TECHNISCHE UNIVERSITÄT DARMSTADT

Impact of ionising radiation on adult neurogenesis: physiological and cellular effects of low and moderate doses of ionising radiation in neural differentiation distinguished by differentiation phase

Vom Fachbereich
Biologie
der Technischen Universität
Darmstadt
zur Erlangung des akademischen
Grades eines
Doctor rerum naturalium
genehmigte Dissertation

von
Dipl.-Biol. Kerstin Rau
geboren am 19.11.1986
in Heppenheim

1. Referent: Prof. Dr. Bodo Laube

2. Referent: Prof. Dr. Gerhard Thiel

Tag der Einreichung: 02.03.2018

Tag der mündlichen Prüfung: 13.04.2018

Darmstadt, 2018

D 17

Kerstin Rau

Impact of ionising radiation on adult neurogenesis: physiological and cellular effects of low and moderate doses of ionising radiation in neural differentiation distinguished by differentiation phase

Darmstadt, Technische Universität Darmstadt

Jahr der Veröffentlichung der Dissertation auf TUprints: 2018

URN: urn:nbn:de:tuda-tuprints-73910

Tag der mündlichen Prüfung: 13.04.2018

Ehrenwörtliche Erklärung

Ich erkläre hiermit ehrenwörtlich, dass ich die vorliegende Arbeit entsprechend den Regeln guter wissenschaftlicher Praxis selbstständig und ohne unzulässige Hilfe Dritter angefertigt habe.

Sämtliche aus fremden Quellen direkt oder indirekt übernommenen Gedanken sowie sämtliche von Anderen direkt oder indirekt übernommenen Daten, Techniken und Materialien sind als solche kenntlich gemacht. Die Arbeit wurde bisher bei keiner anderen Hochschule zu Prüfungszwecken eingereicht.

Darmstadt, den ……

1. Summary

Comprehensive follow-up of brain cancer patients and re-evaluation of medical data revealed a frightening correlation between low and moderate doses of ionising irradiation and induced cognitive dysfunctions. The particular radio sensitivity of adult neurogenesis within the adult brain is suggested as the major contributor in the underlying pathogenesis. Adult neurogenesis describes the differentiation of neural stem cells to mature neurons in the adult brain. Neural differentiation can be separated in three main phases, early progenitor phase, fate specification phase and cell maturation phase. The cellular base of neural differentiation provides a restricted stem cell pool, out of self-renewing neural stem cells (NSCs).

To investigate the impact of low and moderate doses of ionising radiation (IR) on adult neurogenesis we intended to distinguish the differentiation process in its dynamic subpopulations, represented in the individual differentiation phases. Based on ES-derived NSCs we established and characterised a 2D-model system, reflecting the three differentiation phases, of adult neurogenesis.

In the first part of this work we characterised the differentiation of the J1 NSC model system concerning specific marker expression, morphology and functional differentiation markers. The broad characterisation revealed that the J1 model system reflects each of the three differentiation phases, i.e. early progenitor, fate specification and cell maturation in adult neurogenesis on the intra- and intercellular as well as on the functional level in a synchronised, time dependent differentiation. We used the synchronous differentiation of the J1 model system to discriminate the individual differentiation phases by time.

In the second part of this work we analysed the individual radio sensitivity of the distinct differentiation phases. Addressing issues concerning radiotherapy bystander and diagnostic doses, we used low to moderate x-ray doses between 0.25 and 2Gy. To estimate the distinct radio sensitivity of NSCs and the three differentiation phases, we measured the reduction in vitality of the separated subpopulations and estimated the individual LD_{50} of each differentiation phase. NSCs, as well as all three differentiation phases, show an individual radio sensitivity significantly different to the other subpopulations. The proliferative subpopulations, NSCs and early progenitors showed the highest radio sensitivity, whereas the final differentiation phase, cell maturation, showed the lowest. In further analyses we investigated the mechanisms responsible for the IR induced reductions in the individual subpopulations. Within the postmitotic differentiation phases, fate specification and cell maturation, radiation induced apoptosis is the underlying mechanism. In the proliferative subpopulations, the reduction in the number of cells is predominantly mediated by reduced proliferation in NSCs and induced apoptosis in early progenitors.

To investigate the effect of IR on individual differentiation phases further, we irradiated the three defined differentiation phases and analysed the characteristic differentiation properties of the particular differentiation phase by functional, morphological and histochemical markers post IR. Early progenitors, the first subpopulation within the neural differentiation, are affected in their proliferation, but the migration of the surviving cells is not affected by low dose IR, neither is the entry into the postmitotic status. In the next step we analysed J1 cells irradiated in the fate specification phase. The fate determination of the surviving cell population showed a reduced percentage of future neurons post ionising radiation compared to unirradiated samples. The terminal differentiation phase revealed a broad modulation in the phase specific characteristic properties induced by low dose radiation, determined in altered neuronal architecture and a lower density of synaptic markers in

neuroblasts as well as a reduced density of the voltage-gated potassium channels $K_V1.1$. Regarding the functional level we found a long-lasting stagnation in the excitability of the in cell maturation phase irradiated cultures, reflected by a reduced firing rate, decreased coordination in the activity pattern and a loss in spike synchrony.

In the last part of this work we investigated whether the properties of the self-renewing NSCs were also affected by IR. In previous work Dr. Bastian Roth determined that functional characteristics of J1 NSCs are modified post low dose IR, mediated via alterations in K^+ channel currents. In continuative experiments we investigated if low dose IR leads to changes in the morphological and immunohistological characteristic within the J1 NSC population. The follow up of the irradiated NSCs revealed a highly significant increase of the differentiation marker doublecortin (DCX) within the self-renewing population. By using K^+ channel blockers during radiation, we could inhibit the increase in DCX positive cells post low dose IR. In summary we found radiation induced modulations in the phase specific properties of each subpopulation, represented by NSCs and the three differentiation phases, in the third and fourth part of this work.

In conclusion, depending on the differentiation phase, we could identify several specific physiological and cellular effects of low and moderate doses of IR during neural differentiation in a ES-derived neural stem cell line.

2. Zusammenfassung

Umfassende Folgeuntersuchungen von Hirntumorpatienten und die Aufarbeitung medizinischer Daten ergaben eine erschreckende Korrelation zwischen niedrigen und moderaten Dosen ionisierender Strahlung und induzierten kognitiven Dysfunktionen. Die besondere Radiosensitivität der adulten Neurogenese innerhalb des adulten Gehirns wird als wichtigster Faktor für die zugrundeliegende Pathogenese angesehen. Adulte Neurogenese bezeichnet die Differenzierung von neuralen Stammzellen zu reifen Neuronen im adulten Gehirn. Die neurale Differenzierung lässt sich in drei Hauptphasen unterteilen: die frühe Vorläufer-phase, die Zellschicksalsspezifikations-phase und die Zellreifungs-phase. Die zelluläre Basis der neuralen Differenzierung bildet ein begrenzter Stammzellpool aus selbsterneuernden neuralen Stammzellen (NSZs).

Um den Einfluss niedriger und mittlerer Dosen ionisierender Strahlung (IR) auf die adulte Neurogenese zu untersuchen, unterteilten wir den Differenzierungsprozess in seine dynamischen Subpopulationen, die in den einzelnen Differenzierungsphasen abgebildet sind. Basierend auf aus embryonalen Stammzellen generierten neuralen Stammzellen, haben wir ein 2D-Modellsystem entwickelt und charakterisiert, welches die drei Differenzierungsphasen der adulten Neurogenese abbildet.

Im ersten Teil dieser Arbeit haben wir die Differenzierung des J1 NSZ Modellsystems hinsichtlich spezifischer Markerprotein Expression, Morphologie und funktioneller Differenzierungsmarker charakterisiert. Die breite Charakterisierung ergab, dass das J1-Modellsystem jede der drei Differenzierungsphasen, d.h. die frühe Vorläufer-phase, die Zellschicksalsspezifikations-phase und die Zellreifungs-phase der adulten Neurogenese sowohl auf intra- und interzellulärer als auch auf funktioneller Ebene in einer synchronisierten, zeitabhängigen Differenzierung widerspiegelt. Wir nutzten die synchrone Differenzierung des J1-Modellsystems um die einzelnen Differenzierungsphasen zeitlich zu diskriminieren.

Im zweiten Teil dieser Arbeit analysierten wir die individuelle Radiosensitivität der einzelnen Differenzierungsphasen, wobei wir niedrige bis moderate Röntgendosen zwischen 0,25 und 2Gy verwendeten, in Bezug auf Strahlentherapie und diagnostische Dosen. Um die individuellen Radiosensitivität von neuralen Stammzellen und den drei Differenzierungsphasen zu bestimmen, wurde die Abnahme der Vitalität der einzelnen Subpopulationen nach Bestrahlung ermittelt. Zuzüglich wurde die individuelle mittlere letale Dosis (LD_{50}) jeder Differenzierungsphase bestimmt. Neurale Stammzellen wie auch jede der drei Differenzierungsphasen, zeigte eine individuelle Radiosensitivität, die sich signifikant von der der anderen Subpopulationen unterscheidet. Die proliferativen Subpopulationen, neurale Stammzellen und frühe Vorläuferzellen zeigten die höchste Radiosensitivität, während Zellen in der letzten Differenzierungsphase, der Zellreifung-phase, die niedrigste Radiosensitivität zeigte. In weiterführenden Analysen untersuchten wir die Mechanismen, die für die strahleninduzierten Reduktionen in den einzelnen Subpopulationen ursächlich sind. Innerhalb der postmitotischen Differenzierungsphasen, der Zellschicksalsspezifikation-phase und der Zellreifungs-phase, ist die strahleninduzierte Apoptose der zugrundeliegende Mechanismus. In den proliferativen Subpopulationen wird die Reduktion der Zellzahl überwiegend durch eine reduzierte Proliferation in neuralen Stammzellen und einer induzierten Apoptose in der frühen Vorläufer-phase verursacht.

Zur genaueren Untersuchung der Wirkung von ionisierender Strahlung auf einzelne Differenzierungsphasen wurden die drei definierten Differenzierungsphasen getrennt bestrahlt und auf die charakteristischen Differenzierungseigenschaften der jeweiligen Differenzierungsphase mittels

funktioneller, morphologischer und histochemischer Marker analysiert. Frühe Vorläuferzellen, die erste Subpopulation innerhalb der neuralen Differenzierung, sind in der Proliferation beeinträchtigt, aber weder die Migration der überlebenden Zellen noch der Übergang in den postmitotischen Zustand wird durch Niedrigdosisstrahlung beeinflusst. Im nächsten Schritt verfolgten wir die Differenzierung von J1-Zellen, die in der Zellschicksalsspezifikations-phase bestrahlt wurden. Die Zellschicksalsbestimmung der überlebenden Zellpopulation zeigte einen reduzierten Anteil an zukünftigen Neuronen nach ionisierender Strahlung im Vergleich zu unbestrahlten Proben. Die terminale Differenzierungsphase zeigte eine breite Modulation in den phasenspezifischen Eigenschaften, hervorgerufen durch Niedrigdosisstrahlung. Wir konnten Veränderungen in der neuronalen Architektur und einer geringeren Dichte synaptischer Marker in Neuroblasten sowie einer reduzierten Dichte des spannungsabhängigen Kaliumkanals $K_V1.1$ bestimmen. Hinsichtlich der funktionelle Ebene fanden wir eine lang anhaltende Stagnation in der Erregbarkeit der, in der Zellreifungs-phase bestrahlten Kulturen, die sich in reduzierter Feuerrate, verminderter Koordination im Aktivitätsmuster und Verlust in der Spike-Synchronität äußerte.

Im letzten Teil dieser Arbeit untersuchten wir, ob die Merkmale der sich selbst erneuernden neuralen Stammzellen ebenfalls durch Strahlung beeinflusst sind. In vorangegangenen Arbeiten ermittelte Dr. Bastian Roth, dass funktionelle Merkmale von J1 NSZs nach Niedrigdosisbestrahlung verändert sind. In weiterführenden Experimenten überprüften wir, ob Niedrigdosisstrahlung zu Veränderungen der morphologischen und immunhistologischen Merkmale innerhalb der J1-NSZ-Population führt. Die Weiterverfolgung der bestrahlten neuralen Stammzellen ergab einen hoch signifikanten Anstieg des Differenzierungsmarkers Doublecortin (DCX) innerhalb der sich selbsterneuernden Population. Durch die Verwendung von K^+ Kanalblockern während der Bestrahlung konnten wir die Zunahme der DCX-Zellen nach Niedrigdosisstrahlung hemmen. Zusammenfassend fanden wir, im dritten und vierten Teil dieser Arbeit, strahlungsinduzierte Modulationen in den phasenspezifischen Merkmalen jeder Subpopulation, repräsentiert durch neurale Stammzellen und den drei Differenzierungsphasen.

Abschließend konnten wir, in einer aus ES-generierten neuronalen Stammzelllinie, abhängig von der Differenzierungsphase, mehrere spezifische physiologische und zelluläre Auswirkungen niedriger und moderate Strahlungsdosen während der neuronalen Differenzierung identifizieren.

3. Introduction

3.1. Ionising radiation and cognitive dysfunction

Worldwide radiation exposure is increasing due to recent nuclear accidents, transatlantic flights, space travel, atomic weapons testing and use, and medical treatments [3]. The explosive growth in the use of medical diagnostics and therapeutic radiology has led to a marked increase in the number of individuals receiving exposure to ionising radiation (IR) [4]. Especially in the case of brain tumours, the medical applications of radiation therapy have enabled a more efficient diagnosis and treatment of patients, resulting in increased survival rates and longer post-cancer lifetime. Simultaneously, an increase in late side effects of head irradiation has been observed in follow-ups [5].

Cognitive deficits, including progressive deficits in memory, attention and executive functions represent a significant risk for patients undergoing cranial radiotherapy. Cognitive impairment occur in 50%–90% of adult patients with brain tumours who survive, frequently in the absence of corresponding anatomical abnormalities [6]. Due to the improved radiotherapy treatment techniques, the patients with brain tumour survive longer but they experience the late effects of radiotherapy. Since the population of patients with late symptoms is growing rapidly [7], the current effort is focused on functional consequences of head radiation.

It is difficult to distinguish if the observed cognitive deficits are induced by the cancer disease or by radio treatment side effects. Hall et al. analysed cognitive function in a large population of men at the time of military enlistment, who had received low dose ionising radiation for cutaneous haemangioma as children [8]. Between 1930 and 1959 over 4500 boys received cranial irradiation to treat haemangioma, half of them could be followed up until military enlistment at the age of 18 or 19 years. Hall et al. found an overall statistically significant decreasing probability of attending high school in relation to radiation dose compared to untreated children. In the military enlistment test, a significant dose relation for all cognitive tests reflecting learning ability and logical reasoning was determined [8]. This study clearly verified that ionising radiation of the head has long lasting effects on cognitive abilities [8].

Comparable results have been observed in further studies, Albert et al. reported that American children treated with x-rays for tinea capitis had a higher incidence of psychiatric disorders than chemotherapy-treated children [9]. The cohort was re-evaluated by Ron et al. almost 20 years after the treatment. The treated children had lower examinations scores, IQs and a slightly higher frequency of mental retardation than the control group [10]. In addition, a relationship between IR exposure, psychiatric disorders, dementia and neurodegenerative diseases such as Alzheimer and Parkinson has been suggested [7].

Particularly frightening is that applied doses within 0.04-1.5Gy could be correlated to cognitive deficits [8]. This dose range is overlapping with doses applied in medical imaging technics as computer tomography (CT) scans and x-ray photographs [11]. For this reason, the investigation of underlying mechanisms of radiation induced cognitive dysfunction become highly interesting and relevant.

3.2. The role of adult neurogenesis in learning and memory

Before 1970, the human brain was thought to be radioresistant; acute cellular injury in the central nervous system (CNS) as necrosis or plane apoptosis were not detected until single doses of ≥30Gy [12]. Compared to other organs where lower radiation doses cause severe tissue destruction, head irradiation did not show signs of overt tissue damage, leading to the evaluation of the brain as radioresistant organ [13].

The recovery of adult neurogenesis revealed a sensitive target to radiation within the human brain [5, 14, 15]. Adult neurogenesis is a developmental process of generating new functionally integrated neurons, that occurs throughout life in the hippocampus of the mammalian brain. Significant progress has been made in recent years to decipher how adult neurogenesis contributes to brain functions. The majority of human neurons stay unchanged from birth to death in which only a small fraction is renewed throughout life (**Figure 1**).

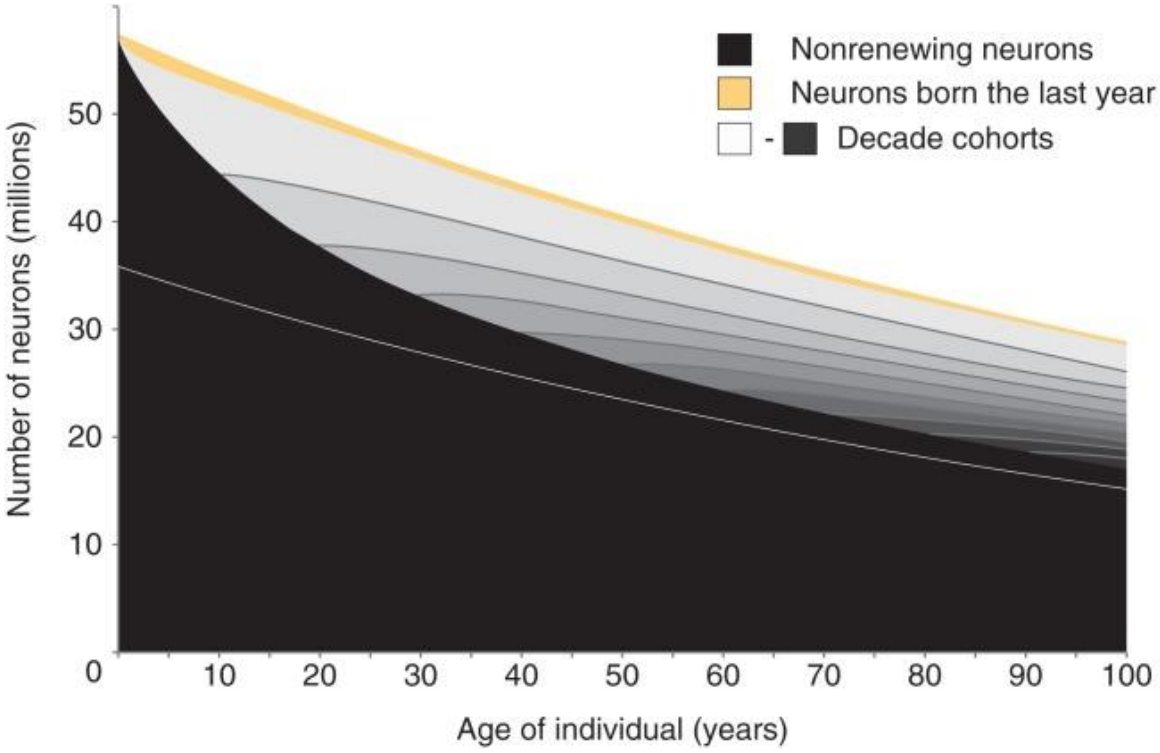

Figure 1 Dynamics of hippocampal neurogenesis in humans. Radiocarbon analyses were used to identify the age of hippocampal neurons. Shown is a schematic representation of the change in neuronal number and turnover in the human hippocampus. The dentate gyrus neurons constitute the population above the white line, and the other subdivisions of the hippocampus are shown below the white line. Neurons generated before birth of the individual are depicted in black, and decade cohorts of new neurons are shown in grayscale. The proportion of cells shown in light gray represents the neurons generated during the last decade, the next shade darker represent the neurons generated the decade before that and so on. New born neurons have specific functional properties, and the neurons generated during the last year are depicted in yellow. Modified from Spalding et al. 2013 [14, 15].

Spalding et al. showed that there are two populations of neurons within the hippocampus, one rather homogenous population (constituting 35% of hippocampal neurons), turning over at a median rate of 1.75% per year, and the other not turning over [15]. The hippocampus is the brain structure crucial for learning and memory, inhibition and dysfunction of hippocampal neurogenesis are associated with impaired learning and memory, cognitive deficits and neurodegenerative diseases [16, 17].

At the cellular level, new born neurons display special properties that are distinct from mature neurons. Synaptic connected new born neurons exhibit hyper-excitability and enhanced synaptic plasticity during a critical period of maturation in the hippocampus, which may allow newly integrated adult-born neurons to make unique contribution to information processing [16]. At the circuitry level, adult-born neurons are responsible for certain special properties of the local circuitry. One potential mechanism is a reduced sensitivity of new born neurons to inhibition from interneurons during the critical maturation period [16]. *In vivo* recording from the dentate gyrus in anesthetized mice has shown that elimination of adult neurogenesis leads to decreased synchronization of dentate neuron firing, suggesting a modulatory role in inter-neuronal communication. At the systemic level, a number of computational models of adult neurogenesis have provided insights on how the addition of new neurons may alter neural network properties and have suggested distinct roles for adult-born neurons at different stages of neuronal maturation [18].

In summary the small number of new born neurons can affect global brain functions via active modifications of mature neuronal firing, synchronization and network oscillations [16, 19]. The function of adult neurogenesis is more than a cell-replacement mechanism in which dying neurons are functionally replaced by new neurons but rather provides new neurons with properties and information-processing capacities that are distinct from those of existing mature neurons [20]. The heterogeneous nature of the hippocampus, with a small new born neuron population that is highly plastic and excitable and a large population of mature granule cells that are sparsely activated with high input specificity, offers unique information-processing capacity that can adapt to dynamic needs over the lifetime [19, 21].

3.3. Adult neurogenesis as underlying pathogenesis of radiation induced cognitive dysfunction

Cognitive dysfunctions observed post cranial irradiation often manifests as deficits in hippocampal-dependent learning and memory [13, 22, 23], suggesting a connection to adult neurogenesis [7, 12, 13, 24]. It has been shown that adult neurogenesis is highly sensitive to ionising radiation, resulting in a massive reduction in new born neurons [12]. Whole brain irradiation leads to apoptosis in hippocampal regions connected to neurogenesis, inhibition or loss in the generation of neurons and the reduction of proliferating cells [5]. Radiation induced deficits in adult neurogenesis are displayed long-lasting or permanent on cellular, circuit and systemic level even after lower doses [5, 24, 25].

It is suggested that the learning and memory deficits are caused by the accumulation of radiation induced dysfunctions on various levels [26]. So far the cellular and molecular mechanisms underlying radiation induced cognitive impairment are not fully characterised but most probably involve loss of adult neurogenesis resulting in altered systemic function [27]. Detailed mechanisms of how these cellular alterations lead to late effects as cognitive impairment remain largely unknown [28].

A better understanding of cellular and tissue mechanisms will balance the risk against benefit in the use of medical radiology and promote the development of new prevention and therapy methods to reduce adverse long-term consequences of radiation.

3.3.1. **Aim of the study**

The understanding of the individual effects of IR on adult neurogenesis is highly relevant. Almost all studies are performed at the heterogeneous neural stem cell niche level which does not reflect the individual reactions of the diverse progenitors towards radiation. Establishment of a model system to distinguish the individual differentiation phases is essential to identify intrinsic radiation induced modifications, could help to understand systemic malfunctions. The main effect of IR in adult neurogenesis is the loss of neuronal cells, therefore differential analyses of the cellular subpopulations would help to evaluate the risk of radiation in the cellular subpopulations within adult neurogenesis. In highly regulative, dynamic processes like the adult neurogenesis, specific properties of each subpopulation play a critical role in the tissue homeostasis and maintenance. Especially low dose irradiation is known to affect the physiological properties of cells. Detailed analyses of the surviving population would give insight if the physiological properties of the irradiated subpopulations are modified and may endanger the differentiation process and the maintenance of functional adult neurogenesis. In this thesis, we established a model system of neural differentiation, distinguishable in differentiation phase dependent subpopulations, by using an ES-derived neural stem cell line. Understanding the impact of IR on individual subpopulations within neural differentiation can shed light on the sensitivity of adult neurogenesis to IR and help to prevent IR induced cognitive deficits.

4. Chapter I: Establishment and characterisation of a suitable model system for neural differentiation in adult neurogenesis

4.1. Introduction

4.1.1. Adult neural stem cells

For a long time, neurogenesis was determined to happen only in early brain development and is terminated after birth [29, 30]. First in 2013 adult neurogenesis was approved in humans [14, 15]. Adult neurogenesis is the generation of new neurons from a pool of adult neural stem cells [31]. These neural stem cells (NSCs) are tripotent stem cells, capable to differentiate into astrocytes, oligodendrocytes and neurons [32].

The adult mammalian brain harbours two main NSC pools, in the subgranular zone (SGZ) in the dentate gyrus (DG) of the hippocampus and in the subventricular zone (SVZ) of the lateral ventricles (LV) [33-37]. Furthermore, recent studies suggest the presence of NSCs in the striatum, part of the basal ganglia [14, 38, 39] as shown in **Figure 2**. Adult neurogenesis generates continuously new neurons throughout life [34, 40], which emphasizes the significance of neurogenesis after birth. Malfunctions in adult neurogenesis are related to limitations in cognitive functions, learning and memory as well as pathological conditions such as epilepsy, schizophrenia and neurodegenerative diseases as Morbus Parkinson, Alzheimer disease or Huntington disease [36, 41-54]. This illustrates clearly that the understanding of adult neurogenesis is of prime importance for diagnostic and therapeutically usage.

4.1.2. Neural stem cell niches

The late discovery of adult neurogenesis is mainly owed to the limitation of sensitive methods. Only the discovery of nucleotide analogs like bromodeoxyuridine (BrdU) combined with neuron specific protein markers and confocal imaging allowed confident identification of adult born neurons [30, 55]. These methods enabled the identification of stem cell niches in several brain regions in multiple species [56, 57]. In mammals, neurogenesis appears to be more limited to the dentate gyrus (DG) and the olfactory bulb (OB). The migration of new born neurons to the OB along the rostral migratory stream from the subventricular zone (SVZ) is often focused in immunohistological studies but remains in humans controversial [58, 59]. The presence of neurogenesis in the dentate gyrus (DG) in humans is generally accepted by the scientific field. In this case new born neurons migrate a short distance to the granule cell (GC) layer in the DG and integrate into the circuitry of the hippocampus [14, 38].

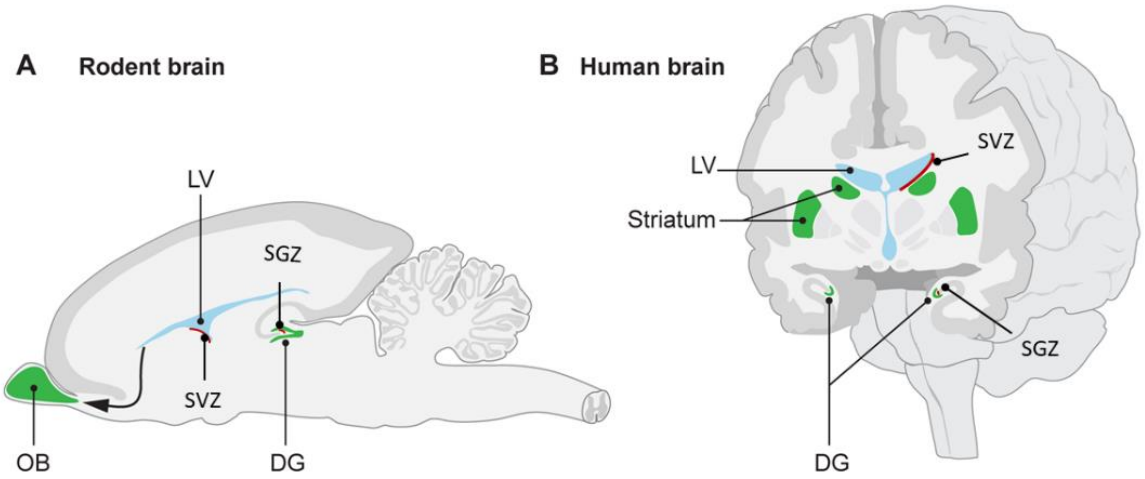

Figure 2 Schematic illustration of adult NSCs in the adult rodent and human brain. New neurons are indicated in green. (**A**) in rodents, neuroblasts which are generated in the subventricular zone (red) lining the lateral ventricle (LV) migrate to the OB, a structure crucial for olfaction, where they integrate as interneurons. (**B**) in humans, neuroblasts are also present in the subventricular zone (red) and new neurons integrate in the adjacent striatum, which plays an essential role in movement coordination, procedural learning, and memory, as well as motivational and emotional control. New neurons are continuously generated in the DG of the hippocampus, a brain structure essential for memory and mood control, in both rodents and humans (**A, B**), modified from Frisen, 2015 [38]

Even if the human neurogenesis of the DG is the main focus in current research the level of new neuron production has been characterised in limited cases[15, 34]. Frisen and colleges used carbon-dating to estimate neurogenesis rate and determined a yearly turnover of 1.75% for neurons and 3.5% for astrocytes in the dentate gyrus [15].

In vivo both stem cell niches (SGZ and SVZ) only generate neurons and astrocytes [60], even if transplantation experiments and *in vitro* experiments showed that the neural stem cells are also capable to generate oligodendrocytes [2, 33, 61-64]. These studies also show that the microenvironment of the stem cell niches not only hosts stem cells but also influences neural differentiation.

4.1.3. **Neural differentiation**

Stem cell niches are defined by the balance of self-renewal to obtain the stem cell pool and the induction of differentiation [32]. Neural differentiation is a complex process strongly regulated by a spatial-chronological gene expression pattern depending on intra- and extracellular signalling and tissue communication [15, 65, 66]. Cell differentiation is the process of the structural and functional specialisation of cells. In neural differentiation the starting point are neural stem cells. In the so called self-renewal phase NSCs proliferate via symmetrical cell division. In the SGZ, the pool of symmetrical dividing stem cells is also referred as radial glia cells (RGCs) or type1 cells [67].

Induced differentiation leads to an asymmetric cell division, generating early progenitors. The population of early progenitor cells generated by asymmetric cell division are also named nonradial

type 2 or intermediate progenitor cells. Type 3 cells are progenitor cells with future neuronal fate in later differentiation [68, 69].

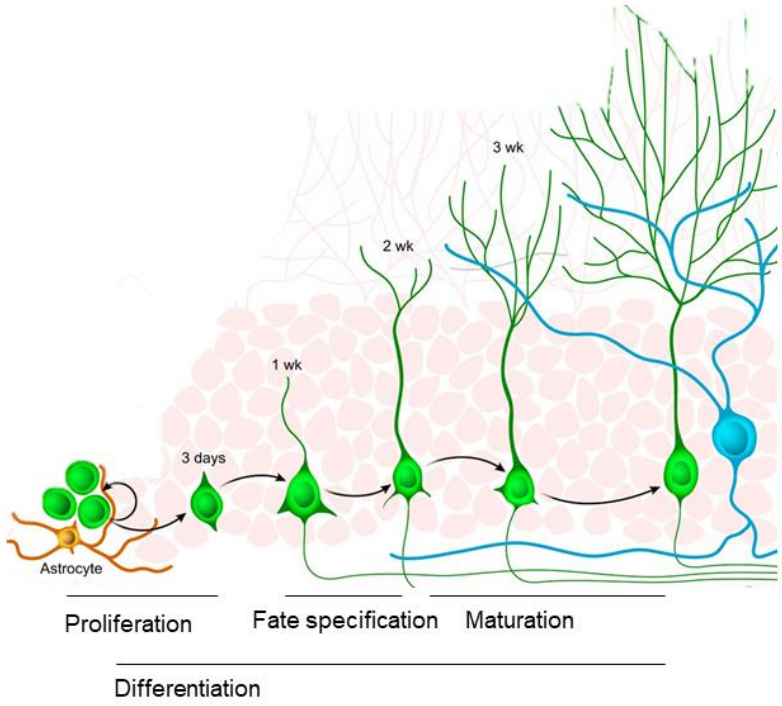

The development of DG stem cells to fully mature neurons. New neurons arise from slowly dividing neural stem cells, also known as radial glial cells, and the more rapidly amplifying, neural progenitor cells. Over the next weeks, cells differentiate into neurons, slowly developing dendritic arborizations and axonal projections. Between 2 and 3 weeks of age, new neurons begin to receive excitatory input from cortical path axons, and by 4–8 weeks, their physiology and anatomy begin to approach those of fully mature neurons. Induced apoptosis is a final differentiation event during maturation, surviving neurons count as differentiated [2].

Figure 3 Schematic illustration of the hippocampal neurogenesis. NSCs harboured in the SGZ pass three differentiation phases (proliferation, fate specification, maturation) while migrating to the hippocampus. Surviving neurons integrate in the hippocampal network and are referred as differentiated. Modified after Aimone et all, 2014 [1].

At the beginning of neural differentiation an amplification phase takes place. The early progenitor cells, developed from an asymmetrical cell division, process a strong proliferation phase, during which the early progenitor population is amplified. After this phase the cells are post-mitotic. During the amplification phase more early progenitors (EP) are generated as enter further differentiation. Some of these EPs stay in a quiescence stage, building a depot of early progenitors [70-72]. These early progenitor cells have a committed differentiation potential and enter directly or after reactivation the fate specialisation [61]. Following the differentiation, the main migration takes place which also leads to morphological transformations [73] as shown **Figure 3**. In preparation for the migrating phase, the tips of the growing neurites, called growth cones, sense the extracellular matrix for molecular interactions with target proteins, like the glycoprotein laminin. The morphological changes, caused by the axonal growth, show the typical apical dendrites on opposite sides leading to a spindle shape. The spindle like morphology is a characteristic for early progenitors (**Figure 3**). In adult neurogenesis neuroblasts from the SVZ migrate in chains and follow the same path, which can be shown in immunohistological studies [74]. Observations of these structures gave the first hints for adult neurogenesis, like the rostral migratory stream mostly known from rodents [58, 74-77]. Later streams of glioblasts were discovered, the so called glial tube, is often located directly beside the neuroblast paths [59, 78].

The surrounding tissue delivers signals for induced and continued differentiation via growth factor gradients [79]. Post mitotic progenitors enter the second differentiation phase, the so-called fate specification. During this phase the neuronal or glial fate determines. This process is accompanied by

morphological and structural cell type specifications. The fate specification is considered to be terminated upon the expression of specific marker proteins as ß Tubulin 3 (ßTub3) or Microtubule-associated protein 2 (MAP2) for neuronal progenitors, or Glial fibrillary acidic protein (GFAP) expression in glial progenitors [2, 14, 32, 34, 80-86]. Beside the protein expression, the morphology of the progenitors develops, neuronal progenitors can be recognized by axonal and dendritic growth, resulting in a typical pyramidal shape [2].

After the fate specification neuronal progenitors can be referred as neuroblasts and glial progenitors as glioblasts [2]. Glio- and neuroblasts enter the final differentiation phase, the cell maturation. In the final differentiation step the morphology, gen- and protein- expression and signalling of mature neurons and astrocytes is evolved [2, 14, 40, 61, 65, 87, 88]. The maturation process in neuroblasts covers multiple levels. Beside intracellular processes as increased axonal and dendritic growth, specialised functional maturation and protein expression, intercellular processes like network integration and synaptic connection play a role [14, 89-91]. One major differentiation event during neuronal maturation is synaptogenesis, which represents the base for intercellular neuronal transmission and coordinated network signalling [2, 39, 49, 92]. In course of the maturation phase most of the neuroblasts (50-70%) undergo apoptosis *in vivo* [93-100]. The synaptic induced programmed cell death is a final differentiation event to eliminate superfluous or malfunctioning neuroblasts [100]. Surviving neuroblasts are classified as differentiated or mature neurons [14, 32, 34, 80, 100]. Despite all, the exact mechanisms inducing and regulating neural differentiation processes are poorly understood [16].

4.1.4. **Regulation in neural neurogenesis: extrinsic and intrinsic factors**

Adult neurogenesis is a highly dynamic process and is regulated by many extrinsic factors as well as intrinsic factors. The neural stem cell niche provides variable growth factor gradients resulting in a highly specialized microenvironment [101]. Some of the main growth factors identified in neural differentiation are Epidermal Growth Factor (EGF), Fibroblast Growth Factor 2 (FGF2) and Brain-Derived Neurotrophic Factor (BDNF). EGF plays a major role in maintaining symmetric divisions and inhibiting differentiation [79]. In isolated NSCs EGF is a key factor to maintain the self-renewal status. FGF2 has one of the most widespread roles in neural differentiation. FGF2 in the absence of EGF, stimulates induced differentiation and increased proliferation. Furthermore, differentiation, migration and neuronal survival is stimulated by FGF2 [79]. The neurotrophin BDNF is also a strong regulator for neuronal survival. It also stimulates late neuronal differentiation events as axonal growth and synaptogenesis. NSCs *in vitro* failed to differentiate into neurons in BDNF free conditions [79]. Neuroblasts also start to express and release BDNF, the expression is regulated by synaptic activity [79, 102].

Additional to growth factor gradients, the extracellular matrix of the neural niche, is a regulating element in neural differentiation [103]. Migration is regulated by interactions between cells and between cells and the extracellular matrix [104]. Laminin is the best investigated example. Presented from surrounding cells, laminin allows the differentiating cells to attach and find their path through the surrounding tissue [49, 54, 66, 84, 87, 105]. Via integrins progenitors bind on laminin, which stimulates axonal growth and organisation [106-108]. The axonal interaction between differentiating progenitors is also regulative for further differentiation. Growing axons permanent emit and retire filopods to establish connections with dendrites [66, 77, 87, 109]. When they successful connect

recruiting of synaptic proteins starts [106]. First presynaptic proteins form an active plate which stimulates postsynaptic protein recruitment and synaptic adhesion[110]. The final formation and maintenance of synapses is dependent of electrical activity [111]. Simultaneous activity of pre- and post-synaptic neurons strengthens the newly formed synapses. Synchronised activities lead to activation of AMPA or NMDA receptors which is followed by neuron specific Na^+ currents. These simultaneous activities resemble the fundamentals of synaptic long-term potentiation (LTP), the biomolecular base of learning and memory [106, 112]. Beside its role in synaptogenesis, electric activity plays a major role in the survival of neuroblasts.

Active input has been shown to be critical for the death and survival of individual neuroblasts during neuronal maturation [100, 113]. During the differentiation progress apoptosis is a major regulative process which starts with established synaptic connections [114-118]. In the adult hippocampus, GABAergic synaptic input promotes the survival of DG neuroblasts [119]. Suppression of GABA excitation in new born neurons also impaired the survival of neuroblasts, a process mediated by the regulation of transcription factor activation (e.g. CREB). Therefore, GABA-mediated depolarization and the subsequent initiation of CREB signalling appear to enhance the survival rate of maturing neurons [120]. The synaptic induced apoptosis is the final event in neuronal differentiation, terminating neural differentiation [121].

4.1.5. **Protein expression during neural differentiation**

On the way from neural stem cell to mature neuron or astrocyte the protein expression of the cells changes fundamentally. To analyse neural differentiation marker proteins are often used to identify the differentiation status of progenitor or stem cells. Some of the key markers during differentiation are nestin, doublecortin (DCX), microtubule-associated protein 2 (MAP2), ß Tubulin 3 (ßTub3) and glial fibrillary acidic protein (GFAP) (see also **Figure 4**).

Nestin is expressed in NSCs [122]. Nestin has been the most extensively used marker to identify stem cells within various areas of the developing nervous system and in cultured cells *in vitro* [123, 124]. Upon differentiation, nestin becomes downregulated and is replaced by fate-specific intermediate filament proteins [125]. One of this cell fate specific intermediate filaments is GFAP, exclusively expressed in astrocytes [126]. The intermediate filament GFAP is the most widely used marker of astrocytes [127]. It is thought to control astrocytic shape, movement, and function.

Correspondingly, the structure proteins ßTub3 and MAP2 are expressed in neurons after fate determination and used as neuron marker [33]. MAP2 is a neuron-specific dendritic protein that is used as a marker of neuronal dendrites [128]. The MAP2 protein plays a role in determining and stabilizing dendritic shape during neuronal development [129]. ßTub3 is a tubulin thought to be involved in morphological specification during differentiation of neuronal cells [130]. Accordingly, immunohistological staining of ßTub3 is found in the cell bodies, dendrites, axons, and axonal terminations of neuroblasts [131, 132]. In contrast to MAP-2, ßTub 3 also visualises axons.

The neuronal migration protein DCX is also a microtubule-associated protein. DCX is one of the earliest differentiation markers in neuronal differentiation already expressed in proliferating progenitors. Because of the early expression of DCX in progenitors, it is used as early differentiation marker which persists in neuroblasts after fate determination [63, 133-136]. DCX is widely expressed by migrating progenitors and is observed in the earliest phase of neuronal differentiation. DCX has a suggested role

in the growth of neuronal processes at the leading edge of the cell [137]. Consistent with this role, DCX immunostaining appears most intense at extremities of neurites and continues into proximal regions of growth cones, but not the tips [138].

Beside the commonly used differentiation marker proteins, synaptic proteins play a key role in functional neuronal differentiation. In proceeding differentiation, neuroblasts start to express synaptic proteins which is the basal setting to form synapses and functional development. Post-synaptic-density-protein 95 (PSD95) is a membrane associated post synaptic guanylate kinase with a PDZ domain [139, 140]. As one of the best studied members of this family, PSD95 is a common marker for excitatory post-synapses [139]. Synaptophysin also known as major synaptic vesicle protein p38, is a glycoprotein essential for synaptic vesicles and synaptic transmission [139, 141-143]. Enriched in presynaptic areas it is a commonly used marker for pre-synapses, in permealized immunostainings synaptophysin is localized cytoplasmic [125, 140, 143-146]. Gephyrin is an anchoring protein that links inhibitory neurotransmitter receptors to the postsynaptic cytoskeleton, which makes it to a postsynaptic marker for inhibitory synapses [147, 148].

4.1.6. **Functional differentiation of neural progenitors**

The differentiation from NSCs to neurons and astrocytes includes also specialisation on the functional level of the progenitors. Differentiating neural cells show specialised ion channel expression during the differentiation process, the differentiation phase dependent expression makes them suitable as differentiation markers. The functional differentiation can be identified using different functional marker characteristics.

Resting membrane potential in neuronal differentiation

One of the functional marker characteristics is the resting membrane potential (V_R). Proliferating NSCs and early progenitors in the adult brain are characterised by an V_R of -40 to -55mV [149-151] During the differentiation progress the progenitors show a lower V_R. In DCX positive progenitors *in vivo* as well as in enriched neuroblast population *in vitro* a V_R of -55mV to -65mV is measured [97, 152, 153]. The more negative V_R in later neuronal differentiation is suggested to be caused by the down regulation of K_{ir} channels (see **Figure 4**) [97, 154]. Mature neurons are characterised by a V_R of around -65mV, it has been shown that a V_R of -65mV is one of the last marker in neuronal differentiation, reached in maturation phase [92, 97]. Beyond the role as marker, the changes in the V_R play a functional role in the differentiation process [155]. It is hypothesized that changes in the V_R of differentiating progenitors alters the Ca^{2+} signalling to control phase specific gene expression [156, 157]. Around 80% of the differentiation relevant genes correspond to V_R dependent regulated genes, in mammalian neurons [97, 155, 157, 158].

Ion channels expression during neuronal differentiation

It is known that specific ion channels control proliferation, differentiation and survival in NSCs. The large K^+ channel super-family is the most studied ion channel group in the context of neurogenesis (**Figure 4**). K^+ channels have been implicated in the regulation of at least three critical events of neurogenesis: cell proliferation, differentiation and migration [159-162]. K^+ channel properties are often influenced by factors known to regulate the distinct steps of neurogenesis, such as cytokines and growth factors [163-166]. K^+ channel expression has been studied in a number of NSC and progenitor models including various embryonic and postnatal cultures from both the VZ and hippocampus, as well

as NSC models derived from other types of stem cells [97]. Both *in situ* and *in vitro* studies have revealed a progression of K^+ channel over the course of neuronal differentiation. Changes in K^+ channels expression (and possibly activity) appear to play a critical role in fine tuning progression from quiescent to proliferative early progenitors [91]. Inhibition of the K^+ channels with high resting conductance (e.g., specific K_{ir} isoforms) could stimulate proliferation in NSCs and early progenitors [167]. Migrating progenitors dramatically change their shape while moving, local swelling and shrinkage are necessary for migrating cells when they are obliged to squeeze through surrounding tissue. K^+ as well as Ca^+ channels are key player in this process [168-172]. In further differentiation, K^+ channel regulates the cell excitability and axon growth [173]. The differentiation phase dependent expression of specific K^+ channels can be used as marker to identify the sub-stages in neuronal differentiation [91]. K_{ir} channels are mainly expressed in proliferating NSCs and early progenitors, the down regulation of K_{ir} channel expression in post mitotic phases, makes K_{ir} channels to a marker of early progenitors and self-renewing NSCs [91]. Post mitotic progenitors show increased expression of delayed-rectifier K^+ channels (K_{DR}), Ca^{2+}-sensitive K^+ channels (K_{Ca}) and A-type K^+ channels (K_A). K_{DR}, K_{Ca} and K_A channels accordingly represent a marker for post mitotic progenitors [91](see also **Figure 4**).

One of the main electrophysiological characteristic in postmitotic neuroblasts during further differentiation are voltage-gated Na^+ channels (Na_v), a fundamental device for action potentials [92, 97, 155]. In later differentiation synaptic activity is an intrinsic intercellular key regulator. To generate action potentials Na_v channels are required. It could be shown that acquiring action potentials is one of the late events in neuronal maturation in adult mice, conducted with voltage gated sodium channel expression [92]. Compared to embryonal neurogenesis, the expression of Na_v channels is delayed, resulting in an late synaptic activity [92]. Elsewise as in embryonal differentiation, Na_v channels display a late differentiation marker in adult neurogenesis, expressed during cell maturation (**Figure 4**). The late expression of Na_v presupposes late coordinated synaptic activity. Hence, coordinated synaptic activity mediated by Na_v channels is one of the latest markers in adult neural differentiation. Carleton et al. suggested the late onset of synaptic transmission in adult neurogenesis may protect the surrounding network from uncontrolled neurotransmitter release and network disruption [92].

Spontaneous activity in neural differentiation

During functional differentiation spontaneous activity is an elementary process correlated with regulative mechanisms [111, 113, 174-178]. The complex patterns of ion channel development that occur in excitable cells can be understood as an ongoing process to a final set of properties. Spontaneous activity regulates a large variety of developmental processes, but still little is known about its role in adult neurogenesis [178, 179].

In course of embryonal neurogenesis early progenitors start to express neurotransmitter receptors as $GABA_A$-receptors. Activation of $GABA_A$-receptors by endogenous GABA, activates voltage-gated Ca^+ channels. The resulting Ca^{2+} transients induce the expression of transcription factors as NeuroD which also lead to the expression of Na_v channels and neuronal markers. Beside GABA receptors, AMPA and NMDA receptors and their activation play regulative roles in inducing spontaneous activity following signalling [174, 179, 180].

Regarding adult neurogenesis, it is known that neuronal progenitors and neuroblasts express voltage-gated Na^+ and Ca^+ channels and transmitter-activated channels similar to those in embryonic cells [49, 53, 90, 121].It has been shown that spontaneous activity also regulates activity-dependent processes in adult neurogenesis[180-182]. Spontaneous activity can regulate the level of excitability of cells by controlling the expression of ion channels involved in fate determination, synaptogenesis and survival

[49, 111, 136, 174-177, 180, 183-188]. Spontaneous synaptic activity emerged soon after entering fate specification phase with increasing spiking activity in further differentiation. The spike frequency and amplitude increased significantly with cell maturation [92, 178]. In cell maturation phase, neuroblasts fire action potentials spontaneously and receive synaptic contacts, suggesting a functionally network integration [92].

Taken together, spontaneous activity represents a fundamental marker of functional differentiation in embryonal and adult neurogenesis, mirroring ion channel and receptor rearrangement and trafficking, network building and intracellular as well as intercellular signalling (see also **Figure 4**).

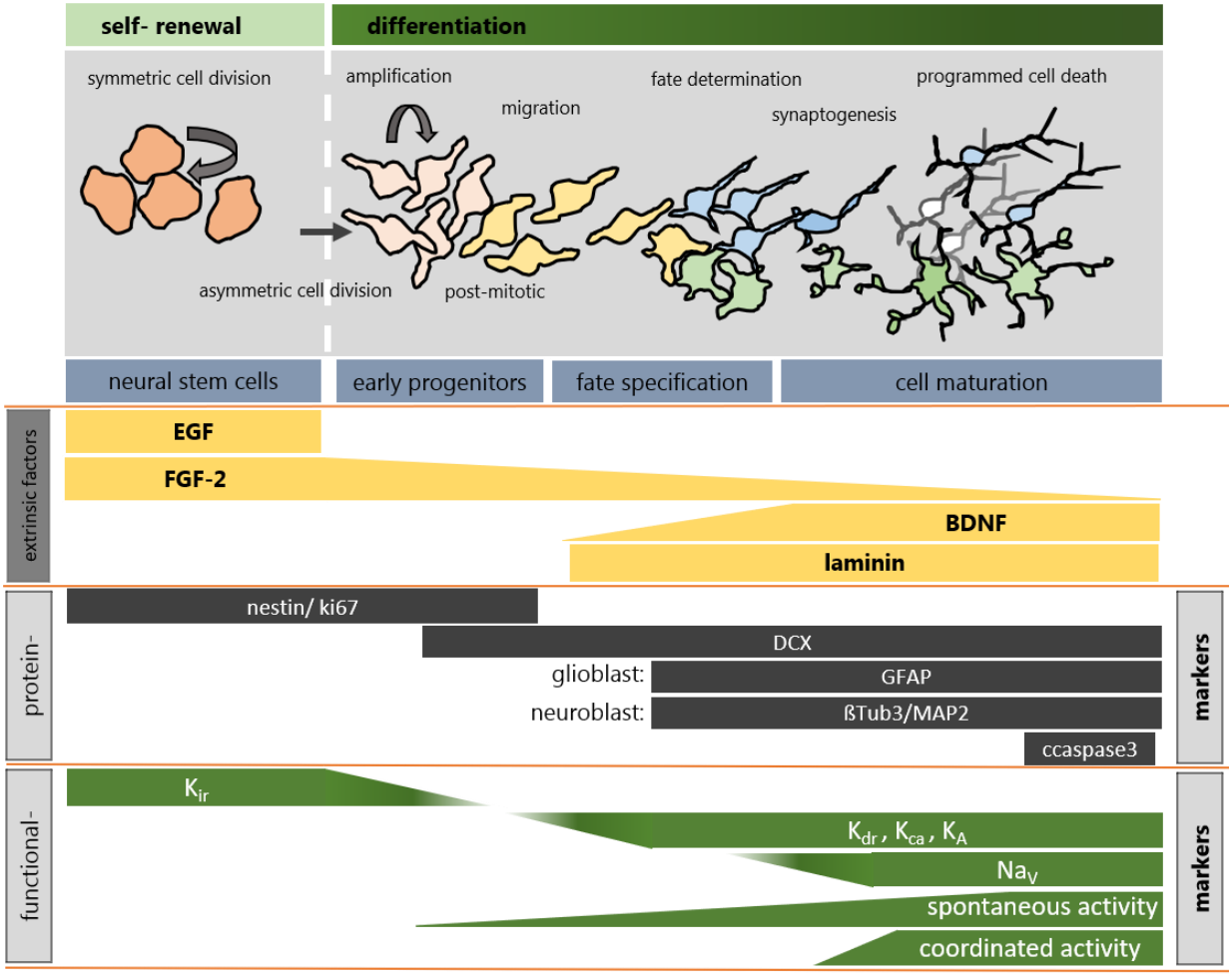

Figure 4 Schematic overview of morphological, functional and protein expression changes in neural differentiation: neural differentiation can be characterised by comprehensive changes on morphological and functional levels. **Morphology**: compared to self-renewing NSCs, early progenitors show a spindle like shape. Entering fate specification phase, future neurons show increased axonal growth, resulting in a pyramidal appearance. In the final cell maturation phase the progenitors show the neuron or astrocyte characteristic morphology. **Extrinsic factors**: the progression in the differentiation course is regulated by extrinsic growth factor gradients (EGF, FGF-2, BDNF) and extracellular proteins (laminin). **Specific protein expression depending on the differentiation status are often used as markers**: NSCs and proliferative progenitors express nestin and ki67. In early differentiation progenitors start to express DCX. Progenitors determined in their fate express neuron- or glia-specific proteins as ßTUB3, MAP2 in neuroblast and GFAP in glioblasts. The apoptotic marker ccaspase3 is a marker for late maturation. **Ion channels are expressed depending on the differentiation phase and can be used as markers**. The expression of selected ion channels involved in regulating the properties of neural differentiation have been summarised by Swayne [91]. In the proliferating, nestin positive phase mainly inward- rectifying K^+ channels (K_{IR}) are identified. In progressing differentiation, future neurons start to express delayed-rectifier-type and Ca^{2+}-sensitive K^+ channels (K_{DR}, K_{Ca}) and A-type K^+ channels (K_A). In later differentiation voltage gated sodium channel (NA_V) are expressed and result in coordinated network activity, a marker for synaptogenesis.

4.1.7. **J1 NSCs a potential model system for neural differentiation?**

Adult neurogenesis is an increasing research target with a growing need for adequate model systems. The limited amount of neurogenesis in adult animals, the complex influence of the microenvironment, as well as the difficult accessibility make *in vivo* studies inappropriate for fundamental research. Isolated cells from neural stem cell niches, could be maintained in culture as neurospheres *in vitro* [189]. Neurospheres consist predominantly of early progenitors mixed with differentiated astrocytes and neurons and undefined progenitors [190]. This mixed cellular population provides a heterogeneous pool that contains only few undifferentiated NSCs, which decrease in the ability to self-renewal [191]. Neurospheres, as well as adherent cultures of primary progenitors show a switch from neurogenic to gliogenic differentiation in longer cultivation, suggesting a loss of the differentiation potential during cultivation [192-194]. The NSCs as well as the progenitors in varying differentiation phases maintained within neurospheres cannot be directly identified and purified [195]. The cellular complexity, heterogeneity and unstable differentiation potential *in vitro* represent limitations of these primary cultures.

Conti. et al. manage to differentiate murine embryonic stem cells to adherent NSCs [191]. By the use of the epidermal growth factor (EGF) he achieved a homogeneous NSCs undergoing continuous symmetrical self-renewal divisions. He could also show that depletion of EGF (and concentration gradients of FGF2 and BDNF) lead to neuronal and glial differentiation in this culture, with a high survival rate and high yield of neuronal cells. The differentiation potential of the introduced model system was stable over 115 passages [191, 196] and unchanged by temporal cryoconservation. Therefore, the J1 NSCs line represents a stable, directly accessible, 2D model system for adult NSCs.

2D neuroblastoma cell lines are also used to investigate neuronal differentiation. These cancer cell lines display neuronal characteristics and show single differentiation markers as ßTub3 expression or post mitotic populations when cultivated with FGF2 or BDNF [197, 198]. These systems fail in representing comprehensive processes as functional differentiation, fate specification or the generation of mature neurons or astrocytes [199, 200].

Conti. et al. already showed that neural differentiation is inducible in J1 NSCs by growth factor modulations in the media, with a promising neuronal percentage [191]. Beside the neuronal markers ßTub3, expression of the synaptic marker synaptophysin and Na_v channels could be detected, 5 days post induced neural differentiation, suggesting at least partly displaying functional neuronal maturation [191]. Taken together, the J1 NSC model system displays a promising 2D model system for neural differentiation.

4.1.8. First aim: establishment of a suitable model system

As roughly described previously, neural cell differentiation is an interminable, complex process, characterised by three main differentiation steps in adult, as well as in embryonal neurogenesis (see also **Figure 3** and **Figure 4**) [201].

The first event in neural differentiation is the proliferation: NSCs perform self- renewal, symmetric divisions to maintain the stem cell pool. Induced differentiation starts with asymmetric division of these cells. The generated **early progenitor** cells pass a short but highly proliferative phase, called amplification phase, which results in a pool of progenitors with committed differentiation potential, but still undetermined cell fate. The first phase of neural differentiation is closely connected to induced migration.

The cell **fate specification** is defined as the second differentiation phase. Fate specification means rearrangement of the intracellular infrastructure for neuronal or astrocytic cell specification. This process is mainly defined by morphological specification, the expression of fate specific proteins and the starting of spontaneous activity. Proteins like GFAP for future astrocytes or ßTub3 for future neurons are the typical cell fate specific proteins and are often used as marker proteins. Determined in the fate, the cells can be referred as neuroblasts or glioblasts [35, 106, 201-204].

The third and final phase of neural differentiation is the **cell maturation.** Neuro- and glioblasts evolve the full properties of neurons or astrocytes, combined with the integration in the existing tissue. The neuronal maturation refers mainly to bioelectrical characteristics, given by the expression and activation of specified ion channels and receptors leading to increasing and coordinated activity [2, 39, 49, 112, 187, 205, 206]. Beside the specialised basic lay-out, dynamic neurite and dendrite growth, movement and activation is important for synaptogenesis and synaptic integration. Neuronal maturation as well as network integration depends on coordinated intercellular communication [39, 49, 109, 110, 207].

All three differentiation phases are intricate processes alone, entangled and depending on each other, even more complicated, which makes *in vivo* studies challenging. *In Vitro* studies are often limited in reflecting diverse differentiation events. The J1 NSC model system has not been investigated regarding individual differentiation phases but appears as a promising model system for complex differentiation events [191]. To investigate the influence of ionising radiation (IR) on specific differentiation phases of adult neurogenesis a well characterized model system is mandatory. As base for further radiation experiments we established and characterized a model for adult neurogenesis, based on the J1 NSC model system, focusing the representation of all three differentiation steps and the capability for varying methods as immunostainings, patch clamp recordings and multi-channel arrays.

4.2. Material and methods

Cell line

All experiments were performed with the murine neural stem cell line J1. This cell line is derived from murine J1 embryonic stem cells to a stable neural stem cell line, as described by Conti, 2005 [191]. Only cells between passage 7 to 20 were used, cultured at 37°C and 5%CO_2.

Differentiation protocol

The used differentiation protocol is based on the use of three sequential individual differentiation media. To start differentiation, undifferentiated cells were harvest and centrifuged. The cell-pellet was resuspended in DI media and seeded on cell culture flasks. The first two days differentiating cells stay in DI media, on differentiation day 3 cells were harvested again and centrifuged. The pellet was resuspended in media DII and seeded on laminin coated cell culture ware. The laminin coating was prepared overnight (3µg/cm$^{2)}$. The differentiating cells stay in media DII until differentiation day 5, for three days. On differentiation day 6 the media was changed to media DIII, for another three days. From differentiation day 9 on cells were cultured in media pD (post-differentiation). During the complete differentiation a daily media change is necessary. The used protocol is based on Conti, 2005 and modified for experimental requirement [191]. Divergent from the published original protocol, the first differentiation step was shortened to two days and cell density was adjusted. Modifications were verified in pre-experiments focusing on cell survival and vitality.

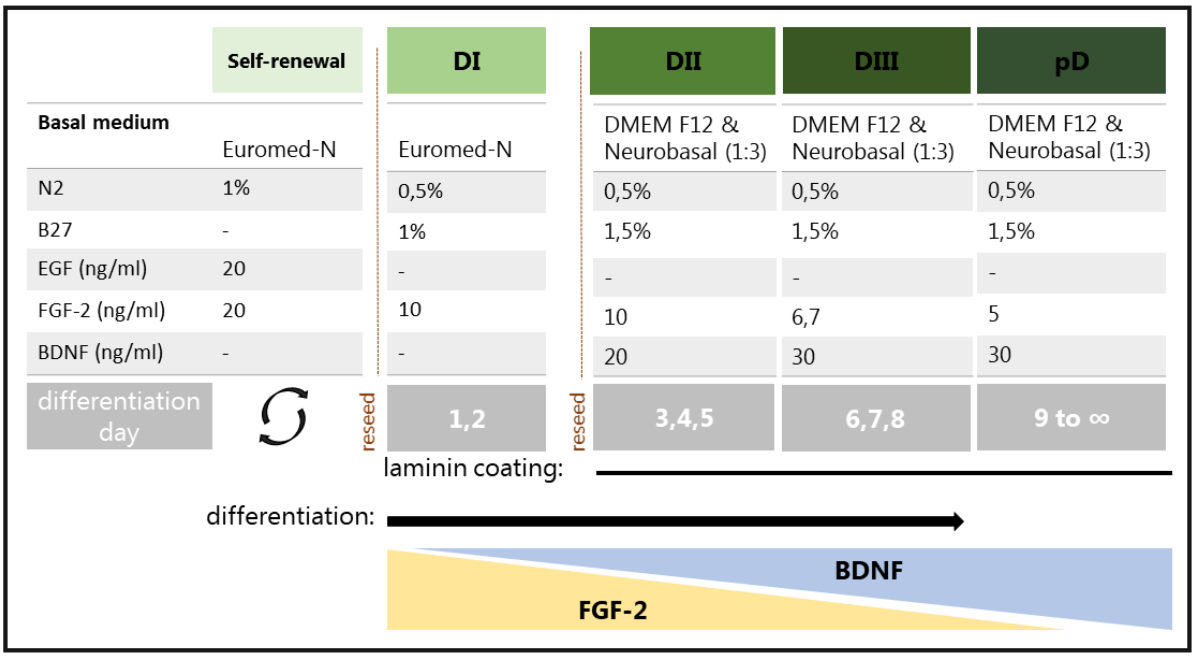

Figure 5 Schematic illustration of the used differentiation protocol; to keep J1 NSCs as homogenous NSC-line, cells were passaged in self-renewal media, maintaining stem cell character via epidermal growth factor (EGF); to induce differentiation cells have to be reseeded in the first differentiation media DI for two days. On differentiation day 3, pre-differentiated cells are reseeded on laminin coated labware and cultured in second differentiation media DII. On differentiation day 6 the media is changed to third differentiation media DIII for three days. According to Conti, 2005 [191] cells are differentiated after day 8, but cells could be cultured for longer in media pD. The composition of the sequential differentiation medias is listed above, basically defined by the increase of brain-derived-neurotrophic factor (BDNF) and the decrease of fibroblast-growth factor 2 (FGF2).

Antibody staining

For antibody staining cells were fixed with 4% PFA, permealized with 0.1% Triton X-100 and blocked overnight. Primary antibody was incubated in antibody buffer (concentrations listed below) overnight at 4°C, secondary antibody was incubated in antibody buffer for one hour at RT.

List of used primary antibodies:

antibody		host			Marker for:	concentration
ßTub3	beta Tubulin 3	m	abcam	ab18207	neurons	1:200
c-cas 3	cleaved caspase 3	r	cell signaling	#9664	apoptosis	1.500
DCX	Doublecortin	r	abcam	ab18723	neural precourser	1:400
GFAP	glial fibrillary acidic protein	r	abcam	ab7260	astrocytes	1:200
Ki67	ki67	r	abcam	ab16667	proliferation	1:100
MAP-2	microtubuli associated protein 2	r	chemicon	MAB3418	neurons	1:200
Nestin	nestin	m	abcam	ab11306	stem cells	1:200
PSD95	post- synaptic density protein 95	m	abcam	ab18258	(post-) synapses	1:200
Synaptophysin	major synaptic vesicle protein p38	r	abcam	ab8049	(pre-) synapses	1:200
Gephyrin	gephyrin	r	synaptic systems	147111	(post-) synapses	1:200
K_V1.1	K_V1.1 channel, extracellular	r	almone labs	Apc161	K^+ channel	1:200

Expression on differentiation marker

To quantify the cells expressing certain differentiation markers, J1 NSCs were differentiated for ten days. Each day cells were fixed and stained for the markers nestin, DCX, MAP2, ß-tubulin3 and GFAP. The samples for each day were photographed with the same exposer time. Cells positive for the certain marker were counted manually and normalized on the total cell number. For each marker staining (only GFAP and ß-tubulin3 were double stained) at least 1000 cells were counted for each day, out of at least 3 individual experiments.

Apoptosis- Assay

Cells were seeded, differentiated and fixed on corresponding differentiation days. Antibody staining against cleaved caspase 3 was performed and cleaved caspase 3 positive cells were counted manually. For each data set at least 1200 cells were analysed in four individual experiments with variable cell passages.

To represent each differentiation step cells were fixed on differentiation day 2 (representing DI), differentiation day 4 (representing DII), differentiation day 7 (representing DIII) and differentiation day 9 (representing pD). Furthermore, undifferentiated cells were fixed.

Proliferation- Assay

Cells were seeded, differentiated and fixed on corresponding differentiation days. Antibody staining against Ki67 was performed and Ki67 positive cells were counted manually. Ki67 is a common marker for mitotic cells [133, 208], caused by the exclusive expression of protein Ki67 in actively proliferating cells. To estimate the growth fraction of the population, cells were seeded, differentiated and fixed

on corresponding differentiation days. Antibody staining against ki67 was performed and ki67 positive cells were counted semiautomatic using the programs imageJ based micromanager 1.4 and scanJ. For each data set at least 1200 cells were analysed in four individual experiments with variable cell passages.

To start differentiation undifferentiated cells were solved and centrifuged. The cell-pellet was resuspended in DI media and seeded on cell culture flasks. The first two days differentiating cells stay in DI media on differentiation day 3 cells were harvested again and centrifuged. The pellet was resuspended in DII media and seeded on laminin coated cell culture ware. The differentiating cells stay in media until differentiation day 5, for three days. On differentiation day 6 the media was changed to DIII media, for another three days. From differentiation day 9 on cells were cultured in pD media. To represent each differentiation step cells were fixed on differentiation day 2 (representing DI), differentiation day 4 (representing DII), differentiation day 7 (representing DIII) and differentiation day 9 (representing pD). Furthermore, undifferentiated cells were fixed.

Patch clamp recordings

For the electrophysiological measurements, the culture medium was removed and replaced by external bath solution containing (in mM) 4 KCl, 140 NaCl, 1 $MgCl_2$, 2 CaCl2, 5 D-Glucose, 10 HEPES /NaOH, pH 7.4. Microelectrodes were made from borosilicate glass capillary tubing using a vertical puller (PC-10, Narishige, Tokyo, Japan) with an open resistance between 8-12 MΩ. The intracellular solution contained (in mM) 50 KCl, 10 NaCl, 60 K-Fluoride 1 EGTA and 10 HEPES/KOH, pH 7.2. The currents were measured at room temperature and provoked with a standard pulse protocol consisting of a 500 ms long step from a holding voltage at -80 mV to 800 ms long test pulses between -140 mV and +60 mV and a 1500 ms long post-pulse at -80 mV. Solution exchange was executed manually by a pressurised-perfusion-system. Membrane currents of cells were recorded in the whole cell configuration (Hamill et al., 1981) with an EPC-7 amplifier (from Heka Electronic, Lambrecht, Germany) under the control of the WinWCP Software (University of Strathclyde, Glasgow, Scotland). Instantaneous currents were sampled 5 ms after onset of the test voltage; in this way the transient-capacitive current was eliminated from the current measurements. The steady-state currents were sampled at the end of the test pulses (usually at 800 ms), at which the slow outward rectifiers were close to their steady state. The time of data collection is indicated in the figures by symbols. Data were analyzed with WinWCP and IGOR software (Wavemetrics, Portland, USA).

On differentiation day 7 and differentiation day 9 it is possible to identify neuron by eye, data from these timepoints are estimated by selectively patching neurons.

Multi electrode array

To quantify membrane potential changes Multi Electrode Arrays (MEA) were used. Cells were seeded on laminin coated MEA chips on differentiation day three (1,2 Mio. Cells/ Chip). To let the cells attach to the ground, first measurements were performed on differentiation day four. During the differentiation measurements were taken at differentiation day eight, eleven, 15,18, 22 and 26. Two hour before measurement media was refreshed. Each measurement was taken over 120s, to avoid noise chips were placed in headstage five minutes before starting. All measurements were performed at 37°C.

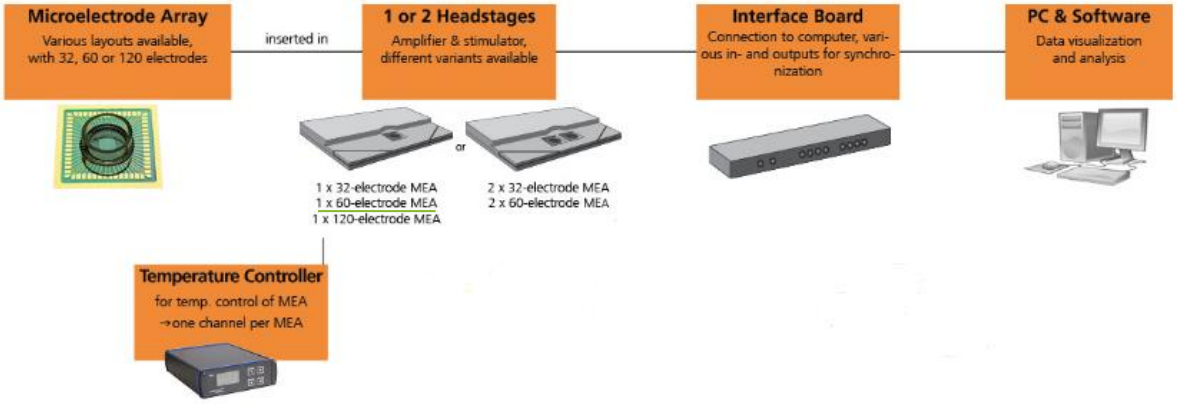

Figure 6 Organization of the MEA 2100 setup used, composed of a 60 electrode MEA-chip, one headstage, connected to temperature controller and interface board; modified from multichannelsystems.de

Parameters for measurement were determined in various pre-experiments. For all results the electrode layout „60MEA200/10iR-Ti“was used, with a sampling rate of 20.000 Hz. To document spontaneous activity spike detector was employed, as threshold the -5x standard deviation of the noise signal of every channel was set.

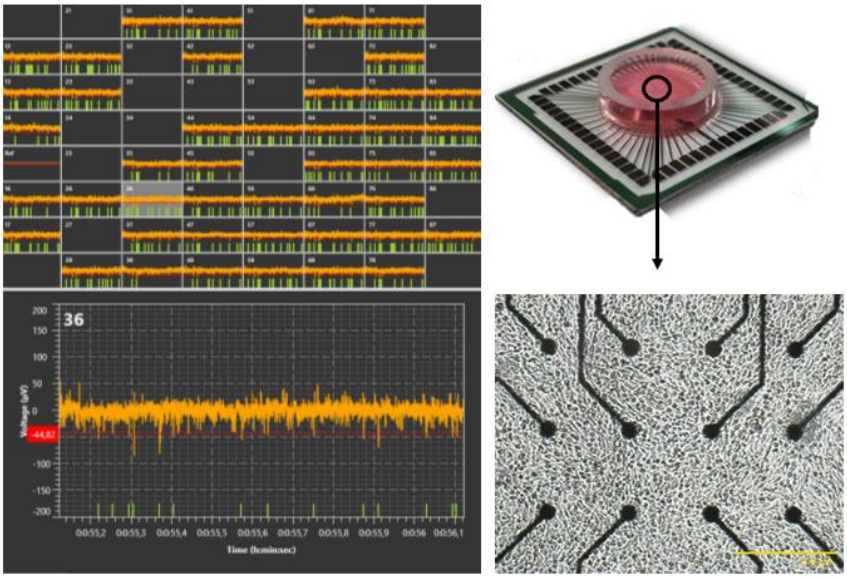

Figure 7 Exemplary presentation of a MEA measurement on differentiation day 4 (left) shown are raw data monitored in spike detector tool with an individual threshold of the -5x standard deviation of the noise signal of each channel, green bars mark detected events in each channel. Results of electrode 36 are depicted enhanced on the lower left. the pictures on the right show a MEA-chip and the cultured cells in the middle of the MEA-chip below (scalebar 250µm).

For data evaluation, multichannel data suite was used to transfer data files into .NEX format. The transformed data was edited in Neuroexplorer 5 version to readout spike detector data and distinguish between signal and noise. Collected data were normalized on first measurement (day 4) per chip. For the scatterplots the detected spikes in each channel were correlated to the timestamp.

4.3. Results

4.3.1. Immunostainings for the expression of marker proteins during J1 NSC differentiation

Neurons, astrocytes, progenitors and stem cells differ in the expression of proteins. Some of these proteins are characteristic for the initiation of a specific differentiation state, these proteins are often used as markers in differentiation studies. To monitor the marker protein expression, we checked for the major marker proteins during the used differentiation protocol. The cells were fixed in self-renewal state and after initiation of differentiation each day for ten days. All samples were stained for the stem and progenitor marker nestin, the progenitor marker DCX, the astrocyte marker GFAP, the neuron markers MAP2 and ßTub3 (**Figure 8**).

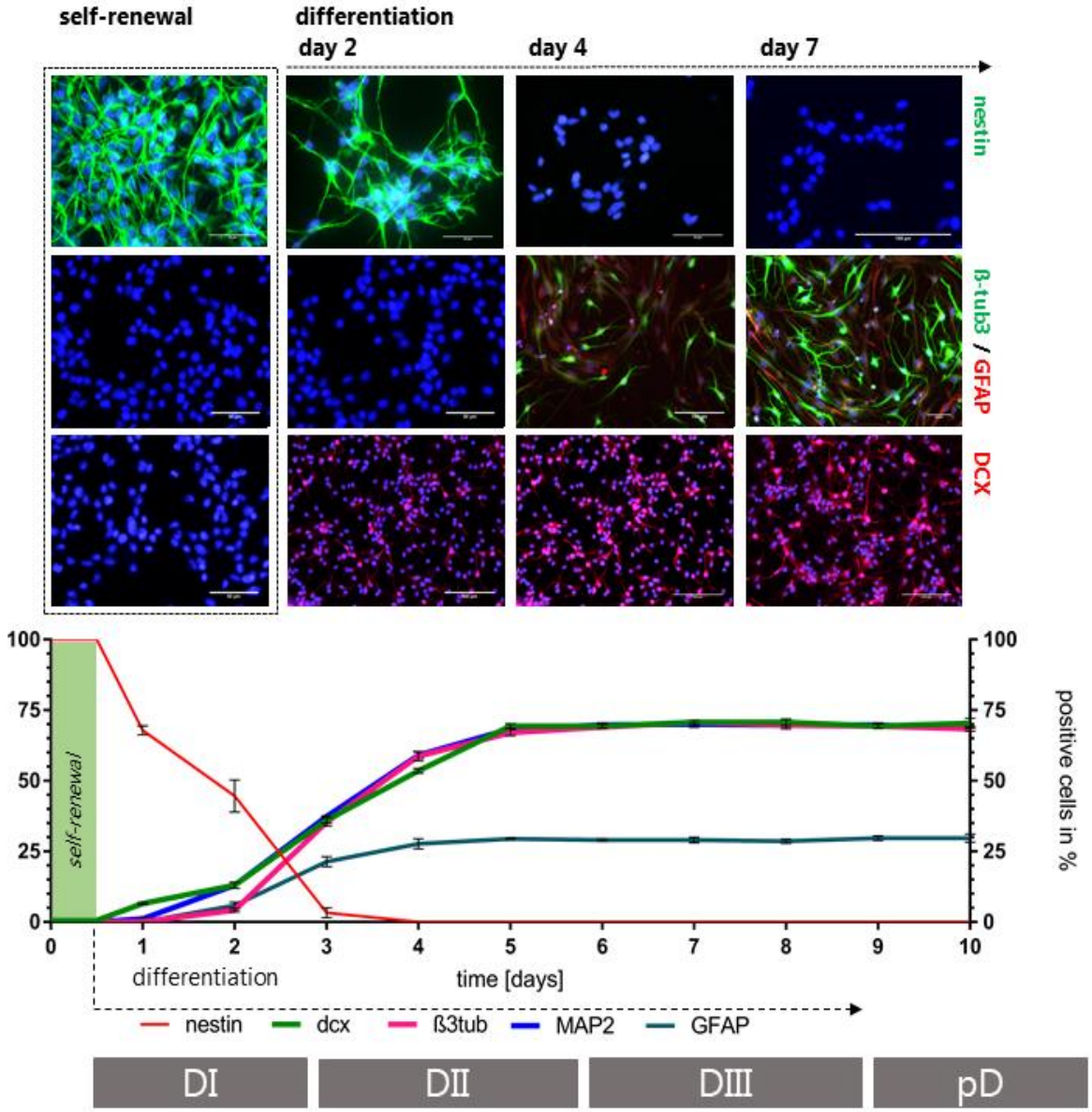

Figure 8 Expression of marker proteins in differentiating J1 NSCs. To distinguish differentiation stages, we analysed the expression of the differentiation markers DCX, ß Tub 3, MAP2, GFAP and the stem cell marker nestin. J1 NSC in self-renewal media and after media induced differentiation were fixed and stained for marker proteins via antibody staining. J1 NSCs were differentiated for 10 days, fixing samples of each day, exemplary photos shown above. On each day cells positive for each marker, were counted and normalized on total cell number (below) plotted are mean with SD. For each marker staining (only GFAP and ß Tub 3 were double stained) at least 1000 cells were counted for each day, out of at least 3 individual experiments. Cell cores were stained using DAPI. Scalebar 50µm.

As shown in **Figure 8** J1 NSCs kept in self-renewal media express homogenously the stem cell marker nestin. In this state no cells positive for the astrocyte marker GFAP and the neuron markers ß Tub3 or MAP2 are detectable. We could confirm these result, published by Conti [191]. The dominant marker for undifferentiated J1 NSCs nestin is detected in 100% of the cells. Only below 1% of cells cultured in self- renewal media are also DCX positive. According to Conti, 2005 [191] differentiation is initialized by reseeding J1 NSCs in EGF free media (media DI). We checked for the first time 12h after initiation of differentiation (day 1) for the expression of marker proteins in the differentiation progress. Nestin is not expressed homogenously anymore on day 1, 67% of the population are positive for nestin, decreasing to 44% on day 2 and 4% on day 3. After differentiation day 3 no cells positive for nestin were detected.

DCX is the first differentiation marker appearing in neural differentiation. With induced differentiation we could find an increase to 6% in the DCX positive subpoplulation. On day 2, 13% of the cells are positive for DCX, raising to 36% on day 3, continuous increasing to a maximum of ~70% on day 5. From day 5 to 10 70% of the cells show a DCX expression.

MAP2 and ßTub3 are markers for neuronal progenitors and neurons, labelling dendrites (MAP2) and axons (ßTub3). We could detect cells positive for MAP2 for the first time on day 2 in 13% of the population. The percentage of cells expressing MAP2 raises until day 5, with 37% on day 3, 62% on day 4 and 70% on day 5. From day 5 to day 10 no differences in the relative number of cells expressing MAP2 were observed. The expression of ßTub3 shows a related distribution over the differentiation course, first detected on differentiation day 2 (4.3%), the ratio of cells positive for ßTub3 raises to 35% on day 3, reaching its maximum on day 5 with ~72%. Like MAP2, ßTub3 is stable expressed by 70% of the population until day 10.

GFAP labels glial progenitors and astrocytes, during J1 differentiation it is first time detected on day 2 in 6% of the cells. The GFAP positive population raises continuous until day 4 (28%) and reaches a maximum of 31% on day 5, stable detected until day 10.

In **Figure 8** we could confirm induced differentiation throughout shifts in the expression of nestin and DCX in the cell population 12h after initiation. From day 4 on, no nestin positive cells could be detected, indicating that with induced differentiation no subpopulation remains undifferentiated and that all cells reached a post mitotic status on day 4. The expression of the differentiation markers DCX, MAP2, ßTub3 and GFAP rises until day 5. Around 70% of the cell population express neuron specific markers (MAP2, ßTub3), while ~30% are positive for the astrocyte marker GFAP from day 5 on. The stable expression until day 10, indicates that the differentiation process regarding the expression of marker proteins is determined from day 5 on. The loss of nestin expression and the spreading expression of neuron and astrocyte specific proteins between differentiation day 3 and 5, reveals that the **fate specification** of differentiating J1 NSCs takes place in this period, resulting in 70% neurons and 30% astrocytes.

In the course of the experiment we also checked for oligodendrocytes, using Olig3 as marker. Below 0.3% of the cells expressed Olig3 tested on differentiation day 6 and 9. Concerning that at least 99.7% of the population differentiates to astrocytes and neurons.

Following the expression of structure associated marker proteins, the extending morphology of the differentiating cells was noticed (see **Figure 8**). The morphological changes during the differentiation protocol are analysed in detail in the following part (4.3.2).

4.3.2. **Morphological changes during J1 differentiation**

The specification of neural stem cells to functional neurons and astrocytes accompanied by the composition of a highly specialised morphology. Beside the specialised proteome pattern also the morphology changes suitable to specific requirements, mainly characterized by growing extensions and intra cellular linking. The appearance of neural stem cells differs clearly form neurons, astrocytes and oligodendrocytes, but also during differentiation typical morphologies are passed (see **Figure 3** and **Figure 4**). The appearance of differentiating cells changes and shows characteristic shapes depending on differentiation phase which makes it is possible to derive differentiation status by the cell morphology. To follow the morphology of J1 NSCs we used a light microscope and photographed each differentiation day for 10 days with a 40x magnification.

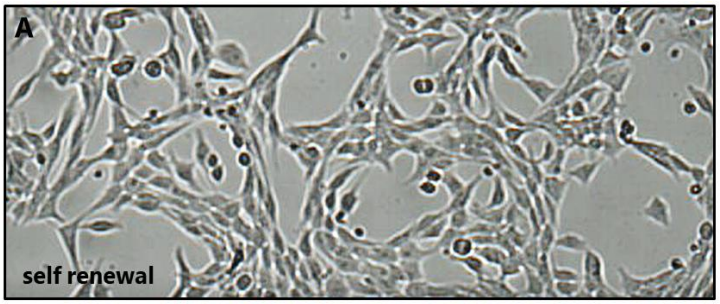

A) J1 NSCs cultured in self-renewal media. The attached cells show a flat, plumb morphology with several rounded, proliferating cells.

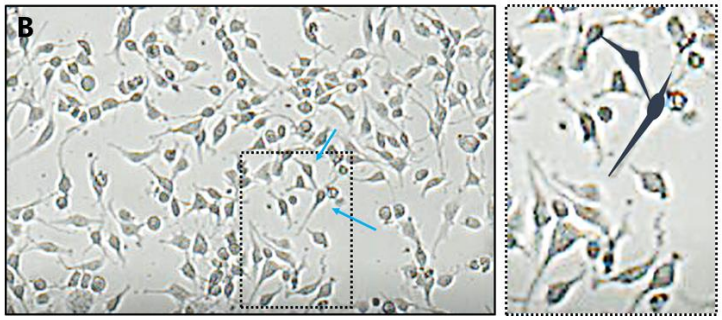

B) J1 NSCs in the first differentiation step, 12h after initiation of differentiation. The cells appear thinner with apical dendrites on opposite sides which leads to the spindle like look (arrows), enlarged on the right. Rounded proliferating cells are recognizable.

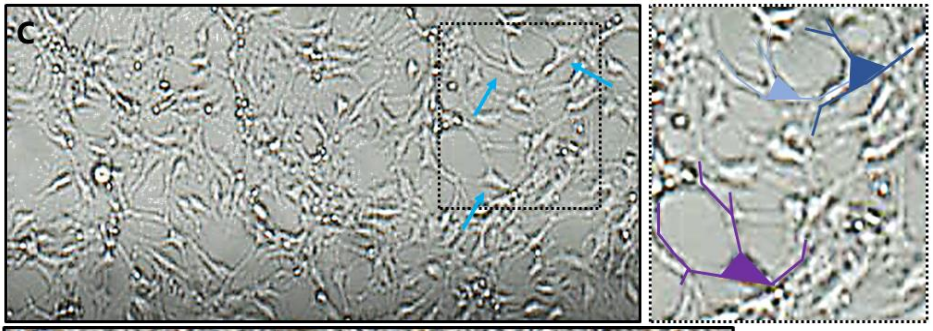

C) J1 NSCs on differentiation day 3, show first cellular extensions. Mostly cells with a pyramidal shape are observed (Arrows), enlarged on the right.

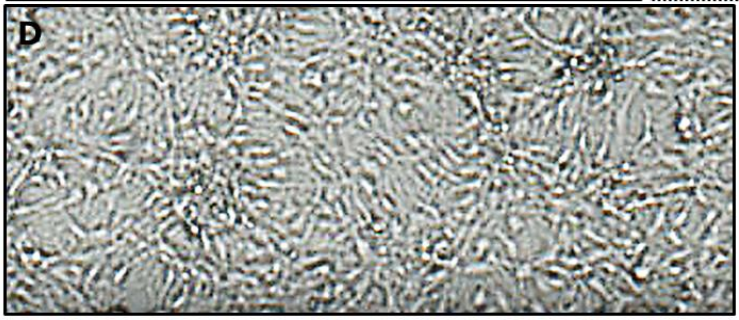

D) On differentiation day 5, all cells show a clear growth in cellular extensions. The cells are highly cross linked, so that single cells are not distinguishable anymore.

Figure 9 Morphology analyses of J1 cells during differentiation, on differentiation day 1, 3 and 5. a) Typical morphology of J1 in self-renewal state and on the first differentiation day (**b).** J1 morphology on third and fifth differentiation day (**c & d)**. To follow morphological changes during differentiation pictures were taken 12h after initializing differentiation (**b**), differentiation day 3 (**c**) and differentiation day 5 (**d**), using a light microscope with 40x magnification.

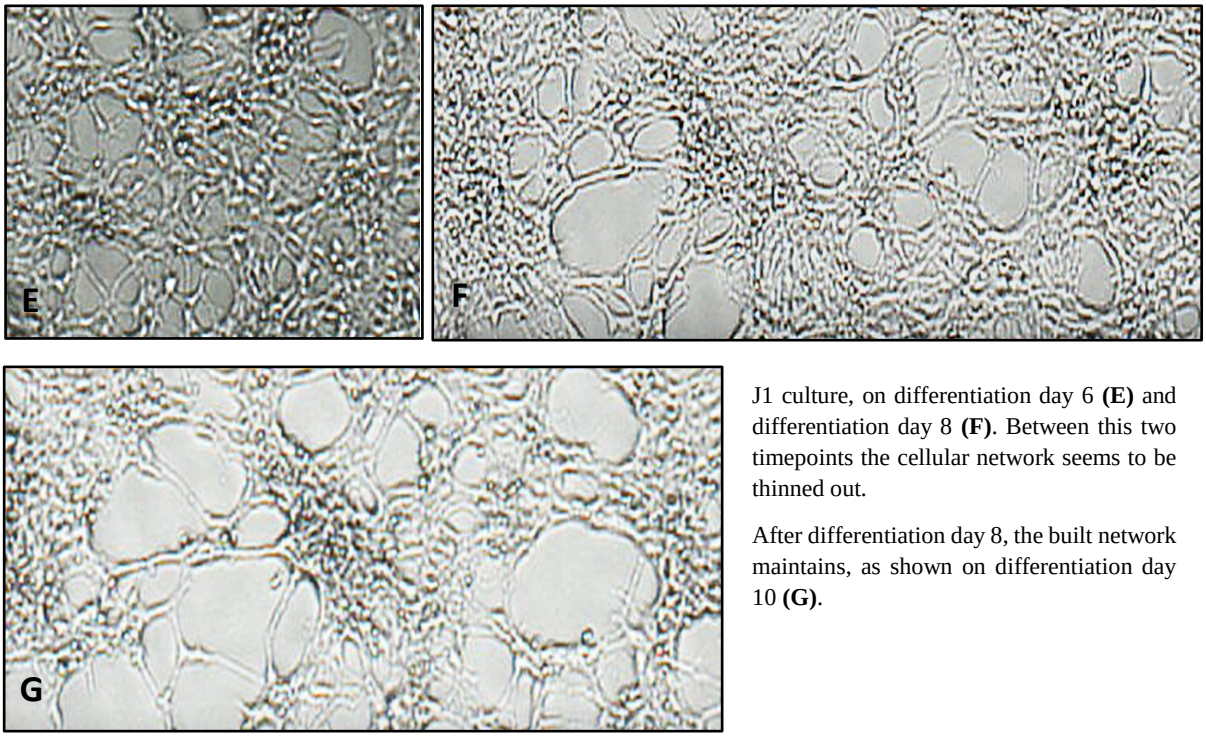

J1 culture, on differentiation day 6 **(E)** and differentiation day 8 **(F)**. Between this two timepoints the cellular network seems to be thinned out.

After differentiation day 8, the built network maintains, as shown on differentiation day 10 **(G)**.

Figure 10 Morphology analyses of J1 cells during differentiation, on differentiation day 6, 8 and 10. e) Typical morphology of J1 culture on differentiation day 6, 8 (**f)** and 10 **(g).** The shown pictures were taken using a light microscope with 40x magnification.

Figure 9 and **Figure 10** show a clear change in the morphology of J1 cells in self renewal and induced differentiation. In the self-renewal state, the adhered J1NSCs resemble a flat, laminar morphology. Proliferating cells can be easyly spotted by their cicular shape (**Figure 9 a**). 12h post induced differentiation, J1 show a clearly changed cell morphology presenting a spindle like shape. The cellbody appears thinner and spread along the two extensions on the opposite sides (**Figure 9 b**). This spindle morpholoy is typical for proliferating early progenitors shown in **Figure 3** and **Figure 4**, suggesting that J1 cells on differentiation day 1 represents early progenitors status on morphological level. Early progenitors are also characterised by the experssion of the marker protein nestin, which is expressed in J1 cells on differntiation day 1 (see **Figure 8**).

After this time the cells are reseeded on laminin coated surfaces, which simulates migration to laminin presenting target cells. Laminin coating is nessesary for the adheasion and survival of the J1 cells in further differentiation [191]. Sustained by differentiation media DII the apperance of the cells changes from spindle-like to pyramidal. Most J1 cells on differentiation day 3 envolve three extensions per cell, the drawn-out cellbody along the extensions leads to the pyramidal look (**Figure 9 c**). In neural differentiation the pyramidal shape is determined by an apical axon and lateral dendrides developing in futur neurons (see **Figure 3**). As shown in **Figure 8** J1 NSCs start developing dendrites and axons, shown by the dendrite marker MAP2 and the axon and dendrite marker ß tubulin 3. This suggests that the pyramidal shaped cells on differntiation day 3, as shown in **Figure 9 c,** are neuronal progenitors with growing axons and dendrites. In the next two days the extensions grow longer and cross link with each other (also shown in ßtub3 and GFAP staining in **Figure 8**). This step could be characterised as fate specification phase in earlier experiments (**Figure 8**). The observed morphology mirrors the reconstruction from early progenitors to neurons, characterised by axonal and dendritic growth and branching. At differntiation day 5 the cells are strongly linked, so that single cells can not be distinguished from each other (**Figure 9 d**). From this time on the built network gets so dense that it is

not possible to follow individual cell morphology. In the following days of the differentiation protocol, the morphology of the built network changes again. Over the time of differentiation day 6 to 8 the network seems to thin out (**Figure 10e & f**) and reaches a morphological stable state after day 8, as shown in **Figure 10 (f & g)**. This indicats that the differentiation is not determined. The so called programmed cell death is a late event in neuronal differentiation, which could cause the observed thinning. This has to be investigated in further experiments monitoring apoptosis. From day 8 on the evolved neuronal network seems stable. It consists of grouped cells, with long connected axons and dendrits. Extensions of different cells link parallel to each other, which leads to thicker strands forming a connection between cell groups.

Following the differentiation of J1 cells, we could identify typical morphological characteristics of neural differentiation. We could identify spindel shaped cells, characteristic for early progenitors on differentiation day 1, followed by growing cellular extensions, leading to a pyramidal shape on day 3, typical for neuronal progenitors (see also **Figure 4**). The relative homogenous cell morphology on day 1 and 3 leads to the suggestion that J1 cells display a synchronaised differntiation progression. From day 5 on increased growth in cellular extensions was observed, making it challenging to identify induvidual cells. Nevertheless, we recognized a thinnig in the built up network between differntiation day 6 and 8, which could be caused by synaptic induced apoptosis, a late differentiation event.

4.3.3. **Proliferative and post mitotic stages during J1 differentiation**

Proliferation only takes place at the beginning of neural differentiation (**Figure 3**, **Figure 4**). Beside the self-renewal of NSCs, only early progenitors pass the cell cycle for a limited number of times. After this amplification phase the progenitors are post mitotic, entering further differentiation phases. To check if and when proliferation appeared in the used differentiation protocol, ki67 antibody staining was used. The stem and progenitor marker nestin is characteristic for proliferating NSCs, although nestin could be shortly detected in postmitotic progenitors [122]. Orientated on the nestin expression (**Figure 8**) J1 cells are expected to leave the cell cycle between differentiation day 1 and 3.

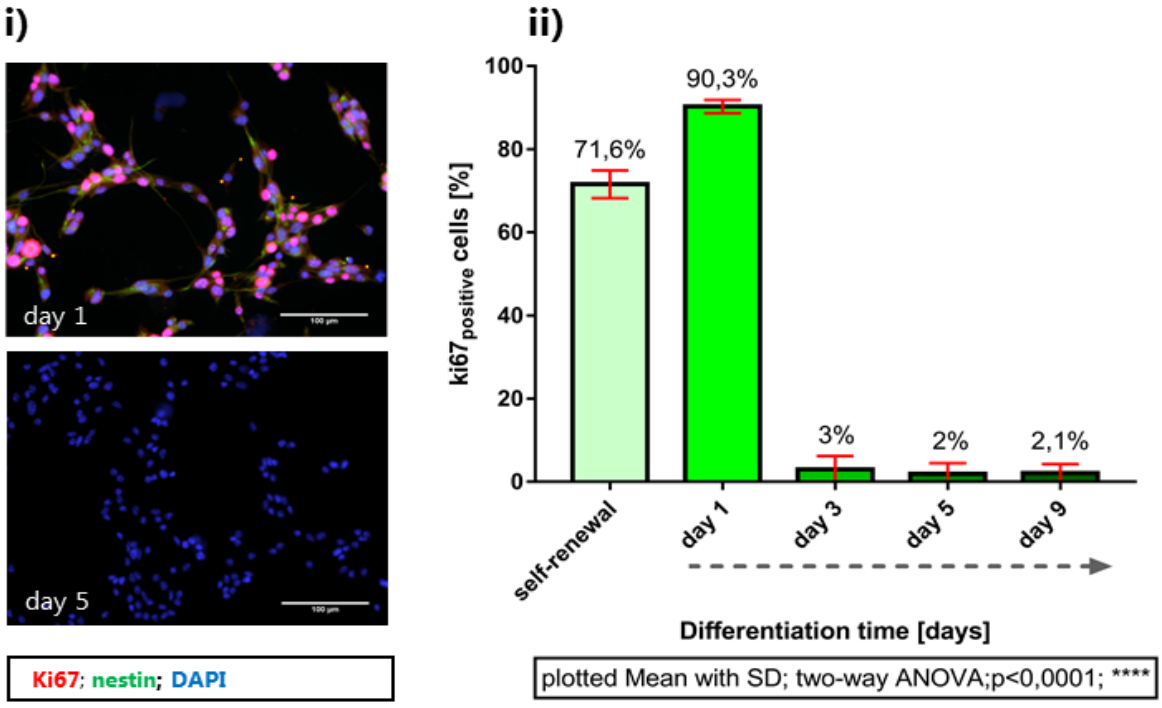

Figure 11 mitotic active cells during J1 differentiation. **i**) exemplary pictures of ki67 and nestin labelling on differentiation day 1 and 5 in J1 NSCs (scalebar 100µm). (**ii**) Using antibody staining again the mitotic cell marker ki67 the percentage of proliferating cells was estimated in self-renewal state and on differentiation day 1,3,5 and 9.

Undifferentiated cells show a ki67 positive fraction of around 72%, initialized differentiation (day 1) increases the growth fraction to 90% and decreases rapidly below 3% (day 3) in the following differentiation days. The growth fraction keeps on a minimum ($\leq$ 3%) in the ongoing differentiation time. While the first two timepoints (self-renewal and differentiation day 1) show stable results, the later timepoints (differentiation day 3,5,9) show variable results represented in tall standard deviations. This and the manual inspection of the staining suggests that this could be measurement error. Additional experiments using EdU labelling verified this suggestion, no EdU positive cells could be found from differentiation day 3 on (data not shown).

It could be clearly shown that J1 NSCs in self-renewal and on the first differentiation day are in a proliferating state. From differentiation day 3 on the J1 cells are post mitotic. The increased mitotic fraction on differentiation day 1, correlated with the nestin expression shown in **Figure 8** , suggesting that the first two day of the differentiation protocol mirrors the amplification phase in early neural differentiation. On differentiation day 3 J1 cells are post mitotic and lost the expression of the stem cell/progenitor marker nestin, indicating that the amplification phase is completed.

Based on the results from **Figure 8** and **Figure 11** J1 cells in the first two differentiation days can be characterized as **early progenitors**, expressing nestin and passing a high proliferative amplification phase. This step is followed by a phase where increasing cell numbers of fate specific marker positive cells are detectable (**Figure 8** & **Figure 11**). Between day 3 and 5 the fate specification increases over the whole cell population, showing 70% of the cells expressing neuron specific markers (MAP2, ßtub3) and 30% expressing the astrocyte specific marker (GFAP) on day 5. The post-mitotic state of the cells confirms the suggestion that differentiation day 3 to day 5 represents the second differentiation step,

the **fate specification** in differentiating J1 cells. The fate specification phase is followed by the cell maturation, the final differentiation phase in neural differentiation characterised by functional maturation and induced apoptosis, the so called programmed cell death.

4.3.4. **Programmed cell death in J1 differntiation**

The previous morphological study showed a thinning of the built-up network between differentiation day 6 and 8, which could be caused by apoptosis. In later differentiation apoptosis is a programmed event to sort out odd new progenitors (**Figure 4**). In the following experiment the apoptosis rate was determined over in differentiation J1 cells. To quantify the apoptotic fraction, cleaved caspase 3 antibody staining was used. Caspase 3 is activated by apoptotic signalling and cleaved into two subunits which can be detected via antibody staining for cleaved caspase 3.

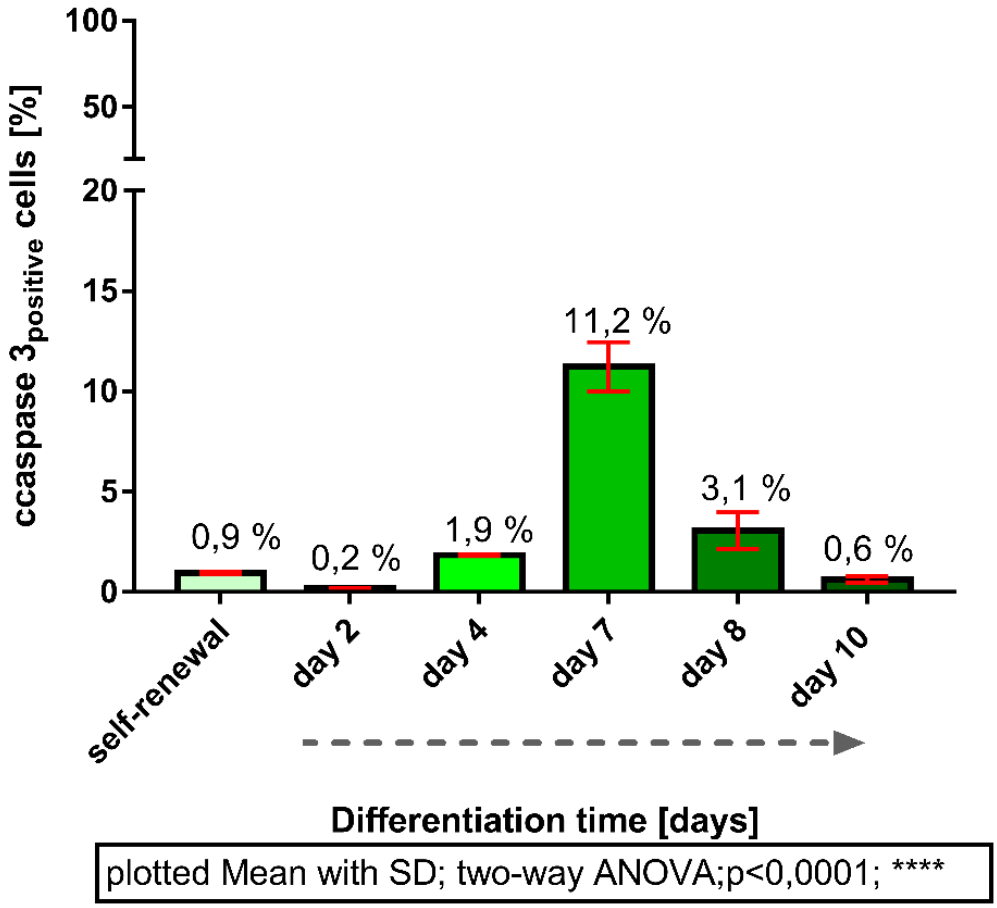

Figure 12 Apoptotic fraction of J1 cells during differentiation. Estimated via cleaved caspase 3 staining on differentiation day 2,4,7,8,10 and in self-renewal state. The highest apoptotic fraction occurs on day 7 with 11.2% and decreases to 3.1% on differentiation day 8. Undifferentiated cells show a distinct lower apoptosis rate with 1%, also day 2,4 and 10 show lower apoptotic fractions with 0.2% on day 2, 1.9% on differentiation day 4 and 0.6% on day 10.

The apoptosis rate during the differentiation protocol stays on a low level below 2% until differentiation day 7-8. On differentiation day 7 over 11% of the cells show apoptotic signalling, which decreases to 3.1% one day later. On day 10 the apoptotic fraction reaches a low level of 0.6% again. The temporally determined and stable apoptotic wave indicates differentiation induced apoptotic signalling reaching the maximum on differentiation day 7. This apoptotic wave represents the

programmed cell death, a differentiation event linked with synaptogenesis in maturating neurons [30, 40, 88, 115, 174, 206, 209, 210].

The results from **Figure 12** suggest that the differentiation phase from day 7 to 8 represents the **maturation** of young neurons and astrocytes, the final differentiation event (see **Figure 3**) in neuronal differentiation. To investigate this suggestion further analyses on a functional level were performed within the J1 differentiation.

4.3.5. **Functional differentiation markers in J1 differentiation**

Resting membrane potential changes in J1 differentiation

The resting membrane potential (V_R) is the base of the electro-biophysical functionality of individual cells, the V_R can also be used as a functional marker during neuronal differentiation. To estimates if the J1 model system also displays a functional differentiation, functional markers as V_R were analysed.

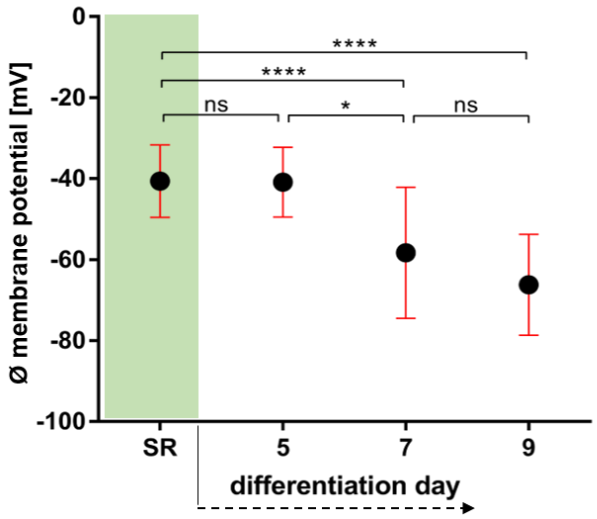

	Ø membrane potential [mV]	SD	n
self-renewal	-40.65	8.95	67
differentiation:			
day 5	-40.9	8.65	10
day 7	-58.3	16.23	6
day 9	-66.24	12.5	15

Figure 13 Identified resting membrane potential of J1 in self-renewal and during differentiation (day 5, day 7, day 9), measured via patch clamp by Dr. Bastian Roth. Tabularly summary of the mean VR of J1 cells in self-renewal and on differentiation day 5, 7 and 9, plotted mean with SD, for statistics unpaired t-test was used (ns: $p > 0.05$; * $p \leq 0{,}05$; *** $p<0.001$; **** $p<0.0001$).

Changes in the V_R has been correlated with progression in the neuronal differentiation and can used as basal functional marker [97]. Estimated in self-renewal state J1 NSCs show a relative low negative membrane potential of -40mV. During the three-stepped differentiation protocol the differentiated cells show a continuous shift to more negative membrane potentials. While the membrane potential on differentiating day 5 (-40.9mV) is similar to the measured membrane potential in self-renewal state (-40.7mV), the membrane potential on differentiation day 7 (-58.3mV) is significantly lowered. On differentiation day 9 the quantified V_R is -66.2 mV, representing the typical membrane potential of neurons (-65mV). This data corresponds to previously published *in vivo* measurements of neurons [211]. NSCs in the adult brain show a V_R of -55 to -40 mV [149-151], also corresponding to the measured results (-40.65mV in self-renewal state). The more negative V_R in post mitotic differentiation is

suggested to be mainly caused by the down regulation of K_{ir} channels. Beside K_{ir} expression, K_{DR}, K_A and Na_v channel expression is restricted to specific differentiation phases, making them suitable as functional differentiation markers.

Expression of characteristic ion channels in J1 differentiation

Neural differentiation goes along with specified ion channel expression, rearrangement and trafficking. Specified potassium channels expression is known to occur during neurogenesis and characterised (see **Figure 4**). In his work, my colleague, Dr. Bastian Roth characterised the functional expression of characteristic ion channels in the used J1 NSCs differentiation protocol via patch clamp recordings. The individual channel types were identified by using specific blockers or regarding specific kinetic characteristics.

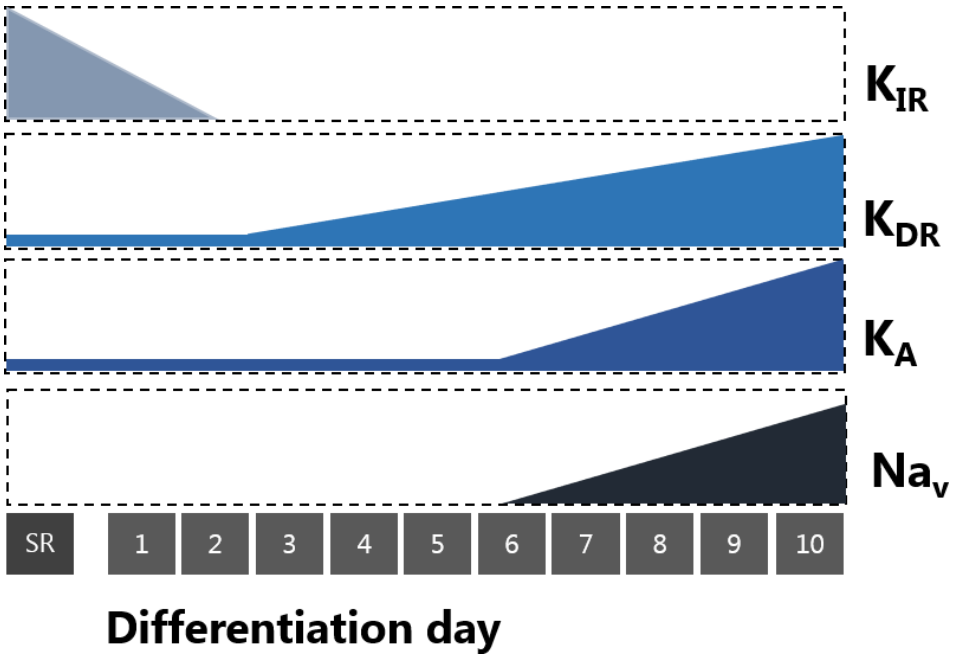

Figure 14 Identified ion channel families and relative quantification during J1 differentiation. Overview of identified ion channel families in self-renewing J1 NSCs and over ten days of differentiation. The results are provided from Dr. Bastian Roth, showing the occurrence of the ion channel types K_{ir}, K_{DR}, K_A and NA_v. in self-renewing J1 NSCs and induced differentiation. The channel typic currents were normalised on their maximum strength and schematic illustrated over the differentiation time course.

In his work Dr. Bastian Roth could identify inward-rectifying K^+ channels (K_{IR}) in self-renewing J1 NSCs, deceasing with induced differentiation. K_{IR} channel specific currents are detectable until differentiation day 3. Delayed-rectifier-type and A-type K^+ channels (K_{DR}, K_A) are detectable to all timepoints, K_{DR} currents increase from day 3 on, K_A currents increase from differentiation day 6 on.

Beside potassium channels Bastian Roth could identify voltage-gated sodium channel (Na_v) activity from day 6 on, increasing in the following differentiation days. Na_v channels are required for the synaptic development, indicating that synaptogenesis could be initialised from day 6 on. The identified channel expression profile strongly correlated with published studies of functional differentiation markers [97] and displays the major ion channel types involved in functional neuronal differentiation (see also **Figure 4**).

Synaptic protein expression in J1 differentiation

The previous results show a functional differentiation regarding ion channels. In the following experiments synapse formation during neuronal differentiation is focused. Synaptogenesis starts with the cell maturation phase in neural differentiation. Depending on successful axon connections, presynaptic proteins form an active plate, which stimulates postsynaptic protein recruitment and synaptic adhesion resulting in synapse formation [110].To check if pre- and post-synaptic sides are developed in our differentiation protocol, we stained J1 cells for PSD95 and Synaptophysin during differentiation. Since axonal and dendritic connections are the base for the generation of synapses we focused of timepoints later than differentiation day 4. As shown in **Figure 8** dendritic and axonal growth starts at differentiation day 3, while the linking between the cells increase in the following days as shown in morphological studies in **Figure 9** and **Figure 10**.

Beside the pre- and post-synaptic markers synaptophysin and PSD95, we labelled for gephyrin a postsynaptic marker for inhibitory synapses[147, 148]. PSD95 is expressed in excitatory glutamatergic synapses [212].

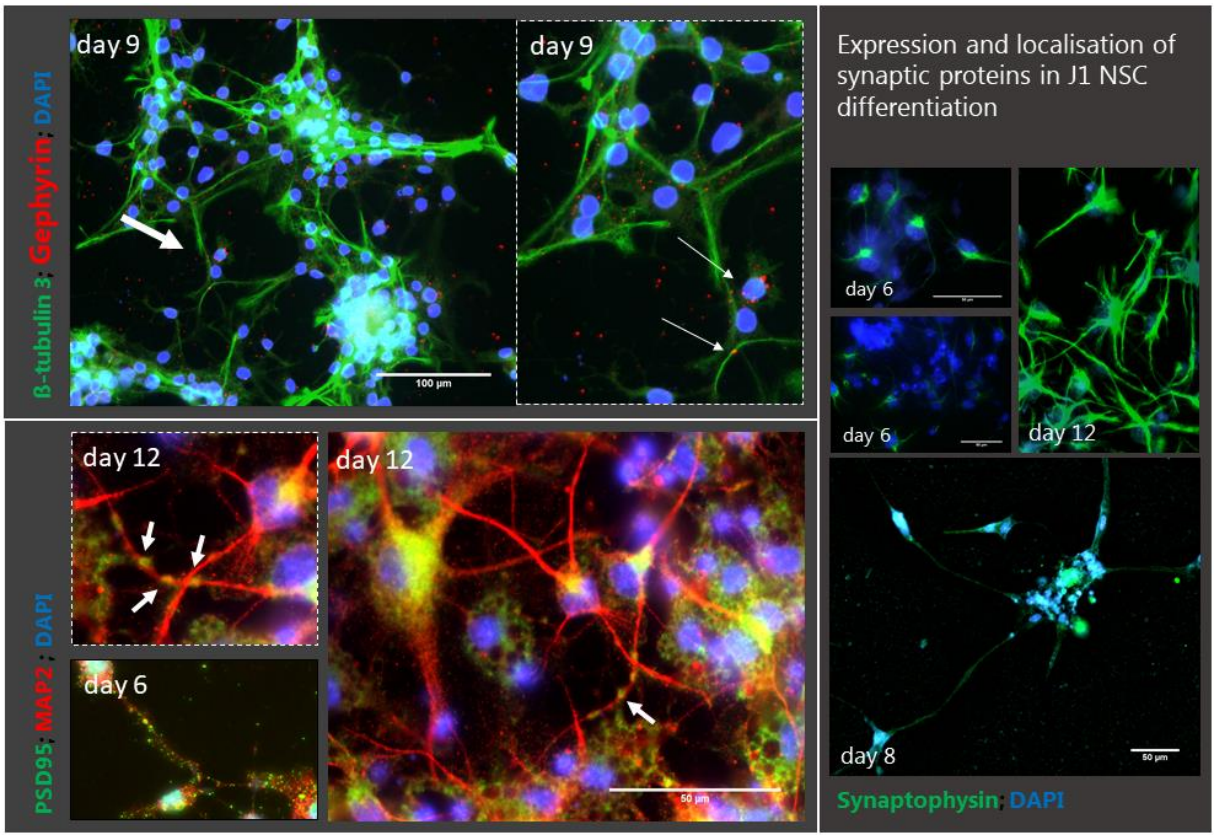

Figure 15 Expression and localization of the synaptic markers synaptophysin, PSD95 and gephyrin in J1 differentiation. **Top left**: The inhibitory postsynaptic marker gephyrin is detectable in J1 cells expressing ß-tubulin 3. On differentiation day 9 gephyrin is located along dendrite endings and around the core. **Bottom left**: The excitatory postsynaptic marker PSD95 in J1 expressing MAP2. PSD95 is detectable on differentiation day 6, localised in clusters along dendrites and axons and around the core in J1 cells. On differentiation day 12 PSD95 clusters are spread along neuronal dendrites. **Right**: the presynaptic marker synaptophysin is expressed on differentiation day 6, mainly localised around the core and less along axons. On differentiation day 8 the localisation is spread along the axons, gaining in intensity on differentiation day 12.

As shown in **Figure 15**, the used differentiation protocol allows the expression of post- and pre-synaptic markers, as well inhibitory and excitatory synapse markers. On differentiation day 6 PSD95 as well as synaptophysin are localised mainly around the cell core. In the following days the density of PSD95 and synaptophysin in the cell extensions rises (data not shown) reaching a stable status on day 12. The expression of the inhibitory postsynaptic marker gephyrin is only detectable in few cells and on a low level, which makes it hard to follow. The first expression of gephyrin was detected on differentiation day 7, localised around the core (data not shown) suggesting that protein expression starts. In the following days more and more gephyrin can be found in dendritic endings, reaching a stable distribution on differentiation day 9.

Nevertheless, it could be shown that pre- and post-synaptic proteins are expressed in J1 NSCs, a basal criterion for synapse formation. The synthesis of these synaptic proteins starts on differentiation day 6, indicating the beginning of the **cell maturation phase** in neuronal differentiation. The rising distribution along axons and dendrites could be owed to contact induced protein recruitment, the first step in synaptogenesis. Correlated with the occurrence of Na_v channels from day 6 on (**Figure 14**) the data suggest initiation of functional synaptogenesis from day 6 on.

We tried to quantify the number of excitatory and inhibitory neurons, which was very challenging because of the entangled dendrites and the low signals for gephyrin. Counted on day 10 we could estimate 17-22% neurons expressing gephyrin and 72-86% neurons expressing PSD95 in the cultured network. The labelling of synaptic markers shows clearly that neural differentiation is not determined of differentiation day 5, but the transition to the **maturation phase** in neural differentiation. To determine the length of maturating and to check if the expression of synaptic proteins actual leads to functional synapses multi electrode arrays were used.

Spontaneous activity in J1 differentiation

While the V_R and specific ion channel expression represents the functional differentiation of individual cells, there is no information about the network activity, neither synaptic activity. During differentiation maturating cells connect and later synapses lead to an organised excitability in the neural network. The electro-biophysical up growth is mediated by spontaneously membrane potential changes, which grow into coordinated network activity modulated by synaptic activity.

To follow spontaneous activity, multi electrode chips were used. These chips are equipped with 60 electrodes on the surface (59 measuring electrodes, 1 reference electrode) which allow extra-cellular recordings of the differentiating cells. To document spontaneous activity, spike detector was employed, as threshold the -5x standard deviation of the noise signal of every channel was set.

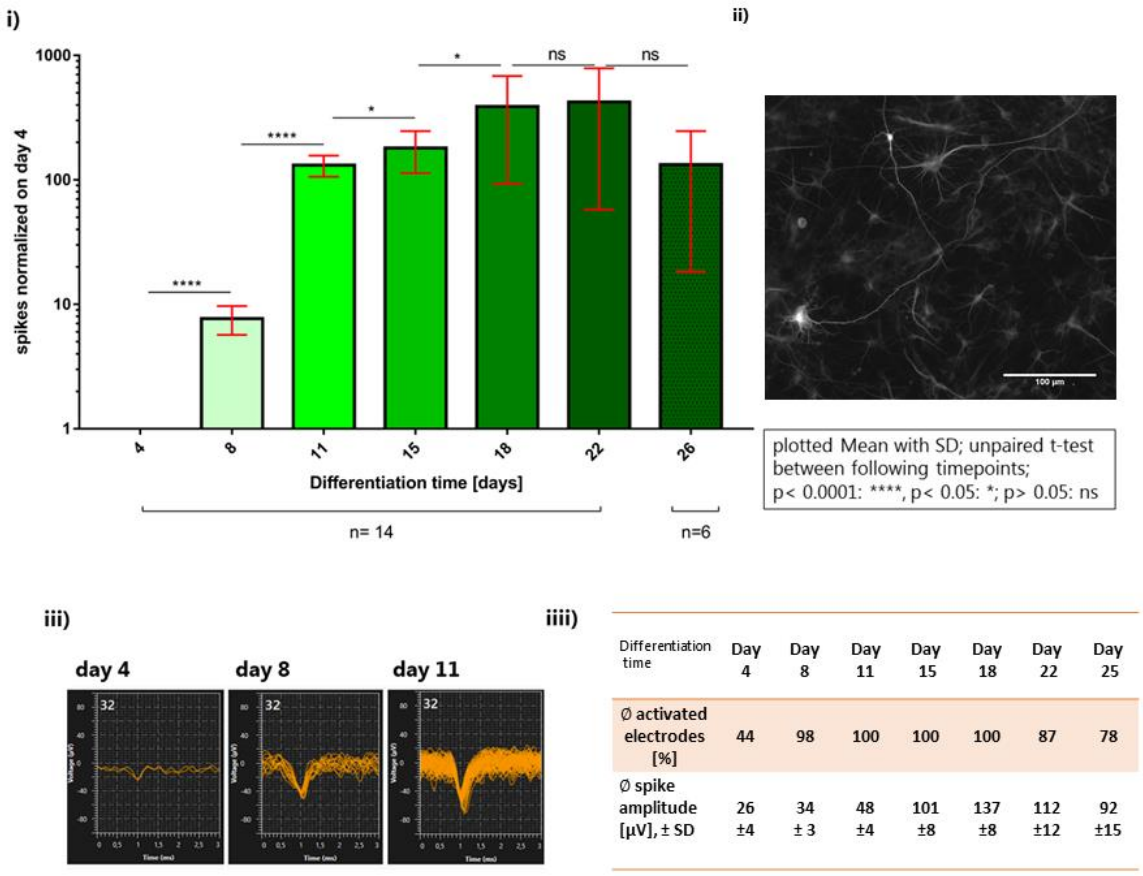

Differentiation time	Day 4	Day 8	Day 11	Day 15	Day 18	Day 22	Day 25
Ø activated electrodes [%]	44	98	100	100	100	87	78
Ø spike amplitude [µV], ± SD	26 ±4	34 ± 3	48 ±4	101 ±8	137 ±8	112 ±12	92 ±15

Figure 16 Spontaneous activity analyses in J1 differentiation, using MEA. i) Spontaneous activity detected via spike detector within 120s, on differentiation day 4,8,11,15,18, 22 and 26. Counted spikes were normalized on the number of estimated spikes on day 4 of each MEA-chip. In all measurements no external stimulus was used, all counted spikes are spontaneously generated. **ii)** exemplarity picture of J1 cells differentiated in MEA chip, on differentiation day 11 labelled with ß Tubulin 3. Scalebar 100µm. **iii)** Overlay of the spike kinetic of electrode 32 in a MEA chip detected over a time of 10 seconds on differentiation day 4,8 and 11 **iiii)** overview of % activated electrodes and average spike amplitude [µV] of the collected measurements (results **i-iii** provided by Selina Kahl).

Via the spike detector tool, used in the MEA measurements, all voltage changes bigger than the -5x standard deviation of the noise signal of every channel were counted. This threshold was estimated in pre-experiments and is represented in literature [213]. The counted spikes were normalized on the number of measured spikes on day 4 for every individual MEA-chip. As shown in **Figure 16 i)** the number of detected spikes increased significant from differentiation day 4 to day 18. Especially from day 4 to day 8 and day 8 to day 11 the counted events increased 10-fold. From day 11 on the increase in the spontaneous activity reduces and results in a decrease starting on day 22, which can be explained by the loss of viable cell cultured in MEA chips. **Figure 16 iii)** shows an overlay of the kinetics of detected spikes within 10s on electrode 32 in one MEA chip, representing that the amplitude of the detected spikes increases from -25µV (day 4), -58µV (day 8) to a maximal amplitude of –73µV (day 11). This can also be seen in **iiii)**, the average amplitude height of all detected spikes grows until day 18, where it reaches the maximum of 137µV. Corresponding to this the percentage of activated electrodes of a MEA-chip raises, reaching ~ 100% on day 8. From day 8 to day 18 all measuring electrodes of a chip detected at least one event over the measured time of 2 minutes.

These results point out that J1 cells reach a higher excitability over the differentiation time, mirrored in increasing spontaneous activity [113]. The main increase in the number of spikes is between differentiation day 4 and 11. The percentage of activated electrodes on the individual measuring days shows the distribution of the spontaneous activity over the network. On differentiation day 8 ~ 100% of the electrodes are activated, indicating that the majority of cells in the network are in an excitable, spontaneous active status from day 8 on. The raising spontaneous activity as well as the spreading over the neural network leads to the suggestion that synaptic signalling in involved. One of the key characteristics of synaptic signalling is coordinated activity, mirrored in synchronously activated areas.

To analyse if a coordinated activity is reached during the J1 differentiation we displayed the measured spontaneous activity in a scatterblot (**Figure 17**).

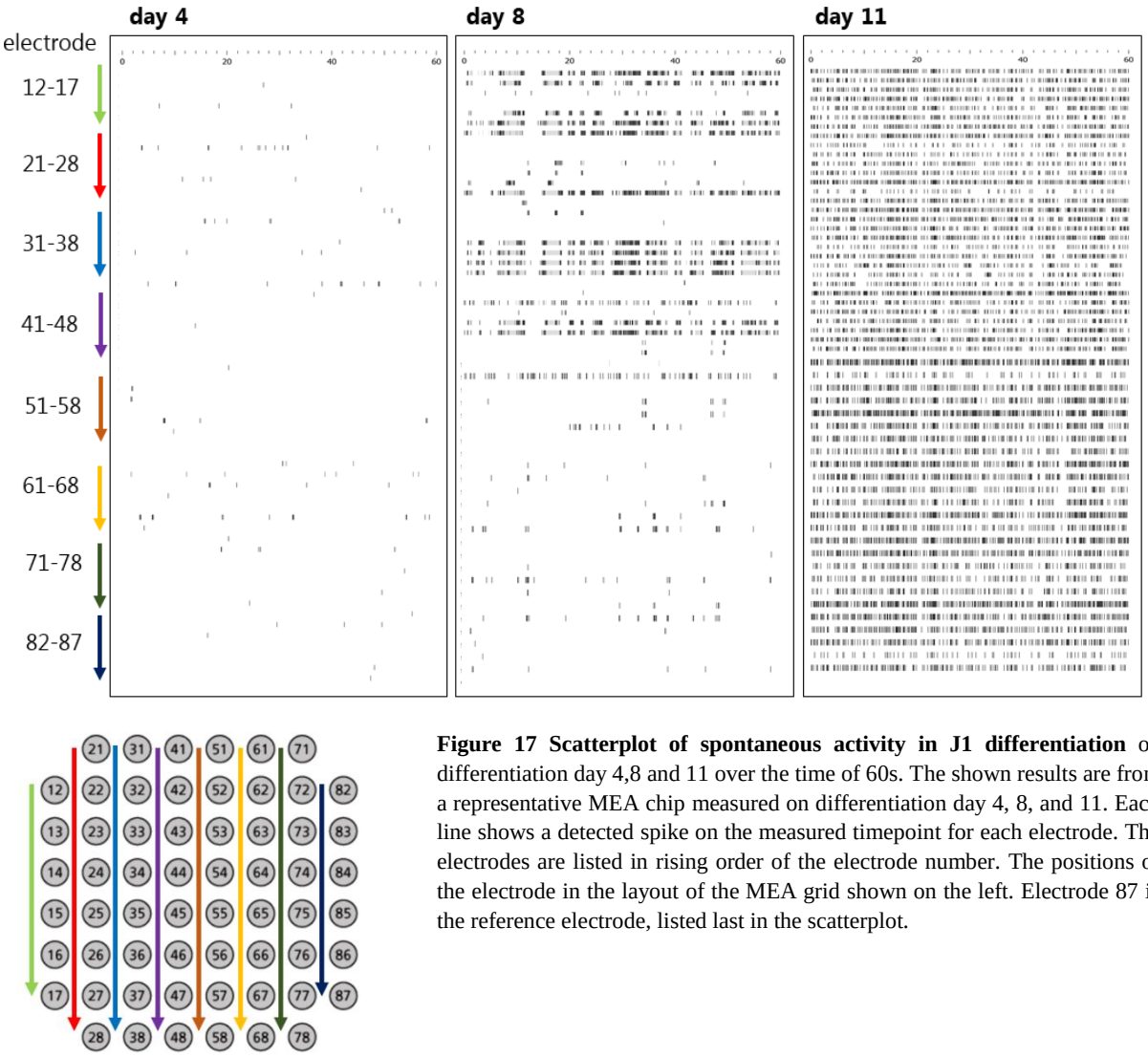

Figure 17 Scatterplot of spontaneous activity in J1 differentiation on differentiation day 4,8 and 11 over the time of 60s. The shown results are from a representative MEA chip measured on differentiation day 4, 8, and 11. Each line shows a detected spike on the measured timepoint for each electrode. The electrodes are listed in rising order of the electrode number. The positions of the electrode in the layout of the MEA grid shown on the left. Electrode 87 is the reference electrode, listed last in the scatterplot.

Figure 17 shows a scatterplot of the detected spikes of each electrode in a representative MEA chip in correlation to the time. The few detected spikes measured on differentiation day 4 do not show any coordination or pattern. On differentiation day 8 a clear coordination in the spike pattern can be recognized. Electrode comprehensive activity pattern are clearly visualized particularly in the upper half of the scatterplot. The temporal coordinated spike pattern in nearby electrodes are a clear sign for synaptic signalling. On differentiation day 11 nearly all detected spikes of all electrodes follow a coordinated pattern, indicating that the spontaneous activity is modulated by synaptic signalling comprehensive the whole network.

Taken together the analyses using MEAs show an electrophysiological differentiation of J1 NSCs to a functional neural network with synaptic signalling since at least differentiation day 8. This can also be substantiated with the presence of synaptic proteins as shown in **Figure 15**. Neural maturation is defined as the last step in neural differentiation mainly characterized by myelination, dendritic branching and synaptogenesis [2, 39, 49, 112, 134, 206, 212]. Increasing dendritic branching between differentiation day 5 and 10 could be show in **Figure 9** and **Figure 10**, expression of synaptic proteins

starting on differentiation day 6 ,as well as the formation of functional synapses on differentiation day 8,could be shown in **Figure 15** and **Figure 17**. These results together with the typical apoptotic wave (**Figure 12**) allow the definition of the **maturating phase** from differentiation day 6 to 8 in the used protocol.

4.3.6. **Overview**

The neural differentiation of J1 NSCs were analysed concerning the expression of marker proteins (4.3.1),morphology (4.3.2), proliferation (4.3.3), apoptosis (4.3.4) and functional differentiation in single cells (4.3.5 membrane potential and ion channels) and on the intercellular network level (4.3.5 multi electrode array). The broad characterisation allowed a precise classification of three differentiation steps summarised in **Figure 18**.

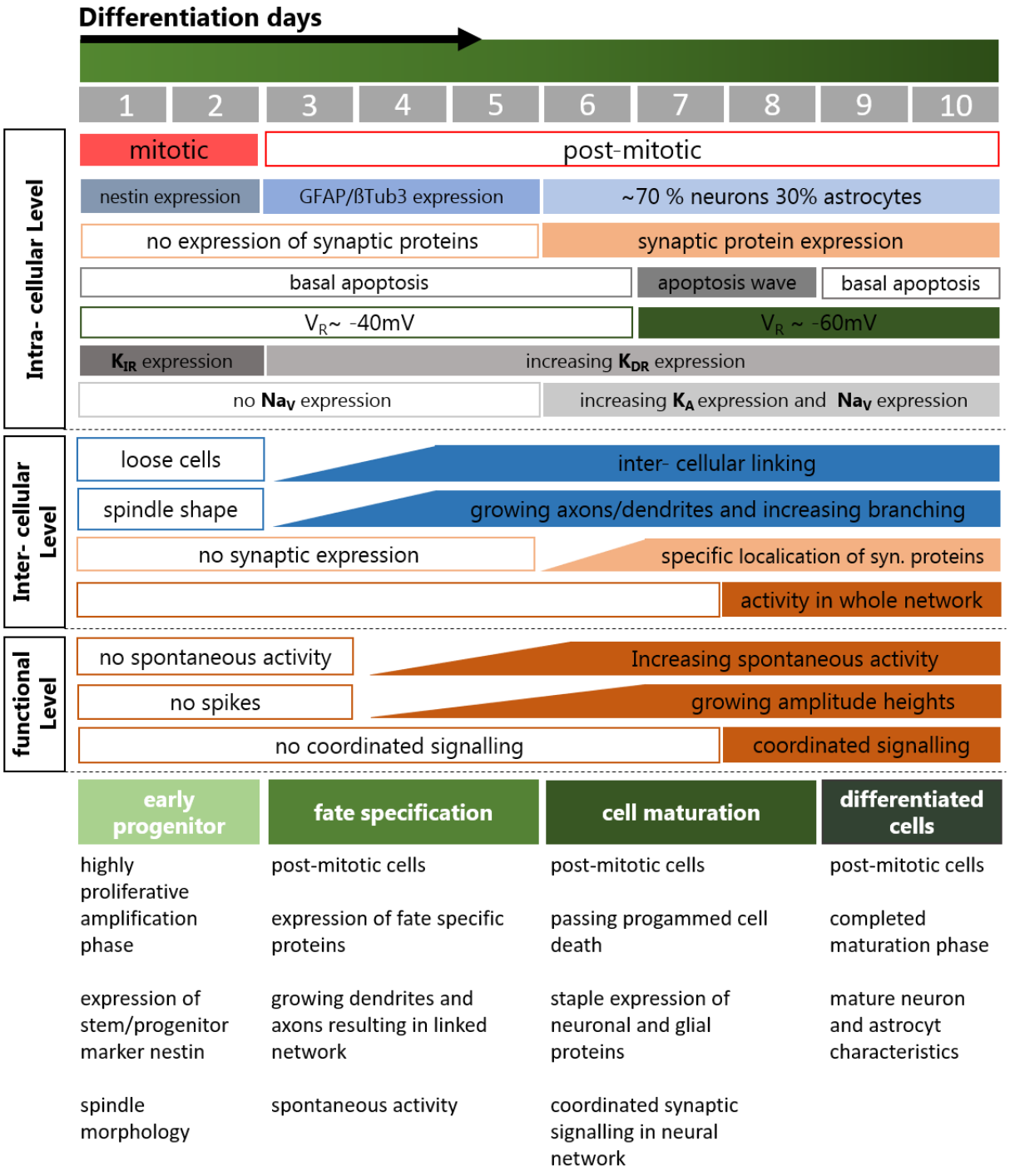

Figure 18 Schematic summary of characterised differentiation events in the J1 model system. The J1 model system shows various differentiation events on intra-, inter- cellular and functional level. The taken results allow to determine the three main differentiation phase **early progenitors**, **fate specification** and **cell maturation**. Based on the broad characterisation it is possible to classify the determined differentiation phases in restricted time periods of the differentiation protocol. The first differentiation phase, early progenitors, ranges from differentiation day 1 to 2. From day 3 to 5 differentiating J1 cells pass the fate specification, followed by the maturating phase from differentiation day 6 to 8. From day 9 on the differentiation is completed and cells can be referred as differentiated neurons and astrocytes.

As previously shown by Conti, J1 NSCs resemble the self-renewal of adult NSCs [191]. J1 NSCs express homogenously the stem/ progenitor marker nestin (**Figure 8**). The proliferating fraction is around 71% (**Figure 11**) with a doubling time of ~28h.

Induced differentiation raises the proliferation fraction over 90% (**Figure 11**) within the first two differentiation days and an accelerated doubling time of ~22h. The morphology of the cells changes dramatically, to a progenitor typical spindle shape (**Figure 9**). Cells in this shape still express nestin, also in first progenitors DCX expression is detectable, but no fate specific proteins. Cells in the first two differentiation days differ clearly from cells in self-renewal phase marked by increased proliferation and changed morphology. According to the determined properties, cells in the first two differentiation days can be characterised as **early progenitors** in the so-called amplification phase.

After differentiation day 2 cells show initially a typical pyramidal morphology, growing into a more branched shape in the following days (**Figure 9**). The acquiring spontaneous activity, the fate specific protein expression (**Figure 8**) plus the post mitotic state (**Figure 11**) represents the **fate specification** step in neural differentiation.

After fate determination, on differentiation day 6, the cell maturation takes place. Neuronal maturation mainly obtains the bioelectric constitution of the neuroblasts conditioned by specialised ion channels resulting in functional activity, as well as synaptogenesis and synaptic activity. The third and final differentiation phase, **cell maturation**, is represents in the J1 model system, characterised by ion channel rearrangement (**Figure 14**), characteristic membrane potential (**Figure 14**) synaptogenesis (**Figure 15**) and exponentially increased network activity (**Figure 16**). The advanced networking between the cells is electrophysiological mirrored in coordinated activity over the culture shown in **Figure 17**. The electrophysiological measurements together with the synaptic immunostaining (**Figure 16**, **Figure 17**) mirror a clear maturation phase resulting in functional synaptic signalling. Also, the occurring apoptosis wave (**Figure 12**) mirrors the so called “programmed cell death” of the maturation phase in neural differentiation, completed on differentiation day 8.

The differentiation of the murine neural stem cell line J1 showed various differentiation events on cellular, inter-cellular and functional level. The estimated results allow a classification of the three defined differentiation phases, **early progenitors**, **fate specification** and **cell maturation**. J1 cells in the first two days of differentiation are **early progenitors**, passing a highly proliferative amplification phase. During this time interval the differentiation process is restricted on the cellular level. The second differentiation step is determined from differentiation day 3 to 5, in this time the **fate specification** takes place. The post-mitotic progenitors start to express neuron or astrocyte specific markers, combined with evolvement to the fate specific morphology and excitability. On differentiation day 5 all cells are determined in their fate. Between differentiation day 6 to 8 J1 cells pass the last differentiation step, the **cell maturation**. In this phase the inter-cellular level gains on importance. The neuroblasts form functional synapses, resulting in organized network signalling. With the end of the programmed cell death the maturation process is terminated.

The differentiating J1 cells have passed all differentiation events after differentiation day 8. From differentiation day 9 on the cultured network consists out of ~70% young neurons and ~30% young astrocytes and can be referred as differentiated or mature cells.

4.4. Discussion

Differentiation phases in the J1 model system

Neural cell differentiation is an interminable, complex process, characterised by three main differentiation phases [201]. The first phase is the early progenitors phase followed by fate specification, the second differentiation phase. The third and final phase of neural cell differentiation is the cell maturation of the neuro- and glioblasts. In the first part of this work a differentiation protocol for the neural stem cell line J1 was estimated and characterised. The three differentiation phases **early progenitors**, **fate specification** and **cell maturation** could be identified and restricted to differentiation days. The media induced differentiation of J1 NSCs, leads to a synchronous differentiation and allows the separation of the cells population in defined differentiation phases depending on the differentiation time. Differentiating J1 cells create a coordinated functional network containing of ~70% neurons and ~30% astrocytes, similar to observations of adult neurogenesis in the DG of mice [60]. The used differentiation protocol ensures a high survival during the differentiation, allowing a quantitative number of cells in each differentiation phase.

J1 NSCs represents a stable cell line representing a homologous population of NSCs in self-renewal phase [191]. The used differentiation protocol allows a synchronous differentiation of the population. The differentiating cells pass the characteristic phases, early progenitors, fate specification and cell maturation, of adult neurogenesis [201]. The characterisation of the differentiation process showed that J1 cells reflect all three differentiation phases in a successive process, within 8 days (**Figure 18**). The identified differentiation phases show the characteristic markers for each phase [201]. The first two days, identified as **early progenitors**, show an increased proliferation (**Figure 11**) and nestin expression (**Figure 8**). The following **fate specification** phase, could be identified from differentiation day three to five, characterised by post mitotic progenitors, archiving fate specific protein expression and morphology (**Figure 8**, **Figure 11**). This phase is also determined by additional functional markers as increasing expression of typical ion channels, which are also mirrored in the J1 population (**Figure 14**). The final **cell maturation** phase starts with completed fate determination, which is the case on differentiation day six within the J1 population (**Figure 8**). In the following days we could identify various characteristics for the maturation, hereby we focused on neuroblasts. J1 neuroblasts mirrors the typical V_R (**Figure 13**), ion channel expression (**Figure 14**) as well as the evolution of coordinated network activity (**Figure 16**, **Figure 17**). The coordinated activity combined with the shown expression of synaptic proteins (**Figure 15**) indicates, functional synaptogenesis in J1 cells. Synaptic communication is also the base for induced apoptosis, a final differentiation event in the cell maturation [100]. In the J1 population the programmed cell death is terminated on differentiation day 8 (**Figure 12**), indicating a completed cell maturation.

Based on our results we can claim that the J1 differentiation represents a suitable model for adult neurogenesis. The estimated data verified that all three differentiation phases are displayed in this J1 model system, escorted by various differentiation events. The homology of the population during the differentiation process also enables the identification of the differentiation status by time. This attribute of the J1 model system is a special benefit compared to many other model systems, struggling with heterologous differentiation stages in the populations. In further experiments we plan to investigate the effect of ionising radiation on discrete differentiation phases, which is nicely possible in the J1 model system.

Comparison to other neural differentiation systems

There are different strategies to study adult neurogenesis, favoured are often murine model systems due to their similar neural organization structures compared to humans. *In vivo* studies are often limited by the possibility to selectively distinct individual differentiation phases [214]. In *in vivo* systems as well as in primary cultures often single differentiation markers such as DCX expression, are used to identify differentiating cells. The proper identification of the differentiation status in these mixed cultures are limited and imprecise compared to the presented J1 model system. Based on the characterisation the precise differentiation status of J1 cells is known and pursuable. Each characterized differentiation step shows a comprehensive differentiation including morphological, cell cycle- dependent, functional and protein expression aspects, comparable to *in vivo* systems or primary cultures.

The main advantages of *in vivo* studies are the possibility to observe tissue effect and whole brain effect [209, 215-218]. Accompanied with *in vivo* studies, these models are often complex and require long analysis, bureaucratic controls and ethical disunions. This also applies for primary culture. Self-renewing J1 NSCs are cultivated as immortal cell line and can be frozen and expanded quickly. In animal studies the neural differentiation process takes 1-3 month [2] (see also **Figure 3**) while J1 cells pass the three differentiation phases within 8 days (see also **Figure 18**). Which offers an oblivious save of time in the experimental process. *In vivo* studies as well as model systems like neurospheres, primary culture or organo slices struggle with polymorphic mixed differentiation stages, which do not allow a precise distinction between separate differentiation steps [86, 219-221]. The separation of cells in defined differentiation phases, possible in the J1 NSC model system, is the key feature for the planed radiation experiments.

Cell lines with neuronal characteristics like neuroblastomas are often very limited in their differentiation probabilities [198, 222, 223]. Often used neuroblastoma cell lines like SHSY or N2a are capable to show morphological changes and the expression of differentiation markers (e.g. DCX) after induced differentiation. Functional differentiation as well as the expression of synaptic markers or synaptic signalling outstrips the possibilities of these model systems [198, 223].

Weighing up pros and cons of available model systems, combined with shown results, the J1 model system provides an accessible and relatively easy to handle model system with manageable complexity. On the other hand, the J1 NSC model system displays not the migration of differentiating cell. The migration, is simulated by reseeding J1 cells on laminin coated surfaces in the second differentiation phase (**Figure 5**). Throughout this simulation, migration is not reflected in the J1 model system. The used model system is isolated from environmental factors as stem cell niche texture, enclosed tissue signalling or non-neural factors. This circumstance could be an advantage or a disadvantage depending on the research target. The J1 NSCs differentiation protocol represents the differentiation of neurons and astrocytes, which are the cell types generated in adult neurogenesis. In embryonal neurogenesis, NSCs also differentiated to oligodendrocytes which is not displayed in J1 differentiation, making it to an adult neurogenesis model system. Comparative antigenic studies also showed, that the J1 NSC model system provides remarkable antigenic similarity to adult NSCs [214].

Taken together the used murine 2D model system shows a quick neural differentiation on inter-cellular, intra-cellular and functional level comparable to adult neurogenesis *in vivo*. The adhered growth on plastic as well as glass surfaces gives J1 NSCs a multi-purpose usability in various methods as immunostainings, patch-clamp or multi electrode arrays. These methods are often limited by the 3D cultivation of primary cultures or the non-adhered growth of neurospheres. Focused on the

functional evaluation the ESC-derived NSC model system shows similar results to primary culture systems, also shown in Ban, 2007 [213].

In the following chapters the aftermaths of ionizing radiation in low dose area will be picked up, focused on single differentiation events in the entirety of neural differentiation. Clearly characterized differentiation phases are the basis for further studies on the impact of ionising radiation on separated differentiation events. The particular properties of the J1 model system displays a suitable system to investigate differentiation phase specific radiation effects in adult neurogenesis.

5. Chapter II: Radio sensitivity of individual differentiation phases in adult neurogenesis

5.1. Introduction

5.1.1. Ionising radiation

As the name implies, ionising radiation (IR) is defined as radiation that carries enough energy to liberate electrons from atoms or molecules, thereby ionising them. IR can be separated in particle radiation and photon radiation. Particle radiation is mainly generated by radioactive decay, resulting in energy-rich subatomic particles hurtling at high speed. Photon radiation is, in contrast to particle radiation, made up of high- energy electromagnetic waves, characterised by the wave-particle duality. Electromagnetic waves are categorized by the frequencies, wavelength and photon energy in the electromagnetic spectrum. Electromagnetic waves with frequency ≥30PHz; wavelength ≤124nm and photon energy ≥10eV are ionising, which covers high energy UV-light, x-rays and gamma rays.

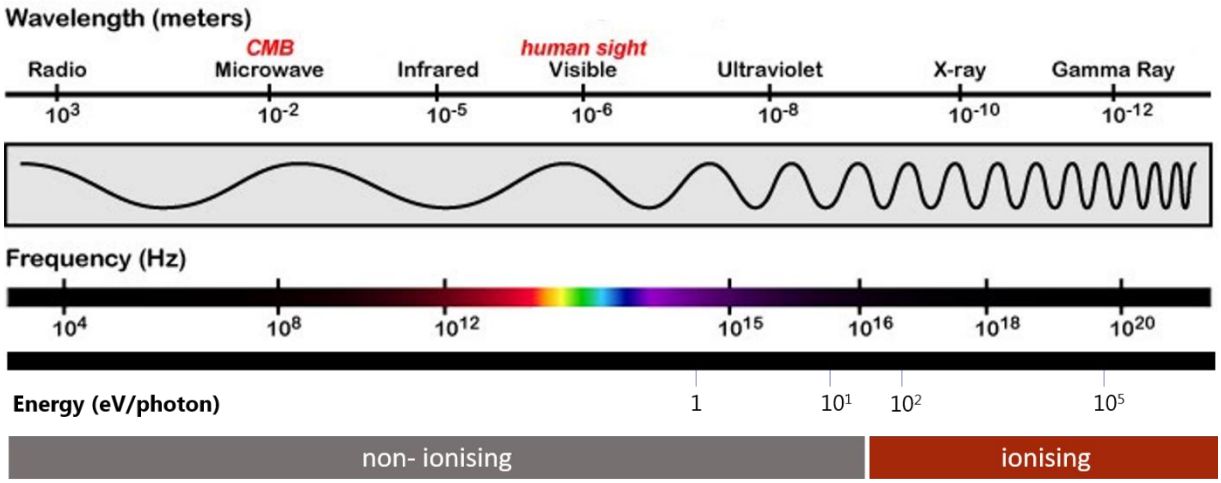

Figure 19 The electromagnetic spectrum showing the relation of frequencies, wavelength and photon energy in electromagnetic waves. The higher ultraviolet part, x-rays and gamma rays carry enough energy to ionise. Figure modified from studybuddy.com

Even though photons are electrically neutral, they can ionize atoms directly through the photoelectric effect and the Compton effect. The possibility to ionise biological tissues makes IR harmful to living organisms. In biological sciences the absorbed dose is mainly used, representing the mean energy imparted to matter per unit mass by ionizing radiation. The unit is Gray (Gy), it is defined as the absorption of one joule of radiation energy per kilogram of matter (1Gy = 1J/kg) [224].

5.1.2. Biological effects of IR

On the cellular level, the DNA is the most critical target to IR. Ionising radiation can, beside other damages, lead to the most toxic lesions, DNA double strand breaks (DSBs). Unrepaired DSBs can lead to apoptosis and are a serious risk for the chromosomal integrity. These critical lesions can be generated by ionising the cellular DNA directly or via so called indirect ionisation. IR has the ability to generate free radicals that may cause indirect DNA damage. The presence of water and oxygen in irradiated cells leads to reactive oxygen species (ROS) which are responsible for indirect damages and are the main effect of photon irradiation. ROS may also provide a source of metabolic stress to which the CNS is particularly susceptible as compared to other tissue types [225-227]. Although the fixation

of double-stranded DNA breaks leading to mitotic catastrophe is the most supported mechanism of radiation-induced cell death [228], it is thought to be more relevant in cells undergoing active cell division. In the mature CNS where mitotic cells are limited, it is suggested that other mechanisms of radiation-induced damage, such as oxidation of the lipid bilayer [225, 229] changes in microvascular permeability, cell-cell junctional complex rearrangements [230], and mitochondrial alterations inducing additional oxidative stress [231], are more important subcellular targets for ionizing radiation. Nevertheless, the toxic effect of IR is mainly due to genetic instability caused by IR induced DNA lesions, especially in proliferating cells.

5.1.3. **Radio sensitivity**

Radio sensitivity is the relative susceptibility of cells, tissues, organs or organisms to the harmful effect of ionizing radiation. Proliferating cells form the most sensitive part, described by the "law of Bergonié and Tribondeau", formulated in 1906 [232-234]. From their observations, they concluded that quickly dividing tumour cells are generally more sensitive than the majority of body cells. In general, it has been found that cell radio sensitivity is directly proportional to the rate of cell division and inversely proportional to the degree of cell differentiation [235]. In short, this means that actively dividing cells or those not fully mature are most sensitive to radiation. Further factors influencing the radio sensitivity are the metabolic rate and the general cell condition [235]. Based on the mentioned factors a specific radio sensitivity for different tissues or organs can be estimated, proliferative tissues as bone marrow, embryonic cells or gonads are categorized as highly sensitive. While muscles, bones and the nervous system is categorised as less sensitive to IR [236].

The high sensitivity of proliferating cells is the basal mechanism behind radiotherapy, a standard treatment for tumours. Fast proliferating cancer cells represent a sensitive target for IR, combined with chemotherapy and surgery, radiotherapy is a common treatment for various cancer types, especially for badly accessible brain cancer [237]. IR is commonly applied to the cancerous tumour because of its ability to control cell growth by damaging the DNA of cancerous tissue leading to cellular death or/and cell cycle arrest. The specific sensitivity of tumorous tissue compared to affected surrounding healthy tissue is basically generated by different radio sensitivities. To reduce the risk for the bystander cells radiation technics for selectively dose deposition in tumorous areas are improved. Nevertheless, healthy tissue is exposed to IR especially when y-radiation is used. Additionally, it has been shown that tumour cells can be hypoxic and therefore less sensitive to y-radiation because most of their effects are mediated by the free radicals produced by ionizing oxygen [1, 225, 238-240].

5.1.4. **Sources of ionising radiation**

Beside radiotherapy IR is used in imaging diagnostic applications in the medical field, as computed tomography (CT) scans or x-rays. The increased use of x-ray, CT scans for medical diagnosis and radiotherapy, diagnostic radiation examination is the largest man-made source of radiation exposure to the general population, contributing ~40% of the total annual worldwide exposure from all sources in advanced countries. Brenner and Hall suggest that ~2% of cancer deaths in the USA over the last 20 years were attributable to diagnostic x-rays [4, 241, 242]. Beside medical applications human populations are exposed to IR from various sources. We all encounter daily natural radiation including cosmic rays, environmental radionuclides or radon decay products typically providing low-dose exposure. IR can also originate from man-made sources in the context of nuclear accidents, nuclear weapons testing and unplanned discharges of radioactive waste [3]. Some individuals are additionally receiving occupational exposure related to nuclear technologies, airline travel or even space

exploration. Increasing contact with IR leads to increasing risk of radiation-induced damage, for this reason, the long-term effects of IR become highly interesting, especially in the low dose area.

5.1.5. **Radiation effects on neural stem cell niches**

Compared to mature neurons and astrocytes, NSCs niches can be characterized as radiation sensitive regions. Cranial irradiation of 10Gy in adult rats led selectively to a highly significant apoptotic fraction of proliferating cells (ki67 positive) in the subgranular zone of the dentate gyrus [243, 244]. Postmitotic neural cells, in contrast, are considered to be more resistant against ionising radiation [245-247]. Hereby no differentiation between progenitors and mature neurons or astrocytes are made, the used dose range was between 5 to 10Gy.

Most of the studies investigating effects of IR in adult neurogenesis regard the whole stem cell niche, and changes within the heterogenous tissue population. Irradiation of the SVZ leads to a reduction in NSC number, decreased proliferation of surviving NSCs and a decline in differentiation capacity into mature neurons [248-251].These effects has been shown to be dose-dependent (2-10Gy were used). Palmer et all showed that a cranial x-ray dose of 10Gy in rats leads, beside a huge decrease in cell proliferation and the growth potential in the SVZ, to a lasting alteration in the differentiation capacity. A 97% reduction in new born neurons was found in rats two months after cranial irradiation. In a second experiment, one month after irradiation (10Gy), primary cultures form the SVZ were isolated and differentiated for five days *in vitro*, resulting in a five times higher neuronal fraction than in the control. A lower dose (2Gy) leads to a 50% reduction of neurons compared to the control in the *in vitro* differentiation [249]. The ratio between neurons and glia cells in both irradiated groups did not differ from the control groups. Monje et al suggest that this may represents a diverse chronic dysfunction within the population after irradiation [25]. Focusing the neural stem cell niche in whole, it is not distinguishable if these effects are caused by the individual radiation responses of progenitors or by the collapse of the neural stem cell niche hierarchy (see **Figure 20**) [1].

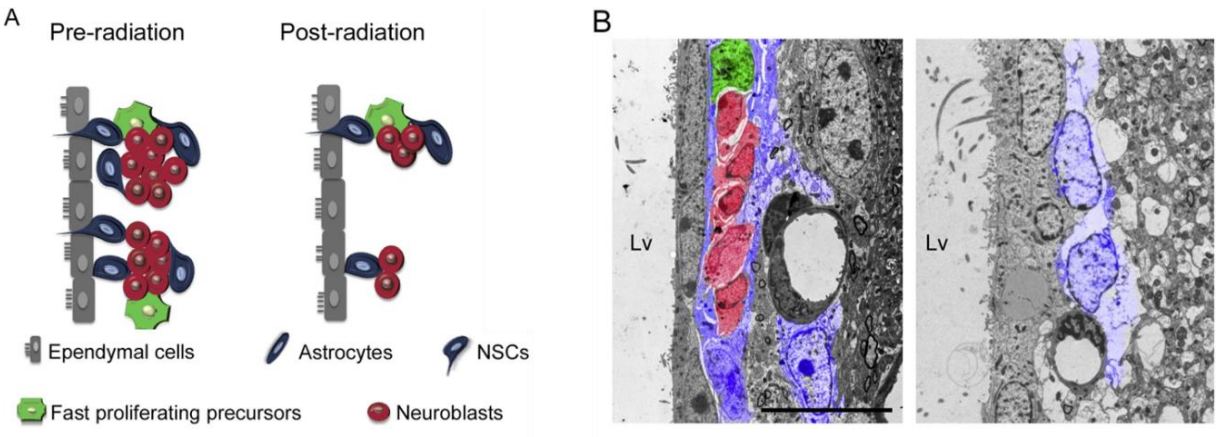

Figure 20 Radiation disrupts the SVZ neurogenic niche. (**A**) Schematic representations of the rodent SVZ. In a pre-radiation condition the SVZ preserves its typical cell organization. Following radiation, the SVZ shows a notable depletion of fast proliferating precursors and neuroblasts. Some astrocytes remain after radiation and ependymal cells are not affected. (**B**) Electron microscopy images of the rodent SVZ pre- and post-radiation. Lv= lateral ventricle, Scale bar 10 µm. Modified after Capilla-Gonzalez [1]

In several studies it could be clearly shown that ionising radiation affects adult neurogenesis. The main effect is the dramatic reduction of the number of (proliferating) cells in stem cell niches and reduction or loss of neurogenesis [185, 238, 248-255]. Electron microscopy studies revealed that, 30 days after SVZ radiation (5-10Gy), the number of NSCs was reduced, fast proliferating precursors cells were practically non-existent, and neuroblasts were scarce [238]. The effects on the proliferative populations were further evaluated by examining the expression of Ki67, a marker of proliferative cells, which showed a notable decrease in the irradiated SVZ [1, 238, 252, 256].

Similar results are obtained for the neurogenic niche in the dentate gyrus. Proliferating cells in this area are particularly sensitive to ionizing irradiation, undergoing apoptosis after doses ranging from 1Gy to 18Gy [250, 251, 257-260]. Mizumatsu et al. and Uberti et al. showed that, the dose response curve for apoptosis in mice DG is biphasic, with a steep response at lower doses (1–2Gy) and a flatter response at higher doses [250, 258] (**Figure 21 i**). In order to assess specific cell populations in the SGZ 12h post irradiation, antibodies against Ki67 and DCX were used. The quantification of positive cells for these antibodies within the SGZ, suggests that early cell loss after x ray doses between 1-2Gy largely represents the response of actively proliferating cells (ki67 positive), whereas the flatter portion of the curve (5–10Gy) is dominated by the response of DCX positive cells (see Figure 21 ii) [13, 250, 251]. These data indicate a decreasing radio sensitivity of in the cause of neural differentiation, determined by the postmitotic status of DCX positive progenitors [250]. The interpretation of these data has become more complicated by the observation that a subpopulation of DCX positive cells also can express Ki67, indicating that they also are capable of proliferation, which may be induced by IR [261].

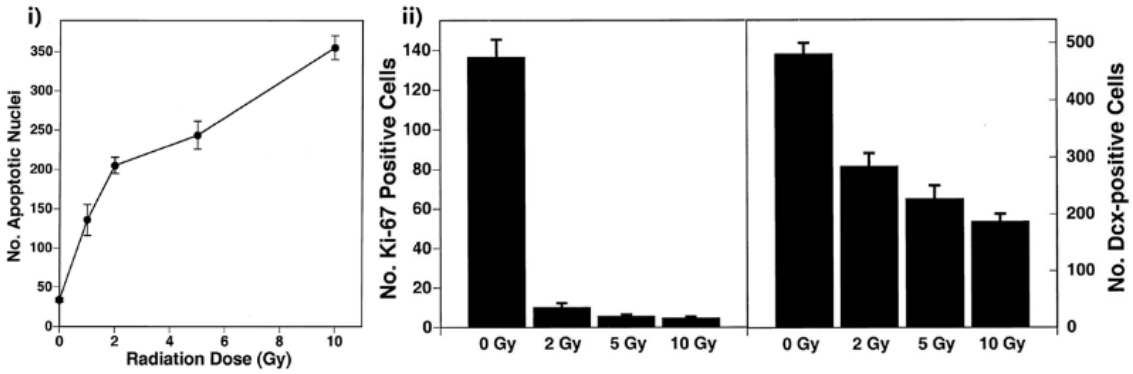

Figure 21 Dose response curves for apoptotic cells in SGZ; the percentage of cell loss for each mouse of a given treatment group (n = 4–5) was compared with sham-irradiated controls, and a percentage cell loss was calculated. Proliferating cells were detected by using an antibody against Ki67; immature neurons were labelled with an antibody against DCX. **i)** Cells in the dentate SGZ undergo dose-dependent apoptosis after low to moderate doses of X-rays. Apoptosis was quantified based on TUNEL labelling and morphological changes in irradiated cells. The steepest part of the response was dominated by loss of actively proliferating cells, whereas the shallower slope, >2Gy, largely represented the response of immature neurons. **ii)** Numbers of proliferating cells (left) and immature neurons (right) in the dentate SGZ are significantly decreased 48 h after irradiation. Antibodies against Ki-67 and DCX were used to detect proliferating cells and immature neurons, respectively. All doses substantially reduced the numbers of proliferating cells, and the dose response from 2 to 10Gy was significant. Immature neurons were also reduced in a dose-dependent fashion. Modified after Mizumatsu [250].

Nevertheless, these data show a decreasing radio sensitivity in DCX positive cells compared to ki67 positive cells, which leads to the suggestion that differentiation progression (mainly postmitotic status) decreases the radio sensitivity in adult neurogenesis. It is hypothesized that the massive reduction of the proliferating fraction determines the long-lasting loss in neurogenesis [13, 250]. Most of the

performed studies used high doses of IR, which do not directly reflect the dose range associated with cognitive deficits (see 3.1 Ionising radiation and cognitive dysfunction).

Taken together, several studies showed a high radio sensitivity of neural stem cell niches, without questions the main effect of IR is dramatic decrease in the proliferating cell population of the neurogenic niches. This leads to a dramatic reduction of the persistent stem cell pool and an ongoing reduction or loss of neurogenesis after IR.

5.1.6. Second aim: identification of particular radio sensitivities in neural differentiation

As summed up before most of the studies focusing effects of IR on neural stem cell differentiation address neural stem cell niches on the whole. Hereby, proliferating cells represent clearly the most sensitive fraction. Although nearly no discrimination between the differentiation phases of the differentiating cells were made, except the proliferative status. In the following chapter we used the previously characterised J1 model system (see chapter 1) to evaluate the radiation sensitivity of differentiating NSCs discriminated by their defined differentiation status, by analysing the survival of separated populations of NSCs and the three differentiation phases, EP, FS, CM post irradiation. Hereby we focus on a dose range below 2Gy.

5.2. Material and methods

Cell irradiation:

The irradiation of J1 NSCs was performed using an x-ray tube equipped with a wolfram-anode, built by the company Philips. X-ray treatment was performed using a power of 19mA, 90 kV voltage and 30cm distance to the IR source, which makes an applied dose of 1,96Gy/min, established by Ficke dosimetry. Depending on the applied dose samples were placed for the calculated timespan in the x-ray tube. To all radiated samples equal control samples were performed and placed in the deactivated x-ray tube for the same time. For samples seeded on glass products (MEA-chips) the treatment time had to be adapted. Irradiation on glass products leads to secondary electrons, so that the dose rate is higher than on plastic products. For samples on glass the radiation time was adapted in the radiometric calculated way.

MTT assay:

MTT-assays were performed in 96-well plates. Undifferentiated J1 NSCs and J1 in the initial differentiation state (DI) were seeded in a density of 10.000 cells per well, 24h later cells were radiated (0; 0.25; 0.5; 0.75; 1; 2Gy). 23h after x-ray treatment MTT reagent was resuspended in the media (15µl/well), cells were incubated 1h at 37°C, 5% CO_2. Afterwards the media was tilted the cells were fixed in 150 µl Isopropanol/0,04N HCl in the dark. All wells were resuspended thoroughly to solve the formazan crystals at the bottom of the wells, directly afterwards the OD of each well was measured using ELISA reader. Cells in later differentiation steps (DII & DIII) were seeded on laminin coated 96 well plates in a density of 30.000 cells per well and differentiated further. 24h before fixation cells were irradiated (0; 0.25; 0.5; 0.75; 1; 2Gy). 1h before fixation 15µl MTT reagent (5mg/ml) was added. For the photometric analyses Tucan ELISA reader was used, measuring absorbance at 570nm and for reference at 630nm as triplet. Determined values were normalized on irradiated samples using Microsoft excel. For each data point at least five individual 96 well plates were measured.

LD_{50} calculation:

Survival curves for x-rays show, in contrast to particle radiation, an initial shoulder in the linear curve progression. The non-linear progression in the lower dose range is caused by the lower linear energy transfer (LET) of x-rays. Increasing LET increases the probability for DSBs, the most toxic radiation induced lesion. To calculate the LD_{50} of the individual differentiation phases we performed a linear fit using graphpad prism. To avoid adulterations in the fit throughout the initial shoulder, the nonlinear part was excluded (data below 1Gy). The estimated data form the previous MTT assay were used, from the dose area 1-5Gy. For the fit all estimated results were used, to estimate the LD_{50} every measurement was fitted and Y=50 was calculated individually.

Proliferation- and apoptosis assay:

Antibody staining was performed as described previously in 4.2 Antibody staining. Radiated samples were fixed 15min after x-ray treatment for ccaspase 3 staining and 3h after x-ray treatment for ki67 staining. The cells were counted semiautomatic using the programs imageJ based micromanager 1.4 and scanJ. For each data set at least 1200 cells were analysed in four individual experiments with variable cell passages. In pre-experiments the timepoints of proliferation minimum (3h after IR) and apoptosis maximum (15min after IR) after treatment was evaluated. All samples were fixed 15min after irradiation for the apoptosis assay and 3h after irradiation for the proliferation assay. The pre-experiments revealed a recovery in the proliferating fraction 12h post IR in SR as well as in EP.

5.3. Results

5.3.1. Radio sensitivity of the individual differentiation phases in neural differentiation

Radio sensitivity is the relative susceptibility to the harmful effect of ionizing radiation. The radiation induced damage could be valued on the level of cells, tissues, organs or organisms. The basal target here is the cellular level, determining higher levels. Sensitivity of cells to radiation correlates directly with the proliferation status of cells. As previously mentioned proliferating cells form the most sensitive fraction to IR (see 5.1.3), which is also validated in neural differentiation. In previous studies differentiating cell are characterize by the expression of DCX and ki67. Since DCX is an early differentiation marker, which is expressed in at least two of three differentiation steps, no further discrimination between the individual differentiation steps was achieved. The proliferation marker ki67 also allows no separation between NSCs and proliferating early progenitors. The J1 model system and its characterisation allows a defined separation of the three differentiation phases, early progenitors (EP), fate specification (FS) and cell maturation (CM), as well as NSCs in self-renewal status (SR). We used this achievement to evaluate the radio sensitivity of the individual differentiation phases in neural differentiation.

To evaluate the radio sensitivity of J1 cells during differentiation a classical toxicity test, MTT assay was used. The MTT assay, called after the dye MTT 3-(4,5-dimethylthiazol-2-yl)-2,5-diphenyltetrazolium bromide, is a colorimetric assay for assessing cell metabolic activity, reflecting the number of viable cells [262]. Viable cells with active metabolism convert MTT into a purple coloured formazan product with a distinguishable absorbance. Apoptotic cells lose the ability to convert the dye, thus the MTT assay can also be used to measure proliferation or apoptosis. To exclude incorrect measurements due to variable metabolic activity throughout the differentiation phases, the radiated samples were normalized on the control sample of corresponding differentiation phase.

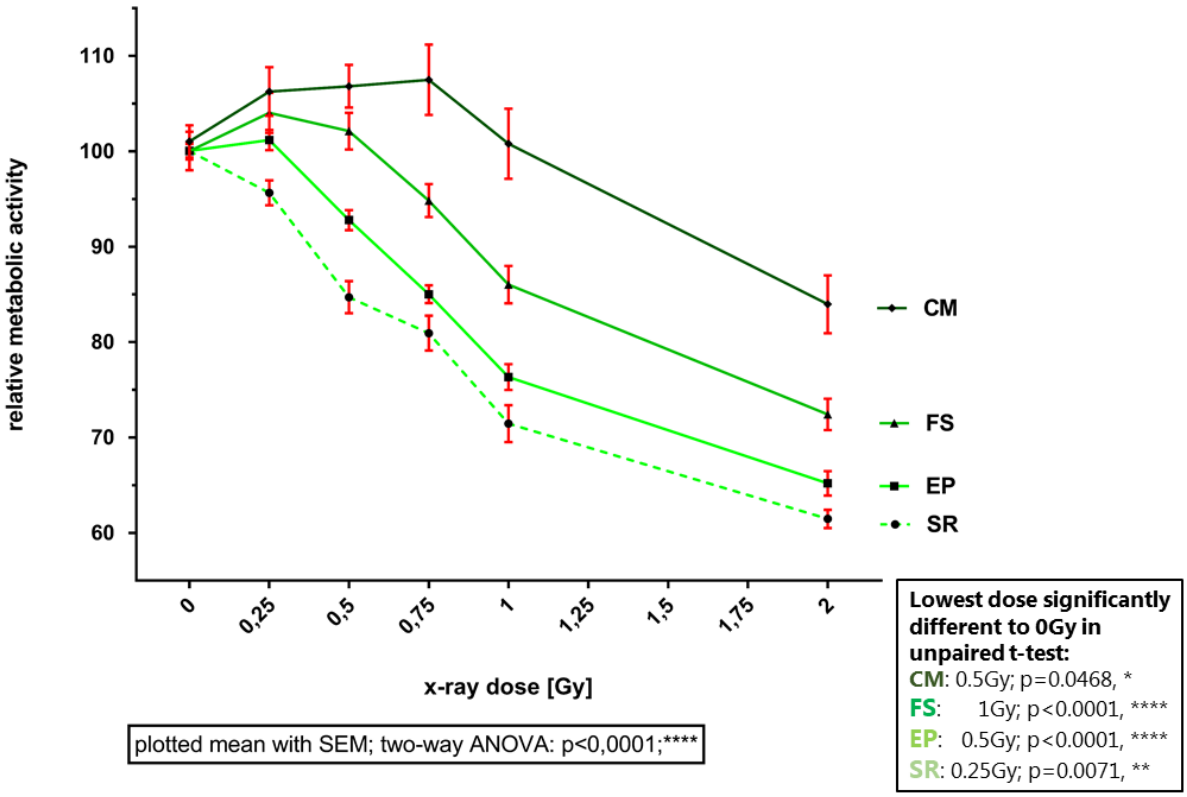

Figure 22 Dose response of individual differentiation phases of J1 NSCs, undifferentiated J1 NSCs (SR) and the three differentiation phases early progenitors (EP, differentiation day 2), fate specification (FS, differentiation day 4) and cell maturation (CM, differentiation day 7) were radiated with 0; 0,25; 0,5; 0,75; 1 and 2Gy. 24h after treatment the metabolic activity was determined via MTT- Assay. All results were normalized on unradiated samples of each differentiation phase, plotted mean with SD. The cytotoxicity of IR is measured via MTT assay, a colorimetric assay to estimate cell metabolic activity (Tetrazolium dye).

To estimate the sensitivity of differentiating cells, MTT assays exposed to 0; 0.25; 0.5; 0.75; 1 and 2Gy, were performed in the three differentiation phases (EP, FS, CM) and self-renewal. All sample were normalized on unirradiated controls, so that the estimated metabolic activity represents the number of cells normalized to control group.

J1 cells show variable reactions to IR depending on the differentiation phase (**Figure 22**). J1 NSCs in self-renewal state show the highest sensitivity to IR. Even to lowest used dose of 250mGy show a significant difference to irradiated cells ($p<0.0071$; **; unpaired t-test). Early progenitors representing the first differentiation phase, which are still proliferative are also highly sensible to IR. While 0.25Gy does not show a significant effect on cells in this proliferating state, 0.5Gy does ($p<0.0001$; ****; unpaired t-test). Presupposed that metabolic activity represents the number of cell, around 7% less cells in the first differentiation phase are detectable 24h after 0.5Gy X-ray treatment. In self-renewal phase the number of cells is already reduced to ~85% after 0.5Gy.

The post-mitotic differentiation phases fate specification and maturation are expected to be less sensitive than the mitotic stages. A lower radio sensitivity of the late differentiation phases could be confirmed in **Figure 22**. Progenitors passing the fate specification, show an average radio sensitivity in comparison to NSC, EP and CM phase. A dose of 1Gy was needed to observe a significant difference between radiated and irradiated cells ($p<0.0001$; ****; unpaired t-test) in this phase, 24h after treatment.

J1 cells in the last differentiation phase (CM), clearly represent the lowest radio sensitivity of all tested groups. In maturation cells, surprisingly the number of cells increases in the lower dose area compared to the control group, indicating proliferation. This differentiation step, representing maturating neuro- and glioblasts shows a significant effect compared to unradiated controls after 0.5Gy (p = 0,0468; *; unpaired t-test). This suggests a stable reaction of cells in the last differentiation phase, but opposite effect as observed in earlier differentiation phases. Instead of decreasing cell numbers, the late progenitors show an increasing cell number 24h after x-ray treatment below1Gy.

Taken together the dose response of J1 cells during differentiation is divers. The highest sensitivity to low dose radiation is clearly shown by J1 NSCs in self-renewal state, showing a decrease of 5% of the population 24h after 0.25Gy x-ray treatment. Early progenitors show a slightly lower radio sensitivity than undifferentiated NSCs. To observe a significant effect compared to the control, a dose of 0.5Gy is needed, showing a decrease of ~7% of the cell number. Also, in cell maturation phase 0.5Gy radiation is enough to observe a significant difference between radiated and unradiated cells. The observed response is, opposite to self-renewal and EP phase, an increase in the cell population 24h after treatment. To obtain a decrease of the cells population, a dose higher than 1Gy is needed. The middle differentiation phase, fate specification, shows a decrease in the cell population 24h after 0.75Gy. To get a significant different response compared to the controls in the fate specification phase, a dose of 1Gy is needed, which leads to a reduction of ~15% in the cell population.

To estimate the toxicity of IR in neurogenesis, the linear regression of the dose response (**Figure 22**) was generated to calculate the LD_{50} of x-rays. The median lethal dose (LD_{50}) is a measure of the toxicity of toxins, radiation or pathogen. The value of LD_{50} is the dose required to kill half of the tested population after a specified test duration. A lower LD_{50} is an indicative of high toxicity. In case of the dose response of NSCs during differentiation, a lower LD_{50} is an indicative of higher sensibility.

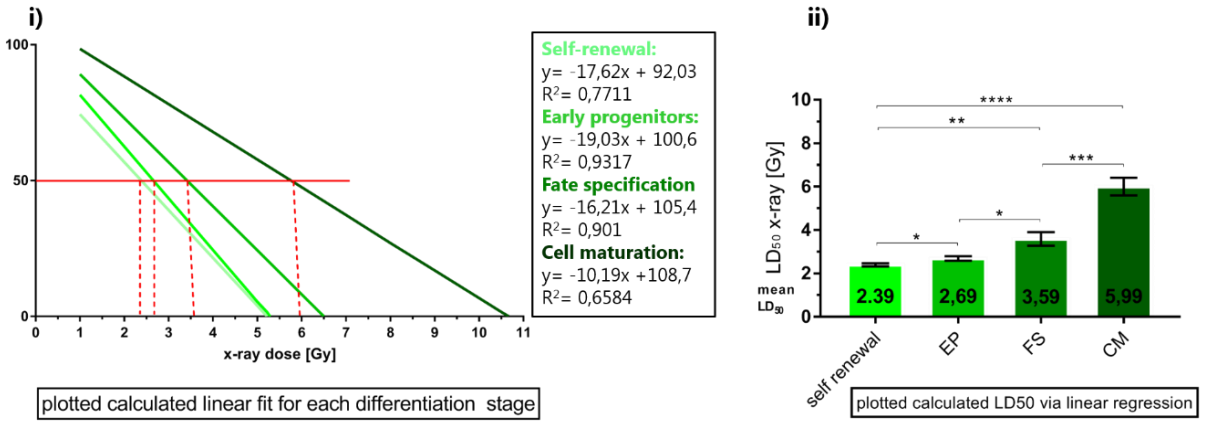

Figure 23 Calculated LD50 via linear regression for every differentiation phase. i) Results of MTT-Assays in **Figure 22** were used to calculate linear fit for J1 NSCs in self-renewal and each differentiation phase. The linear fits were used to estimate LD50 of single x-ray treatment in J1 NSC during differentiation. **ii)** based on the linear regression the LD_{50} for each differentiation phase was calculated. Plotted mean with SD, unpaired t-test (*: $p \leq 0,05$; ** $p \leq 0.01$; *** $p<0.001$; **** $p<0.0001$).

Based on the earlier estimated data (**Figure 22**) the LD_{50} of IR was calculated. The calculated LD_{50} for J1 NSCs in self-renewal and early progenitors are close to each other. The calculated LD_{50} for undifferentiated J1 NSCs (SR) is 2.39Gy; for the initial differentiation phase (EP) it is 2.69Gy. The LD_{50} for the second differentiation phase (fate specification) is 3.59Gy, indicating a slightly lower sensitivity to IR than the earlier phases. For the last differentiation phase (cell maturation) a LD_{50} of 5.99Gy is calculated. Compared to undifferentiated J1 NSCs more than double dose is needed to kill half of the cell population in the maturation phase, indicating a remarkable shift in the sensitivity to IR. **Figure 22** and **Figure 23** show, that in course of differentiation J1 NSCs, get more resistant to IR respective apoptosis 24h after treatment. Because of the tight connection between radio sensitivity and proliferation, these results have been expected. Unexpected are the measured increase in the number of cells in the second and third differentiation step, after radiation in the lower dose area. Increase in the cell number, indicates proliferation. As previously shown in **Figure 11** the fate specification phase and the maturation phase are postmitotic. Radiation induced proliferation would mean a transformation in the course of differentiation in J1 NSCs.

5.3.2. **Apoptosis and proliferation in the individual differentiation phases post IR**

The radio sensitivity of J1 cells during differentiation was estimated via MTT-assay (**Figure 22**). This assay only allows to assume the number of viable cells after x-ray treatment but gives no insight if de- or increased cell numbers are indebted by (reduced) proliferation or apoptosis.

To investigate the increase in the grown cell population of the later differentiation, 24h after IR treatment closely, proliferation and apoptosis assays were performed. To investigate the altered cell number after x-ray treatment closely, immunostainings with the proliferation marker Ki67 and the apoptosis marker ccaspase3 were performed. The previous results of the dose response curve (**Figure 22**) show partly opposed effects of x-ray doses below and above 1Gy. To cover both dose areas, the following assays were performed with 0.5 and 2Gy. In pre-experiments the timepoints of proliferation minimum (3h after IR) and apoptosis maximum (15min after IR) after treatment was evaluated. All samples were fixed 15min after irradiation for the apoptosis assay and 3h after irradiation for the proliferation assay.

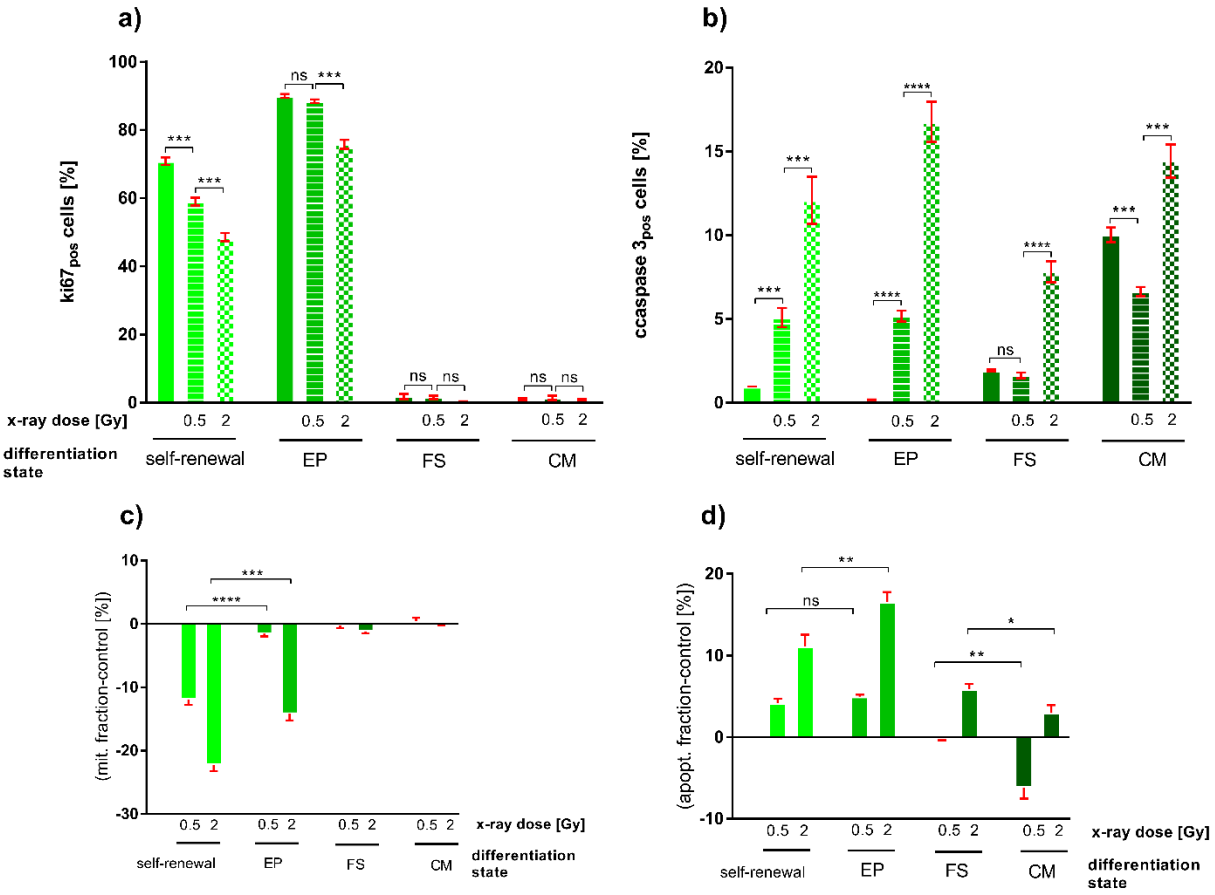

Figure 24 Proliferation and apoptosis of J1 NSCs during differentiation after x-ray treatment. **a)** The mitotic fraction of J1 NSCs in the three differentiation phases and self-renewal phase, estimated via Ki67 staining 3h after x-ray radiation (0; 0.5; 2Gy). **b)** Estimated apoptotic fraction of undifferentiated J1 NSCs and during the three differentiation phases after x-ray treatment (0; 0.5; 2Gy) estimated via cleaved caspase 3 staining, 15min after irradiation. To visualize the difference in the apoptotic fraction and the mitotic fraction to the unradiated control, the percentage of the corresponding control groups were subtracted from the irradiated groups. **c)** percentage of the proliferating fraction subtracted the percentage estimated in the control group. d) percentage of the apoptotic fraction subtracted the percentage estimated in the control group. In all graphs mean with SD is plotted, for statistics unpaired t-test was used (ns: $p > 0.05$; *: $p \leq 0{,}05$; ** $p \leq 0.01$; *** $p<0.001$; **** $p<0.0001$).

Estimated via Ki67 staining, ~70% of the cell population in self-renewal is mitotic active, after 0.5Gy irradiation the mitotic fraction is significantly reduced to ~60%. 3h after a dose of 2Gy the mitotic fraction decreases to ~50%. The first differentiation step is characterized by increased proliferation, the mitotic fraction is ~90%, slightly reduced by 0.5Gy. 2Gy x-ray treatment leads to a significant reduction of ~15% in the mitotic fraction (**Figure 24**). Both radiation doses (0.5 and 2Gy) do not change the postmitotic state of second and third differentiation phase (FS; CM) as shown in **Figure 24 a,c .** In the late differentiation phases (FS, CM) a couple of positive cells for the mitotic marker Ki67 appeared in an irregular pattern, to recheck this EdU assays were used (data not shown). The thymidine analogue EdU was added to the media directly before irradiation (0; 0.5; 2Gy), 3h after treatment the cells were fixed. Neither in radiated, nor in the unirradiated control cells EdU incorporation was found. To review the methodical process, the EdU experiments were repeated with self-renewing cells and early progenitors (EP). Both groups (self-renewal, EP) showed consentaneous results to the presented Ki67 staining (**Figure 24 a, c**) with and without radiation treatment (data not shown). The operated control experiments verify the postmitotic status of J1 NSCs after the first differentiation step, even after irradiation.

The two proliferating groups (SR, EP) show dose dependent reductions in the mitotic fraction 3h after IR. 0.5Gy x-ray treatment reduces the mitotic fraction by 12% in self-renewing J1 NSCs and by 1.5% in early progenitors (EP). Also, the second dose 2Gy reduces the mitotic fraction of undifferentiated cell (SR) nearly 10% more than in J1cells in the first differentiation phase (EP). This suggests that the radiation response of undifferentiated J1 NSCs is more sensitive concerning proliferation than in early progenitors.

Radiation induced apoptosis is a common effect of IR, used in tumourtherapie. Hereby highly proliferating cancer cells are the target, but also surrounding cells are affected. To estimate radiation induced apoptosis in J1 NSCs in the course of differentiation the apoptotic marker cleaved caspase 3 was used (**Figure 24 b, d**). The two proliferating phases of J1 NSCs (SR, EP) show a comparable increase in apoptotic cells after IR (**Figure 24 b, d**). Both groups (SR, EP) show a significant increase of ~5% in the apoptotic fraction after 0.5Gy x-ray. The highly amplifying progenitors in the first differentiation phase (EP) show a 16%, undifferentiated J1 NSCs an 11% elevated apoptotic fraction after 2Gy IR.

The postmitotic differentiation phases (FS, CM) displayed a lower radio sensitivity than the proliferating J1 NSCs (self- renewal and EP) in the previous experiments (**Figure 22**). This could also be shown in the analyses of radiation induced apoptosis via the marker cleaved caspase 3. Progenitors passing the fate specification phase, represented in the second differentiation phase (FS) show almost no apoptotic reaction after 0.5Gy IR. 2Gy of x-ray treatment results significantly in ~ 6% increase in ccaspse 3 positive in the EP population. A comparable increase of apoptotic cells is already detectable after 0.5Gy in the proliferating cell phases (SR, EP). These results show that a nearly a fourfold dose is needed to induce apoptosis in FS than in SR and EP.

The neuro- and glioblasts mirrored in the last differentiation step (CM) show a diverse reaction to IR respecting apoptosis. The lower applied doses reduce the apoptotic fraction significant compared to control samples. The lower dose (0.5Gy) reduces the apoptotic fraction ~6%, while the higher dose (2Gy) enhances the apoptotic fraction ~3% compared to unirradiated samples. In contrast to undifferentiated cells and cells in earlier differentiation phases, showing dose depending induced apoptosis, low dose (0.5Gy) IR leads to a reduced apoptosis in the last differentiation step. Even if the result is unexpected, it corresponds to previous results taken in **Figure 22**. The higher number in viable cells after low dose IR in the later differentiation of J1 NSCs could be explained by supressed apoptosis, not by reactivated proliferation.

2Gy of x-ray induces increased apoptosis compared to unirradiated cells in the fate specification phase, leading to 3% increase in the apoptotic fraction. The induced apoptotic rate after 2Gy is even lower than detected in the second differentiation phase (FS), suggesting that even a higher dose of IR is needed to induce apoptosis in the final differentiation phase (CM).

Taken together we could show that the two proliferating phases (SR, EP) show comparable apoptotic fractions after low dose IR (0.5Gy). The moderate dose of 2Gy induces a significant higher apoptosis in the EP population. Undifferentiated NSCs (SR) show additionally a higher reduction in the proliferating fraction 3h after irradiation. The second and third differentiation phase (FS, CM) show no changes in post mitotic status post IR. The radiation-induced induction of apoptosis in these differentiation phases is clearly reduced compared to SR and EP cells. In FS and CM cells increased apoptosis is only detectable after 2Gy. While the fate specification phase nearly shows no apoptotic reaction to low dose (0.5Gy) IR, the cell maturation phase even shows a reduction in the apoptotic fraction. The diverse radiation responses result in individual radio sensitivities of the differentiation phases, as shown in **Figure 22**.

5.4. Discussion

Radio sensitivity, respective the lethal effect on cells, is clearly linked with cell proliferation, making stem cells dangerously sensitive to IR. This has also been observed previous *in vivo* studies, in whole animal/brain radiation stem cell niches represent areas with the highest apoptosis rate after treatment. To investigate the radio sensitivity of NSCs during neural differentiation, a dose response curve was made using MTT assay (**Figure 22**). In the estimated dose response curve, the number of viable cells 24h post IR of the three differentiation phases during neurogenesis are reflected.

The single differentiation phases representing amplifying progenitors, fate specification phase and maturating progenitors, as well as undifferentiated NSCs show discrete effects to IR. In self-renewing J1 cells IR leads to the highest reduction in the number of cells in a dose dependent manner 24h after treatment as shown in **Figure 22**. X-ray leads to a reduction in the mitotic fraction in J1 NSCs and to elevation in apoptosis which results in the decreased cell number. During the first differentiation step (EP) cells show a distinct response to IR, the naturally higher proliferation rate in this step is less reduced, while the apoptotic fraction is significantly higher than in undifferentiated cells (**Figure 24**). Combined, this leads to a light, but significant increased survival of the early progenitor population, compared to self-renewing NSCs (**Figure 22**). Resulting in a light degradation in the radio sensitivity compared to cells in self-renewal state, represented in the calculated LD_{50} of IR in undifferentiated J1 NSCs (LD_{50} =2.39Gy) and early progenitors (LD_{50} =2.69Gy) (**Figure 23**).

The post-mitotic differentiation phases FS and CM show as expected a higher number in surviving cells (**Figure 22**) compared to the proliferating phases, and reduced radio sensitivity (**Figure 22**), mirrored in the calculated LD_{50} 3.59Gy for the second differentiation phase and 5,99Gy for the third differentiation phase (**Figure 23**). Surprisingly the dose response curve of the last differentiation phase showed an increase in the cell number after IR below 1Gy (**Figure 22**). The following proliferation- and apoptosis experiments conclude that this is the result of a lower apoptosis rate compared to unirradiated cells in this phase (**Figure 24**). J1 cells in the second differentiation phase (FS) show nearly no reaction to lower IR (0.5Gy) respective apoptosis (**Figure 24**).

5.4.1. **Radio sensitivity in proliferating differentiation phases**

The global cellular radiation response can be distinguished in two main mechanisms, cell cycle arrest and apoptosis. Cell cycle arrests, mediated by checkpoint activation is the initial step of damage repair, resulting in decreased proliferation. Radiation induced apoptosis is an intrinsic tissue protection mechanism to eliminate damaged cell.

Previous studies showed that SVZ NSCs are capable to detect and initiate the process of maintaining genomic integrity by slowing progression through the cell cycle [220]. A global mechanism providing damaged cells time to repair DNA damages. In postmitotic progenitors in contrast the radiation response is restricted to apoptosis, leading to an elimination of these population after higher IR doses [220, 263]. Some studies suggested a re-entry in the cell cycle of postmitotic progenitor after IR to repair DNA damages [249, 264, 265]. In our results we could not observe radiation induced proliferation in the postmitotic differentiation phases (**Figure 24**).

The reduced proliferation in NSCs after radiation is predominantly mediated by G2/M- checkpoint activation and altered progression in the cell cycle, associated with regulation of p53 and PCNA [35, 83, 95, 208, 219, 220, 258, 263, 266, 267]. Additionally, IR leads to the activation of the G1/S-

checkpoint and the intra S-checkpoint in self-renewing NSCs, which has been previously shown in the J1 NSC model system [268-270].

Proliferating progenitors show a lack of G1/S- checkpoint activation owed by p21 repression, while self-renewing NSCs also activate G1/S- checkpoint post IR [220, 263, 266, 267]. Roque et al suggests that the absence of the p21-dependent cell cycle arrest at the G1/S transition after DNA damage is a general characteristic of neural progenitors [266]. The lack of the G1/S- checkpoint could explain the higher proliferating fraction post IR observed in EP, compared to self-renewing cells (**Figure 24**). The accessibility of the G1/S- checkpoint in the SR population leads to an increased induction of cell cycle arrest post IR, mirrored in the significant more reduced proliferation, compared to early progenitors (**Figure 24**).

Roque et al could show that most proliferating progenitors entering S phase just after irradiation, died within 4 h post IR during S phase [266], concluding that the lack of G1/S checkpoint is partially compensated by elimination of damaged cells via the intra-S-checkpoint [263, 266]. This suggestion would also explain the significant increased apoptotic fraction in EP cells, compared to SR cells (**Figure 24**). The radiation response of early progenitors is shifted towards apoptosis, reducing the probability to repair radiation induced damages in this phase, compared to self-renewing NSCs. In long term studies the increased apoptosis makes the early progenitor population more sensitive to IR, in comparison to self-renewing NSCs [263, 266]. The limited possibility to repair IR damages leads to a faster elimination of the progenitor population compared to self-renewing NSCs in long term survival [263, 266].

5.4.2. **Radio sensitivity in postmitotic differentiation phases**

Postmitotic progenitors in FS or CM phase left the cell cycle and do not re-enter cell cycle progression. A re-entry in the cell cycle progression in these differentiation phases would mean a change in the differentiation course or de-differentiation. Our results show that IR does not lead to a re-entry of the cell cycle progression in the postmitotic FS and CM cells (**Figure 24**). Which suggest that the progression in differentiation, concerning proliferation is not affected by IR in the later differentiation phases.

In vivo experiment already showed the production of new neurons was significantly dose dependent reduced after x-ray treatment [25, 243, 250, 251, 271]. Li and Cheng postulated 2016 a resistance to radiation induced (5Gy) apoptosis in progenitors after fate determination in mice [272]. This effect could not be repeated in our experiment, even though progenitors in FS and CM are clearly less sensitive to IR than previous differentiation phases (**Figure 22** and **Figure 23**), radiation induced apoptosis is detectable. In the FS state, we could show a reduction in the population in doses above ~1Gy (**Figure 22**, **Figure 24**). The CM phase showed an even lower radio sensitivity than the previous EP phase. IR in the lower dose area (≤1Gy) leads to an increase of the CM population (**Figure 22**). We could show that the increase in the CM population is owed by reduced apoptosis in irradiated CM cells compared to unirradiated CM cells (**Figure 24**). The cell death is a regulatory event in this differentiation phase, which may be inhibited by lower doses of IR, suggesting a IR induced modulation of the differentiation course in the final differentiation phase. The reduced apoptosis post 0.5Gy observed in CM phase may be an indicator for a delay or arrest in the differentiation process. Doses above 1Gy lead to a reduction of the CM phase population and an increased apoptosis compared to unirradiated controls.

Nevertheless, the both postmitotic differentiation phases FS and CM show clearly different radio sensitivities suggesting that the lower radio sensitivity of postmitotic progenitors is not only determined by the absence of proliferation.

Mature neurons are not particular sensitive to apoptosis [95], the higher tolerance of mature neurons to apoptosis occurs by up-regulating survival signalling, including protein kinase B (Akt) pathway [273],tropomyosin receptor kinase A (TrkA) pathways [274], and nuclear factor-κappa B (NF-κB) signalling cascades [99]. The induction of these survival mechanisms in the late differentiation may be the cause of the lower sensitivity towards IR in CM cells than in FS cells.

In the neural differentiation model system ReNcell VM cells, a significant 6-fold increase of anti-apoptotic protein BCL-2 compared to proliferating cells could be measured [95]. The upregulation of BCL-2 is detectable in the same time range as fate determination. The anti-apoptotic BCL-2 protein is suggested to have a neuroprotective function. BCL-2 overexpression was shown to induce enhanced apoptosis resistance [275, 276], extensive neurite outgrowth [277] and a decreased expression of pro-apoptotic BAX and BAK [278] is induced by an overexpression of BCL-2 in neural cells. BCL-2 expression was already shown in J1 NSCs [279].

These data suggest that starting with the fate determination of neural progenitors, the upregulation of anti-apoptotic processes is induced, resulting in an increasing apoptotic resistance in the final differentiation phase [95] and would explain the different radio sensitivities in the postmitotic differentiation phases.

Summary

Most studies agreed that the IR induced apoptosis affects undifferentiated cells and early progenitors dose dependent in the stem cell niches (*i.e.*, proliferating Ki-67-positive cells) [25, 243, 250, 251, 271]. Only few studies investigate further differentiation phases. Mizumatsu et al could show that also DCX positive cells in the SGZ are affected by IR to a greater extent than those that had migrated into the GCL. He suggests that as cells migrated further away from the SGZ became less sensitive to irradiation but could not clear if this response represented different environmental factors or simply the fact that the cells were becoming more differentiated [250]. Excluding the environmental factor in our *in vitro* experiment we can clearly say, that lower radio sensitivity dues the further differentiation, displayed between every differentiation phase.

Based on our results a discrimination of differentiating cells by DCX or ki67 expression is not sufficient. Ki67 expressing cells in the neural stem cell niche are represented by NSCs and high amplifying progenitors (EP), these cells represent the most sensitive fraction IR. In our results we could confirm these findings, both cell phases show comparable sensitivities to IR. The reduced cell numbers 24h after irradiation are a result of decreased proliferation and induced apoptosis. The decrease in the cell number in self-renewing NSCs is mainly mediated to reduced proliferation. Early progenitors show a more stable proliferation after IR and a slightly higher apoptosis.

Taken together we could estimate the specific radio sensitivity of differentiating J1 cells discriminated by their defined differentiation status. Using the characterised J1 model system it could be confirmed that proliferating cells represents the most sensitive fraction. Leaving the cell cycle alone causes not a higher radio sensitivity, which is clearly shown in the unequal radio sensitivities of the post mitotic differentiation phases fate specification and cell maturation. The decedent radio sensitivity of the

following differentiation phases indicates that differentiating J1 cells also gain in anti-apoptotic mechanisms during the differentiation process. The high radio sensitivity of the two proliferating populations present a susceptibility of adult neurogenesis towards IR, since these populations are the base for the input of new cells in further differentiation. Nevertheless, it is open if surviving cells of each differentiation phase show an undisturbed further differentiation.

6. Chapter III: Phase specific radiation effects on functional and morphological differentiation

6.1. Introduction

6.1.1. Ionising radiation and adult neurogenesis

A lot of data determine the importance of adult neurogenesis for hippocampal learning and memory [36, 43, 45, 46, 49, 207, 280-299]. As expected, radiation-induced learning and memory deficits in animal models [300, 301] are accompanied by an increase in hippocampal apoptosis [243, 251], a decrease in hippocampal proliferation and a decrease in adult neurogenesis [251, 302, 303]. It is clear that postnatal neurogenesis plays a critical role in hippocampal function and that radiation-induced alterations in neurogenesis contribute to cognitive deficits [19, 47, 282, 304]. Mice exposed to whole-brain x-rays ranging from 2 to 10Gy at the age of 21 days exhibited persistent decrease in neurogenesis that correlated with spatial memory retention deficits three months after the exposure [305]. A further study, using adult rats that were exposed to a single cranial dose of 10Gy, showed strongly reduced neuronal precursor proliferation and 97% less mature neurons in the irradiated hippocampus compared to sham-exposed hippocampus of control animals [249]. Focal irradiation using a 10Gy dose to the hippocampus of 2-month-old mice, induced significant decrease in neurogenesis and cell proliferation after 3 months. The irradiated mice also showed a decline in cognitive function [13]. Similar results, a coinciding reduction in neurogenesis and cognitive decline, have been observed after whole-brain radiation in several other studies [240, 306, 307].

6.1.2. Radiation effects on neuronal morphology and synaptic plasticity

In contrast to the reduction in cells, little is known about affected physiology in surviving cells in adult neurogenesis post IR. Still, radiation-induced adverse effects on cognition could be promoted by alterations in functional properties of surviving cells that impact the cranial structure and synaptic plasticity. Several studies found modifications in neuronal morphology and synaptic plasticity but could not discriminate if this is caused by IR itself or reduced/disturbed adult neurogenesis.

Parihar and Limol found changes in the neuronal architecture in young neurons after γ-irradiation [308]. 2-month-old mice were cranial irradiated with 1 and 10Gy, 10 and 30 days after the granule cell layer were analysed. To both timepoints a dose dependent decrease in dendric branching and synaptophysin expression was found. In contrast the expression of PSD95 was increased in a dose dependent manner after IR [308]. In a second study proton radiation was used (0.1 and 1Gy) [309]. For 1Gy all previous results could be resumed. For 0.1Gy no differences in the neuronal architecture was found, while the increased expression of PSD95 and decreased expression of synaptophysin was also detectable [309]. In a comparable study adult mice were cranial irradiated with 10Gy γ-radiation [310]. One week and one month after treatment a significant reduction in spine density in neurons of the DG was found. Radiation-induced effects on the expression of proteins involved in neuronal function have additionally been detected. Pyramidal neurons in the CA1 region were also analysed, but no differences in the spine density between irradiated and control animals were found, indicating a region-specific effect [310]. In all three studies also, alterations in the spine morphology was found after radiation [308-310].

Long-term increase in the expression of postsynaptic density protein (PSD-95) and microtubule-associated protein 2 (MAP2) after x-ray exposure has been reported in mice [311, 312]. Previous studies have shown the essential role of these proteins in spine formation, stability and maturation of dendrites [313, 314]. Dendrites, the branched projections of a neuron, are essential for the synaptic contact. Correspondingly, dendritic morphology dictates many aspects of neural function, including signal propagation and information processing. Structural changes often correlate with severe cognitive disorders and mental retardation [315-318].

Studies in rodents have shown radiation-induced alteration in the expression of genes, essential for the regulation of excitatory synaptic transmission [303, 319, 320]. Irradiation was also shown to cause removal of excitatory NMDA receptors from the cell surface and increased surface expression of GABA receptors [312, 321]. These factors are essentially involved in the synaptic plasticity and cell maturation. IR induced changes may result in inhibition or disturbance of the cell maturation. Nevertheless, it should be mentioned that the lowest dose used in these rodent studies was 10Gy.

6.1.3. **Reactive oxygen species (ROS)**

In general terms, ROS have been considered for many years as toxic molecules leading to the oxidation of cellular macromolecules such as membrane lipids, proteins and DNA [322, 323]. ROS have been largely associated with oxidative stress, modifying the redox status of the cell [324, 325] and linked to various diseases [323, 326-331]. Undoubtedly, abnormally high and dysregulated ROS production leads to oxidative stress and cell death, but the regulation of ROS levels in response to cellular demands is critical for normal cell behaviour [332]. Accumulating evidence suggests that ROS could be considered as second messengers involved in numerous signalling pathways [333-335] also playing a role in neurogenesis and neural differentiation [336-338].

The high energy protons generated by IR mainly leads to ejection of electrons from water molecules via hydrolysis in biological systems [339] .In the presence of oxygen, the free electrons interact with oxygen and form superoxide radicals ($O_2^{\bullet -}$). Superoxide radicals then induce cascades generating H_2O_2 via enzymatic or spontaneous dismutation. H_2O_2 in turn generates hydroxyl radicals ($OH^{\bullet -}$) via Fenton reaction or Haber-Weiss reaction [340, 341]. In view of ROS, irradiation implies oxidative stress on biological systems beside direct radiation damages, which can cause long lasting and functional deficits. The production of H_2O_2 and the downstream changes in redox-sensitive signalling pathways can last for months and sometimes years after the initial irradiation [342, 343]. The sustained elevation of ROS in tissues and cells leads to a shift in the redox homeostasis which could alter the course of cell proliferation, differentiation, and long-term survival [344].

Endogenous ROS in cells can be generated via two sources [345]. The major site of ROS production is the inner mitochondrial membrane. During respiration electrons are transited to oxygen from mitochondrial respiratory complex I and III, which generate superoxide ($O_2\cdot^-$). Which is dismutated to hydrogen peroxide (H_2O_2) via superoxide dismutase (SOD2). Additionally, in cytosol, the NADPH-oxidase (NOX) enzymes catalyse the conversion of O_2 into $O_{2\bullet}{}^-$, which is coupled to the transformation of NADPH into $NADP^+$ [156, 346-348]. The generated superoxide is dismutated to H_2O_2 by the cytosolic SOD1. Cytosolic as well as mitochondrial H_2O_2 can be eliminated by catalase or glutathione-peroxidase [349]. Typically, ROS are associated with cell malfunction and disease [350, 351] even if there is a growing body of literature supporting crucial roles for ROS in the regulation of cell signalling [352, 353]

growth [354, 355], Ca^{2+} signalling [356-358], adhesion, and control of redox sensitive gene expression [352].

In the cause of neural differentiation, early progenitors show an elevated ROS level, caused by the energy intensive amplification phase [359]. In the following differentiation steps, neuronal progenitors keep a high ROS level [360-362], while glial progenitors as well as NSCs show low ROS levels [360, 363]. Modifications in the native ROS levels resulted in altered differentiation, mainly regarding induction, proliferation and fate specification [227, 336, 337, 344, 359, 360, 364-366]. This findings strength the suggestion that ROS plays a regulative role in neural differentiation and that radiation induced ROS modifications can led to misregulation in the differentiation process.

6.1.4. **Third aim: differentiation properties of neural progenitors post low dose IR divided by differentiation phase**

We could evaluate the radio sensitivity of differentiating NSCs depending on their differentiation phase (see chapter 2). The three differentiation phases early progenitors, fate specification and cell maturation show a discrete sensitivity, resulting in discriminative survival of the individual populations post IR. Discriminations between differentiation phases, especially in the postmitotic phase is rarely performed even though cells in the fate specification and cell maturation phase display significant differences in the radiation sensitivity. Equally the impact of IR on the functional and morphological differentiation of the surviving progenitors is rarely followed. The J1 model system allows to follow the differentiation of irradiated differentiation phases. To investigate the effect of IR on individual differentiation phases further, we irradiated the three defined differentiation phases and evaluated the impact of IR on characteristic differentiation properties of the particular differentiation phase by functional, morphological, molecular and histochemical markers. The obtained results could help to predict the risk of IR on surviving progenitors and their contribution to remaining neurogenesis excluding environmental factors.

6.2. Material and methods

Migration assay:

To analyse migration, µ-slide chemotaxis (IBIDI) were used (see **Figure 25**). Following the product instruction, the separation area was filed with 15% Matrigel in PBS. The Matrigel was hardened overnight in the incubator (37°C, 5% CO_2). On the next day, the target chamber was coated with laminin (3µg/$cm^{2)}$. To start the migration assay, undifferentiated J1 NSCs were resuspended in the first differentiation media (DI) and seeded in the start chamber (15000cells/chamber). The target chamber was filled with the second differentiation media (DII). The first 24h allows the cells to grow adhered on the surface of the start chamber. One day after seeding the early progenitors were irradiated, controls were placed in the deactivated x-ray tube for the same time. 24h after irradiation the number of cells in the target chamber was counted manually. To exclude previously migrated cells the target chamber was photographed before irradiation, possibly migrated cells were counted and subtracted from the estimated number 24h later. To confirm the if the migrated cells are postmitotic we stained the cells of the target chamber for ki67.

For each data set (0; 0.5 and 1Gy) 12 migration chambers were analysed, in four individual experiments, including variable cell passages. Matrigel concentration, migration time and seeded number of cells were estimated in pre-experiments.

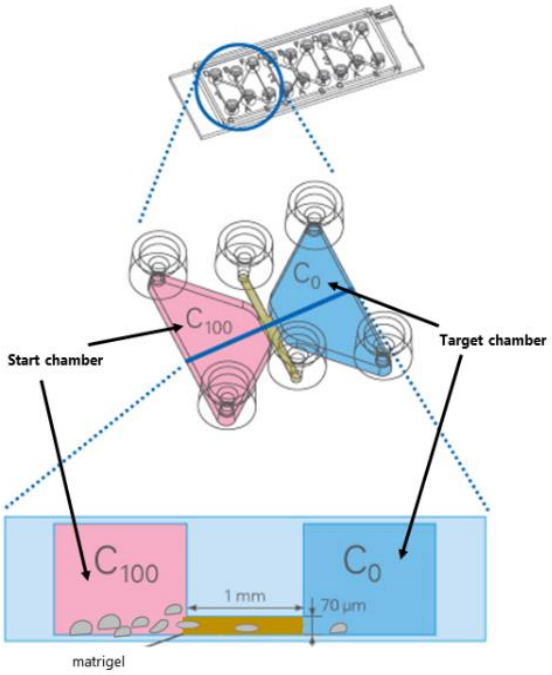

Figure 25 composition of the used migration chamber. The used "µ-slide chemotaxis" is a two-chamber slide. The start and target chamber are separated by a small matrigel stripe (15%), ensuring a stable gradient for over 48h. The start chamber was filled with J1 NSCs in the first differentiation media (DI), the target chamber was filled with the second differentiation media (DII) and coated with laminin. Modified from IBIDI product description.

Fluorescence intensity quantification:

For the quantification of the $K_V1.1$ channel or synaptic protein intensity antibody staining were performed as described previously (4.2 Antibody staining). Stained samples were photographed via a fluorescence microscope using the same exposure time. To estimate each channel intensity imageJ was used. A color histogram was made, separating each channel intensity in 255 bins. On the basis of the plotted histogram noise and signal area was distinguished for each channel. The intensity values of the estimated signal area were exported in mircosoft excel and normalized on each other (red/blue; green/blue; green/red). For the shown diagrams graph pad prism was used. The protocol is based on published fluorescence intensity quantifications [367-370].

For each data set min. 30 photos of each staining and treatment were analysed, out of at least three individual experiments.

Multi electrode analyses- synchrony:

To estimate the synchrony of the activity pattern, measured via MEA recordings Neuro Explorer 5 was used. Datafiles of each measurement were imported in Neuro Explorer 5, allowing to read out the timestamp of each detected spike. These data files were used for the synchrony vs. time tool. This graph shows the distance from this spike to the closest spike (timestamp) in the reference event. This analysis is useful to identify neurons in sync with the reference neuron [178]. To do this, it is needed to select inverted distance. Then, high values indicate spikes that are close to each other.

A high inverted distance shows almost-synchronous spikes with the reference. For each spike that occurred, the distance from this spike to the closest spike (timestamp) in the reference event is estimated. If distance is inverted, one is divided through the closest distance (y= (1/ (distance [s])).

The synchrony analyses were performed for exemplary measurements of a MEA-chip of each treatment (0; 0.5; 1Gy) on differentiation day 4, 8, 11,15. In pre-analyses the mean frequency of each electrode was estimated, the electrode representing the mean spike frequency was set as reference electrode. In following analyses, the inverted distances of each electrode were estimated. Plotted in the shown graph **Figure 30** are the maximal inverted distance of each electrode within 60s recording time. The highest inverted distance estimated was 40, which represents a distance of 0.025s between two spikes (in different electrodes).

Inverted distance: **40 = 1/0.025s**

6.3. Results

6.3.1. Irradiation of the individual differentiation phases concerning IR induced effects on phase specific differentiation properties

Beside reduced proliferation and apoptosis, ionising radiation is suspected to induce changes in the differentiation properties of adult neurogenesis. To investigate the impact of IR on differentiation characteristics, J1 cells were radiated in defined differentiation phases and checked for changes in phase specific differentiation events.

6.3.2. Radiation induced effects on early progenitor properties

Radiation induced effects on migration

The main characteristic of early progenitors is increased proliferation, which makes them particularly sensitive to IR as shown in part 5.3.1 previously. Another key characteristic of early progenitors is initialized migration, which has not been addressed in this work so far. To include the induced migration, we changed the differentiation protocol for this experiment. Instead of simulating migration by reseeding cells on laminin coated surfaces we used a two-chamber system, separated by Matrigel (see 6.2 migration assay). The cells were irradiated (0; 0.5; 1Gy) on differentiation day 2, 24h later, on differentiation day 3 the number of cells in the target chamber were counted.

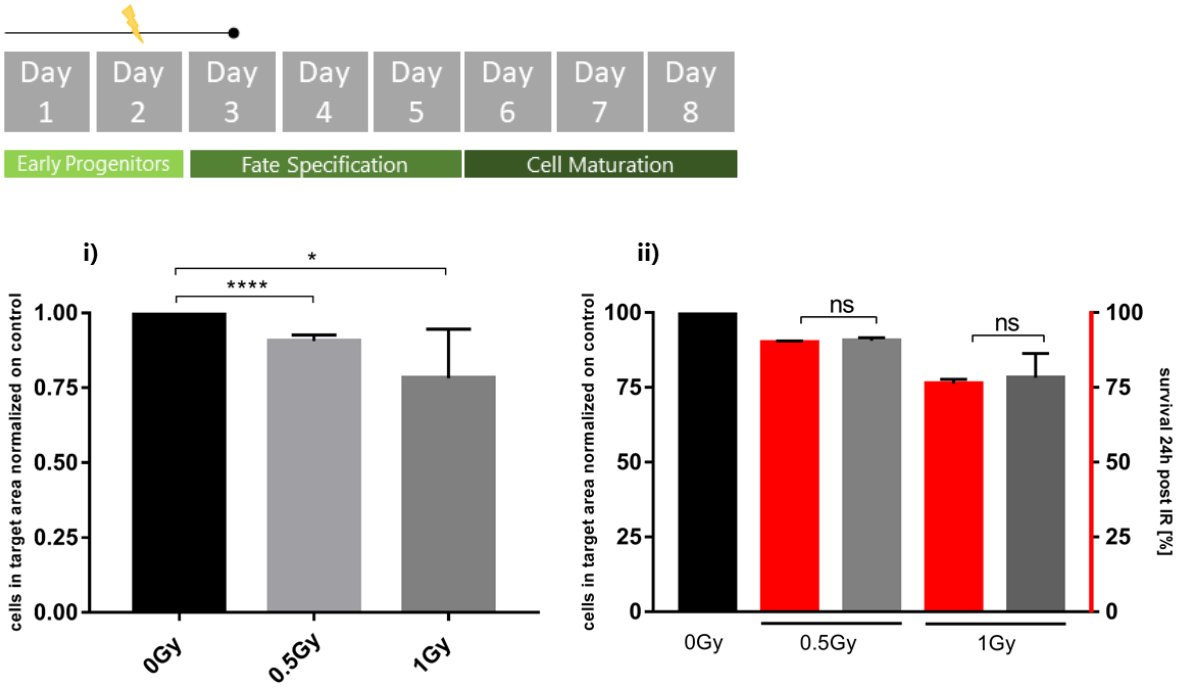

Figure 26 Early progenitor migration 24h post irradiation i) number of migrated cells 24h after irradiation (0;0.5;1Gy) normalized on unirradiated cells. Radiation leads to a significant decrease of cells migrated to the target area. **ii)** The percentage of cells migrated to the target area after irradiation compared to the surviving fraction after irradiation (red bars). The surviving fraction for early progenitors 24h after 0.5 and 1Gy was estimated in **Figure 22**. Plotted mean with SD, unpaired t-test (ns: $p > 0.05$; *: $p \leq 0,05$; **** $p<0.0001$).

As shown in **Figure 26** the number of migrated cells was clearly reduced 24h after irradiation in a dose dependent manner. Early progenitors radiated with 0.5Gy show 10% less cell migrated cells in the target area, radiation with 1Gy leads to a reduction of ~25% (**Figure 26i**). In previous experiments (**Figure 22**) we could show that the surviving fraction of early progenitors 24h after o.5Gy is 90.6% and after 1Gy 76.3% compared to unirradiated early progenitors. These results resemble nearly exactly the percentage of migrated cells after irradiation, shown in **Figure 26 ii**. This data indicate that all surviving cells also migrated in the target area, which leads to the conclusion that IR does not affect the migration of surviving early progenitors, neither the initiation of migration.

To verify that the cells migrated to the target area are postmitotic, we performed antibody staining for ki67. Unirradiated and irradiated (0.5; 1Gy) cells in the target chamber did not show any positive cells for the mitotic marker ki67 on differentiation day 3 (data not shown). The absence of ki67 positive cells reveals that the migrated cells are postmitotic.

6.3.3. **Radiation induced effects on fate specification phase properties**

Radiation induced effects on fate specification

On day four (FS) J1 cells have passed the amplification phase and are postmitotic. The second differentiation step, lasting from day three to five (FS), represents the fate specification phase of differentiating neural progenitors. From day three on, fate specific markers (GFAP, ßTub3) are detectable within the cell population and increasing in the following days. From day six on all cells are determined in their fate and positive for an astrocyte or neuron marker.

To check if the fate determination is influenced by IR, J1 cells were differentiated for six days and radiated on day four with 0; 0.5 and 1Gy x-ray. On day 6 the irradiated and unirradiated cultures were fixed and stained for the astrocyte marker GFAP and the neuron marker ßTub3. Afterwards the percentage of neurons and astrocytes were counted manually on the microscope.

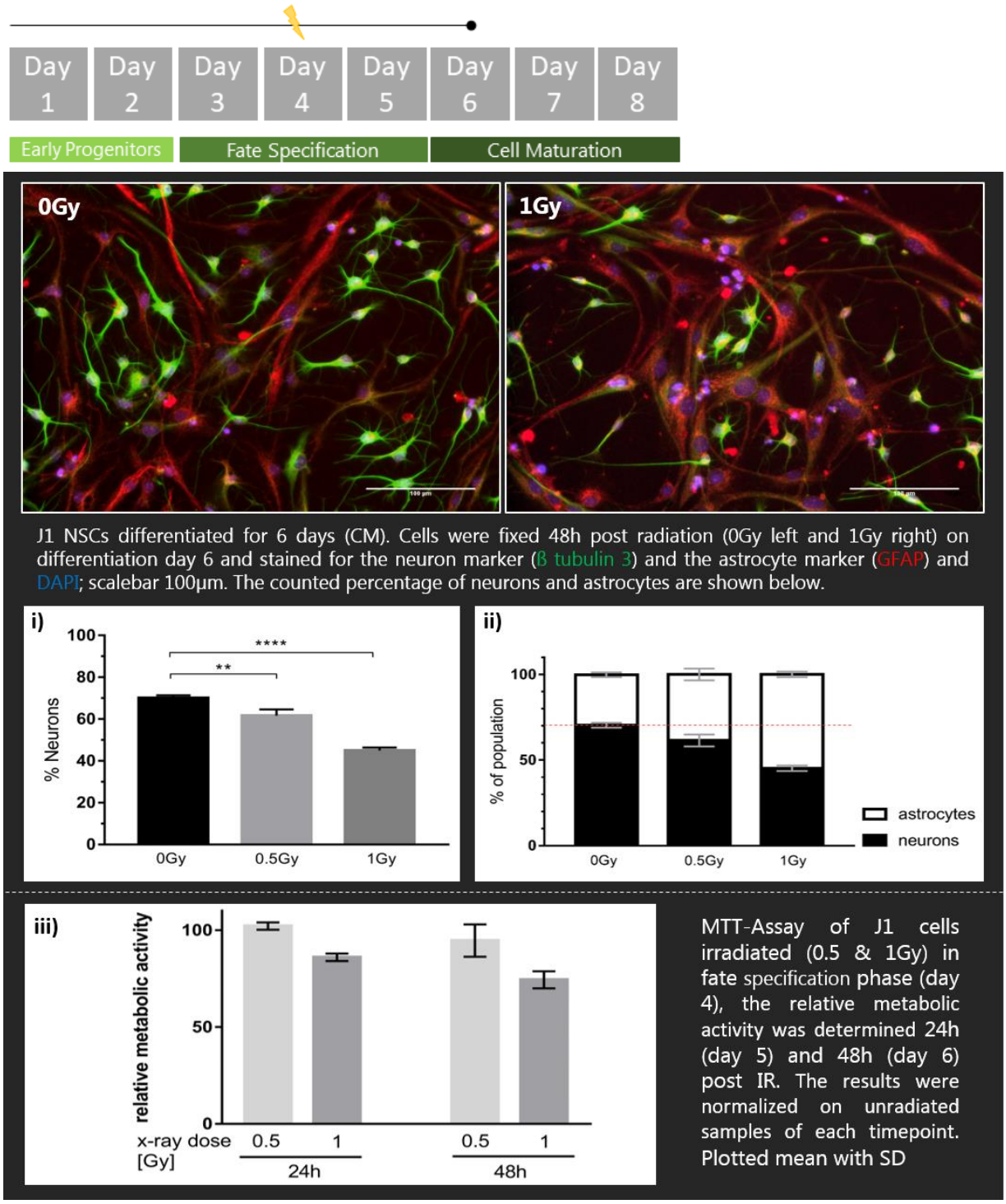

Figure 27 Fate specification in J1 cells, irradiated during FS phase; **above**: exemplary pictures of unirradiated and irradiated J1 NSCs on differentiation day 6, 2 days post irradiation (1Gy). The immunostaining was used to discriminate between future astrocytes (GFAP positive (red)) and future neurons (ß tubulin 3 positive (green)). **i**) bar chart of the counted percentage of neurons in radiated (0.5; 1Gy) and control cultures; unpaired t-test (** $p \leq 0.01$; **** $p<0.0001$). **ii)** Distribution of neuroblasts and glioblasts in cultured samples 2 days after irradiation (0; 0.5; 1Gy) in percent. **iii)** surviving cell number of J1 irradiated on day 4 (0.5,1Gy) 24h and 48h post IR, estimated via MTT-Assay.

To investigate if cell fate specification is affected by IR during the second differentiation step, we used antibody staining against neuron and astrocyte marker proteins. As shown in **Figure 27i** the percentage of neuroblasts decreases after irradiation. The reduction of neuroblasts increases with raised radiation dose, after 0.5Gy 63% of the population can be identified as neuroblasts, after 1Gy ~ 45%. Unirradiated J1 NSCs show ~70% neuroblasts after fate specification (see also **Figure 8**). Parallel to the reduction of ß tubulin 3 positive cells, the percentage of GFAP positive cells increases (**Figure 27 ii**). In all analysed samples (~50000 cells total) only 11 cells were found, that could not be collated to ßTub3 or GFAP. The summarized estimated percentage in neuroblast (ßTub3 positive) and glioblast (GFAP positive) on differentiation day 6, after irradiation is ~100%. which shows that the cell fate is determined on differentiation day 6 also after irradiation (0.5, 1Gy) during the fate specification phase. The fate determination on differentiation day 6, 48h post irradiation indicates that the fate specification is altered but not delayed after IR treatment.

In previous experiments we focused on the survival 24h post IR (see **Figure 22** and **Figure 24**) to compare the altered fate distribution, the survival of J1 in fate specification phase 48h post IR was determined (**Figure 27 iii**). The surviving fraction of J1, 48h post 1Gy irradiation is ~74%, accordingly the population is 26% reduced. The percentage of neuroblasts is ~25% reduced post 1Gy compared to unirradiated controls (**Figure 27 i, ii**). 48h post 0.5Gy, the FS population is reduced to ~94% compared to unirradiated controls, the reduction in neuroblasts measured is ~7%. These results suggest that the reduction in ßTub3 positive cells, 48h post IR, is caused by neuroblast specific apoptosis.

6.3.4. **Radiation induced effects on cell maturation properties**

Radiation induced effects on cell maturation on functional network activity

The final differentiation step, cell maturation, is mainly characterized by the maturation of functional signal transmission in the differentiating network. The base for neural signal transmission are electric excitability, synaptic connections and functional synaptogenesis. To check if the cell maturation is influenced by IR during the final differentiation phase, multi-electrode arrays (MEA) were used. J1 NSCs were differentiated on MEA chips and irradiated on differentiation day 7. Methodical settings, measurement days and cell numbers were chosen as established previously (4.3.5).

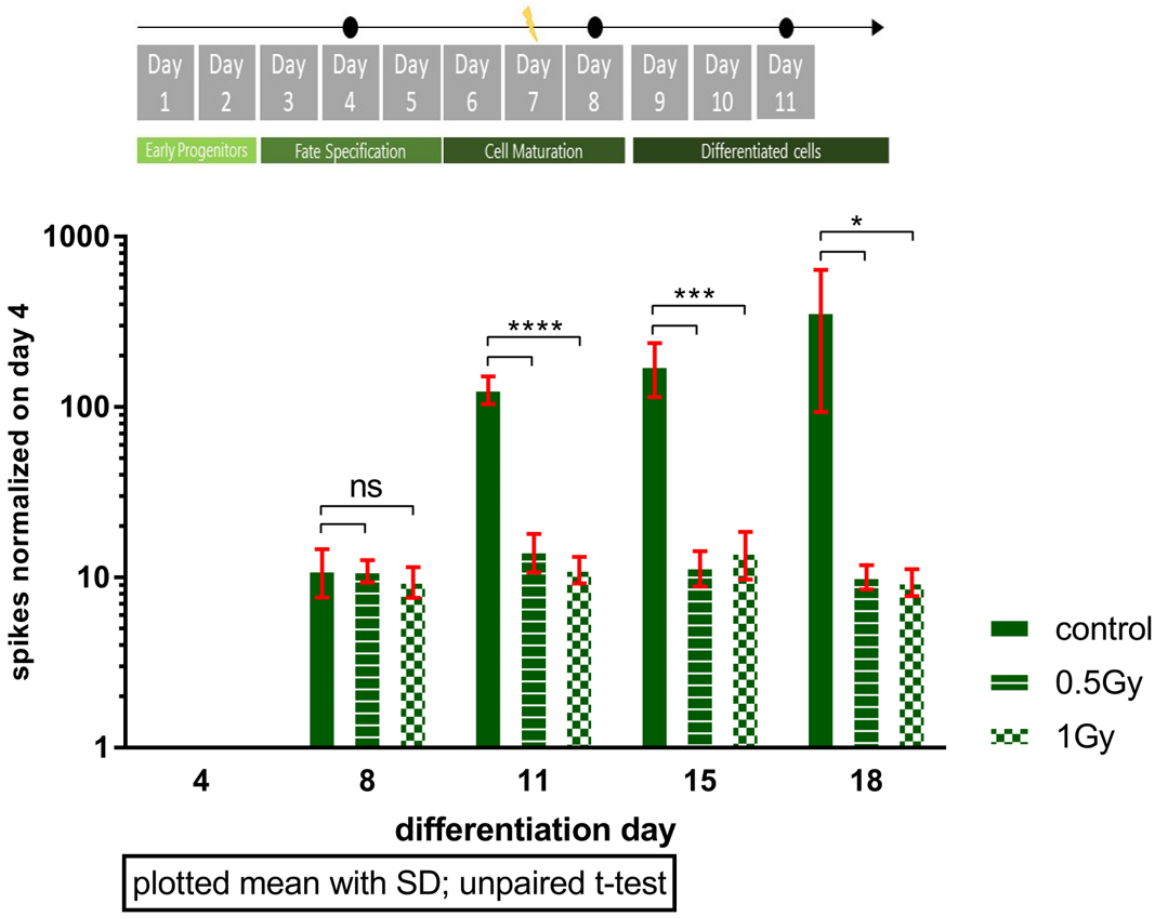

Figure 28 Spontaneous activity of J1 cells irradiated in CM phase (0; 0.5; 1Gy) on differentiation day 7. Spontaneous activity was detected via spike detector within 120s, on differentiation day 4,8,11,15 and 18. Counted spikes were normalized on the number of estimated spikes on day 4 of each MEA-chip. In all measurements no external stimulus was used, all counted spikes are spontaneously generated. n=14 (control); n=4 (0.5Gy); n=4 (1Gy). Plotted mean with SD, unpaired t-test (ns: $p > 0.05$; *: $p \leq 0,05$; *** $p<0.001$; **** $p<0.0001$).

J1 cells show an exponential increase in the spontaneous activity from differentiation day 4 to 18. Irradiation on differentiation day 7 leads to a nearly stable number of detected spikes from differentiation day 8 to 18 independent of the applied dose (0.5 or 1Gy). In both irradiated experiments (0.5 and 1Gy) the samples were significantly different (from day 11 on) to the control experiments, but not to each other. These results indicate a long-lasting stagnation in the spontaneous activity of

differentiating J1 cells post irradiation in the cell maturation phase. Induced apoptosis as the cause of the reduced activity can be excluded. According to previous results (see Figure 22) 0.5 and 1Gy do not reduce the number of cells irradiated in the final differentiation phase. To verify the number of cells, the cells in the MEA chips were counted on differentiation day 11, showing a comparable number of cells in all measured samples. In the previous characterisation (chapter 1; 4.3.5) we could show an increase in coordinated activity from day 8 on, caused by synaptic signalling. To check if the synaptic signalling is disturbed after irradiation we analysed scatterplots of the irradiated samples.

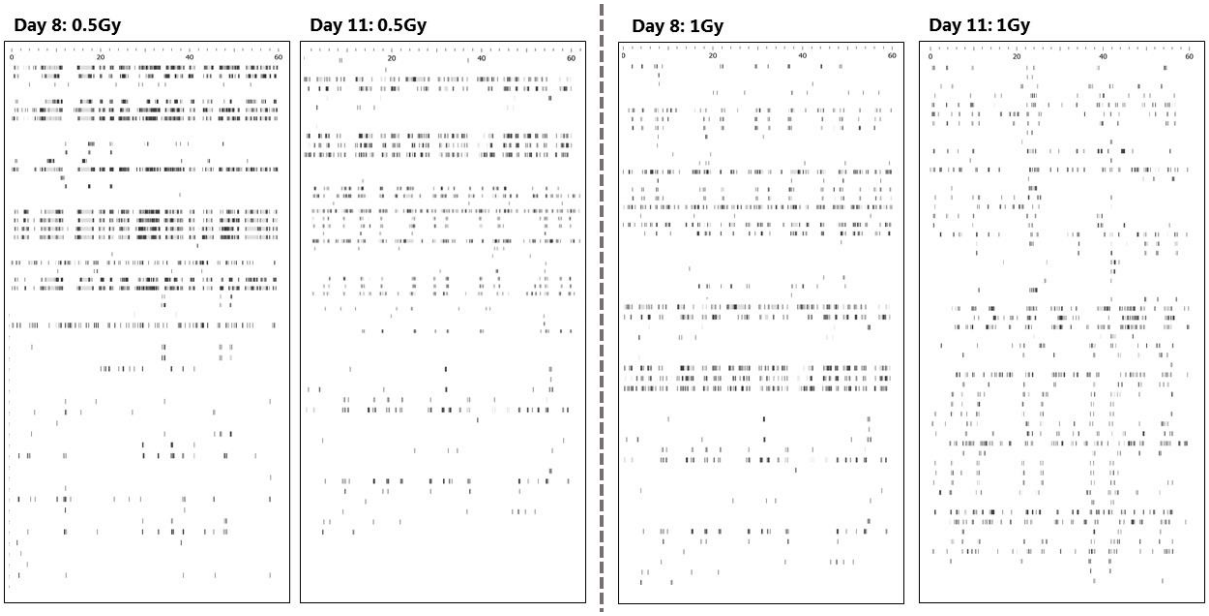

Figure 29 Exemplary scatterplots of representative MEA measurements post irradiation, on differentiation day 8 and 11. **Left**: scatterplot of an individual MEA chip irradiated with 0.5Gy on differentiation day 7, shown are counted spikes on differentiation day 8 and 11. Each line shows a detected spike on the measured timepoint for each electrode over a time of 60s. **Right**: scatterplot of an individual MEA chip irradiated with 1Gy on differentiation day 7, shown are counted spikes on differentiation day 8 and 11. Each line shows a detected spike on the measured timepoint for each electrode over a time of 60s.

As shown in **Figure 29** irradiated J1 cells loose in coordinated activity between differentiation day 8 and 11. In unirradiated samples scatterplots of differentiation day 11 are characterized by highly coordinated activity, with a high synchronous firing rate in all channels (see **Figure 17**). Irradiated samples of both doses (0.5 and 1Gy) show a reduction in the spontaneous activity as well as in coordination over all 59 measuring electrodes compared to unirradiated samples (**Figure 17** and **Figure 29**). The activity pattern of irradiated samples does not differ from results from differentiation day 11 on the following measurement days, day 15 and day 18 (data not shown) which is also represented in the stable spontaneous activity (**Figure 28**). Taken together, irradiation in the cell maturating phase leads to a long-lasting change in the spontaneous activity and activity pattern of J1 cells. Since the results of irradiated samples on differentiation day 8 (24h after IR) are comparable to control samples in spontaneous activity (**Figure 28**) and activity pattern (see **Figure 17** and **Figure 29**) the IR induced changes are not direct (within 24h) detectable. In the follow up of the irradiated samples a clear difference is detectable, both doses (0.5; 1Gy) show no exponential rise in the spontaneous activity (**Figure 28**) neither increasing coordination in the activity pattern (**Figure 29**) as observed in unirradiated cultures. Especially the changed activity pattern suggests that the irradiated cultures failed in establish and strengthen synchronous signal transmission.

To investigate the reduction in synchrony further, the inverted spike distance was estimated in representative measurements of each treatment (0; 0.5; 1Gy). The inverted distance between spikes specifies the synchrony between detected spikes in different electrodes, higher values indicate higher synchrony.

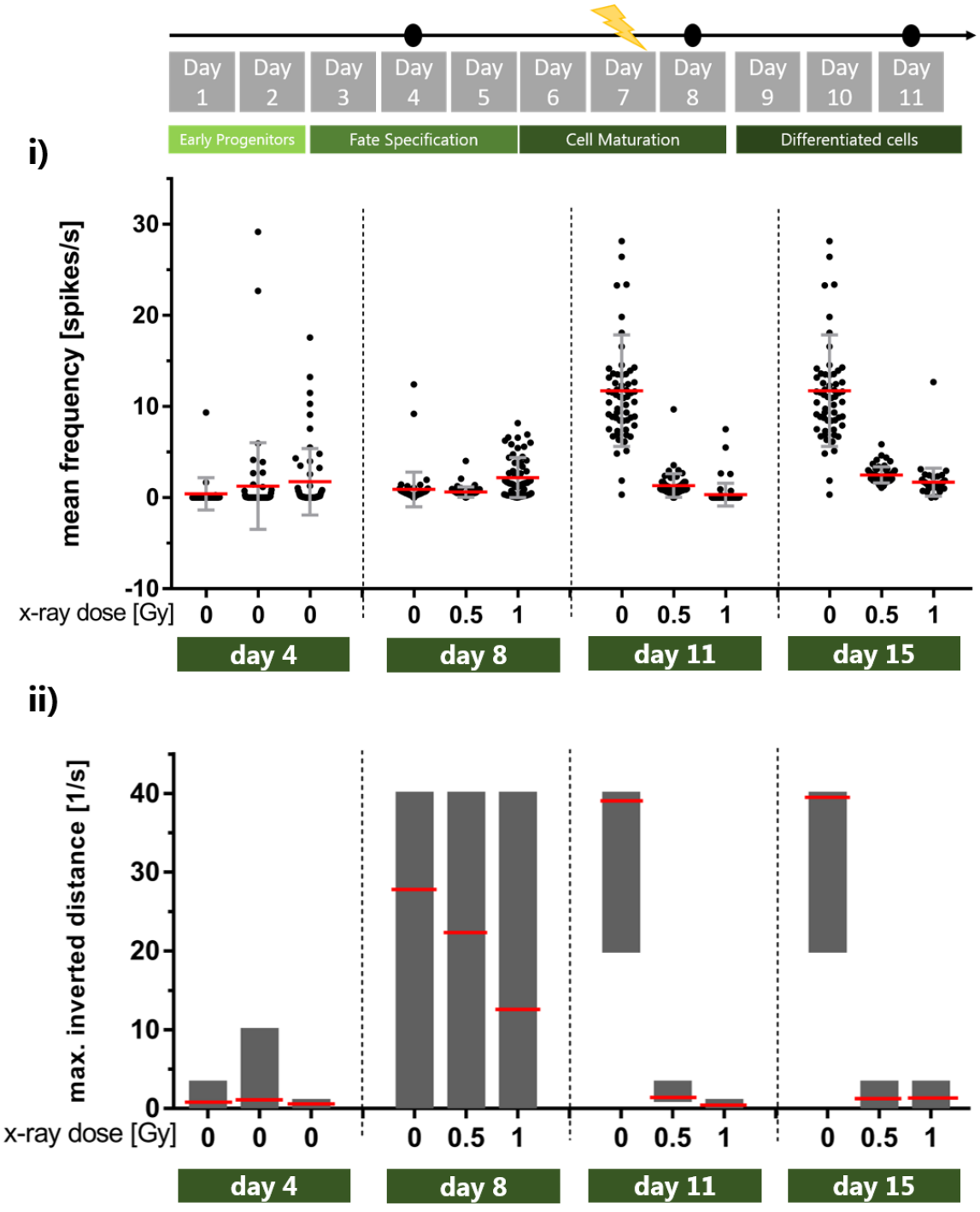

Figure 30 Synchrony analyses in MEA measurements of J1 cells irradiated in CM phase (0; 0,5; 1Gy) on differentiation day 4,8,11,15. **i)** spike frequency of exemplary unradiated and radiated J1 on differentiation day 4,8,11,15. MEA chips were irradiated on differentiation day 7. Plotted is mean spike frequency [spikes/s] of each of the 59 electrodes in one MEA chip, red line indicates mean, grey lines SD. **ii)** Synchrony analyses of the exemplary MEA chips for each treatment (0; 0.5; 1Gy) on differentiation day 4,8,11,15. Plotted is the maximal inverted distance of each 58 electrodes to the reference electrode (electrode with mean frequency). The flying bars reveal the area between the highest and lowest value of each chip, red lines indicate mean. The highest inverted distance estimated was 40, which represents 0.025s between two spikes (in different electrodes). Inverted distance = 40 = 1/0.025s

To quantify the synchrony of the network activity in representative MEA chips over the time we estimated the inverted distance of spikes to a reference electrode. As reference electrode, the electrode with a firing rate representing the mean of all mean frequencies was set. **Figure 30 i)** shows the mean frequency of each electrode of a representative MEA chip of each treatment (0; 0.5; 1Gy) over the recording time of 60s. In the unirradiated sample the mean frequency of all electrodes rises from day 8 to 11, while both irradiated samples show a more or less stable spike rate over the complete time course.

In **Figure 30 ii)** the maximal inverted spike distance (ID_{max}) was quantified, a value representing the synchrony of intra-electrode activity. All samples show a low maximal ID_{max} in all electrodes, indicating no synchrony in the activity pattern on day 4. On differentiation day 8 (24h post IR) all samples show a clear increase in the ID_{max}, the ID_{max} of all samples spread from the highest to the lowest measured values, indicating that there are electrodes in each MEA chip, that recorded synchronic spikes and some that did not. The both irradiated samples (0.5; 1Gy) show a dose dependent reduction in the mean ID_{max} of all electrodes, revealing that less synchronic recordings are measured post IR than in the control culture.

On differentiation day 11 the unirradiated culture shows a high synchrony, with ID_{max} of 20 to 40 for all electrodes, which represents an inter spike distance of 0.05 to 0.025s. This declares, that each electrode was at least one time during the measurement (60s) highly synchronized to the reference electrode, which is a clear sign of coordinated global network activity, which is also shown on day 15.

The irradiated MEA chips in contrast, show a massive loss in synchrony on differentiation day 11, representing the status of day 4. The reduced ID_{max} are also detected on day 15, in the radiated samples (0.5; 1Gy). The measured mean ID_{max} of the radiated samples range between 0.5 and 1.7 on day 11 and 15, which represents a spike distance of 2 to 0.58s. These results suggest, that IR on differentiation day 7 leads to loos of coordinated global network activity in J1 NSCs. Even though, 24h post IR a synchrony between the electrodes were found, a complete decrease is measured on day 11 and 15.

Taken together J1 NSCs irradiated in the cell maturation phase show a lasting stagnation in the spontaneous activity, decreased coordination in the activity pattern, reduced firing rate and loos in spike synchrony. All these results suggest that x-ray treatment during the CM phase leads to loss of synaptic coordination which may be caused by malfunction in synaptic maintenance and/or synaptic transmission.

Radiation induced effects on synaptic protein expression in maturating progenitors

The final differentiation phase is characterised by the functional maturation of the neuro- and glioblasts, represented by the expression of synaptic proteins among others. In previous results we could show that the activity pattern of J1 NSCs is changed after IR in this phase. The coordination of the network activity is controlled by synaptic signalling. To check if altered expression of synaptic proteins is affected by IR, we quantified the presence of synaptic proteins post irradiation in the cell maturation phase.

To quantify the synaptic proteins in neuronal differentiation after x-ray treatment, antibody staining for the pre-synaptic protein synaptophysin and the post-synaptic proteins PSD95 and Gephyrin was used. J1 NSCs were differentiated for 9 days, on differentiation day 7 (CM) cells were irradiated with 0; 0.5; 1Gy. To avoid the influence of IR induced apoptosis doses ≤ 1Gy were chosen (see **Figure 22**).

48h after radiation cells were fixed, stained and photographed via fluorescent microscope. Afterward the fluorescent intensity was quantified using ImageJ.

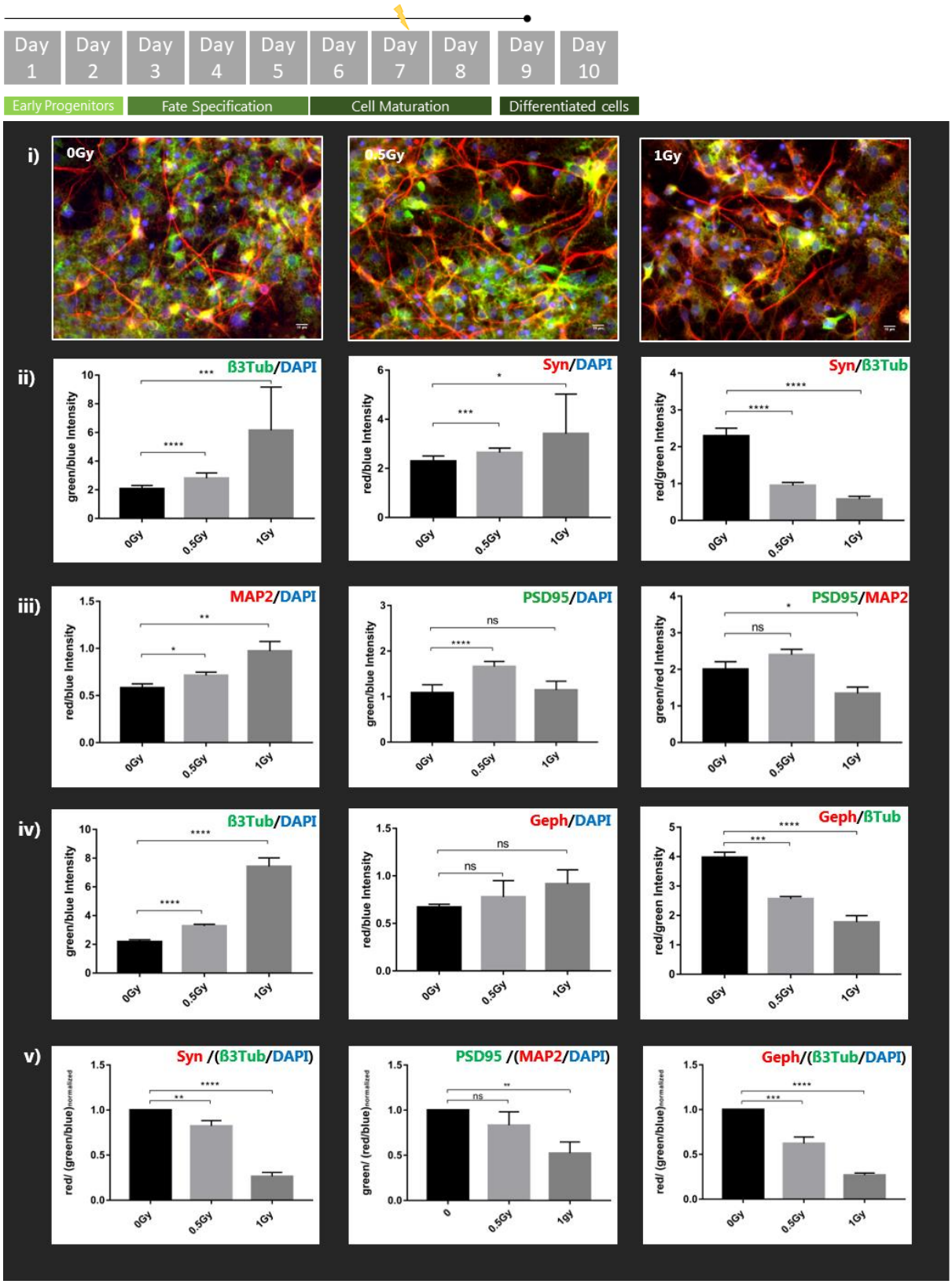

Figure 31 Quantification of synaptic protein fluorescence intensity in J1 cells irradiated in CM phase i) exemplary photos of J1 NSC on differentiation day 9, 48h after irradiation 0; 0.5; 1Gy stained for the neuron marker MAP2 (red) and post-synaptic density protein 95 (green). DAPI (blue), scalebar 10µm. **ii)** quantification of the staining for the pre-synaptic marker

synaptophysin (red), normalized on neuron marker ß-Tubulin 3 (green) and DAPI (blue). **iii**) quantification of the staining for the excitatory post-synaptic marker PSD95, normalized on neuron marker MAP2 and DAPI. **iv**) quantification of the staining for the inhibitory post-synaptic marker Gephyrin (red), normalized on neuron marker ß-tubulin 3 (green) and DAPI (blue). **v**) quantification of synaptic markers normalized on neuron marker per DAPI, in irradiated and unirradiated J1 cells. Unradiated (0Gy) results were set as 1. **ii-v**) plotted mean with SD, unpaired t-test (ns: $p > 0.05$; *: $p \leq 0,05$; ** $p \leq 0.01$; *** $p<0.001$; **** $p<0.0001$).

As shown in **Figure 31** the expression of the pre-and post-synaptic markers in J1 NSCs 48h after irradiation (0; 0.5; 1Gy) were quantified using intensity quantification of each channel. Beside the synaptic proteins all samples were stained for a neuron marker (MAP2 in PSD95 samples and ßTub3 in synaptophysin and gephyrin samples) and the cell core marker DAPI. Normalization of the neuron marker on DAPI shows in all three antibody stainings a significant increase in the neuron marker intensity compared to DAPI intensity in a dose dependent manner (**Figure 31 ii-iv** left blots). Normalization of the intensity of synaptophysin on the intensity of DAPI shows an increase after IR in a dose dependent manner. This is also shown in the intensity of PSD95 normalized on DAPI post 0.5Gy. The intensity of gephyrin normalized on DAPI shows no significant increase after IR. Since J1 cells in the cell maturation phase are postmitotic, the DAPI intensity could be referred as cell number, indicating that the expression of synaptic proteins per cell increases after irradiation for synaptophysin in a dose dependency. For 0.5Gy an increase could also be shown for PSD95.

So, after irradiation J1 cells show a higher intensity of neuronal proteins (MAP2 and ßTub3) and the synaptic proteins PSD95 and synaptophysin per cell. If we normalize the synaptic intensity on the neuronal intensity of each staining, irradiation leads to a significant dose dependent decrease for synaptophysin and gephyrin. PSD95 intensity normalized on the intensity of MAP2 shows a significant decrease for 1Gy x-ray dose.

The conform results of the normalization of the neuron markers intensity on DAPI intensity leads to the suggestion that IR shifts to an increase in neuronal markers in the cultured network, which would also explain the increase in synaptic intensity per DAPI intensity. The fluorescence intensity mirrors the concentration of the defined signal in the analysed staining. Considering this the increase in the neuron marker intensity/DAPI intensity, could also be interpreted as a morphologic change of the neuronal structure, resulting in an increase in neuronal surface. The result, that the intensity for the dendritic marker MAP2 /cell increases less than the intensity of the dendritic and axonal marker ßTub3, suggests that this result could be due to altered neuronal morphology. The comparison of the increase of the dendritic intensity (MAP2) per cell to the axonal and dendritic intensity (ß-tubulin 3) suggest a major increased in axonal growth and a minor increase in dendritic growth post IR. This interpretation strongly agrees with the results from the normalization of the synaptic marker intensity/DAPI. The intensity of the presynaptic marker synaptophysin shows a significant increase post IR. Since presynapses are axonal synapses, an increased axonal surface leads to more presynases. The intensity of the postsynaptic marker gephyrin normalized on DAPI intensity, shows an insignificant dose dependent increase. For the postsynaptic marker PSD95 we could confirm a significant increase in the intensity normalized on the DAPI intensity, post 0.5Gy but not for 1Gy IR. Considering that the dendritic growth post irradiation is a minor effect, the effect of radiation induced alterations of dendritic localized postsynapses is even weaker and can hardly be detected in the experimental setup.

The normalization of the synaptic marker intensity on the neuronal marker intensity shows a decrease for gephyrin and synaptophysin after IR. As shown previously, we detected an increase in the intensity of ßTub3 and synaptophysin normalized on DAPI intensity post irradiation, indicating an induced

axonal growth attended with more presynapses per cell. The normalization of synaptophysin intensity on the ßTub3 intensity shows a highly significant decrease post IR. These results suggest that the radiation induced increase in ßTub3 and synaptophysin follow independent kinetics, which results in a lower presynaptic density post irradiation.

The intensity of both postsynaptic markers PSD95 and gephyrin normalized on the neuronal marker intensity show comparable results. The intensity of the excitatory marker PSD95 normalized on the dendritic marker intensity (MAP2) shows a significant decrease 48h post 1Gy IR, but a slight insignificant increase post 0.5Gy IR. The decease of the PSD95 intensity normalized on the MAP2 intensity post 1Gy, suggest a lower density of the excitatory postsynapses post IR, similar to synaptophysin. The intensity of the inhibitory postsynaptic marker gephyrin normalized on the neuronal marker ß-tubulin 3 shows a significant decrease depending on the IR dose. Indicating a significant reduction in the density of inhibitory postsynapses on the neuronal surface.

The normalisation of the synaptic markers intensities of the normalized neuron markers (**Figure 31 v**) represents the synaptic marker concentration on neuronal surface per cell. For all three used synaptic markers (synaptophysin, PSD95, gephyrin) a significant dose dependent decrease was observed (except PSD95 post 0.5Gy). These results suggest that the density of post- and presynaptic markers per neuron is reduced, in a dose dependent manner 48h post IR in the cell maturation phase.

Taken together we could show conformable responses of immature neurons irradiated in the cell maturation phase. The estimated data suggest an increased axonal and dendritic surface 48h post 0.5 and 1Gy irradiation. The neurons show a lower density of the presynaptic marker synaptophysin and the postsynaptic excitatory marker PSD95 as well as the postsynaptic inhibitory marker gephyrin. The neuronal reduction in synaptic proteins verifies the result from the previously electrophysiological data, indicating that x-ray treatment maturating neurons leads malfunction in synaptic maintenance and resulting in damaged synaptic transmission.

Radiation induced effects on K_V1.1 channel density in J1 cell irradiated in CM phase

In the FS phase of J1 cells an increase in K_{DR} channels was observed by Dr. Bastian Roth (**Figure 14**), a member of this group is the voltage activated K_V1.1, prominent in neuronal cells and associated with adjusting the bio-electrical activity of neurons [371]. K_V1.1 is known to be located on the soma, axons, synaptic terminals and dendrites [372], with a high dense clusters at axonal initial segments determining neuronal polarity [373, 374].

K_V1 voltage-gated potassium channels are of major importance in adjusting the bio-electrical activity of future neurons. Through an ion conductive pore, they mediate the outflow of K^+ across the lipid bilayer of the surface membrane in response to depolarization, regulating the resting membrane potential and excitability, timing and frequency of action potentials during repetitive spike trains, and the release of neurotransmitters at axon terminals [375]. K_V1.1 channels are basal regulators for the excitability of neuroblasts and synaptic transmission. Inactivation of these axonal K_V1 channels accounts for the ability of neuronal depolarization to broaden axonal action potentials and regulate local synaptic transmission in the brain [376]. Thus, the axonal K_V1 channel activity may regulate the strength of synaptic transmission by modulating the action potential duration and firing pattern as well as the extent of action potential invasion into axonal branches [377]. To check if the precondition for synaptic transmission on the base of K_V1.1 presence is disturbed by IR we stained for K_V1.1, post irradiation in the cell maturation phase of J1 cells.

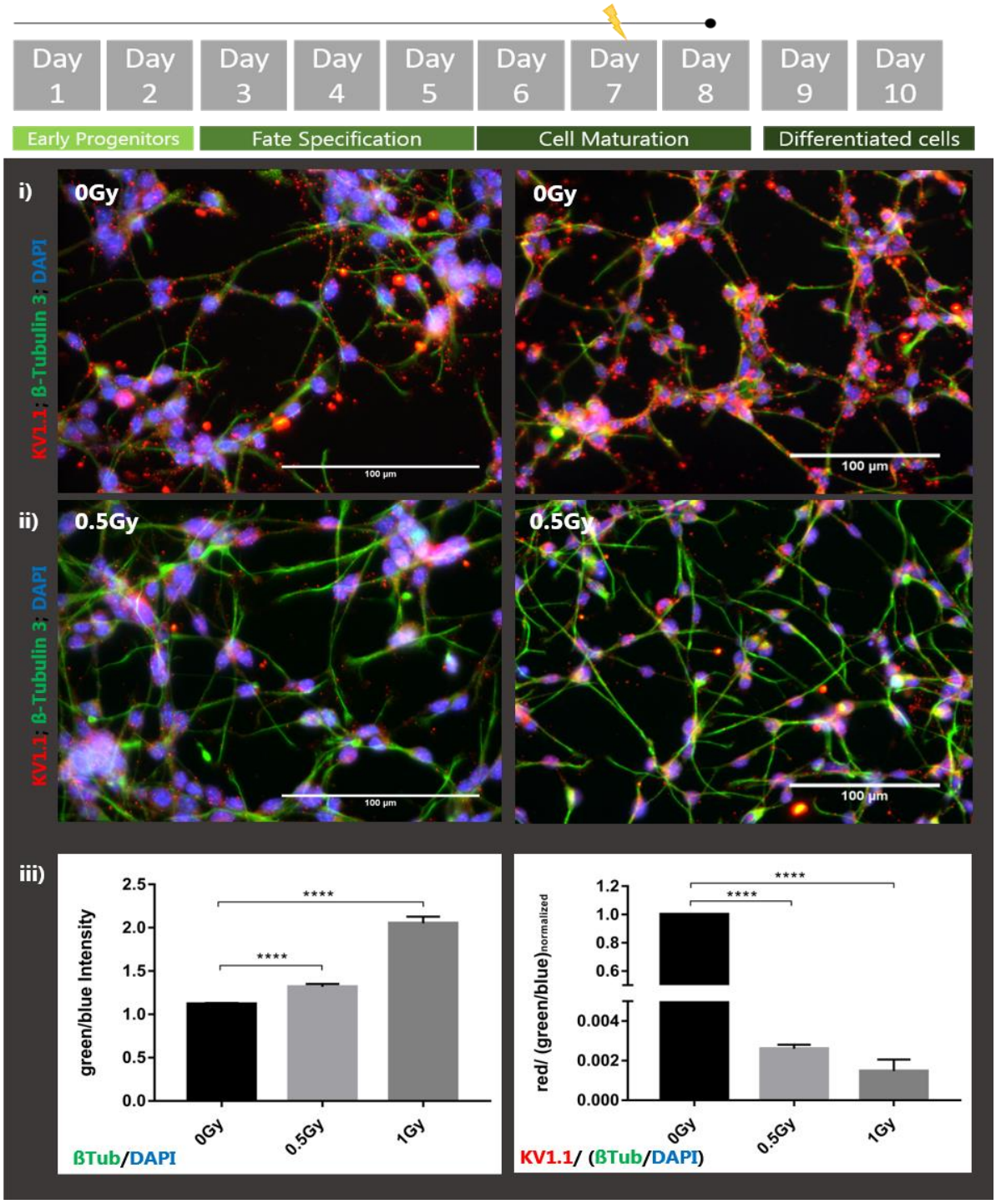

Figure 32 Immunostaining for the voltage-gated potassium channel K_V1.1 in J1 cell irradiated in CM phase (0Gy, 0.5Gy, 1Gy). Exemplary pictures of unirradiated (i) and irradiated (ii) J1 NSCs on differentiation day 8. To quantify the reduction in the K_V1.1presence, the intensity of each channels was analysed. **iii) left:** quantification of neuron marker ß-Tubulin 3 intensity (green) normalized on cell core marker (blue) in irradiated and unirradiated J1 cells. **right:** quantification of K_V1.1 intensity (red) normalized on ßTub3 per DAPI, in irradiated and unirradiated J1 cells. Unirradiated (0Gy) results were set as 1, showing an ~380-fold higher intensity of K_V1.1/(ßTub3/DAPI) than J1 post 0.5Gy and a ~660-fold than J1 post 1Gy.plotted mean with SD; unpaired t-test (**** $p<0.0001$).

The double staining of the neuronal marker ßTub3 and K_V1.1, shows clearly that K_V1.1 channels are expressed in J1 neuroblast on differentiation day 8 (**Figure 32**). The K_V1.1 channels are localized along the axons with a higher density at the axonal endings. Signal for K_V1.1 are also detectable around the cell core, which might be the ER. 24h after 0.5Gy of IR the amount of K_V1.1 signals in the neuroblast seems to be reduced. The remaining K_V1.1 signals seem mainly localized in the axonal terminals and in the ER region.

The quantification of the fluorescence intensities 24h post IR shows an increase in the ßTub3 intensity normalized on DAPI, which indicates induced axonal growth. The normalization of K_V1.1 signal intensity per neuron (**Figure 32 iii**, left) shows a massive highly significant reduction post IR. These results show clearly that 0.5 and 1Gy x-ray leads to a highly significant decrease in the K_V1.1 density in maturating neurons 24h post IR. K_V1.1 channels are key player in synaptogenesis and synaptic maintenance, the reduction of K_V1.1 may be the basal mechanism in higher functional deficits observed in J1 cells post IR in the cell maturation phase.

6.4. Discussion

6.4.1. Radiation induced effects on phase specific differentiation properties

The used J1 model system allows a discrimination between the three phases (early progenitors, fate specification, cell maturation) of neural differentiation characterised by phase specific differentiation events (see chapter 1). In contrast to *in vivo* or primary culture experiments, it is possible to analyse neural progenitors in defined differentiation phases. Each of these differentiation phase shows a distinct sensitivity towards IR (see chapter 2). Published data suggest that beside apoptosis, altered differentiation properties of the surviving cells is a radiation induced occurrence in neurogenesis. To investigate the influence of IR on the characteristics of surviving progenitor cells, we analysed phase specific differentiation events after irradiation.

6.4.2. Radiation induced effects on early progenitor properties

Neural differentiation starts with the early progenitor phase, mainly characterised by a high cell proliferation and initialized migration. Beside the cell amplification the migration to target molecules and along growth factor gradients (e.g. laminin, BDNF), is a basal process in neural differentiation, providing the further differentiation process and the hierarchic structure of neural stem cell niches.

As shown before IR during the early progenitor phase leads to an inhibition of proliferation and induced apoptosis (**Figure 24**), resulting in a reduced cell number (**Figure 22**). In further experiments we could shows that the migration itself is not affected by IR during this phase (**Figure 26**). The reduced number of migrated J1cells is owed by the reduced number of cell post IR. The reduction of the early progenitor population post 0.5 and 1Gy irradiation are caused by cell cycle arrest and apoptosis as described in chapter 5. The migration assay indicates that neither the initiation, nor the migration itself is affected by 0.5 or 1Gy irradiation in the early progenitor phase. These results suggest that the surviving early progenitors show an unaffected further differentiation post IR, concerning migration.

Several studies could show a lack of migrating progenitors in neural stem cell niches post IR [1, 96, 238, 253]. *In vivo* studies could not discriminate whether irradiation affects the migration properties of early progenitors or irradiation induced reduction of the cell population or damages in the environmental structures caused the lack of migrating progenitors. Isolated proliferating cells from irradiated (10Gy) mice SVZs were capable to proliferate *in vitro* but lack the ability to generate migrating neuroblasts [238]. Which indicates that IR may affect the induction of migration in proliferation progenitors. Altered migration behaviour post IR could been found in other cell systems like glioblastoma [378] and other cancer cells [379, 380].

Our results suggest that the migration properties of early progenitors itself is not altered by irradiation and the observed lack in migrating cells is based on the decrease in the population post IR. As shown before (see chapter 2) the proliferation phases in neurogenesis also reflect the highest radio sensitivities during neurogenesis. Our results, that the migration properties of surviving early progenitors are not affected by IR, agree with result of transplantation experiments. Ki67 positive cells isolated from irradiated SVZs, transplanted in unirradiated brains regained the ability to proliferate, migrate and gave rise to neuronal and glial progenitors [249]. The other way around, unirradiated cells transplanted in irradiated brains, show a high reduction on proliferation, migration and neuronal and glial progenitors [249]. Similar results show experiments with a localized radiation technique, precise irradiation (10Gy) of the rostral migratory stream, showed that unirradiated progenitors failed to

migrate through the irradiated area. These data cumulated with our findings suggest that migratory alteration is not due to an intrinsic disruption in the migratory machinery of early progenitors, but rather may be caused to disturbance of environmental migratory signalling *in situ* [238, 381-386].

6.4.3. **Radiation induced effects on fate specification phase properties**

The second differentiation phase (FS) is characterised by the fate specification of postmitotic progenitors. J1 cells in FS phase show a higher radio resistance than the proliferative phases (SR, EP) which may be owed by the post mitotic status of cells.

In previous experiments could be shown that IR during the FS phase does not change the postmitotic status of the cells (**Figure 24**). The unchanged postmitotic status indicates that the differentiation course of the FS progenitors is not retrogressive or discontinued post IR concerning proliferation. To check if the fate specification of differentiating J1 cells is affected by x-rays, FS progenitors were irradiated in the critical differentiation step and analysed in the neuro-glioblast ratio 48h later.

Altered astrocyte-neuron ratio in neurogenesis has been repeatedly observed post IR. Irradiation of J1 cells in the FS phase showed a significant reduction of neuroblasts 48h post 0,5 and 1Gy, in a dose dependant manner. Since all analysed cells of the population are determined in its fate to this time, a delay in the progression of the differentiation could be excluded. The estimated survival of the population 48h post IR, showed that the reduction in in the population resemble nearly exactly the reduction in neuroblasts observed to this timepoint (**Figure 27**). These results lead to the conclusion that future neurons in this differentiation phase reveal a specific sensitivity to IR compared to future astrocytes. An early-neuroblast-specific radiation induced apoptosis could also be shown *in vivo* [250, 272]. Li et al. failed to observe any apoptotic cells that were positive for GFAP in the intermediate progenitor population, as well as apoptotic cells positive for late neuronal markers post IR (≥ 5Gy). Combined with our results, this suggest that neuronal progenitors pass a transient radiosensitive status during early neuronal fate specification. Li et al. suggested that in later neuronal differentiation the neuroblast loss the specific sensitivity towards IR [272]. Our data may confirm this suggestion, based on the significantly lower radio sensitivity of the next differentiation phase (CM) (chapter 2), indicating that neuroblast specific sensitivity in FS is transient.

The neuroblast specific sensitivity towards IR in the FS phase reflects a particular endangerment for adult neurogenesis, selectively affecting the input of future neurons in the hippocampus. Focusing neurogenesis, the evaluation of the lower radio sensitivity in the FS phase has to be relativized.

In our experiments we could also observe that the radiation induced loss of cells seems to be delayed (**Figure 27**). IR induced apoptosis during neural differentiation is usually terminated 24h post treatment [95, 243, 248, 250, 263, 272, 387, 388]. In the FS phase we could not observe a loss in the cell number 24h post 0,5Gy, while 48h post IR the population was slightly reduced to 94% (**Figure 27**). Also post 1Gy we observed a more reduced cell number 48h than 24h after x-ray treatment, indicating varied apoptosis kinetics.

Irradiation is known to activate p53 and induced apoptosis. It has been showed that the majority of NSCs did not demonstrate p53 upregulation after irradiation [272], whereas increased p53 nuclear immunoreactivity was observed in early progenitors and neuroblasts after irradiation *in vivo* [243, 258, 263, 272, 389]. Also neurons show a p53 dependent radiation induced apoptosis *in vivo* [390]. These data suggest that NSCs and neuronal progenitors as well as neurons show differential apoptotic response after IR. It has been described that in early progenitors, future neurons and neurons the IR

induced apoptosis is mediated by p53 [243, 258, 263, 272, 389]. p53 knockout mice showed a massive reduction of apoptotic cells and a significant elevation in the number of immature neurons after lower doses (below 5Gy) compared to wildtype mice [389]. Which leads to the suggestion that the neuronal specific radio sensitivity in the fate specification phase is p53 mediated. Also the unchanged number of young astrocytes and glioblasts in the p53 knockout mice [389] indicates that IR does not lead to p53 mediated apoptosis in this progenitors.

There is no literature of the apoptotic response of post mitotic progenitors passing fate specification to IR. But the collected data suggest that the glioblast-neuroblast specific radiation response is established in the FS phase. The acute radio sensitivity in the second differentiation phase is restricted to future neurons and may be caused by neuronal specific signalling. Astrocytes resemble the highest radio resistance in the adult brain compared with neurons and oligodentrocytes [5, 391]. Single irradiation with doses below 8Gy did not affect the numbers of GFAP-expressing astrocytes in vivo [5, 391]. The high radio resistance is caused by differential radiation response [215, 392-395] and more effective ROS buffer systems [5, 396-398]. Evolvement of these astrocyte specific characteristics may contribute to the higher radio resistance of future astrocytes during FS phase.

ROS as mediator for cell type specific radiation sensitivity in FS phase?

Differential cell type specific development of astrocyte and neuronal characteristics concerning radiation response and ROS tolerance during this differentiation phase may cause the specific radio sensitivity of future neurons, which require the acute loss of new neurons post IR [250, 272].

About differences in early glioblasts and early neuroblasts in this specific differentiation phase is little known. Nevertheless it has been shown that postmitotic neuroblast show one of the highest native ROS level estimated during neurogenesis [360-362].The elevated ROS level is exclusive characteristic for neuronal progenitors, so that it is even used to distinguish neuronal and glial progenitors [360, 364]. During neurogenesis the native ROS level rises with induced differentiation, amplifying early progenitors show a higher ROS level than NSCs. In the further differentiation future neuroblasts enhance the ROS level while future astrocytes lower the ROS level [360-362]. The lower ROS level of glioblasts may be a hint to developed ROS buffer systems in future astrocytes.

Radiation induced elevation in the cellular ROS level has been shown during neurogenesis [399-401]. Neural precursor cells isolated from rat SVZs *in vitro* showed a significant increase in ROS after exposure to x-rays, and compared to controls, the levels of ROS were elevated at each dose and post irradiation time [389]. ROS levels exhibited statistically significant fluctuations, increasing in a dose-dependent manner over the first 12 h before dropping at 18 h and rising again at 24 h. The elevated ROS levels also showed an important correlation between apoptosis and increased ROS [389]. Limoli et al. linked the differential apoptotic peaks with IR induced ROS mediated oxidative stress-activated pathways [389], which may explain the delayed apoptotic reaction observed in future neurons in FS phase (**Figure 27**). p53 dependent ROS induced apoptosis has been shown in different phases of neural and neuronal differentiation [349, 388, 389, 402-405].

The high native ROS level combined with the IR induced ROS elevation may determine the specific radio sensitivity of neuronal progenitors in the FS phase. It has been shown that astrocytes are more resistant towards radiation/ROS induced apoptosis [406]. Marker et al. hypothesized this resistance is caused by a higher vitamin E content in astrocytes, the main protection for membrane lipid peroxidation [406-408]. Controversial results showed that neurons acquire higher levels of ROS prior to undergoing apoptosis [328, 360, 409-411] but did not include the higher baseline levels of ROS in

neurons. IR induced ROS together with high intrinsic levels of ROS may result in a level of oxidative stress that cannot be compensated by intrinsic mechanisms operating in neuronal progenitors.

Summary

Reduced neuron/astrocyte ratio is an often-observed result in neurogenesis post IR [204, 227, 249, 263, 272, 332, 412-418]. *In vivo* studies showed a long-lasting decline in the production of new neurons as well as an acute loss of neuroblasts and new neurons post IR. The generation of astrocytes seems not (or less) affected by IR which leads to a shift in the astrocyte-neuron ratio observed in long time studies [249, 251, 302, 419, 420]. Since the generation of new neurons is described as the critical function of adult neurogenesis, the reduction of the neuronal linage is often associated with neurological deficits, observed as late effect post cranial radiation [5, 25, 421, 422]. Several studies could show that IR induces molecular changes in the proliferating fraction and the cellular microenvironment, leading to limitations in the differentiation potential of NSCs and early progenitors [26, 227, 389, 423-427]. These changes in the differentiation potency explains the long-lasting loss of neurons but not the acute reduction of new neurons [97, 218-220, 428-430]. The cause of the acute reduction of new neurons is often hypothesized with paused differentiation, since immature neurons show a relative low radio sensitivity [218, 220, 244, 431]. Our result combined with *in vivo* data [250, 272] suggest that temporary neuron specific radio sensitivity in FS phase may be the cause of the acute loss in new neurons post IR.

6.4.4. **Radiation induced effects on cell maturation phase properties**

The final phase in neural differentiation is cell maturation, this differentiation phase resembles the lowest radio sensitivity of the three differentiation phases (see chapter 2). The final differentiation phase is characterised by the establishment of functional signal transmission in the differentiating network. The base for the neuronal signal transmission are electric excitability, synaptic connections and functional synaptogenesis of immature neurons. Since the cell maturation is a complex process we checked for radiation induced modulation on different levels post IR.

24h post IR (0.5,1Gy) we could verify a massive reduction in the density of voltage-gated potassium channels KV1.1 in the new neurons (**Figure 32**). The neuroblasts show an increased axonal and dendritic surface 48h post 0.5 and 1Gy irradiation (**Figure 31**). Additionally, we could reveal a lower density of the presynaptic marker synaptophysin and the excitatory postsynaptic marker PSD95 as well as the inhibitory postsynaptic marker gephyrin. The reduction in synaptic proteins density fits to the result from the electrophysiological measurements, which showed malfunction in synaptic transmission (**Figure 29**, **Figure 30**) and spontaneous activity up to eleven days post IR (**Figure 28**). Taken together J1 cells irradiated in the CM phase show a lasting stagnation in the spontaneous activity, decreased coordination in the activity pattern, reduced firing rate and loos in spike synchrony on the functional level. All these results suggest that x-ray treatment during the final differentiation phase leads to loss of synaptic coordination which may be caused by malfunction in synaptic maintenance and/or synaptic transmission. The higher synchrony of the activity pattern on day 8 (24h post IR) than in the following days (**Figure 29**, **Figure 30**) indicates no direct loss of the synaptic transmission. These data suggest even more that IR during the final differentiation phase affects the synaptic maintenance.

The disrupted synaptic signalling in the CM phase of J1 cells post irradiation may also explain the inhibition of native apoptosis observed previously in chapter 2 (**Figure 24**). 0.5Gy reduced the apoptotic fraction significant compared to control samples while the 2Gy enhanced the apoptotic fraction ~3% compared to unradiated samples. During the CM phase, the so called programmed cell death, is a final differentiation event. It is known that the apoptotic signalling is mediated via synaptic transmission [30, 40, 88, 115, 174, 206, 209, 210]. The dysfunction in synaptic signalling observed in maturating neuroblasts (**Figure 29**, **Figure 30**) may disturb the apoptotic network signalling. The inhibition of programmed cell death via low dose IR, reflects a malfunction in terminal differentiation during adult neurogenesis.

Long-lasting reduction in synaptic density post a single dose of cranial irradiation (5Gy), has also been observed *in vivo* [432, 433]. Croniola et al. showed a 20% reduction in postsynaptic density in dentate granule cells 2 months post-irradiation [432]. More detailed analyses of spine morphology showed a significant increase in thin spines and a significant decrease in mushroom spines in neurons in the dentate gyrus [310] suggesting a potential change in synaptic activities following cranial irradiation. All these studies suggest enhanced oxidative stress as keyplayer in the observed modifications post IR. The structure and density of dendritic spines are important factors in synaptic functions, and dynamic changes in the shapes and sizes of dendritic spines can affect synaptic stability and synaptic strength [308, 310, 312, 318]. These studies indicate that maintenance of synaptic connections, via maintenance of dendritic synapses, may be fundamental for deficits in cognitive functions following cranial irradiation [310, 432, 433].

ROS as mediator for radiation induced functional deficits in CM phase?

Recent data suggests that ROS should be considered as second messengers involved in numerous neuronal signalling pathways in health and disease [333-335, 398]. Indeed, ROS fulfils several criteria of second messenger molecules, such as the ability to amplify a cellular signal triggered by the primary ligand. In addition, ROS have the special attribute of “chemical interconversion” [434]. The superoxide anion derived from NOX enzymes is rapidly converted into hydrogen peroxide, either spontaneously or enzymatically by SOD. In turn, hydrogen peroxide can be transformed into the hydroxyl radical in the cytoplasm [435]. Another feature of ROS, consistent with their role as possible second messengers, is that the synthesis of superoxide anions and hydrogen peroxide (but not hydroxyl radicals) is finely regulated [332, 436-438]. The need of the precise regulation becomes apparent regarding axonal growth depending on ROS (see **Figure 33**) [332].

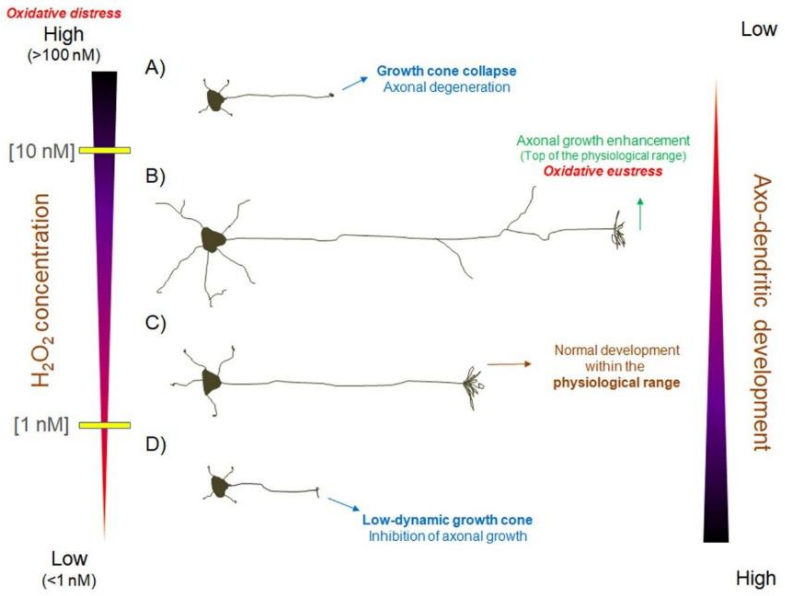

Figure 33 Influence of ROS on neuronal axon growth. Hydrogen peroxide (H_2O_2) the most stable ROS, drives either negative or positive outcomes for neuronal development depending on its concentration. A) Abnormally high and deregulated H_2O_2 production favours an oxidative distress condition, leading to the collapse of the axonal growth cone in neurons and subsequently axonal degeneration. B, C) Elevated levels of ROS within the physiological range (10nM) enhances both axonal and dendritic growth (B). Moderate to low H_2O_2 concentrations are instrumental for normal neuronal axonal growth, as well as axonal regeneration (C). D) Abnormally low H_2O_2 concentration (by instance, below 1nM), which may occur due to the loss of function of the NOX 2 complex, impairs both the polarization of hippocampal neurons and axonal growth, inhibiting neuronal development. Modified from Wilson [332]

Sies postulated recently that the physiological concentration of ROS ranges between 1 and 10nM [325], higher and lower concentrations are referred as toxic and lead to inhibition of axonal and dendritic growth (**Figure 33**) [434, 439-441]. Within the physiological range, elevated levels of ROS promote both axonal and dendritic growth [332, 442] compared to normal development [441, 443-445]. Irradiation in the CM phase of J1 cells showed an increase in axonal and dendritic markers 48h post IR (0.5,1Gy) compared to unirradiated J1 cells (**Figure 31**), indicating an elevated ROS level within the physiological range. Wilson et al. suggest that ROS promote axonal development through ER Ca^{2+} release mediated by the ryanodine receptor (RyR), which activates Rac1 [442]. Rac1 is GTP-binding proteins that control the assembly and disassembly of the actin cytoskeleton [446]. However, the postulated signal way may not be the only ROS mediated regulation mechanism for modified axonal and dendritic growth. Both F-actin and microtubules are susceptible to redox posttranslational modifications that affect the dynamic properties of the cytoskeleton and this may have a direct effect on the morphology of neurons during maturation [447-450].

It seems that highly regulated ROS levels are instrumental in shaping neurons, which is crucial for mature neuronal functions such as synapses and neurotransmission [442]. The similar phenotype (increased axonal and dendritic growth) in our experiments leads to hypothesis that the applied x-ray doses (o.5,1Gy) leads to an elevation in the ROS level, within the non-toxic range. This disruption in the precise ROS regulation may lead to misregulation in downstream signalling pathways leading to malfunctions in neuronal maturation.

The reduced density in of $K_V1.1$ channels as well as synaptic proteins (**Figure 31**, **Figure 32**) may be a side effect of the raised axonal and dendritic growth. The uneven reductions in the synaptic proteins

as well as the $K_V1.1$ channel suggests independent regulation. It has been shown that Rac 1 modulates development of excitatory synapses [451, 452]. It is also known that the expression and recruitment of synaptic proteins, as well as the synaptic maintenance is activity dependent [111, 174-177]. Spontaneous activity can regulate the level of excitability of cells by controlling the expression of ion channels generating it, synaptogenesis and survival [49, 111, 136, 174-177, 180, 183-188]. We observed a stagnation in the spontaneous activity post IR in the maturation phase (**Figure 28**). The massive reduction in the spontaneous activity compared to unirradiated samples suggests that the deficit in spontaneous activity also results in a deficit of activity-dependent processes in neuronal maturation [180-182]. The depletion of synaptic signalling observed post IR may be the outcome of reduced activity caused by decreased excitability. The excitability of neurons is defined by ion channel layout and activity. IR as well as ROS is known to affect various ion channels, like intracellular Inositol 1,4,5-trisphosphate (IP_3) receptors or RyRs [442, 453-455]. The main function of these receptors is the release of Ca^{2+} from the ER in response to activation of the plasma membrane receptors and phospholipase C. The released Ca^{2+} mediates further signalling circuits including glutamatergic, adrenergic and cholinergic signalling.

Beside the intracellular Ca^{2+} channels, it is known that among others, potassium channels are mediated by IR/ROS [456, 457]. Many types of K^+ channels including voltage-gated (K_V) [458-466], 2-P domains [467], calcium-activated (K_{Ca}) [468] and G-protein coupled inwardly rectifying (GIRK) [469] K^+ channels can be modified by oxidizing agents *in vivo* and *in vitro*. K^+ channels modulation plays a potential role in neuronal radiation response [464, 470]. KCNB1, a voltage gated potassium channel, form when exposed to H_2O_2, oligomers held together by disulfide [471, 472]. KCNB1 oligomers are detected in the brains of mice post oxidative stress [471, 473]. These oligomerized KCNB1 channels do not conduct current *in vitro* [473] and probably *in vivo* [473]. It has been suggested that moderate levels of oxidized KCNB1 channels affect hippocampal and cortical excitability and are suspected to cause spatial learning and memory impairment experienced during normal aging or post oxidative stress [456]. Another family of K^+ channels, K_{Ca} channels play a role in the regulation of a number of physiological functions including neuronal excitability [474]. K_{Ca} channels show a complex redox-dependence. A number of their methionine and cysteine residues can be oxidized, leading to changes in the permeability and gating properties of these channels [468, 475, 476]. It could been shown that in hippocampal neurons, ROS enhance K_{Ca} activity via an increase in the open probability [477]. Regarding the wide influence of ROS, respectively low dose IR, on ion channel functionality, it is supposable that the observed reduction in spontaneous activity (**Figure 28**) is mediated via altered excitability post IR.

A direct interaction between $K_V1.1$ and ROS is not known [457]. The reduced density of $K_V1.1$ found 24h post IR in maturating J1 cells (**Figure 32**) points more to reduced expression than oxidation in $K_V1.1$ channels. During synaptogenesis $K_V1.1$ channels are involved in regulating neuronal excitability and modulating activity[374]. Some studies suggest a that $K_V1.1$ plays a key role in induced neuronal apoptosis [478-482]. A protein kinase C (PKC) dependent pathway regulates $K_V1.1$ gene expression and leads to neuronal apoptosis via permanent up regulation of $K_V1.1$ expression [482]. The pro-apoptotic pathway could converse act as anti-apoptotic pathway, preventing apoptosis by down regulating $K_V1.1$ expression [482]. $K_V1.1$ inactivation has already been postulated as endogenous neuroprotective mechanism in primary rat neuron [479, 483]. Considering the possible neuroprotective function, the reduced $K_V1.1$ level, could also act as anti-apoptotic mechanism in maturating neuroblasts. This hypothesis would also explain the reduced apoptosis post 0.5Gy observed in CM phase (**Figure 24**).

Summary

Taken together we could identify several functional deficits in progenitors passing CM phase post IR. In contrast to the earlier differentiation phases (EP, FS) radiation induced apoptosis plays a minor role. J1 cells in CM phase show the lowest radio sensitivity during the J1 differentiation (**Figure 22**). Post irradiation in CM phase we could observe a long-term survival (**Figure 28**), typical neuronal marker expression (MAP2, ßTub3; **Figure 31**), synaptic marker expression (**Figure 31**), typical ion channels expression (**Figure 32**) and spontaneous activity in the cells (**Figure 28**, **Figure 29**, **Figure 30**), suggesting an unaffected maturation. A closer look reveals a modulation in these characteristics, as lower density in synaptic proteins and $K_V1.1$ channels (**Figure 31**, **Figure 32**), increased dendritic and axonal growth (**Figure 31**), reduction in spontaneous activity (**Figure 28**, **Figure 30**) and malfunction in coordinated signalling (**Figure 29**, **Figure 30**), in the irradiated cultures. Especially the lost in the ability to generate coordinated, synaptic network signalling indicates a malfunction of maturating progenitors in adult neurogenesis. A growing body of data suggests that the functional deficits in CM cells may by mediated by disturbed ROS signalling post IR.

6.4.5. **Overview of IR induced effects on differentiation phase specific differentiation properties**

Each differentiation phase is defined by typical differentiation events (see chapter 1). The homogenous differentiation of the J1 cells offers the possibility to investigate the influence of IR on the properties of the separated differentiation phases.

The first differentiation phase, EP, is characterised by amplification of the cell number and the initiation of migration. In our experiments we could reveal that IR reduces the early progenitor population via IR induced apoptosis and reduced proliferation (see chapter 2; **Figure 22**, **Figure 24**). The reduced population of early progenitors post irradiation did not show differences in the migration, neither the initiation of migration. Which indicates that surviving early progenitors are able to induce further differentiation events (e.g. migration) post IR.

The second differentiation phase, FS, is manly characterised by fate specification of post mitotic progenitors, showing a reduced radio sensitivity compared early progenitors (see chapter 2; **Figure 22**, **Figure 24**). We could point out that reduction in the FS population post IR is caused by apoptosis (**Figure 24**). Irradiation of J1 cells in the FS phase showed a significant reduction of neuroblasts, similar the reduction in the whole culture, suggesting a neuroblast specific radio sensitivity in the FS phase. The fate determination of the surviving culture is not delayed, indicating a no affection in the progression of the further differentiation.

The final differentiation phase, CM, showed by far the lowest radio sensitivity in the differentiation progress (**Figure 22**, **Figure 24**). Irradiation of J1 cells in CM phase reveals a high survival rate (**Figure 22**) and a comparable phenotype as in unirradiated cultures. Detailed analyses exhibited malfunctions on various levels of the maturation characteristics (see 6.3.4). In contrast to the earlier differentiation phases (EP, FS), IR leads to an arrest or failure in the differentiation progress in J1 cells during CM phase. Suggesting that maturating J1 cells cannot terminate the final differentiation phase post IR.

Regarding adult neurogenesis the neuroblast specific sensitivity towards IR in the FS phase reflects a particular endangerment, selectively affecting the input of future neurons in the hippocampus beside

high radio sensitivity of early progenitors, estimated previously (chapter 2). The incomplete maturation in CM phase post IR reflects additionally a malfunction in the input of new neurons. The limited excitability of the immature neurons post IR creates also an endangerment of hippocampal information-processing. It has been shown that the high excitability of immature and new neurons particularly contributes to the hippocampal function [20] (see also 3.2 The role of adult neurogenesis in learning and memory). Beside the loss of neuronal input, IR may affect adult neurogenesis also on comprehensive functional level, determined in the interaction between highly excitable immature neurons and sparsely activated mature neurons.

7. Chapter IV: IR induced changes in the properties of the self-renewing J1 NSCs population

7.1. Introduction

7.1.1. Radiation induced differentiation in adult neural stem cells

The long-lasting decline in adult neurogenesis post IR is contributed to a permanent reduced stem cell pool in the adult brain [1, 25]. Beside IR induced apoptosis in the self-renewing stem cells (see chapter 2), IR induced differentiation is suggested to cause the reduction in the stem cell pool, leading to a permanent depletion of neural stem cells even after a single, moderate dose of IR [218, 484]. It has been shown that IR (8Gy) leads to a senescent subpopulation in neural stem cell pool, expressing immunohistological differentiation markers [279, 485]. Radiation induced differentiation, resulting in a permanent reduction of the stem cell pool has been hypothesized in various stem cells *in vivo* and *in vitro* [486-488]. The permanent reduction of the neural stem cell pool is a disadvantage for the recovery of the neural stem cell niche post IR induced apoptosis and may cause the constant deficits in adult neurogenesis post radiation [484].

7.1.2. Radiation induced changes in the functional properties of self-renewing J1 NSCs

As described previously neural differentiation can be characterised using morphological, functional or immunohistological markers (see chapter 1). Even though, functional properties as membrane potential or specific ion channel conductance are typical for specific differentiation phases, mostly specific marker protein expression is used to define the differentiation phase of progenitors in neurogenesis. Dr. Bastian Roth investigates the functional characteristics in neural differentiation using the J1 model system and the effect of IR on specific functional characteristics. In this work he could identify changes in functional characteristics in self- renewing J1 NSCs post IR.

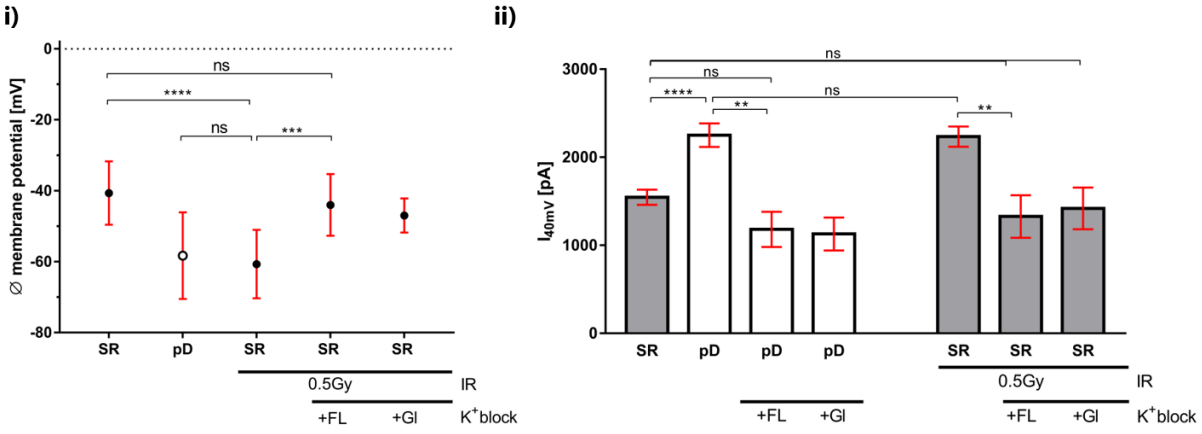

Figure 34 Altered functional characteristics in J1 NSCs post IR. **i**) J1 NSCs show a reduced V_R 24h post 0.5Gy IR. The lowered V_R in SR cells post IR is similar to V_R measured in differentiated J1 NSCs (differentiation day 9; pD). The V_R of irradiated J1 NSCs did not show a reduction in the presence of the K^+ channel blockers (20µM fluoxetine (FL) and 50µM glibenclamide (Gl)) during the V_R measurement. **ii**) Peak conductance at 40mV of J1 in SR and differentiated (differentiation day 9; pD). Differentiated J1 cells show a raised I_{40mV} than J1 in SR. The increase in the I_{40mV} is blockable in the presence of 20µM fluoxetine (FL) and 100µM glibenclamide (Gl). For this measurement differentiated J1 cells were perfused with external solution containing 100µM glibenclamide or 20µM fluoxetine. 0.5Gy IR leads to an increase in the I_{40mV} 24h post IR similar to differentiated J1 cells (pD). The increase in I_{40mV} 24h post IR in J1 SR is blocked, when the cells are incubated in 20µM fluoxetine (FL) or 100µM glibenclamide (Gl) during irradiation. **i-ii**) plotted mean with SD, unpaired t-test, (ns: $p > 0.05$; ** $p \leq 0.01$; *** $p<0,001$; **** $p<0.0001$).

Dr. Bastian Roth could show that low dose irradiated (0.5Gy) J1 NSCs have a significant higher K^+ conductance and a lower membrane potential than the control group (**Figure 34**). The elevated membrane potential as well as the increased K^+ conductance are functional characteristics for differentiated neurons (**Figure 13**) mainly mediated via $K_V3.1$ and K_{ATP} channel currents (**Figure 34**). Upon the characterisation of the functional differentiation, Dr. Bastian Roth could identify the establishment of the reduced V_R upon the CM phase (**Figure 13**) in the established differentiation protocol. In further analyses Dr. Bastian Roth could identify that increased $K_V3.1$ and K_{ATP} channel conductance as the main cause for the elevated K^+ conductance and the lowered membrane potential in differentiated J1 cells as well as in irradiated J1 NSCs. $K_V3.1$ and K_{ATP} channel are blockable with glibenclamide respectivly fluoxetine [489-491]. J1 NSCs irradiated in the presence of glibenclamide or fluoxetine did not show a reduction in the V_R 24h post 0.5Gy (**Figure 34 i**), suggesting that the reduced V_R post low dose IR is mediated via $K_V3.1$ and K_{ATP} channels. Dr. Bastian Roth could also show that the IR induced increase in the I_{40mV} of J1 NSCs is blockable with the addition of glibenclamide and fluoxetine during irradiation (**Figure 34 ii**). The reduced V_R and increased I_{40mV} in self-renewing J1 NSCs persists at least for 48h post IR (data not shown).

7.1.3. **Fourth aim: radiation induced changes in self-renewing J1 NSCs**

The self-renewal of the NSC population is the basal source of adult neurogenesis. The presented results (**Figure 34**) indicate low dose IR induced changes of the functional characteristics within the SR population of J1 NSCs. The long-lasting alteration of the V_R and I_{40mV} post IR suggests a $K_V3.1/K_{ATP}$ channel mediated change in the SR characteristics, which may endanger the self-renewing NSC population. In continuative experiments we investigate if low dose IR leads also to changes in the morphological and immunohistological characteristic within the NSC population.

7.2. Material and methods:

Antibodystaining

Antibodystainings were performed as described in chapter 1. For each staining four individual experiments were performed. In each experiment at least 3x 1000cells per staining were analysed, 24h and 72h post IR (0.5Gy and 0Gy). DCX positive cells were counted manually in five individual experiments (3x1000 cells per experiment) 24h and 72h post IR (0.5Gy and 0Gy).

Proliferation assay

To identify proliferating cells within the culture we used ki67 staining. Cells were stained and counted as described in chapter 1. We performed four individual experiments (2x 1500cells per experiment) for each timepoint (24h,72h) and each dose (0.5Gy and 0Gy).

K^+ channel blocker

To block K^+ channel during IR we used the reversible $K_V3.1$ channel blocker fluoxetine (Sigma; IC50: 13µM) [492] and the K_{ATP} channel blocker glibenclamide (Sigma; IC50: 25µM) [493]. For self-renewing J1 NSCs irradiated in the presents of the K^+ channels blockers, we added fluoxetine and glibenclamide in the SR media directly before irradiation. The total blocker concentration diluted in the media was 20µM for fluoxetine and 50µM for glibenclamide. 12h after addition we removed the blocker via media exchange. We also performed a media exchange in the control cultures simultaneously.

7.3. Results:

7.3.1. Late differentiation markers in self-renewing J1 NSCs post low dose IR

In chapter 1, we characterised the differentiation of J1 cell using morphological, immunohistological and functional markers. As shown in **Figure 34**, Dr. Bastian Roth could show that undifferentiated J1 cells show an increased K^+ conductance and reduced V_R, 24h post low dose irradiation (**Figure 34**). The functional characteristics (V_R and I_{40mV}) in J1 NSCs post IR, correlate to V_R and I_{40mV} measured in J1 cells post differentiation. Differentiated J1 cells are defined by a postmitotic status, specific morphology and specific marker protein expression (see chapter 1, **Figure 18**). We checked irradiated J1 NSCs for morphological and immunohistological differentiation markers typical for differentiated cells and late differentiation (see **Figure 8** and **Figure 10**).

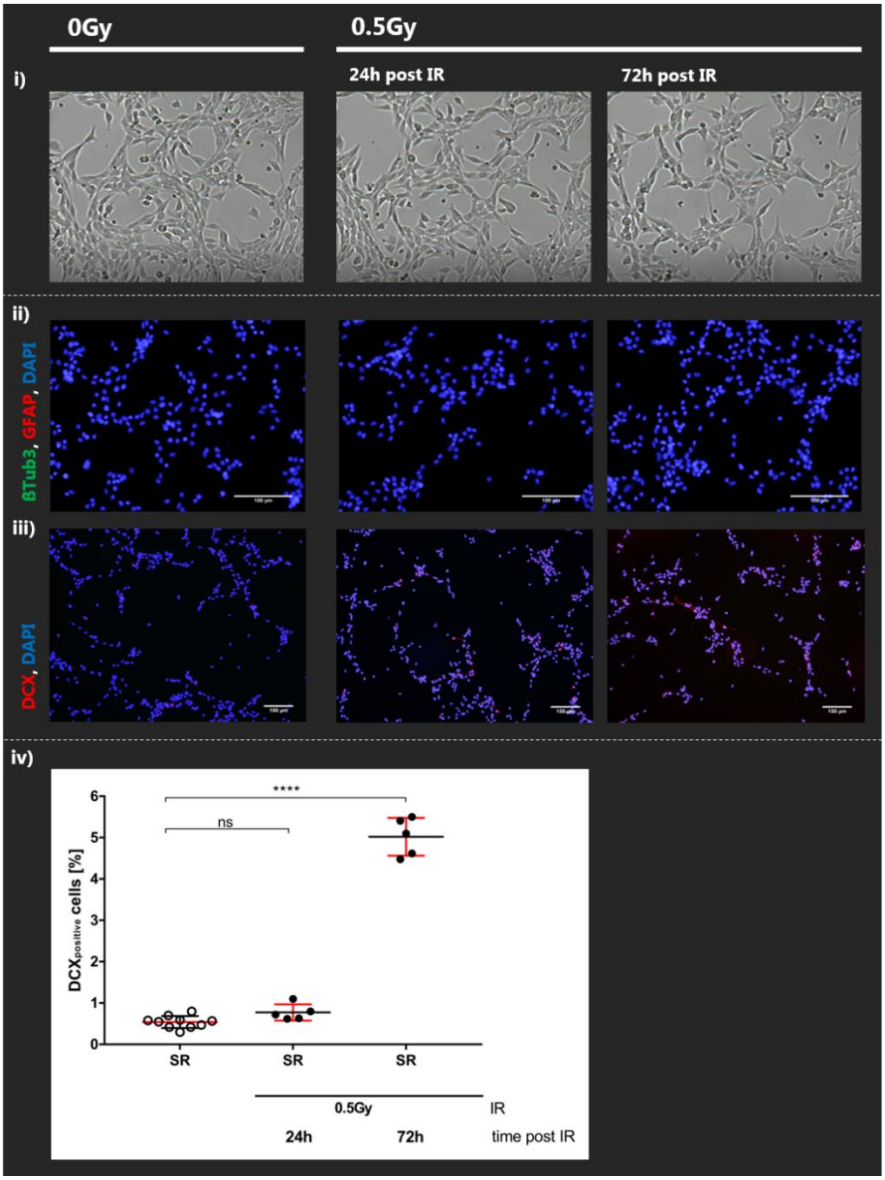

Figure 35 Morphological and immunohistological differentiation markers in J1 NSCs post IR (0.5Gy). We analysed J1 NSCs (SR) irradiated with 0.5Gy, 24h and 72h post IR on morphological markers **(i)** and specific marker expression **(ii, iii)**. **(i)** representative pictures of unirradiated and irradiated J1 NSCs, 24h and 72h post IR. **(ii)** representative pictures of the expression of cell fate specific differentiation markers, ßTub3 (green) and GFAP (red), in irradiated and unirradiated J1 NSCs 24h and 72h post IR. Scalebar 100µm. **(iii)** Expression of the differentiation marker DCX (red), 24h and 72h post IR. Scalebar

100µm. **(iv)** Quantification of DCX positive cells in J1 NSCs, 24h and 72h post IR (0.5Gy). Plotted mean with SD, unpaired t-test, (ns: $p > 0.05$; **** $p<0.0001$).

Differentiated J1 show a typical morphology, defined by cellular extensions and highly linking between individual cells (see **Figure 10**). Irradiated J1 NSCs show no morphological differences compared to unirradiated J1 NSCs (**Figure 35 i**). Undifferentiated J1 cells both 24h and 72h post IR (0.5Gy) resemble a typical morphology for J1 in self-renewal status (see also **Figure 9**), characterised by a flat, plumb cell shape without axonal or dendritic growth.

Using the differentiation protocol, we could detect cells expressing the fate specific proteins GFAP or ßTub3 from differentiation day 2 on, increasing until differentiation day 5 (**Figure 8**). Irradiated J1 NSCs did not show any cells expressing GFAP or ßTub3 24h, neither 72h post low dose irradiation (**Figure 35 ii**). DCX is an early differentiation marker, increasing from differentiation day 1 in the cell population in the established differentiation protocol (**Figure 8**). In self-renewing J1 cells we could detected ~0.5% cells expressing DCX (**Figure 8**, **Figure 35**), post 0.5Gy we found an increase of DCX positive cells within J1 NSCs (**Figure 35 iii**). The quantification of DCX positive cells in J1 NSCs post 0.5Gy IR, revealed a highly significant increase in DCX positive cells 72h but not 24h post IR. Unirradiated J1 NSCs show a stable population between 0.3-0.7% DCX positive cells (controls for both timepoints were summed in unirradiated SR) as shown in **Figure 35 iv**. 24h post 0.5Gy we could not detect a significant increase in the number of DCX positive cells in the population. J1 NSCs, 72h post 0.5Gy, show ~5% DCX positive cells within the population, which resembles a 10-fold higher number in DCX expressing cells compared to unirradiated J1 NSCs.

Taken together we could not confirm changes in the characteristic of J1 NSCs 24h post 0.5Gy using morphological and immunohistological markers. We did not find any morphological changes, ßTub3 or GFAP expression 24h as well as 72h post IR in the SR population. Certainly, we could verify a highly significant 10-fold increase in DCX positive cells 72h post 0.5Gy within the SR population.

7.3.2. **Early differentiation markers in self-renewing J1 NSCs post low dose IR**

In neural differentiation DCX expression is strongly correlated to the post mitotic status of progenitors, highly increasing with the termination of the early progenitor phase (see chapter 1, **Figure 8** and **Figure 11**). With the increase of DCX positive cells in the neural differentiation J1 progenitors also lost the expression of stem cell marker protein nestin (**Figure 8**). Decrease of nestin positive cells, as well as reduced proliferation are typical markers for early differentiation in neurogenesis. In further experiments we analysed if the increasing DCX expression within the J1 NSC population post IR, can be correlated to a raising postmitotic status and decreased nestin expression in the self- renewing J1 cells.

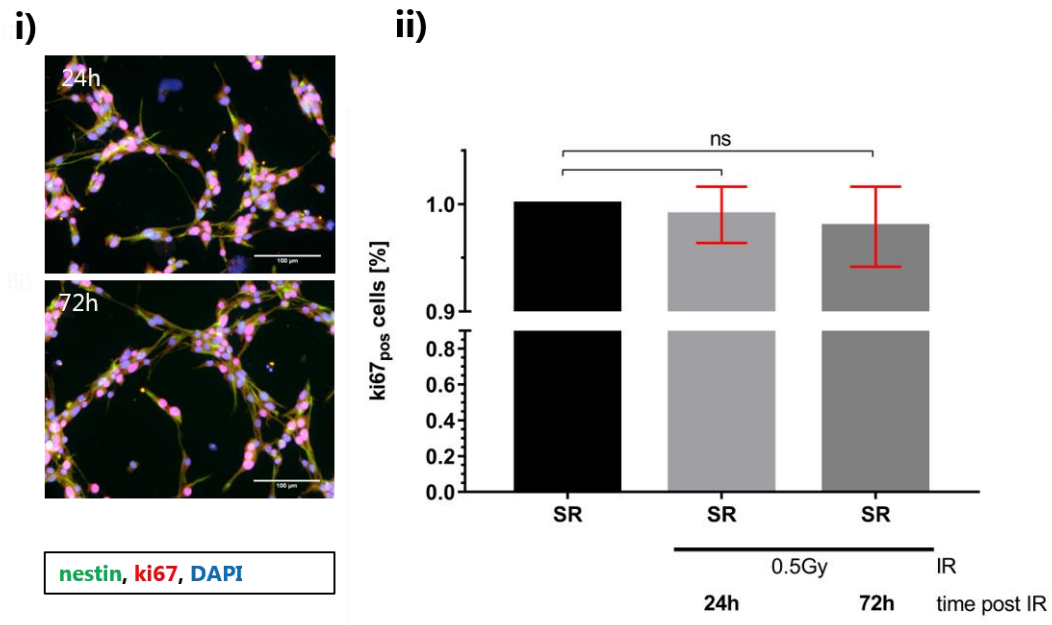

Figure 36 Proliferation and nestin expression in J1 NSCs post low dose IR (0.5Gy). To check if the proliferation and expression of the stem cell marker nestin is changed in SR cells population post 0.5Gy, we used antibody staining against the stem cell marker nestin (green) and the mitotic cell marker ki67 (red). **i**) exemplary pictures of ki67 and nestin labelling in the J1 NSC population 24h and 72h post 0.5Gy, untreated cells are shown in **Figure 11**. (scalebar 100µm). **ii**) We used the proliferation marker ki67 to quantify mitotic active cells 24h and 72h post IR in J1 NSC. The percentage of ki67 positive cells in irradiated populations were normalized on the percentage of ki67 positive cells in control population. plotted mean with SD, unpaired t-test, (ns: $p > 0.05$).

We used the early differentiation markers nestin and ki67 to find induced differentiation in undifferentiated J1 NSCs 24h and 72h post 0.5Gy IR. Nestin is homogenously expressed in the self-renewing J1 population and decreases in the early progenitor phase (**Figure 8**). In the irradiated J1 NSC cultures we found a stable nestin expression in all cells 24h and 72h post IR, as well as in unirradiated J1 NSCs (data not shown) indicating that the number of nestin expressing cells is not altered in J1 NSCs post 0.5Gy x-ray treatment.

Untreated J1 NSCs show a ki67 positive cell fraction of around 72% (**Figure 11**), 24h and 72h after 0.5Gy observed a slight reduction in the number of ki67 positive cells within the culture. Normalized on the control, the mean number of ki67 positive cells decreases to ~98% 24h post 0.5Gy IR and to ~96% 72h post 0.5Gy IR. Using unpaired t-test we could not statistically verify differences between the irradiated and unirradiated populations.

In summary we could not detected a significant difference between unirradiated and irradiated (0.5Gy) J1 NSCs, regarding the early differentiation marker expression nestin and ki67. Concerning morphological and immunohistological markers we failed to observe any differences in early and later differentiation markers between unirradiated J1 NSCs and J1 NSCs 24h post 0.5Gy. Also, 72h post IR we could not find significant changes between irradiated and unirradiated J1 NCSs, with exception of the percentage of DCX expressing cells. Corresponding to the functional changes (V_R and I_{40mV}), characterised by Dr. Bastian Roth (**Figure 34**), the 10-fold increase in DCX positive cells post 0.5Gy resembles a highly significant increase in a immunohistological differentiation marker in J1 NSCs post IR.

7.3.3. Correlation between $K_V3.1/K_{ATP}$ channel mediated functional changes and increased DCX expression in the self-renewing NSC population post low dose IR

By checking early and later morphological and immunohistological differentiation markers, we found an increase in DCX positive cells in irradiated J1 NSCs. To check if the raised DCX positive subpopulation in undifferentiated J1 NSCs is correlated to the functional phenotype (**Figure 34**) we used the potassium channels blockers fluoxetine and glibenclamide during irradiation.

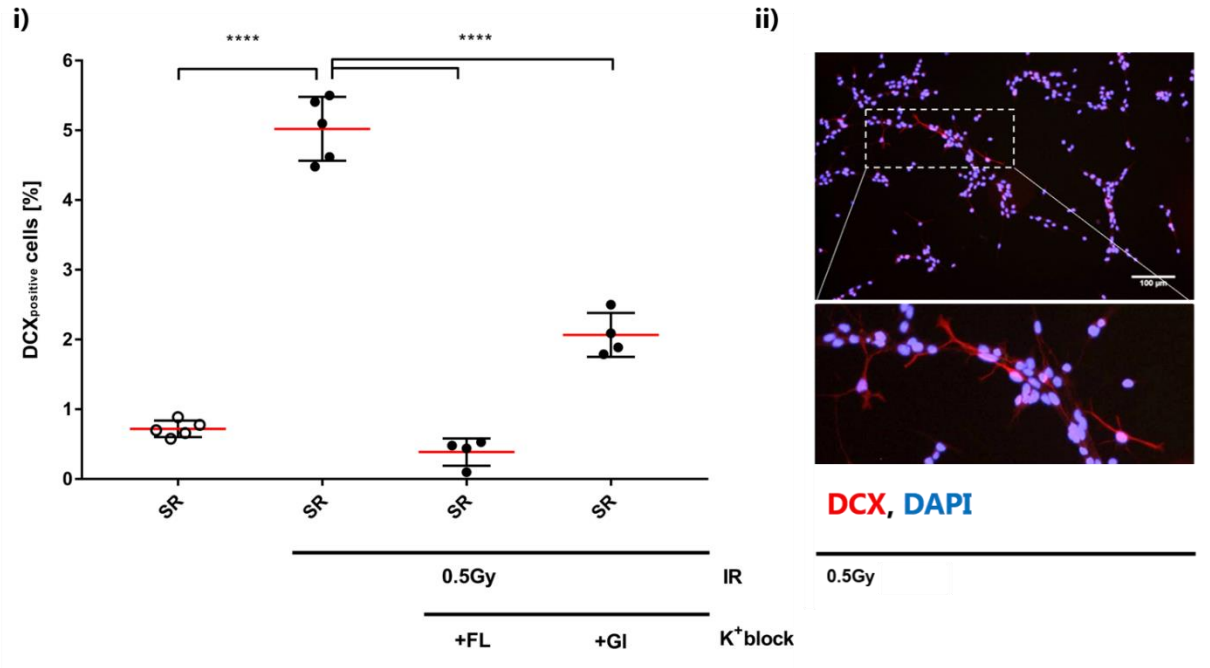

Figure 37 Correlation between DCX positive cells and potassium conductance. Undifferentiated J1-NSCs were irradiated with 0.5Gy with and without the K^+ channel blockers fluoxetine (FL, 20µM) and glibenclamide (Gl, 50µM). Irradiated J1 NSCs show in contrast to unirradiated J1 NSCs (SR) a higher level of $DCX_{positive}$ cells. Treatment with 20µM Fluoxetine or 50µM glibenclamide leads to significant decreased $DCX_{positive}$ cells 72h post IR (n=4, p **** < 0,0001, unpaired t-test). Left: exemplary immunostaining of undifferentiated J1 NSCs, 72h after irradiation, stained for DCX (red) and DAPI (blue). Scalebar: 100µm.

As shown in **Figure 37** irradiation in the presence of the K^+ channel blockers fluoxetine or glibenclamide inhibits the increase of DCX positive cells 72h post IR. Unirradiated J1 NSCs reveal a stable fraction of ~0.5% DCX positive cells, 72h post 0.5Gy the fraction of DCX positive cells significantly increase to ~5%. Addition of fluoxetine and glibenclamide during irradiation blocks the increase in the DCX positive cells within the culture. J1 NSCs 72h post irradiation with 0.5Gy, treated with 20µM fluoxetine show ~0.3%, cells treated with 50µM ~1.7% DCX positive cells. Treatment of unirradiated J1 NSCs with fluoxetine and glibenclamide did not alter the percentage of DCX positive cells within the culture (data not shown). The inhibition of the increase in the DCX positive cell fraction, via K^+ channel blockers indicates

a correlation between the increased K^+ conductance (**Figure 34**) and DCX expression in J1 NSCs post 0.5Gy IR.

Taken together J1 NSCs show a lowered membrane potential when irradiated with 0.5Gy IR (**Figure 34**). Dr. Bastian Roth could attribute the alterations in the membrane potential to a long-lasting IR induced, increased K^+ conductance. Blocking of the responsible K^+ channels reveals the IR induced effect on the membrane potential and K^+ conductance. Beside the changes in the functional properties, characterised by Dr. Bastian Roth, we could also verify an increase in the immunohistological differentiation marker DCX within the irradiated SR population. Comparable to the reduced V_R and increased I_{40mV}, induced by 0.5Gy IR, the increase in the DCX positive cell population is blockable by fluoxetine and glibenclamide. These results suggest that the increase in DCX positive cells 72h post IR is mediated by fluoxetine/glibenclamide sensitive potassium channels.

7.4. Discussion

The neural stem pool is the base for neural differentiation. Proliferating NSCs guaranty the persistence of life long adult neurogenesis. In chapter 2 we could show that the number of J1 NSCs is dramatically reduced even after low dose IR (**Figure 22**) which causes a temporal decline in differentiation capacity into mature neurons [248-251]. In comparison with the differentiation phases, self-renewing NSCs show the highest sensitivity to IR (**Figure 22**). Even low doses as 0.5Gy lead to a significant reduction to ~85% of the population 24h post IR. The decreased cell population is caused by a reduction in the mitotic fraction (3h post IR) and by IR induced apoptosis (**Figure 24**).

7.4.1. Radiation induced changes in the characteristic properties of self-renewing J1 NSCs post low dose IR

In more detailed analyses Dr. Bastian Roth could show that, 0.5Gy IR induces long-lasting changes of the functional characteristics within the SR population of J1 NSCs. Modified V_R and I_{40mV} post IR suggests a $K_V3.1/K_{ATP}$ channel mediated change in the functional SR characteristics (**Figure 34**). As described in chapter 1, various K^+ channels types are expressed depending on the differentiation phase (**Figure 4**) and appear to play a critical role in fine tuning of neural differentiation [91]. We investigated the surviving J1 NSC population on further changes in SR typical characteristics beside the acute reduction in the population. The self-renewal status of NSCs is mainly defined by a stable proliferation and the absence of differentiation markers [191]. Concerning immunohistological markers nestin is one the few specific markers exclusively expressed in NSCs and EP (see **Figure 4**). Low dose irradiation (0.5Gy) did not change the homogenously expression of nestin within the SR population, 24h and 72h post IR (**Figure 36**).

Even though it is known that K^+ channel are key players in cell proliferation [494] we could not determine a significant change in the mitotic fraction within the irradiated SR population 24h and 72h post 0.5Gy IR (**Figure 36 ii**). These results indicate that the proliferation of the NSC population, aside from the contemporary inhibition (see **Figure 24**), is not affected by low dose irradiation. Also, the unchanged homogenously nestin expression indicates a consistent stem cell character in the irradiated NSC population 24h and 72h post 0.5Gy IR.

DCX is the first differentiation marker occurring in neural differentiation (see **Figure 4** and **Figure 8**), J1 NSCs in self-renewal status show a low subpopulation (~0,5%) of DCX positive cells. We could define a highly significant 10-fold increase in the number of DCX expressing cells, 72h post 0.5Gy IR. Regarding further immunohistological differentiation markers as GFAP or ßTub3 we could not find any expression 24h as well as 72h post IR in the SR population (**Figure 35 ii**). Regarding the cell morphology irradiated J1 NSCs show no morphological differences compared to unirradiated J1 NSCs (**Figure 35 i**). J1 NSCs both 24h and 72h post IR (0.5Gy) resemble a typical morphology for J1 in self-renewal status (see also **Figure 9**), characterised by a flat, plumb cell shape without axonal or dendritic growth.

In summery surviving J1 NSCs did not show any characteristic changes 24h post 0.5Gy IR, except the reduced V_R and the increased I_{40mV}, determined by Dr. Bastian Roth. The pursuit of the irradiated NSC population revealed an increase in the DCX positive cell number 72h post IR, indicating an altered protein expression in a subpopulation within the NSC population.

K^+ channel dependent DCX expression in self-renewing J1 NSCs

To check if the increased DCX positive subpopulation within the NSC population 72h post 0.5Gy can be correlated with the reduced V_R and increased I_{40mV} estimated 24h post IR, we used the K^+ channel blocker fluoxetine and glibenclamide. J1 NSC irradiated in the presence of the $K_V3.1/K_{ATP}$ channel blockers did not show altered functional characteristics 24h post 0.5Gy (**Figure 34**) and no increase in the DCX positive cell number 72h post IR (**Figure 37**). The unaltered number in DCX positive cells, when irradiated with fluoxetine and glibenclamide, suggest that the increase in DCX expressing cells 72h post IR is mediated by fluoxetine/glibenclamide sensitive potassium channels.

A large phase of neurogenesis is associated with the expression of DCX. This phase ranges from the EP to CM phase. DCX expression is thought to be mostly specific for future neurons, since nearly all DCX-positive cells express early neuronal antigens but lack antigens specific for glial cells, undifferentiated cells, or apoptotic cells [132]. Concerning DCX expression at early phases of adult neurogenesis, a brief overlap with nestin expression has been found [495]. Nevertheless, DCX expression is a sign of induced differentiation in neural differentiation [134]. Even though we could not find further signs of induced differentiation, the significant increase in the DCX positive subpopulation suggests induced differentiation within the self-renewing NSC population post low dose IR.

The dependence of the DCX expression in J1 NSCs to fluoxetine/glibenclamide sensitive potassium channels leads to the conclusion that IR induced changes in functional characteristic may originate further alterations in the cellular properties.

K^+ channels are known for their sensitivity towards IR and ROS [496, 497] (see also chapter 3) and their regulative role in neural differentiation [91]. We could not find any information about the role of $K_V3.1$ and K_{ATP} channels in self-renewing NSCs in the literature, but it is known that fluoxetine and glibenclamide modulate adult neurogenesis. Fluoxetine specifically increases proliferation of hippocampal early progenitors, but not of NSCs *in vivo* [498]. The increased number of early progenitors manifested later as an increase in the number of new neurons in the DG [499]. Similar results were shown for glibenclamide [500, 501]. Glibenclamide also leads to an increased number in neurons in neurospheres [502]. In summery neither glibenclamide nor fluoxetine affect self-renewing NSCs but increases proliferation in early progenitors. These data suggest that the activation/expression of glibenclamide/fluoxetine sensitive channels is a characteristic difference between NSCs and early progenitors and may modulate the balance between the NSC and early progenitor population. A similar hypothesis has been suggested by Yang and Fan [503, 504].

Taken together, the radiation induced increase in fluoxetine/glibenclamide sensitive potassium conductance (**Figure 34**) shown by Dr. Bastian Roth may affect the maintenance of the neural stem cell population and induce differentiation within the irradiated population. We could determine a 10- fold increase of the differentiation marker DCX within the NSC population post 0.5Gy, mediated by fluoxetine/glibenclamide sensitive potassium channels. These IR induced changes in the characteristics and homogeneity of the neural stem cell population may cause a lasting decline in the stem cell pool of adult neurogenesis. Especially the low induction dose of 0.5Gy, reflects an endangerment of the persistence and maintenance of the self-renewing population, deserving further investigation.

8. Conclusion

Comprehensive follow-up of brain cancer patients and retrospective studies revealed a frightening correlation between cranial irradiation and long lasting cognitive deficits [7, 12, 24, 422]. The particular radio sensitivity of adult neurogenesis is suggested as major contributor in the underlying pathogenesis [5]. The life-long generation of new neurons in defined stem cell niches contributes essential to the hippocampal dynamics [19, 21]. Radiation induced inhibition of adult neurogenesis is therefore thought to be associated with massive dysfunctions in hippocampal learning and memory [24, 28, 238, 243, 305].

Adult neurogenesis describes the differentiation of neural stem cells to mature neurons in the adult brain [34]. This process is highly complex and not fully understood [16]. The neural differentiation is separated in three main phases, early progenitor phase, fate specification phase and cell maturation phase [61]. Each differentiation phase includes multiple differentiation events which together lead to highly specialised mature cells [2]. Although neurons are understood as the essential mature cell type, neural differentiation also generates new astrocytes. Neural differentiation takes place in limited restricted regions of the adult brain, the stem cell niches [32]. These stem cell niches are hierarchic organised tissues, harbouring NSCs and progenitors of each phase closely connected. The cellular base of neural differentiation are self-renewing NSCs, providing a restricted stem cell pool via symmetrical cell division [101]. Induced differentiation leads to an asymmetric cell division creating early progenitors. Early progenitors are proliferating cells with a reduced stem cell potency. The early progenitor cells pass a transient amplification phase, before they reach a postmitotic status. During the first differentiation phase the migration within the neural stem cell niche is initialised. The migration follows extracellular growth factor gradients stimulating the further differentiation progression. Together with the leave of the cell cycle, differentiating progenitor enter the second differentiation phase, the fate specification. During this differentiation phase the postmitotic progenitors determine their future fate. *In vivo* adult neural differentiation generates only neurons (50-70%) and astrocytes (30-50%), while *in vitro* also oligodentrocytes are possible [14]. The fate specification is accompanied with intracellular and morphological cell specification, as specific protein expression and axonal growth. The fate specification is followed by the final differentiation phase, the cell maturation. During this phase the glio- and neuroblasts specialise their structural and functional properties and integrate in the neural network. The main characteristics in the terminal neuronal differentiation are high excitability and functional synaptic integration. The cell maturation phase is terminated with a synaptic mediated apoptotic wave, the programmed cell death. Surviving neuroblasts count as mature new neurons. It is shown that immature neurons in the last differentiation phase contribute critical to the hippocampal information-processing [505]. The high excitability of the small subpopulation is thought to be essential for modulation of neuronal synchronization and network oscillations and may contribute to the critical role of adult neurogenesis in learning and memory.

It has been shown that IR leads to a nearly complete loss of adult neurogenesis, apparent in the reduction of all cell types within the adult stem cell niche [1]. Radiation induced apoptosis detracts the cellular base of adult neurogenesis in the adult brain [5]. The diverse properties of the individual differentiation phases suggest that they also display diverse reactions towards IR. To investigate the impact of IR to individual differentiation phases, a model system is needed which allows the distinct separation of the three differentiation phase subpopulations.

The very limited number of adult neurogenesis makes *in vivo* studies challenging [34]. *In vitro* studies are mostly performed in heterogeneous primary cultures struggling with mixed undefined differentiation phase [24]. In the first part of this work we established and characterised a suitable model system to investigate radiation induced reductions in defined differentiation phases within adult neurogenesis.

We used ES-derived J1NSCs and established a 2D differentiation protocol. Subsequent we characterised the differentiating J1 cells concerning specific marker expression, morphology and functional differentiation markers. The broad characterisation revealed that the J1 model system reflects each of the three differentiation phases, i.e. early progenitor (EP), fate specification (FS) and cell maturation (CM) in adult neurogenesis on the intra- and intercellular as well as on the functional level. The self-renewal status (SR) of J1 NSCs has already been analysed by Conti, 2005 [191]. J1 NSCs in self-renewal show a stable proliferation and homogenous stem cell characteristics defined by stem cell marker expression and differentiation capacity [191]. Media induced differentiation leads to a homogenous early progenitor population within the first two days, characterised by increased proliferation and decreasing stem cell marker expression. From differentiation day three on the J1 population is postmitotic, gaining morphological and functional markers of the fate specification phase. We could determine an increase in the expression of the fate specific proteins ßTub3 and GFAP within the J1 population. On differentiation day five all cells are determined in their fate, resulting in ~70% neuronal progenitors and ~30% astrocytic progenitors within the culture. After the fate commitment, differentiating J1 cells enter the final differentiation phase, the cell maturation. Regarding cell maturation we mainly focused on the neuronal differentiation. J1 neuroblasts pass a functional differentiation defined by a neuron typic V_R of -60mV, specific ion channel expression and highly increasing excitability, reflected in raising spontaneous activity. During the maturation phase we could detect pre- and post-synaptic protein expression, characteristical for inhibitory and excitatory synapses. Using MEA analyses, we also observe coordinate network activity characteristic for synaptic signalling. The cell maturation phase is terminated by the programmed cell death, occurring on differentiation day seven in the J1 model system. In summary the J1 NSCs system reflects a comprehensive differentiation on intra- and intercellular as well as on functional and morphological level, comparable to adult neurogenesis in the hippocampus. The synchronised, time dependent differentiation of the homogenous J1 progenitor population allows the discrimination of the three differentiation phases by time. We used the synchronous, time dependent differentiation of the estimated J1 system as the base of our radiation experiments, allowing the separation and individual follow up of all three differentiation phases in adult neurogenesis.

The main impact of IR is the loss of cells, defined by a specific radio sensitivity compared to mature brain cells [1]. The reduction of the neurogenic niche population limits the input of new neurons in the hippocampus and prohibits adult neurogenesis [238]. Most studies discriminated the stem cell niche subpopulation only by proliferative and postmitotic cells [1, 272]. In the second part of this work, we analysed the individual radio sensitivity of the subpopulations discriminated by the distinct differentiation status. Additionally, most studies focusing on IR induced effects on adult neurogenesis used high radiation doses (≥ 5Gy). Concerning radiotherapy bystander and diagnostic doses, we focused on a lower dose range between 0.25 and 2Gy.

To estimate the distinct radio sensitivity of NSCs and the three differentiation phases we measured the reduction of the separated subpopulations and estimated the individual LD_{50} of each differentiation phase. The NSC population showed the greatest reduction 24h post IR, reflected in a LD_{50} of 2.4Gy. The early progenitor population revealed a slightly higher survival 24h post IR, mirrored

in a LD_{50} of 2.7Gy. The third differentiation phase, fate specification, showed a lower radio sensitivity compared to the proliferative subpopulations, verified in a LD_{50} of 3.6Gy. In the final differentiation phase, cell maturation, the radio sensitivity of the population is clearly reduced. To achieve a reduction in the population a dose above 1Gy is needed, the estimated LD_{50} is 6Gy. NSCs as well as all three differentiation phases show an individual radio sensitivity, significant different to the others. These data clearly revealed that the radiation response of the stem cell niche population is diverse. The particular high radio sensitivity of the NSCs and early progenitors endangers adult neurogenesis at the basal cell production, inhibiting the input of new cells by the reduction of the fundamental cell pool providing cells for the neural differentiation.

In further analyses we investigate the mechanisms responsible for the IR induced reductions in the individual subpopulations. Within the postmitotic differentiation phases fate specification and cell maturation, radiation induced apoptosis is the underlying mechanism. IR leads to a reduced induction of apoptosis in the maturating population indicating a gain in anti-apoptotic properties in the terminal differentiation phase of neural differentiation. In later experiments we could show that the IR induced apoptosis in fate specification phase, is restricted to future neurons, particularly endangering the adult neurogenesis by modifying the native ratio of future neurons and astrocytes.

In the proliferative cell populations, NSCs and early progenitors, IR leads to temporally inhibition of the proliferation additionally to IR induced apoptosis. The reduction in the number of cells is predominantly mediated by reduced proliferation in NSCs and induced apoptosis in early progenitors, which enables a better recovery in the self-renewing population [263, 266]. Regarding neural differentiation the IR induced apoptosis within the first two differentiation phases (EP and FS) endangers particularly the survival of neuronal progenitors, leading to a decline in adult neurogenesis. The terminal differentiation phase (CM) shows a significant higher survival post IR, indicating that the interaction between the immature and mature neurons in the hippocampus is not directly affected by IR [243].

In the second part of this work we could clearly show, that low and moderate doses of IR lead to significant reduction in three (SR, EP, FS) of the four subpopulations responsible for adult neurogenesis. The radio sensitivity of the subpopulations decreases with the progression in differentiation, making the basal populations of neural differentiation mostly affected. In the hierarchic organisation of the neural stem cell niche, these subpopulations (SR and EP) provide the cellular input in the differentiation process. The IR induced reduction of the fundamental cell populations inhibits adult neurogenesis until the subpopulations are restored, thus making the loss of cells as the main aspect in IR induced inhibition of adult neurogenesis [238, 431].

The use of a moderate dose range indicates a quantitative survival in each subpopulation, raising the question if observed cognitive deficits can be exclusively founded in IR induced loss of cells. To determine if low dose IR affects the neural differentiation itself, we followed the differentiation of surviving irradiated progenitors separated by differentiation phase. To verify that the progression in neural differentiation is unaltered we checked in the third part of this work for characteristic properties of each individual differentiation phase till the entry of the next differentiation phase.

Early progenitors, the first subpopulation within the neural differentiation, is characterised by a high proliferation and induced migration. Low dose IR affects the proliferation of early progenitors as described previously. The migration of early progenitor cells along growth factor gradients presupposes the entry in the fate specification phase. Simulating a growth factor gradient, we could verify that the migration of the surviving early progenitors is not affected by low dose IR. The migrated

cells showed a homogeneous postmitotic status indicating an unaffected entry in the fate specification phase. In the next step we followed the fate specification phase post irradiation. Surviving progenitors, irradiated in fate specification phase also showed an unaltered progression to the differentiation phase, indicated by the determined fate of the population on differentiation day six. Even though, the neuron specific sensitivity towards IR altered the future neuron/astrocyte ratio and the characteristic properties in this subpopulation. The terminal differentiation phase, cell maturation, is nearly resistant to radiation induced apoptosis in the low to moderate dose range and is suggested to have a minor influence on the inhibition of adult neurogenesis post IR. Irradiation of the distinct cell maturation phase revealed an inconspicuous phenotype, more precise analyses revealed a broad long-lasting modulation of the functional properties. The immature neurons show typical axonal and dendritic protein expression but show an altered neuronal architecture post low dose radiation, determined in increased axonal and dendritic growth. We could also determine a lower density of the presynaptic marker synaptophysin and the excitatory postsynaptic marker PSD95 as well as the inhibitory postsynaptic marker gephyrin in irradiated immature neurons as well as a reduced density of the voltage-gated potassium channels $K_V1.1$. Regarding the functional level we found a long-lasting stagnation in the excitability of the in cell maturation phase irradiated cultures, determined in reduced firing rate, decreased coordination in the activity pattern and loss in spike synchrony. All these results suggest that low dose x-ray treatment during the final differentiation phase inhibits the characteristic high excitability of immature neurons and leads to malfunction in synaptic transmission. Low dose irradiation additionally inhibits the programmed cell death, the terminal differentiation event in neuronal differentiation, indicating disturbed progression in the differentiation course. The precise analyses of the terminal differentiation phase revealed massive and lasting malfunctions in structural and functional properties within the cell maturation phase post IR.

Immature neurons in the cell maturation phase play an essential role in the hippocampal information-processing [505]. The high excitability of the young subpopulation contributes critical to the activation and synchronisation of the pre-existing hippocampal circuits [21]. The influence of immature neurons on the oscillations and synchrony of neuronal hippocampal activity is correlated to dynamic hippocampus-dependent spatial learning and memory and it is suggested that the immature subpopulation is not only required to acquire new information but also to use previously consolidated spatial memories [18, 21].

It is thought, that IR influences the hippocampal learning and memory by the induced loss of cells in the adult neurogenesis, inhibiting the input of new cells in the critical subpopulation [19, 27]. Based on our data we suggest that the critical cell population itself is affected by low dose IR, in its essential properties. The malfunction of the excitability in the cell maturation phase may be an additional impact of (low) dose radiation to adult neurogenesis and associated cognitive deficits. The “hyperexcitability” of immature neurons, persists post terminated differentiation [18, 21, 505]. Adult-born neurons excitability changes over time similar to those of embryonal born neurons, this modulation is suggested to take years and stabilises the hippocampal heterogeneity of highly excitability new born/ immature neurons and lower excitable embryonal born neurons [21, 505]. The follow up of J1 cell, irradiated in cell maturation phase, determined that the reduced excitability persists up to ten days post differentiation (8 days). Assuming that our results represent an *in vivo* situation, the lasting reduced excitability would probably influence the hippocampal dynamics for years. Based on our result we conclude that IR does not only affect the survival of differentiating NSCs, but also the functional characteristics, which may lead to systemic deficits.

We could not determine the mechanism how IR modulates the properties of maturation cells. The alteration of regulatory elements as activity, synaptogenesis and ion channel density, supposes mutual regulative dysfunction, which may manipulate further differentiation processes and/or are results of a basal downstream dysfunction. Nevertheless, we could correlate some of the IR induced malfunctions to similar phenotypes induced by ROS, which leads to the hypothesis that ROS, in its function as second messenger is a key regulator in the IR induced modifications on differentiation phase specific properties.

NSCs are the fundamental cell population in adult neurogenesis and neural differentiation, providing the maintenance of the neural stem cell niche and cellular recovery post IR [1, 238]. In the second part we already showed that the number of NSCs is reduced by IR, in the last past of this work we investigate if the properties of the self-renewing NSCs are also affected by IR. In previous work Dr. Bastian Roth determined that functional characteristics of J1 NSCs (V_R and I_{40mV}) are modified post low dose IR, mediated via $K_V3.1/K_{ATP}$ channels. In continuative experiments we investigated if low dose IR leads also to changes in the morphological and immunohistological characteristic within the NSC population. The follow up of the irradiated NSCs revealed a highly significant 10-fold increase of the differentiation marker DCX within the self-renewing population, 72h post 0.5Gy. By using $K_V3.1/K_{ATP}$ channel blockers during radiation, we could inhibit the increase in DCX positive cells post low dose IR, indicating that the expression of DCX is also mediated by $K_V3.1/K_{ATP}$ channels. These results verify that low dose IR affects the typical properties and homogeneity of the neural stem cell population, which may reflect an endangerment of the persistence and maintenance of the self-renewing population post IR and consequently the input of cells in neural differentiation.

Combined we found radiation induced modulations in the phase specific properties of each subpopulation, represented by the differentiation phase, in the third and fourth part of this work. The neural stem cell niche is a complex, mutual regulated, hierarchic organized tissue composed of dynamic subpopulations [32]. Each subpopulation is defined by specific properties, providing the niche internal regulation and homeostasis [19, 238]. Radiation induced modulations in the individual properties of each subpopulation, may disturb the mutual enrichment and regulation of the neural stem cell niche and destabilize the hierarchic structure [1]. Instability in the hierarchic organization post IR, provided by altered characteristic of the composed subpopulations may lead to malfunctions in the neural stem cell niche homeostasis and contribute to further dysregulation in the adult neurogenesis and reduced cellular input.

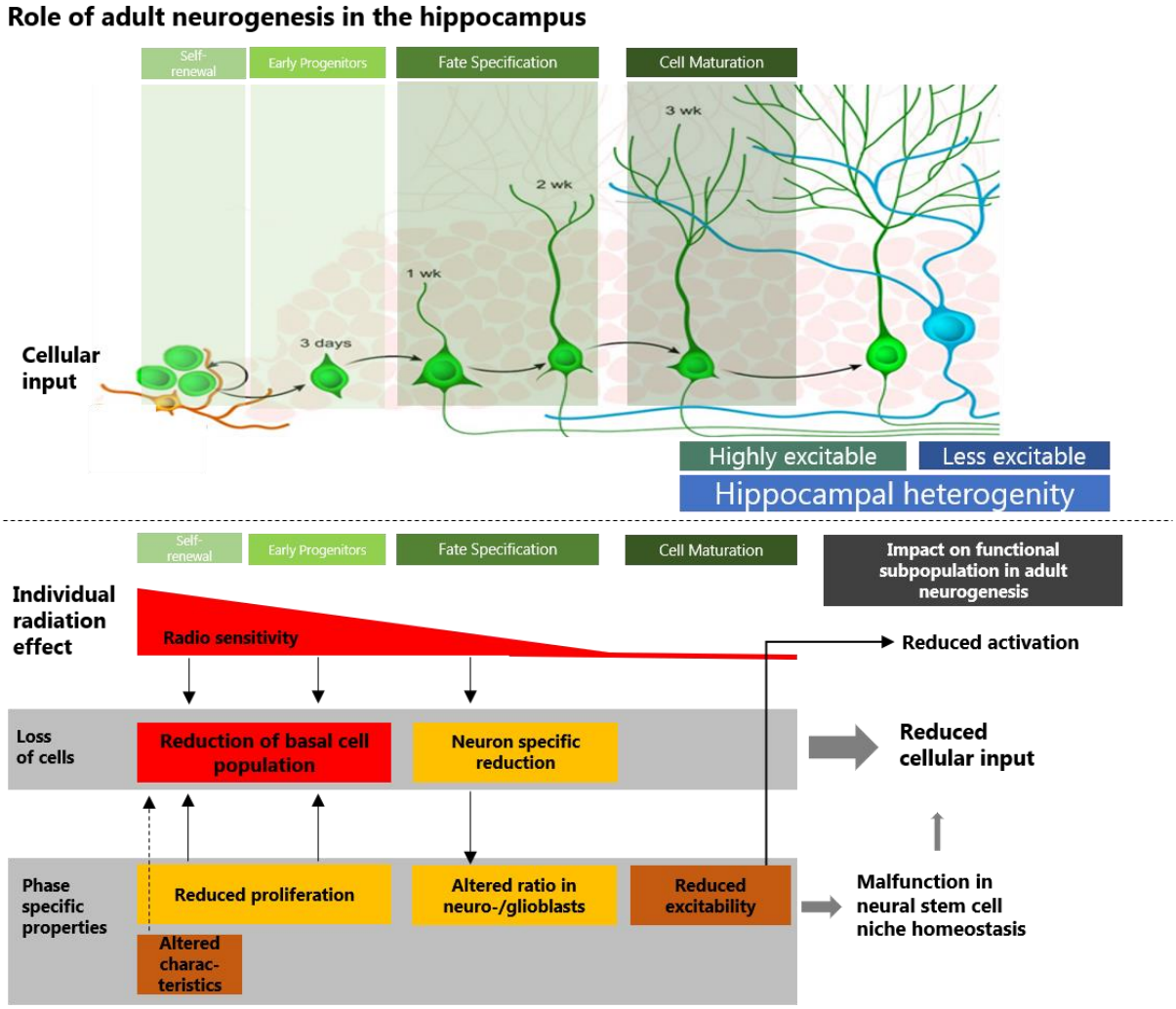

Figure 38 Schematic overview of the role of adult neurogenesis in the hippocampus correlated to IR induced effects in separated differentiation phases and the hypothesised influence in adult neurogenesis. **Above**: adult neurogenesis provides a highly excitable subpopulation of immature/new neurons within the hippocampal circuits. The heterogeneity of the new highly excitable subpopulation and the less excitable "old" neurons provide a dynamic network correlated to hippocampus-dependent spatial learning and memory. Modified after Aimone et all, 2014 [1]. **Below**: Phase specific radiation effects estimated in J1 differentiation. IR leads to a loss of cells within the differentiation progress. Self-renewing NSCs and early progenitors are mostly affected via radiation induced apoptosis and reduced proliferation. In the fate specification phase IR leads to a neuron specific reduction in the subpopulation. The loss of cells within the differentiation progress may result in reduced cellular input in the highly excitable subpopulation in the hippocampal heterogeneity. IR induced altered properties in the characteristics of the subpopulations may affect the neural stem cell niche homeostasis and additionally reduces the cellular input. The reduced excitability in the cell maturation phase post IR may directly affect the maintenance of the hippocampal heterogeneity.

In conclusion, the discrimination of neural differentiation in the underlying subpopulation revealed distinct effects of low to moderate dose radiation within adult neurogenesis. Beside the loss of cells within the subpopulations, we could determine phase specific physiological deficits in the surviving cell populations post irradiation. The radiation induced alterations in the phase specific properties display an endangerment for the homeostasis of the neural stem cell niche. We could also determine

long-lasting massive functional deficits in immature neurons post IR. Immature and new neurons built the critical subpopulation in adult neurogenesis dependent hippocampal information-processing. The modified excitability of maturating neurons post IR may directly affect the hippocampal function. Based on our model system, we hypothesize that IR does not only affect the adult neurogenesis by reducing the cell populations providing the input of new neurons in the crucial population generating the hippocampal heterogeneity but also affects the specific properties of this subpopulation directly.

Radiation induced modifications affecting the specialised physiological properties in the surviving subpopulations of adult neurogenesis may reflect an additional impact in radiation induced malfunctions correlated to cognitive deficits. If our results are verified *in vivo* this would be a new target to prevent and restore radiation induced cognitive deficits.

9. Literature

1. Capilla-Gonzalez, V., et al., *Implications of irradiating the subventricular zone stem cell niche.* Stem Cell Research, 2016. **16**(2): p. 387-396.
2. Aimone, J.B., et al., *Regulation and function of adult neurogenesis: from genes to cognition.* Physiol Rev, 2014. **94**(4): p. 991-1026.
3. Hall, E.J., *Radiation and life.* Bull N Y Acad Med, 1989. **65**(4): p. 430-8.
4. Brenner, D.J. and E.J. Hall, *Current concepts - Computed tomography - An increasing source of radiation exposure.* New England Journal of Medicine, 2007. **357**(22): p. 2277-2284.
5. Balentova, S. and M. Adamkov, *Molecular, Cellular and Functional Effects of Radiation-Induced Brain Injury: A Review.* Int J Mol Sci, 2015. **16**(11): p. 27796-815.
6. Johannesen, T.B., et al., *Radiological and clinical assessment of long-term brain tumour survivors after radiotherapy.* Radiother Oncol, 2003. **69**(2): p. 169-76.
7. Kempf, S.J., et al., *Long-term effects of ionising radiation on the brain: cause for concern?* Radiat Environ Biophys, 2013. **52**(1): p. 5-16.
8. Hall, P., et al., *Effect of low doses of ionising radiation in infancy on cognitive function in adulthood: Swedish population based cohort study.* BMJ, 2004. **328**(7430): p. 19.
9. Albert, R.E., et al., *Follow-up study of patients treated by x-ray epilation for tinea capitis. II. Results of clinical and laboratory examinations.* Arch Environ Health, 1968. **17**(6): p. 919-34.
10. Ron, E., et al., *Mental function following scalp irradiation during childhood.* Am J Epidemiol, 1982. **116**(1): p. 149-60.
11. Brenner, D., et al., *Estimated risks of radiation-induced fatal cancer from pediatric CT.* AJR Am J Roentgenol, 2001. **176**(2): p. 289-96.
12. Greene-Schloesser, D. and M.E. Robbins, *Radiation-induced cognitive impairment--from bench to bedside.* Neuro Oncol, 2012. **14 Suppl 4**: p. iv37-44.
13. Raber, J., et al., *Radiation-induced cognitive impairments are associated with changes in indicators of hippocampal neurogenesis.* Radiation Research, 2004. **162**(1): p. 39-47.
14. Bergmann, O., K.L. Spalding, and J. Frisen, *Adult Neurogenesis in Humans.* Cold Spring Harb Perspect Biol, 2015. **7**(7): p. a018994.
15. Spalding, K.L., et al., *Dynamics of hippocampal neurogenesis in adult humans.* Cell, 2013. **153**(6): p. 1219-1227.
16. Ming, G.L. and H. Song, *Adult neurogenesis in the mammalian brain: significant answers and significant questions.* Neuron, 2011. **70**(4): p. 687-702.
17. Zhao, C., W. Deng, and F.H. Gage, *Mechanisms and functional implications of adult neurogenesis.* Cell, 2008. **132**(4): p. 645-60.
18. Aimone, J.B. and F.H. Gage, *Modeling new neuron function: a history of using computational neuroscience to study adult neurogenesis.* Eur J Neurosci, 2011. **33**(6): p. 1160-9.
19. Toda, T. and F.H. Gage, *Review: adult neurogenesis contributes to hippocampal plasticity.* Cell Tissue Res, 2017.
20. Ge, S., et al., *A critical period for enhanced synaptic plasticity in newly generated neurons of the adult brain.* Neuron, 2007. **54**(4): p. 559-66.
21. Pons-Espinal, M., M.M. de Lagran, and M. Dierssen, *Functional implications of hippocampal adult neurogenesis in intellectual disabilities.* Amino Acids, 2013. **45**(1): p. 113-31.

22. Abayomi, O.K., *Pathogenesis of irradiation-induced cognitive dysfunction.* Acta Oncol, 1996. **35**(6): p. 659-63.
23. Roman, D.D. and P.W. Sperduto, *Neuropsychological effects of cranial radiation: current knowledge and future directions.* Int J Radiat Oncol Biol Phys, 1995. **31**(4): p. 983-98.
24. Hladik, D. and S. Tapio, *Effects of ionizing radiation on the mammalian brain.* Mutat Res, 2016. **770**(Pt B): p. 219-230.
25. Monje, M.L. and T. Palmer, *Radiation injury and neurogenesis.* Curr Opin Neurol, 2003. **16**(2): p. 129-34.
26. Andres-Mach, M., R. Rola, and J.R. Fike, *Radiation effects on neural precursor cells in the dentate gyrus.* Cell Tissue Res, 2008. **331**(1): p. 251-62.
27. Lee, Y.W., et al., *Whole brain radiation-induced cognitive impairment: pathophysiological mechanisms and therapeutic targets.* Biomol Ther (Seoul), 2012. **20**(4): p. 357-70.
28. Greene-Schloesser, D., E. Moore, and M.E. Robbins, *Molecular pathways: radiation-induced cognitive impairment.* Clin Cancer Res, 2013. **19**(9): p. 2294-300.
29. Cajal, R.y., *Les nouvelles idées sur la structure du système nerveux chez l'homme et chez les vertébrés.* Azoulay, 1894. **1**.
30. Gross, C.G., *Neurogenesis in the adult brain: death of a dogma.* Nat Rev Neurosci, 2000. **1**(1): p. 67-73.
31. Goncalves, J.T., S.T. Schafer, and F.H. Gage, *Adult Neurogenesis in the Hippocampus: From Stem Cells to Behavior.* Cell, 2016. **167**(4): p. 897-914.
32. Conover, J.C. and R.Q. Notti, *The neural stem cell niche.* Cell Tissue Res, 2008. **331**(1): p. 211-24.
33. Roy, N.S., et al., *In vitro neurogenesis by progenitor cells isolated from the adult human hippocampus.* Nat Med, 2000. **6**(3): p. 271-7.
34. Eriksson, P.S., et al., *Neurogenesis in the adult human hippocampus.* Nat Med, 1998. **4**(11): p. 1313-7.
35. Gotz, M. and W.B. Huttner, *The cell biology of neurogenesis.* Nat Rev Mol Cell Biol, 2005. **6**(10): p. 777-88.
36. Decimo, I., et al., *Neural stem cell niches in health and diseases.* Curr Pharm Des, 2012. **18**(13): p. 1755-83.
37. Kriegstein, A. and A. Alvarez-Buylla, *The glial nature of embryonic and adult neural stem cells.* Annu Rev Neurosci, 2009. **32**: p. 149-84.
38. Ernst, A. and J. Frisen, *Adult neurogenesis in humans- common and unique traits in mammals.* PLoS Biol, 2015. **13**(1): p. e1002045.
39. Vadodaria, K.C. and S. Jessberger, *Maturation and integration of adult born hippocampal neurons: signal convergence onto small Rho GTPases.* Front Synaptic Neurosci, 2013. **5**: p. 4.
40. Gould, E., et al., *Hippocampal neurogenesis in adult Old World primates.* Proc Natl Acad Sci U S A, 1999. **96**(9): p. 5263-7.
41. Marxreiter, F., M. Regensburger, and J. Winkler, *Adult neurogenesis in Parkinson's disease.* Cell Mol Life Sci, 2013. **70**(3): p. 459-73.
42. Fuster-Matanzo, A., et al., *Role of neuroinflammation in adult neurogenesis and Alzheimer disease: therapeutic approaches.* Mediators Inflamm, 2013. **2013**: p. 260925.
43. Xu, H., et al., *The function of BMP4 during neurogenesis in the adult hippocampus in Alzheimer's disease.* Ageing Res Rev, 2013. **12**(1): p. 157-64.
44. Pla, P., et al., *Huntingtin acts non cell-autonomously on hippocampal neurogenesis and controls anxiety-related behaviors in adult mouse.* PLoS One, 2013. **8**(9): p. e73902.

45. Ben Abdallah, N.M., et al., *Impaired long-term memory retention: common denominator for acutely or genetically reduced hippocampal neurogenesis in adult mice.* Behav Brain Res, 2013. **252**: p. 275-86.
46. Cheng, M.F., *Hypothalamic neurogenesis in the adult brain.* Front Neuroendocrinol, 2013. **34**(3): p. 167-78.
47. Gould, E., et al., *Learning enhances adult neurogenesis in the hippocampal formation.* Nat Neurosci, 1999. **2**(3): p. 260-5.
48. Gould, E., et al., *Neurogenesis in adulthood: a possible role in learning.* Trends Cogn Sci, 1999. **3**(5): p. 186-192.
49. Gu, Y., S. Janoschka, and S. Ge, *Neurogenesis and hippocampal plasticity in adult brain.* Curr Top Behav Neurosci, 2013. **15**: p. 31-48.
50. Li, E., et al., *Ghrelin directly stimulates adult hippocampal neurogenesis: implications for learning and memory.* Endocr J, 2013. **60**(6): p. 781-9.
51. Ouchi, Y., et al., *Reduced adult hippocampal neurogenesis and working memory deficits in the Dgcr8-deficient mouse model of 22q11.2 deletion-associated schizophrenia can be rescued by IGF2.* J Neurosci, 2013. **33**(22): p. 9408-19.
52. Pan, Y.W., D.R. Storm, and Z. Xia, *Role of adult neurogenesis in hippocampus-dependent memory, contextual fear extinction and remote contextual memory: new insights from ERK5 MAP kinase.* Neurobiol Learn Mem, 2013. **105**: p. 81-92.
53. Vivar, C., M.C. Potter, and H. van Praag, *All about running: synaptic plasticity, growth factors and adult hippocampal neurogenesis.* Curr Top Behav Neurosci, 2013. **15**: p. 189-210.
54. Cayre, M., P. Canoll, and J.E. Goldman, *Cell migration in the normal and pathological postnatal mammalian brain.* Prog Neurobiol, 2009. **88**(1): p. 41-63.
55. Kaplan, M.S., *Environment complexity stimulates visual cortex neurogenesis: death of a dogma and a research career.* Trends Neurosci, 2001. **24**(10): p. 617-20.
56. Nottebohm, F., *Why are some neurons replaced in adult brain?* Journal of Neuroscience, 2002. **22**(3): p. 624-628.
57. Zupanc, G.K.H., *A comparative approach towards the understanding of adult neurogenesis.* Brain Behavior and Evolution, 2001. **58**(5): p. 246-249.
58. Merkle, F.T., et al., *Radial glia give rise to adult neural stem cells in the subventricular zone.* Proceedings of the National Academy of Sciences of the United States of America, 2004. **101**(50): p. 17528-17532.
59. Sanai, N., et al., *Unique astrocyte ribbon in adult human brain contains neural stem cells but lacks chain migration.* Nature, 2004. **427**(6976): p. 740-744.
60. Bonaguidi, M.A., et al., *In Vivo Clonal Analysis Reveals Self-Renewing and Multipotent Adult Neural Stem Cell Characteristics.* Cell, 2011. **145**(7): p. 1142-1155.
61. Gage, F.H., *Mammalian neural stem cells.* Science, 2000. **287**(5457): p. 1433-1438.
62. Palmer, T.D., et al., *Fibroblast growth factor-2 activates a latent neurogenic program in neural stem cells from diverse regions of the adult CNS.* Journal of Neuroscience, 1999. **19**(19): p. 8487-8497.
63. Seidenfaden, R., et al., *Glial conversion of SVZ-derived committed neuronal precursors after ectopic grafting into the adult brain.* Mol Cell Neurosci, 2006. **32**(1-2): p. 187-98.
64. Shihabuddin, L.S., et al., *Adult spinal cord stem cells generate neurons after transplantation in the adult dentate gyrus.* Journal of Neuroscience, 2000. **20**(23): p. 8727-8735.
65. Kempermann, G., L. Wiskott, and F.H. Gage, *Functional significance of adult neurogenesis.* Curr Opin Neurobiol, 2004. **14**(2): p. 186-91.

66. Honda, T., H. Tabata, and K. Nakajima, *Cellular and molecular mechanisms of neuronal migration in neocortical development.* Semin Cell Dev Biol, 2003. **14**(3): p. 169-74.
67. Bonaguidi, M.A., et al., *A unifying hypothesis on mammalian neural stem cell properties in the adult hippocampus.* Curr Opin Neurobiol, 2012. **22**(5): p. 754-61.
68. Encinas, J.M., et al., *Division-coupled astrocytic differentiation and age-related depletion of neural stem cells in the adult hippocampus.* Cell Stem Cell, 2011. **8**(5): p. 566-79.
69. Hodge, R.D., et al., *Intermediate progenitors in adult hippocampal neurogenesis: Tbr2 expression and coordinate regulation of neuronal output.* J Neurosci, 2008. **28**(14): p. 3707-17.
70. Fuentealba, L.C., et al., *Embryonic Origin of Postnatal Neural Stem Cells.* Cell, 2015. **161**(7): p. 1644-55.
71. Jhaveri, D.J., et al., *Purification of neural precursor cells reveals the presence of distinct, stimulus-specific subpopulations of quiescent precursors in the adult mouse hippocampus.* J Neurosci, 2015. **35**(21): p. 8132-44.
72. Luzzati, F., et al., *Quiescent neuronal progenitors are activated in the juvenile guinea pig lateral striatum and give rise to transient neurons.* Development, 2014. **141**(21): p. 4065-75.
73. Farkas, L.M. and W.B. Huttner, *The cell biology of neural stem and progenitor cells and its significance for their proliferation versus differentiation during mammalian brain development.* Curr Opin Cell Biol, 2008. **20**(6): p. 707-15.
74. Lois, C., J.M. Garcia-Verdugo, and A. Alvarez-Buylla, *Chain migration of neuronal precursors.* Science, 1996. **271**(5251): p. 978-81.
75. Agoston, Z., et al., *Meis2 is a Pax6 co-factor in neurogenesis and dopaminergic periglomerular fate specification in the adult olfactory bulb.* Development, 2014. **141**(1): p. 28-38.
76. Ramon-Cueto, A., et al., *Long-distance axonal regeneration in the transected adult rat spinal cord is promoted by olfactory ensheathing glia transplants.* J Neurosci, 1998. **18**(10): p. 3803-15.
77. Van Schepdael, A., et al., *Mechanisms of cell migration in the adult brain: modelling subventricular neurogenesis.* Comput Methods Biomech Biomed Engin, 2013. **16**(10): p. 1096-105.
78. Doetsch, F., et al., *Subventricular zone astrocytes are neural stem cells in the adult mammalian brain.* Cell, 1999. **97**(6): p. 703-16.
79. Oliveira, S.L., et al., *Functions of neurotrophins and growth factors in neurogenesis and brain repair.* Cytometry A, 2013. **83**(1): p. 76-89.
80. Benarroch, E.E., *Adult neurogenesis in the dentate gyrus: general concepts and potential implications.* Neurology, 2013. **81**(16): p. 1443-52.
81. Berg, D.A., et al., *Neurotransmitter-mediated control of neurogenesis in the adult vertebrate brain.* Development, 2013. **140**(12): p. 2548-61.
82. Chambers, R.A., *Adult hippocampal neurogenesis in the pathogenesis of addiction and dual diagnosis disorders.* Drug Alcohol Depend, 2013. **130**(1-3): p. 1-12.
83. Cheffer, A., A. Tarnok, and H. Ulrich, *Cell cycle regulation during neurogenesis in the embryonic and adult brain.* Stem Cell Rev, 2013. **9**(6): p. 794-805.
84. David, L.S., M. Schachner, and A. Saghatelyan, *The extracellular matrix glycoprotein tenascin-R affects adult but not developmental neurogenesis in the olfactory bulb.* J Neurosci, 2013. **33**(25): p. 10324-39.
85. Drew, L.J., S. Fusi, and R. Hen, *Adult neurogenesis in the mammalian hippocampus: why the dentate gyrus?* Learn Mem, 2013. **20**(12): p. 710-29.

86. Gil-Perotin, S., et al., *Adult neural stem cells from the subventricular zone: a review of the neurosphere assay.* Anat Rec (Hoboken), 2013. **296**(9): p. 1435-52.
87. Faigle, R. and H. Song, *Signaling mechanisms regulating adult neural stem cells and neurogenesis.* Biochim Biophys Acta, 2013. **1830**(2): p. 2435-48.
88. Gould, E., et al., *Neurogenesis in the neocortex of adult primates.* Science, 1999. **286**(5439): p. 548-52.
89. Sawada, M. and K. Sawamoto, *Mechanisms of neurogenesis in the normal and injured adult brain.* Keio J Med, 2013. **62**(1): p. 13-28.
90. Schmidt-Hieber, C., P. Jonas, and J. Bischofberger, *Enhanced synaptic plasticity in newly generated granule cells of the adult hippocampus.* Nature, 2004. **429**(6988): p. 184-7.
91. Swayne, L.A. and L.E. Wicki-Stordeur, *Ion channels in postnatal neurogenesis Potential targets for brain repair.* Channels, 2012. **6**(2): p. 69-74.
92. Carleton, A., et al., *Becoming a new neuron in the adult olfactory bulb.* Nature Neuroscience, 2003. **6**(5): p. 507-518.
93. Giachino, C., et al., *GABA suppresses neurogenesis in the adult hippocampus through GABAB receptors.* Development, 2014. **141**(1): p. 83-90.
94. Heron, P.M., et al., *Molecular events in the cell types of the olfactory epithelium during adult neurogenesis.* Mol Brain, 2013. **6**: p. 49.
95. Jaeger, A., et al., *Characterization of Apoptosis Signaling Cascades During the Differentiation Process of Human Neural ReNcell VM Progenitor Cells In Vitro.* Cellular and Molecular Neurobiology, 2015. **35**(8): p. 1203-1216.
96. Mandairon, N., F. Jourdan, and A. Didier, *Deprivation of sensory inputs to the olfactory bulb up-regulates cell death and proliferation in the subventricular zone of adult mice.* Neuroscience, 2003. **119**(2): p. 507-16.
97. Yasuda, T. and D.J. Adams, *Physiological roles of ion channels in adult neural stem cells and their progeny.* Journal of Neurochemistry, 2010. **114**(4): p. 946-959.
98. Zhang, L., et al., *Survivin, a key component of the Wnt/beta-catenin signaling pathway, contributes to traumatic brain injury-induced adult neurogenesis in the mouse dentate gyrus.* Int J Mol Med, 2013. **32**(4): p. 867-75.
99. Zhang, Y., et al., *Involvement of NF kappa B signaling in mediating the effects of GRK5 on neural stem cells.* Brain Research, 2015. **1608**: p. 31-39.
100. Ryu, J.R., et al., *Control of adult neurogenesis by programmed cell death in the mammalian brain.* Mol Brain, 2016. **9**: p. 43.
101. Rezza, A., R. Sennett, and M. Rendl, *Adult stem cell niches: cellular and molecular components.* Curr Top Dev Biol, 2014. **107**: p. 333-72.
102. Bekinschtein, P., et al., *Persistence of long-term memory storage requires a late protein synthesis- and BDNF- dependent phase in the hippocampus.* Neuron, 2007. **53**(2): p. 261-77.
103. Meran, L., A. Baulies, and V.S.W. Li, *Intestinal Stem Cell Niche: The Extracellular Matrix and Cellular Components.* Stem Cells International, 2017. **2017**: p. 7970385.
104. Platel, J.C., K.A. Dave, and A. Bordey, *Control of neuroblast production and migration by converging GABA and glutamate signals in the postnatal forebrain.* Journal of Physiology-London, 2008. **586**(16): p. 3739-3743.
105. Brus, M., et al., *Dynamics of olfactory and hippocampal neurogenesis in adult sheep.* J Comp Neurol, 2013. **521**(1): p. 169-88.
106. Fox, M.A. and H. Umemori, *Seeking long-term relationship: axon and target communicate to organize synaptic differentiation.* J Neurochem, 2006. **97**(5): p. 1215-31.

107. Ramon-Cueto, A. and M. Nieto-Sampedro, *Glial cells from adult rat olfactory bulb: immunocytochemical properties of pure cultures of ensheathing cells.* Neuroscience, 1992. **47**(1): p. 213-20.
108. Rubio, M.P., C. Munoz-Quiles, and A. Ramon-Cueto, *Adult olfactory bulbs from primates provide reliable ensheathing glia for cell therapy.* Glia, 2008. **56**(5): p. 539-51.
109. Wainwright, S.R. and L.A. Galea, *The neural plasticity theory of depression: assessing the roles of adult neurogenesis and PSA-NCAM within the hippocampus.* Neural Plast, 2013. **2013**: p. 805497.
110. Perez-Domper, P., S. Gradari, and J.L. Trejo, *The growth factors cascade and the dendrito-/synapto-genesis versus cell survival in adult hippocampal neurogenesis: the chicken or the egg.* Ageing Res Rev, 2013. **12**(3): p. 777-85.
111. Zito, K. and K. Svoboda, *Activity-dependent synaptogenesis in the adult Mammalian cortex.* Neuron, 2002. **35**(6): p. 1015-7.
112. Sanes, J.R. and J.W. Lichtman, *Induction, assembly, maturation and maintenance of a postsynaptic apparatus.* Nat Rev Neurosci, 2001. **2**(11): p. 791-805.
113. Odawara, A., et al., *Long-term electrophysiological activity and pharmacological response of a human induced pluripotent stem cell-derived neuron and astrocyte co-culture.* Biochem Biophys Res Commun, 2014. **443**(4): p. 1176-81.
114. Traniello, I.M., et al., *Age-related changes in stem cell dynamics, neurogenesis, apoptosis, and gliosis in the adult brain: a novel teleost fish model of negligible senescence.* Dev Neurobiol, 2014. **74**(5): p. 514-30.
115. Dayer, A.G., et al., *Short-term and long-term survival of new neurons in the rat dentate gyrus.* J Comp Neurol, 2003. **460**(4): p. 563-72.
116. Ghosh, A., J. Carnahan, and M.E. Greenberg, *Requirement for BDNF in activity-dependent survival of cortical neurons.* Science, 1994. **263**(5153): p. 1618-23.
117. Latchney, S.E., et al., *Deletion or activation of the aryl hydrocarbon receptor alters adult hippocampal neurogenesis and contextual fear memory.* J Neurochem, 2013. **125**(3): p. 430-45.
118. Lee, T.T., et al., *Sex, drugs, and adult neurogenesis: sex-dependent effects of escalating adolescent cannabinoid exposure on adult hippocampal neurogenesis, stress reactivity, and amphetamine sensitization.* Hippocampus, 2014. **24**(3): p. 280-92.
119. Song, J., et al., *Parvalbumin interneurons mediate neuronal circuitry-neurogenesis coupling in the adult hippocampus.* Nat Neurosci, 2013. **16**(12): p. 1728-30.
120. Jagasia, R., et al., *GABA-cAMP response element-binding protein signaling regulates maturation and survival of newly generated neurons in the adult hippocampus.* J Neurosci, 2009. **29**(25): p. 7966-77.
121. Esposito, M.S., et al., *Neuronal differentiation in the adult hippocampus recapitulates embryonic development.* J Neurosci, 2005. **25**(44): p. 10074-86.
122. Suzuki, S., et al., *The neural stem/progenitor cell marker nestin is expressed in proliferative endothelial cells, but not in mature vasculature.* J Histochem Cytochem, 2010. **58**(8): p. 721-30.
123. Frederiksen, K. and R.D. McKay, *Proliferation and differentiation of rat neuroepithelial precursor cells in vivo.* J Neurosci, 1988. **8**(4): p. 1144-51.
124. Ji, R., et al., *TAM receptors affect adult brain neurogenesis by negative regulation of microglial cell activation.* J Immunol, 2013. **191**(12): p. 6165-77.
125. Carpenter, M.K., et al., *Enrichment of neurons and neural precursors from human embryonic stem cells.* Exp Neurol, 2001. **172**(2): p. 383-97.

126. Ferensztajn-Rochowiak, E., et al., *Stem cells, pluripotency and glial cell markers in peripheral blood of bipolar patients on long-term lithium treatment.* Prog Neuropsychopharmacol Biol Psychiatry, 2018. **80**(Pt A): p. 28-33.
127. Eng, L.F., R.S. Ghirnikar, and Y.L. Lee, *Glial fibrillary acidic protein: GFAP-thirty-one years (1969-2000).* Neurochem Res, 2000. **25**(9-10): p. 1439-51.
128. Izant, J.G. and J.R. McIntosh, *Microtubule-associated proteins: a monoclonal antibody to MAP2 binds to differentiated neurons.* Proc Natl Acad Sci U S A, 1980. **77**(8): p. 4741-5.
129. Huber, G. and A. Matus, *Differences in the cellular distributions of two microtubule-associated proteins, MAP1 and MAP2, in rat brain.* J Neurosci, 1984. **4**(1): p. 151-60.
130. Lee, M.K., et al., *The expression and posttranslational modification of a neuron-specific beta-tubulin isotype during chick embryogenesis.* Cell Motil Cytoskeleton, 1990. **17**(2): p. 118-32.
131. von Bohlen Und Halbach, O., *Immunohistological markers for staging neurogenesis in adult hippocampus.* Cell Tissue Res, 2007. **329**(3): p. 409-20.
132. von Bohlen und Halbach, O., *Immunohistological markers for proliferative events, gliogenesis, and neurogenesis within the adult hippocampus.* Cell Tissue Res, 2011. **345**(1): p. 1-19.
133. Cavegn, N., et al., *Habitat-specific shaping of proliferation and neuronal differentiation in adult hippocampal neurogenesis of wild rodents.* Front Neurosci, 2013. **7**: p. 59.
134. Dhaliwal, J., et al., *Doublecortin (DCX) is not Essential for Survival and Differentiation of Newborn Neurons in the Adult Mouse Dentate Gyrus.* Front Neurosci, 2015. **9**: p. 494.
135. Encinas, J.M., et al., *A developmental perspective on adult hippocampal neurogenesis.* Int J Dev Neurosci, 2013. **31**(7): p. 640-5.
136. Kremer, T., et al., *Analysis of adult neurogenesis: evidence for a prominent "non-neurogenic" DCX-protein pool in rodent brain.* PLoS One, 2013. **8**(5): p. e59269.
137. Francis, F., et al., *Doublecortin is a developmentally regulated, microtubule-associated protein expressed in migrating and differentiating neurons.* Neuron, 1999. **23**(2): p. 247-56.
138. Friocourt, G., et al., *Doublecortin functions at the extremities of growing neuronal processes.* Cereb Cortex, 2003. **13**(6): p. 620-6.
139. Chai, J., et al., *[Distribution of postsynaptic density protein 95 (PSD95) and synaptophysin during neuronal maturation].* Xi Bao Yu Fen Zi Mian Yi Xue Za Zhi, 2016. **32**(12): p. 1619-1622.
140. Buckby, L.E., et al., *Comparison of neuroplastin and synaptic marker protein expression in acute and cultured organotypic hippocampal slices from rat.* Brain Res Dev Brain Res, 2004. **150**(1): p. 1-7.
141. Glantz, L.A., et al., *Synaptophysin and postsynaptic density protein 95 in the human prefrontal cortex from mid-gestation into early adulthood.* Neuroscience, 2007. **149**(3): p. 582-91.
142. Hilbe, M., et al., *Synaptophysin: an immunohistochemical marker for animal dysautonomias.* J Comp Pathol, 2005. **132**(2-3): p. 223-7.
143. Kolos, Y.A., I.P. Grigoriyev, and D.E. Korzhevskyi, *[A synaptic marker synaptophysin].* Morfologiia, 2015. **147**(1): p. 78-82.
144. Kwon, S.E. and E.R. Chapman, *Synaptophysin regulates the kinetics of synaptic vesicle endocytosis in central neurons.* Neuron, 2011. **70**(5): p. 847-54.
145. Sarnat, H.B., L. Flores-Sarnat, and C.L. Trevenen, *Synaptophysin immunoreactivity in the human hippocampus and neocortex from 6 to 41 weeks of gestation.* J Neuropathol Exp Neurol, 2010. **69**(3): p. 234-45.

146. Valtorta, F., et al., *Synaptophysin: leading actor or walk-on role in synaptic vesicle exocytosis?* Bioessays, 2004. **26**(4): p. 445-53.
147. Alvarez, F.J., *Gephyrin and the regulation of synaptic strength and dynamics at glycinergic inhibitory synapses.* Brain Res Bull, 2017. **129**: p. 50-65.
148. Choii, G. and J. Ko, *Gephyrin: a central GABAergic synapse organizer.* Exp Mol Med, 2015. **47**: p. e158.
149. Owens, D.F., et al., *Excitatory GABA responses in embryonic and neonatal cortical slices demonstrated by gramicidin perforated-patch recordings and calcium imaging.* J Neurosci, 1996. **16**(20): p. 6414-23.
150. Nguyen, L., et al., *Functional glycine receptors are expressed by postnatal nestin-positive neural stem/progenitor cells.* Eur J Neurosci, 2002. **15**(8): p. 1299-305.
151. Cesetti, T., et al., *Analysis of stem cell lineage progression in the neonatal subventricular zone identifies EGFR+/NG2- cells as transit-amplifying precursors.* Stem Cells, 2009. **27**(6): p. 1443-54.
152. Resnick, S.M., et al., *Longitudinal magnetic resonance imaging studies of older adults: a shrinking brain.* J Neurosci, 2003. **23**(8): p. 3295-301.
153. Yasuda, T., P.F. Bartlett, and D.J. Adams, *Kir and Kv channels regulate electrical properties and proliferation of adult neural precursor cells.* Molecular and Cellular Neuroscience, 2008. **37**(2): p. 284-297.
154. Yasuda, T., P.F. Bartlett, and D.J. Adams, *K-ir and K-v channels regulate electrical properties and proliferation of adult neural precursor cells.* Molecular and Cellular Neuroscience, 2008. **37**(2): p. 284-297.
155. Sundelacruz, S., M. Levin, and D.L. Kaplan, *Role of membrane potential in the regulation of cell proliferation and differentiation.* Stem Cell Rev, 2009. **5**(3): p. 231-46.
156. Bokoch, G.M. and B.A. Diebold, *Current molecular models for NADPH oxidase regulation by Rac GTPase.* Blood, 2002. **100**(8): p. 2692-2696.
157. Okazawa, S.N.a.M., *Membrane potential-regulated Ca 2+signalling in development and maturation of mammalian cerebellar granule cells.* J Physiol

2006. **575.2**
158. Tirone, F., et al., *Genetic control of adult neurogenesis: interplay of differentiation, proliferation and survival modulates new neurons function, and memory circuits.* Front Cell Neurosci, 2013. **7**: p. 59.
159. Puro, D.G., F. Roberge, and C.C. Chan, *Retinal glial cell proliferation and ion channels: a possible link.* Invest Ophthalmol Vis Sci, 1989. **30**(3): p. 521-9.
160. Dubois, J.M. and B. Rouzairedubois, *Role of Potassium Channels in Mitogenesis.* Progress in Biophysics & Molecular Biology, 1993. **59**(1): p. 1-21.
161. Schlichter, L.C., et al., *Properties of K+ and Cl- channels and their involvement in proliferation of rat microglial cells.* Glia, 1996. **17**(3): p. 225-236.
162. Schwab, A., *Function and spatial distribution of ion channels and transporters in cell migration.* American Journal of Physiology-Renal Physiology, 2001. **280**(5): p. F739-F747.
163. Bowlby, M.R., et al., *Modulation of the Kv1.3 potassium channel by receptor tyrosine kinases.* Journal of General Physiology, 1997. **110**(5): p. 601-610.
164. Gamper, N., et al., *IGF-1 up-regulates K+ channels via PI3-kinase, PDK1 and SGK1.* Pflugers Archiv-European Journal of Physiology, 2002. **443**(4): p. 625-634.
165. Perillan, P.R., et al., *Transforming growth factor-beta(1) regulates Kir2.3 inward rectifier K+ channels via phospholipase C and protein kinase C-delta in reactive astrocytes from adult rat brain.* Journal of Biological Chemistry, 2002. **277**(3): p. 1974-1980.

166. Timpe, L.C. and W.J. Fantl, *Modulation of a Voltage-Activated Potassium Channel by Peptide Growth-Factor Receptors.* Journal of Neuroscience, 1994. **14**(3): p. 1195-1201.
167. Zhou, X., et al., *Potential role of KCNQ/M-channels in regulating neuronal differentiation in mouse hippocampal and embryonic stem cell-derived neuronal cultures.* Experimental Neurology, 2011. **229**(2): p. 471-483.
168. Schwab, A., et al., *Potassium channels keep mobile cells on the go.* Physiology, 2008. **23**(4): p. 212-220.
169. Schwab, A., et al., *Oscillating activity of a Ca(2+)-sensitive K+ channel. A prerequisite for migration of transformed Madin-Darby canine kidney focus cells.* J Clin Invest, 1994. **93**(4): p. 1631-6.
170. Pettit, E.J. and F.S. Fay, *Cytosolic free calcium and the cytoskeleton in the control of leukocyte chemotaxis.* Physiol Rev, 1998. **78**(4): p. 949-67.
171. Yu, S.P., *Regulation and critical role of potassium homeostasis in apoptosis.* Prog Neurobiol, 2003. **70**(4): p. 363-86.
172. Schwab, A., et al., *Migration of transformed renal epithelial cells is regulated by K+ channel modulation of actin cytoskeleton and cell volume.* Pflugers Archiv-European Journal of Physiology, 1999. **438**(3): p. 330-337.
173. El Bejjani, R. and M. Hammarlund, *Neural Regeneration in Caenorhabditis elegans.* Annual Review of Genetics, Vol 46, 2012. **46**: p. 499-513.
174. Mennerick, S. and C.F. Zorumski, *Neural activity and survival in the developing nervous system.* Mol Neurobiol, 2000. **22**(1-3): p. 41-54.
175. LoTurco, J.J., et al., *GABA and glutamate depolarize cortical progenitor cells and inhibit DNA synthesis.* Neuron, 1995. **15**(6): p. 1287-98.
176. Liu, X., et al., *Nonsynaptic GABA signaling in postnatal subventricular zone controls proliferation of GFAP-expressing progenitors.* Nat Neurosci, 2005. **8**(9): p. 1179-87.
177. Weissman, T.A., et al., *Calcium waves propagate through radial glial cells and modulate proliferation in the developing neocortex.* Neuron, 2004. **43**(5): p. 647-61.
178. Kayama, T., et al., *Temporally coordinated spiking activity of human induced pluripotent stem cell-derived neurons co-cultured with astrocytes.* Biochem Biophys Res Commun, 2018. **495**(1): p. 1028-1033.
179. Spitzer, N.C., *Electrical activity in early neuronal development.* Nature, 2006. **444**(7120): p. 707-12.
180. Ikrar, T., et al., *Adult neurogenesis modifies excitability of the dentate gyrus.* Front Neural Circuits, 2013. **7**: p. 204.
181. Tozuka, Y., et al., *GABAergic excitation promotes neuronal differentiation in adult hippocampal progenitor cells.* Neuron, 2005. **47**(6): p. 803-15.
182. Ge, S., et al., *GABA regulates synaptic integration of newly generated neurons in the adult brain.* Nature, 2006. **439**(7076): p. 589-93.
183. D'Amico, L.A., D. Boujard, and P. Coumailleau, *The neurogenic factor NeuroD1 is expressed in post-mitotic cells during juvenile and adult Xenopus neurogenesis and not in progenitor or radial glial cells.* PLoS One, 2013. **8**(6): p. e66487.
184. Goda, Y. and G.W. Davis, *Mechanisms of synapse assembly and disassembly.* Neuron, 2003. **40**(2): p. 243-64.
185. Guo, J.J.U., et al., *Neuronal activity modifies the DNA methylation landscape in the adult brain.* Nature Neuroscience, 2011. **14**(10): p. 1345-U172.
186. Huang, Z.J. and P. Scheiffele, *GABA and neuroligin signaling: linking synaptic activity and adhesion in inhibitory synapse development.* Curr Opin Neurobiol, 2008. **18**(1): p. 77-83.

187. Platel, J.C. and W. Kelsch, *Role of NMDA receptors in adult neurogenesis: an ontogenetic (re)view on activity-dependent development.* Cell Mol Life Sci, 2013. **70**(19): p. 3591-601.
188. Pontes, A., Y. Zhang, and W. Hu, *Novel functions of GABA signaling in adult neurogenesis.* Front Biol (Beijing), 2013. **8**(5).
189. Reynolds, B.A. and S. Weiss, *Generation of neurons and astrocytes from isolated cells of the adult mammalian central nervous system.* Science, 1992. **255**(5052): p. 1707-10.
190. Garcion, E., et al., *Generation of an environmental niche for neural stem cell development by the extracellular matrix molecule tenascin C.* Development, 2004. **131**(14): p. 3423-32.
191. Conti, L., et al., *Niche-independent symmetrical self-renewal of a mammalian tissue stem cell.* PLoS Biol, 2005. **3**(9): p. e283.
192. Temple, S., *Division and differentiation of isolated CNS blast cells in microculture.* Nature, 1989. **340**(6233): p. 471-3.
193. Temple, S., *The development of neural stem cells.* Nature, 2001. **414**(6859): p. 112-7.
194. Palmer, T.D., J. Takahashi, and F.H. Gage, *The adult rat hippocampus contains primordial neural stem cells.* Mol Cell Neurosci, 1997. **8**(6): p. 389-404.
195. Suslov, O.N., et al., *Neural stem cell heterogeneity demonstrated by molecular phenotyping of clonal neurospheres.* Proc Natl Acad Sci U S A, 2002. **99**(22): p. 14506-11.
196. Sun, Y., et al., *Long-term tripotent differentiation capacity of human neural stem (NS) cells in adherent culture.* Mol Cell Neurosci, 2008. **38**(2): p. 245-58.
197. Fiore, G., et al., *Differentiation state affects morphine induced cell regulation in neuroblastoma cultured cells.* Neurosci Lett, 2013. **555**: p. 51-6.
198. Matthay, K.K., et al., *Neuroblastoma.* Nat Rev Dis Primers, 2016. **2**: p. 16078.
199. Xie, H.R., L.S. Hu, and G.Y. Li, *SH-SY5Y human neuroblastoma cell line: in vitro cell model of dopaminergic neurons in Parkinson's disease.* Chin Med J (Engl), 2010. **123**(8): p. 1086-92.
200. Prasad, K.N., *Differentiation of neuroblastoma cells in culture.* Biol Rev Camb Philos Soc, 1975. **50**(2): p. 129-65.
201. Pino, A., et al., *New neurons in adult brain: distribution, molecular mechanisms and therapies.* Biochem Pharmacol, 2017. **141**: p. 4-22.
202. Ninkovic, J. and M. Gotz, *Fate specification in the adult brain--lessons for eliciting neurogenesis from glial cells.* Bioessays, 2013. **35**(3): p. 242-52.
203. Xie, Y. and W.E. Lowry, *Manipulation of neural progenitor fate through the oxygen sensing pathway.* Methods, 2017.
204. Zhuang, P.W., et al., *Baicalin regulates neuronal fate decision in neural stem/progenitor cells and stimulates hippocampal neurogenesis in adult rats.* CNS Neurosci Ther, 2013. **19**(3): p. 154-62.
205. Huang, Z.J., et al., *BDNF regulates the maturation of inhibition and the critical period of plasticity in mouse visual cortex.* Cell, 1999. **98**(6): p. 739-55.
206. Low, V.F., et al., *Neurogenesis and progenitor cell distribution in the subgranular zone and subventricular zone of the adult sheep brain.* Neuroscience, 2013. **244**: p. 173-87.
207. Kumazawa-Manita, N., et al., *Tool use specific adult neurogenesis and synaptogenesis in rodent (Octodon degus) hippocampus.* PLoS One, 2013. **8**(3): p. e58649.
208. Jurikova, M., et al., *Ki67, PCNA, and MCM proteins: Markers of proliferation in the diagnosis of breast cancer.* Acta Histochem, 2016. **118**(5): p. 544-52.
209. Chen, Z. and T.D. Palmer, *Differential roles of TNFR1 and TNFR2 signaling in adult hippocampal neurogenesis.* Brain Behav Immun, 2013. **30**: p. 45-53.

210. Christie, K.J., A. Turbic, and A.M. Turnley, *Adult hippocampal neurogenesis, Rho kinase inhibition and enhancement of neuronal survival.* Neuroscience, 2013. **247**: p. 75-83.
211. Kandel, *Principles of Neural Science, fifth edition.* 2013.
212. El-Husseini, A.E., et al., *PSD-95 involvement in maturation of excitatory synapses.* Science, 2000. **290**(5495): p. 1364-8.
213. Ban, J., et al., *Embryonic stem cell-derived neurons form functional networks in vitro.* Stem Cells, 2007. **25**(3): p. 738-49.
214. Conti, L. and E. Cattaneo, *Neural stem cell systems: physiological players or in vitro entities? (vol 11, pg 170, 2010).* Nature Reviews Neuroscience, 2010. **11**(11): p. 782-782.
215. Balentova, S., et al., *Effect of whole-brain irradiation on the specific brain regions in a rat model: Metabolic and histopathological changes.* Neurotoxicology, 2017. **60**: p. 70-81.
216. Dong, X., et al., *Relationship between irradiation-induced neuro-inflammatory environments and impaired cognitive function in the developing brain of mice.* Int J Radiat Biol, 2015. **91**(3): p. 224-39.
217. Pineda, J.R., et al., *Vascular-derived TGF-beta increases in the stem cell niche and perturbs neurogenesis during aging and following irradiation in the adult mouse brain.* EMBO Mol Med, 2013. **5**(4): p. 548-62.
218. Prager, I., et al., *Dose-dependent short- and long-term effects of ionizing irradiation on neural stem cells in murine hippocampal tissue cultures: neuroprotective potential of resveratrol.* Brain Behav, 2016. **6**(10): p. e00548.
219. Armesilla-Diaz, A., et al., *p53 regulates the self-renewal and differentiation of neural precursors.* Neuroscience, 2009. **158**(4): p. 1378-89.
220. Chen, H., et al., *Ionizing Radiation Perturbs Cell Cycle Progression of Neural Precursors in the Subventricular Zone Without Affecting Their Long-Term Self-Renewal.* ASN Neuro, 2015. **7**(3).
221. Belenguer, G., et al., *Isolation, culture and analysis of adult subependymal neural stem cells.* Differentiation, 2016. **91**(4-5): p. 28-41.
222. Mateo-Lozano, S., et al., *Regulation of Differentiation by Calcium-Sensing Receptor in Normal and Tumoral Developing Nervous System.* Front Physiol, 2016. **7**: p. 169.
223. Xicoy, H., B. Wieringa, and G.J. Martens, *The SH-SY5Y cell line in Parkinson's disease research: a systematic review.* Mol Neurodegener, 2017. **12**(1): p. 10.
224. (BIPM), B.I.d.P.e.M., *the international system of units (SI).* 2010.
225. Smart, D., *Radiation Toxicity in the Central Nervous System: Mechanisms and Strategies for Injury Reduction.* Seminars in Radiation Oncology, 2017. **27**(4): p. 332-339.
226. Cordes, M.C., et al., *Distress, anxiety and depression in patients with brain metastases before and after radiotherapy.* Bmc Cancer, 2014. **14**.
227. Tseng, B.P., et al., *Functional Consequences of Radiation-Induced Oxidative Stress in Cultured Neural Stem Cells and the Brain Exposed to Charged Particle Irradiation.* Antioxidants & Redox Signaling, 2014. **20**(9): p. 1410-1422.
228. Cornforth, M.N. and J.S. Bedford, *X-Ray-Induced Breakage and Rejoining of Human Interphase Chromosomes.* Science, 1983. **222**(4628): p. 1141-1143.
229. Giusti, A.M., et al., *Human cell membrane oxidative damage induced by single and fractionated doses of ionizing radiation: a fluorescence spectroscopy study.* International Journal of Radiation Biology, 1998. **74**(5): p. 595-605.
230. Azzam, E.I., S.M. de Toledo, and J.B. Little, *Expression of CONNEXIN43 is highly sensitive to ionizing radiation and other environmental stresses.* Cancer Research, 2003. **63**(21): p. 7128-7135.

231. Dayal, D., et al., *Mitochondrial Complex II Dysfunction Can Contribute Significantly to Genomic Instability after Exposure to Ionizing Radiation.* Radiation Research, 2009. **172**(6): p. 737-745.
232. Bergonié, J.T., L., *De Quelques Résultats de la Radiotherapie et Essai de Fixation d'une Technique Rationnelle.* Comptes Rendus des Séances de l'Académie des Sciences, 1906.
233. Bergonié, J.T., L., *Interpretation of Some Results of Radiotherapy and an Attempt at Determining a Logical Technique of Treatment / De Quelques Résultats de la Radiotherapie et Essai de Fixation d'une Technique Rationnelle.* Radiation Research, 1959.
234. Pawlik, T.M. and K. Keyomarsi, *Role of cell cycle in mediating sensitivity to radiotherapy.* International Journal of Radiation Oncology Biology Physics, 2004. **59**(4): p. 928-942.
235. Rubin, P. and G.W. Casarett, *Clinical Radiation Pathology as Applied to Curative Radiotherapy.* Cancer, 1968. **22**(4): p. 767-&.
236. Stewart, F.A., et al., *ICRP publication 118: ICRP statement on tissue reactions and early and late effects of radiation in normal tissues and organs--threshold doses for tissue reactions in a radiation protection context.* Ann ICRP, 2012. **41**(1-2): p. 1-322.
237. Kantor, G., et al., *Radiation therapy for glial tumors: Technical aspects and clinical indications.* Cancer Radiotherapie, 2008. **12**(6-7): p. 687-694.
238. Achanta, P., et al., *Subventricular Zone Localized Irradiation Affects the Generation of Proliferating Neural Precursor Cells and the Migration of Neuroblasts.* Stem Cells, 2012. **30**(11): p. 2548-2560.
239. Belka, C., et al., *Radiation induced CNS toxicity--molecular and cellular mechanisms.* Br J Cancer, 2001. **85**(9): p. 1233-9.
240. Kim, J.S., et al., *Neurobiological toxicity of radiation in hippocampal cells.* Histology and Histopathology, 2013. **28**(3): p. 301-310.
241. Doll, R. and R. Peto, *The Causes of Cancer - Quantitative Estimates of Avoidable Risks of Cancer in the United-States Today.* Journal of the National Cancer Institute, 1981. **66**(6): p. 1191-&.
242. Berrington de Gonzalez, A. and S. Darby, *Risk of cancer from diagnostic X-rays: estimates for the UK and 14 other countries.* Lancet, 2004. **363**(9406): p. 345-51.
243. Peissner, W., et al., *Ionizing radiation-induced apoptosis of proliferating stem cells in the dentate gyrus of the adult rat hippocampus.* Molecular Brain Research, 1999. **71**(1): p. 61-68.
244. Verheyde, J. and M.A. Benotmane, *Unraveling the fundamental molecular mechanisms of morphological and cognitive defects in the irradiated brain.* Brain Res Rev, 2007. **53**(2): p. 312-20.
245. Schultheiss, T.E., et al., *Radiation response of the central nervous system.* Int J Radiat Oncol Biol Phys, 1995. **31**(5): p. 1093-112.
246. Rezvani, M., J.W. Hopewell, and M.E. Robbins, *Initiation of non-neoplastic late effects: the role of endothelium and connective tissue.* Stem Cells, 1995. **13 Suppl 1**: p. 248-56.
247. Parent, J.M., et al., *Dentate granule cell neurogenesis is increased by seizures and contributes to aberrant network reorganization in the adult rat hippocampus.* Journal of Neuroscience, 1997. **17**(10): p. 3727-3738.
248. Bellinzona, M., et al., *Apoptosis is induced in the subependyma of young adult rats by ionizing irradiation.* Neuroscience Letters, 1996. **208**(3): p. 163-166.
249. Monje, M.L., et al., *Irradiation induces neural precursor-cell dysfunction.* Nature Medicine, 2002. **8**(9): p. 955-962.

250. Mizumatsu, S., et al., *Extreme sensitivity of adult neurogenesis to low doses of X-irradiation.* Cancer Res, 2003. **63**(14): p. 4021-7.
251. Tada, E., et al., *X-irradiation causes a prolonged reduction in cell proliferation in the dentate gyrus of adult rats.* Neuroscience, 2000. **99**(1): p. 33-41.
252. Capilla-Gonzalez, V., et al., *The Subventricular Zone Is Able to Respond to a Demyelinating Lesion After Localized Radiation.* Stem Cells, 2014. **32**(1): p. 59-69.
253. Lazarini, F., et al., *Cellular and Behavioral Effects of Cranial Irradiation of the Subventricular Zone in Adult Mice.* Plos One, 2009. **4**(9).
254. Fukuda, A., et al., *Age-dependent sensitivity of the developing brain to irradiation is correlated with the number and vulnerability of progenitor cells (vol 92, pg 569, 2005).* Journal of Neurochemistry, 2005. **95**(6): p. 1802-1802.
255. Ford, E.C., et al., *Localized CT-Guided Irradiation Inhibits Neurogenesis in Specific Regions of the Adult Mouse Brain.* Radiation Research, 2011. **175**(6): p. 774-783.
256. Capilla-Gonzalez, V., et al., *Age- Related Changes in Astrocytic and Ependymal Cells of the Subventricular Zone.* Glia, 2014. **62**(5): p. 790-803.
257. Nagai, R., et al., *Selective vulnerability to radiation in the hippocampal dentate granule cells.* Surgical Neurology, 2000. **53**(5): p. 503-506.
258. Uberti, D., et al., *p53 is dispensable for apoptosis but controls neurogenesis of mouse dentate gyrus cells following gamma-irradiation.* Molecular Brain Research, 2001. **93**(1): p. 81-89.
259. Lonergan, P.E., et al., *Neuroprotective effect of eicosapentaenoic acid in hippocampus of rats exposed to gamma-irradiation.* Journal of Biological Chemistry, 2002. **277**(23): p. 20804-20811.
260. Santarelli, L., et al., *Requirement of hippocampal neurogenesis for the behavioral effects of antidepressants.* Science, 2003. **301**(5634): p. 805-809.
261. Kronenberg, G., et al., *Subpopulations of proliferating cells of the adult hippocampus respond differently to physiologic neurogenic stimuli.* Journal of Comparative Neurology, 2003. **467**(4): p. 455-463.
262. Riss, M., Niles, *Assay Guidance Manual.* Cell Viability Assays, 2016.
263. Etienne, O., et al., *Variation of radiation-sensitivity of neural stem and progenitor cell populations within the developing mouse brain.* International Journal of Radiation Biology, 2012. **88**(10): p. 694-702.
264. Daynac, M., et al., *Quiescent neural stem cells exit dormancy upon alteration of GABAAR signaling following radiation damage.* Stem Cell Res, 2013. **11**(1): p. 516-28.
265. Herrup, K. and Y. Yang, *Cell cycle regulation in the postmitotic neuron: oxymoron or new biology?* Nat Rev Neurosci, 2007. **8**(5): p. 368-78.
266. Roque, T., et al., *Lack of a p21waf1/Cip-Dependent G1/S Checkpoint in Neural Stem and Progenitor Cells After DNA Damage In Vivo.* Stem Cells, 2012. **30**(3): p. 537-547.
267. Sokolov, M. and R. Neumann, *Lessons Learned about Human Stem Cell Responses to Ionizing Radiation Exposures: A Long Road Still Ahead of Us.* International Journal of Molecular Sciences, 2013. **14**(8): p. 15695-15723.
268. Schneider, L. and F.D. di Fagagna, *Neural stem cells exposed to BrdU lose their global DNA methylation and undergo astrocytic differentiation.* Nucleic Acids Research, 2012. **40**(12): p. 5332-5342.
269. Schneider, L., et al., *DNA Damage in Mammalian Neural Stem Cells Leads to Astrocytic Differentiation Mediated by BMP2 Signaling through JAK-STAT.* Stem Cell Reports, 2013. **1**(2): p. 123-138.

270. Schneider, L., M. Fumagalli, and F.D. di Fagagna, *Terminally differentiated astrocytes lack DNA damage response signaling and are radioresistant but retain DNA repair proficiency.* Cell Death and Differentiation, 2012. **19**(4): p. 582-591.
271. Danzer, S., *Mossy Fiber Sprouting in the Epileptic Brain: Taking on the Lernaean Hydra.* Epilepsy Currents, 2017. **17**(1): p. 50-51.
272. Li, Y.Q., Z. Cheng, and S. Wong, *Differential Apoptosis Radiosensitivity of Neural Progenitors in Adult Mouse Hippocampus.* Int J Mol Sci, 2016. **17**(5).
273. Cheung, Y.T., et al., *Effects of all-trans-retinoic acid on human SH-SY5Y neuroblastoma as in vitro model in neurotoxicity research.* Neurotoxicology, 2009. **30**(1): p. 127-135.
274. Culmsee, C., et al., *Nerve growth factor survival signaling in cultured hippocampal neurons is mediated through TRKA and requires the common neurotrophin receptor p75.* Neuroscience, 2002. **115**(4): p. 1089-1108.
275. Martinou, J.C., et al., *Overexpression of Bcl-2 in Transgenic Mice Protects Neurons from Naturally-Occurring Cell-Death and Experimental-Ischemia.* Neuron, 1994. **13**(4): p. 1017-1030.
276. Wang, C.X., et al., *Cyclin-dependent kinase-5 prevents neuronal apoptosis through ERK-mediated upregulation of Bcl-2.* Cell Death and Differentiation, 2006. **13**(7): p. 1203-1212.
277. Zhang, K.Z., et al., *BCL2 regulates neural differentiation.* Proceedings of the National Academy of Sciences of the United States of America, 1996. **93**(9): p. 4504-4508.
278. Youle, R.J., *Cellular demolition and the rules of engagement.* Science, 2007. **315**(5813): p. 776-777.
279. Schneider, L., *Survival of Neural Stem Cells Undergoing DNA Damage-Induced Astrocytic Differentiation in Self-Renewal-Promoting Conditions In Vitro.* Plos One, 2014. **9**(1).
280. van Praag, H., et al., *Running enhances neurogenesis, learning, and long-term potentiation in mice.* Proceedings of the National Academy of Sciences of the United States of America, 1999. **96**(23): p. 13427-13431.
281. Lemaire, V., et al., *Prenatal stress produces learning deficits associated with an inhibition of neurogenesis in the hippocampus.* Proceedings of the National Academy of Sciences of the United States of America, 2000. **97**(20): p. 11032-11037.
282. Shors, T.J., et al., *Neurogenesis in the adult is involved in the formation of trace memories (vol 410, 372, 2001).* Nature, 2001. **414**(6866): p. 938-938.
283. Kempermann, G., *Possible functions for adult hippocampal neurogenesis.* Journal of Neurochemistry, 2002. **81**: p. 42-42.
284. Kempermann, G., *Why new neurons? Possible functions for adult hippocampal neurogenesis.* Journal of Neuroscience, 2002. **22**(3): p. 635-638.
285. Prickaerts, J., et al., *Learning and adult neurogenesis: Survival with or without proliferation?* Neurobiology of Learning and Memory, 2004. **81**(1): p. 1-11.
286. Snyder, J.S., et al., *A role for adult neurogenesis in spatial long-term memory.* Neuroscience, 2005. **130**(4): p. 843-852.
287. Garthe, A. and G. Kempermann, *An old test for new neurons: refining the Morris water maze to study the functional relevance of adult hippocampal neurogenesis.* Front Neurosci, 2013. **7**: p. 63.
288. Kwon, S.J., et al., *Low-intensity treadmill exercise and/or bright light promote neurogenesis in adult rat brain.* Neural Regen Res, 2013. **8**(10): p. 922-9.
289. Leuner, B., E. Gould, and T.J. Shors, *Is there a link between adult neurogenesis and learning?* Hippocampus, 2006. **16**(3): p. 216-224.
290. Canales, J.J., *Deficient plasticity in the hippocampus and the spiral of addiction: focus on adult neurogenesis.* Curr Top Behav Neurosci, 2013. **15**: p. 293-312.

291. Hagemann, T.L., R. Paylor, and A. Messing, *Deficits in adult neurogenesis, contextual fear conditioning, and spatial learning in a Gfap mutant mouse model of Alexander disease.* J Neurosci, 2013. **33**(47): p. 18698-706.
292. Ho, N.F., et al., *In vivo imaging of adult human hippocampal neurogenesis: progress, pitfalls and promise.* Mol Psychiatry, 2013. **18**(4): p. 404-16.
293. Kohman, R.A., et al., *Effects of minocycline on spatial learning, hippocampal neurogenesis and microglia in aged and adult mice.* Behav Brain Res, 2013. **242**: p. 17-24.
294. Mendez-David, I., et al., *Adult hippocampal neurogenesis: an actor in the antidepressant-like action.* Ann Pharm Fr, 2013. **71**(3): p. 143-9.
295. Pristera, A., et al., *Impact of N-tau on adult hippocampal neurogenesis, anxiety, and memory.* Neurobiol Aging, 2013. **34**(11): p. 2551-63.
296. Puzzo, D., et al., *F3/Contactin promotes hippocampal neurogenesis, synaptic plasticity, and memory in adult mice.* Hippocampus, 2013. **23**(12): p. 1367-82.
297. Tiwari, S.K., et al., *Curcumin-loaded nanoparticles potently induce adult neurogenesis and reverse cognitive deficits in Alzheimer's disease model via canonical Wnt/beta-catenin pathway.* ACS Nano, 2014. **8**(1): p. 76-103.
298. Urbach, A., et al., *Cyclin D2 knockout mice with depleted adult neurogenesis learn Barnes maze task.* Behav Neurosci, 2013. **127**(1): p. 1-8.
299. Zhao, Z., et al., *Ghrelin administration enhances neurogenesis but impairs spatial learning and memory in adult mice.* Neuroscience, 2014. **257**: p. 175-85.
300. Hodges, H., et al., *Late behavioural and neuropathological effects of local brain irradiation in the rat.* Behavioural Brain Research, 1998. **91**(1-2): p. 99-114.
301. Sienkiewicz, Z.J., R.G.E. Haylock, and R.D. Saunders, *Prenatal Irradiation and Spatial Memory in Mice - Investigation of Dose-Response Relationship.* International Journal of Radiation Biology, 1994. **65**(5): p. 611-618.
302. Parent, J.M., et al., *Inhibition of dentate granule cell neurogenesis with brain irradiation does not prevent seizure-induced mossy fiber synaptic reorganization in the rat.* J Neurosci, 1999. **19**(11): p. 4508-19.
303. Snyder, J.S., N. Kee, and J.M. Wojtowicz, *Effects of adult neurogenesis on synaptic plasticity in the rat dentate gyrus.* J Neurophysiol, 2001. **85**(6): p. 2423-31.
304. Kempermann, G., H.G. Kuhn, and F.H. Gage, *More hippocampal neurons in adult mice living in an enriched environment.* Nature, 1997. **386**(6624): p. 493-5.
305. Rola, R., et al., *Radiation-induced impairment of hippocampal neurogenesis is associated with cognitive deficits in young mice.* Experimental Neurology, 2004. **188**(2): p. 316-330.
306. Yoneoka, Y., et al., *An experimental study of radiation-induced cognitive dysfunction in an adult rat model.* British Journal of Radiology, 1999. **72**(864): p. 1196-1201.
307. Brown, W.R., et al., *Capillary loss precedes the cognitive impairment induced by fractionated whole-brain irradiation: A potential rat model of vascular dementia.* Journal of the Neurological Sciences, 2007. **257**(1-2): p. 67-71.
308. Parihar, V.K. and C.L. Limoli, *Cranial irradiation compromises neuronal architecture in the hippocampus.* Proc Natl Acad Sci U S A, 2013. **110**(31): p. 12822-7.
309. Parihar, V.K., et al., *Persistent changes in neuronal structure and synaptic plasticity caused by proton irradiation.* Brain Struct Funct, 2015. **220**(2): p. 1161-71.
310. Chakraborti, A., et al., *Cranial Irradiation Alters Dendritic Spine Density and Morphology in the Hippocampus.* Plos One, 2012. **7**(7).
311. Casciati, A., et al., *Age-related effects of X-ray irradiation on mouse hippocampus.* Oncotarget, 2016. **7**(19): p. 28040-28058.

312. Kempf, S.J., et al., *The cognitive defects of neonatally irradiated mice are accompanied by changed synaptic plasticity, adult neurogenesis and neuroinflammation.* Molecular Neurodegeneration, 2014. **9**.
313. Harada, A., et al., *MAP2 is required for dendrite elongation, PKA anchoring in dendrites, and proper PKA signal transduction.* Molecular Biology of the Cell, 2002. **13**: p. 325a-325a.
314. Woods, G.F., et al., *Loss of PSD-95 enrichment is not a prerequisite for spine retraction.* J Neurosci, 2011. **31**(34): p. 12129-38.
315. Huttenlocher, P.R., *Dendritic and Synaptic Pathology in Mental-Retardation.* Pediatric Neurology, 1991. **7**(2): p. 79-85.
316. Tronel, S., et al., *Spatial learning sculpts the dendritic arbor of adult-born hippocampal neurons.* Proceedings of the National Academy of Sciences of the United States of America, 2010. **107**(17): p. 7963-7968.
317. Terry, R.D., et al., *Some Morphometric Aspects of the Brain in Senile Dementia of the Alzheimer Type.* Journal of Neuropathology and Experimental Neurology, 1981. **40**(3): p. 314-314.
318. Kaufmann, W.E. and H.W. Moser, *Dendritic anomalies in disorders associated with mental retardation.* Cerebral Cortex, 2000. **10**(10): p. 981-991.
319. Rosi, S., et al., *Cranial irradiation alters the behaviorally induced immediate-early gene arc (activity-regulated cytoskeleton-associated protein).* Cancer Res, 2008. **68**(23): p. 9763-70.
320. Wu, P.H., et al., *Radiation induces acute alterations in neuronal function.* PLoS One, 2012. **7**(5): p. e37677.
321. Shi, L., et al., *Spatial learning and memory deficits after whole-brain irradiation are associated with changes in NMDA receptor subunits in the hippocampus.* Radiat Res, 2006. **166**(6): p. 892-9.
322. Halliwell, B., *Reactive Oxygen Species in Living Systems - Source, Biochemistry, and Role in Human-Disease.* American Journal of Medicine, 1991. **91**: p. S14-S22.
323. Dasuri, K., L. Zhang, and J.N. Keller, *Oxidative stress, neurodegeneration, and the balance of protein degradation and protein synthesis.* Free Radical Biology and Medicine, 2013. **62**: p. 170-185.
324. Andersen, J.K., *Oxidative stress in neurodegeneration: cause or consequence?* Nature Medicine, 2004. **10**(7): p. S18-S25.
325. Sies, H., *Hydrogen peroxide as a central redox signaling molecule in physiological oxidative stress: Oxidative eustress.* Redox Biology, 2017. **11**: p. 613-619.
326. Trachootham, D., J. Alexandre, and P. Huang, *Targeting cancer cells by ROS-mediated mechanisms: a radical therapeutic approach?* Nature Reviews Drug Discovery, 2009. **8**(7): p. 579-591.
327. Paravicini, T.M. and R.M. Touyz, *Redox signaling in hypertension.* Cardiovascular Research, 2006. **71**(2): p. 247-258.
328. Barsukova, A.G., D. Bourdette, and M. Forte, *Mitochondrial calcium and its regulation in neurodegeneration induced by oxidative stress.* European Journal of Neuroscience, 2011. **34**(3): p. 437-447.
329. Shukla, V., S.K. Mishra, and H.C. Pant, *Oxidative stress in neurodegeneration.* Adv Pharmacol Sci, 2011. **2011**: p. 572634.
330. Singh, B.K., et al., *Oxidative stress in zinc-induced dopaminergic neurodegeneration: Implications of superoxide dismutase and heme oxygenase-1.* Free Radical Research, 2011. **45**(10): p. 1207-1222.
331. Wang, L.Q., K.J. Colodner, and M.B. Feany, *Protein Misfolding and Oxidative Stress Promote Glial-Mediated Neurodegeneration in an Alexander Disease Model.* Journal of Neuroscience, 2011. **31**(8): p. 2868-2877.

332. Wilson, C., E. Munoz-Palma, and C. Gonzalez-Billault, *From birth to death: A role for reactive oxygen species in neuronal development.* Semin Cell Dev Biol, 2017.
333. Borquez, D.A., et al., *Dissecting the role of redox signaling in neuronal development.* J Neurochem, 2016. **137**(4): p. 506-17.
334. Ray, P.D., B.W. Huang, and Y. Tsuji, *Reactive oxygen species (ROS) homeostasis and redox regulation in cellular signaling.* Cell Signal, 2012. **24**(5): p. 981-90.
335. Weidinger, A. and A.V. Kozlov, *Biological Activities of Reactive Oxygen and Nitrogen Species: Oxidative Stress versus Signal Transduction.* Biomolecules, 2015. **5**(2): p. 472-84.
336. Iqbal, M.A. and E. Eftekharpour, *Regulatory Role of Redox Balance in Determination of Neural Precursor Cell Fate.* Stem Cells International, 2017. **2017**: p. 9209127.
337. Limoli, C.L., et al., *Redox changes induced in hippocampal precursor cells by heavy ion irradiation.* Radiation and Environmental Biophysics, 2007. **46**(2): p. 167-172.
338. Nunez, M.T., et al., *Iron toxicity in neurodegeneration.* Biometals, 2012. **25**(4): p. 761-776.
339. Riley, P.A., *Free-Radicals in Biology - Oxidative Stress and the Effects of Ionizing-Radiation.* International Journal of Radiation Biology, 1994. **65**(1): p. 27-33.
340. Liochev, S.I. and I. Fridovich, *The Haber-Weiss cycle - 70 years later: an alternative view.* Redox Report, 2002. **7**(1): p. 55-57.
341. von Sonntag, C., *Advanced oxidation processes: mechanistic aspects.* Water Science and Technology, 2008. **58**(5): p. 1015-1021.
342. Limoli, C.L., et al., *Apoptosis, reproductive failure, and oxidative stress in Chinese hamster ovary cells with compromised genomic integrity.* Cancer Research, 1998. **58**(16): p. 3712-3718.
343. Rola, R., et al., *Lack of extracellular superoxide dismutase (EC-SOD) in the microenvironment impacts radiation-induced changes in neurogenesis.* Free Radical Biology and Medicine, 2007. **42**(8): p. 1133-1145.
344. Huang, T.T., Y. Zou, and R. Corniola, *Oxidative stress and adult neurogenesis-Effects of radiation and superoxide dismutase deficiency.* Seminars in Cell & Developmental Biology, 2012. **23**(7): p. 738-744.
345. Dickinson, B.C. and C.J. Chang, *Chemistry and biology of reactive oxygen species in signaling or stress responses.* Nature Chemical Biology, 2011. **7**(8): p. 504-511.
346. DeCoursey, T.E. and E. Ligeti, *Regulation and termination of NADPH oxidase activity.* Cellular and Molecular Life Sciences, 2005. **62**(19-20): p. 2173-2193.
347. Glogauer, M., et al., *Rac1 deletion in mouse neutrophils has selective effects on neutrophil functions.* Journal of Immunology, 2003. **170**(11): p. 5652-5657.
348. Lambeth, J.D., T. Kawahara, and B. Diebold, *Regulation of Nox and Duox enzymatic activity and expression.* Free Radical Biology and Medicine, 2007. **43**(3): p. 319-331.
349. Zou, Z.Z., et al., *Induction of reactive oxygen species: an emerging approach for cancer therapy.* Apoptosis, 2017. **22**(11): p. 1321-1335.
350. Vaquero, E.C., et al., *Reactive oxygen species produced by NAD(P)H oxidase inhibit apoptosis in pancreatic cancer cells.* Journal of Biological Chemistry, 2004. **279**(33): p. 34643-34654.
351. Furukawa, A., et al., *H2O2 accelerates cellular senescence by accumulation of acetylated p53 via decrease in the function of SIRT1 by NAD(+) depletion.* Cellular Physiology and Biochemistry, 2007. **20**(1-4): p. 45-54.
352. Kwon, J., et al., *The Nonphagocytic NADPH Oxidase Duox1 Mediates a Positive Feedback Loop During T Cell Receptor Signaling.* Science Signaling, 2010. **3**(133).
353. Mahadev, K., et al., *The NAD(P)H oxidase homolog Nox4 modulates insulin-stimulated generation of H2O2 and plays an integral role in insulin signal transduction.* Molecular and Cellular Biology, 2004. **24**(5): p. 1844-1854.

354. Burhans, W.C. and N.H. Heintz, *The cell cycle is a redox cycle: Linking phase-specific targets to cell fate.* Free Radical Biology and Medicine, 2009. **47**(9): p. 1282-1293.
355. Mofarrahi, M., et al., *Regulation of proliferation of skeletal muscle precursor cells by NADPH oxidase.* Antioxidants & Redox Signaling, 2008. **10**(3): p. 559-574.
356. Kaplan, P., et al., *Free radical-induced protein modification and inhibition of Ca2+-ATPase of cardiac sarcoplasmic reticulum.* Molecular and Cellular Biochemistry, 2003. **248**(1-2): p. 41-47.
357. Hidalgo, C., et al., *A transverse tubule NADPH oxidase activity stimulates calcium release from isolated triads via ryanodine receptor type 1 S-glutathionylation.* Journal of Biological Chemistry, 2006. **281**(36): p. 26473-26482.
358. Tirone, F. and J.A. Cox, *NADPH oxidase 5 (NOX5) interacts with and is regulated by calmodulin.* Febs Letters, 2007. **581**(6): p. 1202-1208.
359. Walton, N.M., et al., *Adult Neurogenesis Transiently Generates Oxidative Stress.* Plos One, 2012. **7**(4).
360. Tsatmali, M., E.C. Walcott, and K.L. Crossin, *Newborn neurons acquire high levels of reactive oxygen species and increased mitochondrial proteins upon differentiation from progenitors.* Brain Research, 2005. **1040**(1-2): p. 137-150.
361. Amoureux, M.C., et al., *N-CAM binding inhibits the proliferation of hippocampal progenitor cells and promotes their differentiation to a neuronal phenotype.* Journal of Neuroscience, 2000. **20**(10): p. 3631-3640.
362. Sporns, O., G.M. Edelman, and K.L. Crossin, *The Neural Cell-Adhesion Molecule (N-Cam) Inhibits Proliferation in Primary Cultures of Rat Astrocytes.* Proceedings of the National Academy of Sciences of the United States of America, 1995. **92**(2): p. 542-546.
363. Lucas, G.W.G.H.J., *Long-term monitoring of spontaneous single unit activity from neuronal monolayer networks cultured on photoetched multielectrode surfaces.* J. Electrophysiol. Tech., 1982. **9**: p. 55-69.
364. Tsatmali, M., et al., *Reactive oxygen species modulate the differentiation of neurons in clonal cortical cultures.* Molecular and Cellular Neuroscience, 2006. **33**(4): p. 345-357.
365. Katoh, S., et al., *Hyperoxia induces the differentiated neuronal phenotype of PC12 cells by producing reactive oxygen species.* Biochemical and Biophysical Research Communications, 1997. **241**(2): p. 347-351.
366. Suzukawa, K., et al., *Nerve growth factor-induced neuronal differentiation requires generation of Rac1-regulated reactive oxygen species.* Journal of Biological Chemistry, 2000. **275**(18): p. 13175-13178.
367. McCloy, R.A., et al., *Partial inhibition of Cdk1 in G 2 phase overrides the SAC and decouples mitotic events.* Cell Cycle, 2014. **13**(9): p. 1400-12.
368. Burgess, A., et al., *Loss of human Greatwall results in G2 arrest and multiple mitotic defects due to deregulation of the cyclin B-Cdc2/PP2A balance.* Proceedings of the National Academy of Sciences of the United States of America, 2010. **107**(28): p. 12564-12569.
369. Gavet, O. and J. Pines, *Progressive Activation of CyclinB1-Cdk1 Coordinates Entry to Mitosis.* Developmental Cell, 2010. **18**(4): p. 533-543.
370. Potapova, T.A., et al., *Mitotic progression becomes irreversible in prometaphase and collapses when Wee1 and Cdc25 are inhibited.* Molecular Biology of the Cell, 2011. **22**(8): p. 1191-1206.
371. Ovsepian, S.V., et al., *Distinctive role of KV1.1 subunit in the biology and functions of low threshold K+ channels with implications for neurological disease.* Pharmacology & Therapeutics, 2016. **159**: p. 93-101.

372. Kirizs, T., et al., *Distinct axo-somato-dendritic distributions of three potassium channels in CA1 hippocampal pyramidal cells.* European Journal of Neuroscience, 2014. **39**(11): p. 1771-1783.
373. Ho, T.S.Y. and M.N. Rasband, *Maintenance of Neuronal Polarity.* Developmental Neurobiology, 2011. **71**(6): p. 474-482.
374. Robbins, C.A. and B.L. Tempel, *Kv1.1 and Kv1.2: Similar channels, different seizure models.* Epilepsia, 2012. **53**: p. 134-141.
375. Debanne, D., et al., *Axon physiology.* Physiol Rev, 2011. **91**(2): p. 555-602.
376. Foust, A.J., et al., *Somatic Membrane Potential and Kv1 Channels Control Spike Repolarization in Cortical Axon Collaterals and Presynaptic Boutons.* Journal of Neuroscience, 2011. **31**(43): p. 15490-15498.
377. Bucher, D. and J.M. Goaillard, *Beyond faithful conduction: Short-term dynamics, neuromodulation, and long-term regulation of spike propagation in the axon.* Progress in Neurobiology, 2011. **94**(4): p. 307-346.
378. Falk, A.T., et al., *[Radiation-induces increased tumor cell aggressiveness of tumors of the glioblastomas?].* Bull Cancer, 2014. **101**(9): p. 876-80.
379. Boehme, K.A., et al., *Chondrosarcoma: A Rare Misfortune in Aging Human Cartilage? The Role of Stem and Progenitor Cells in Proliferation, Malignant Degeneration and Therapeutic Resistance.* Int J Mol Sci, 2018. **19**(1).
380. Vilalta, M., M. Rafat, and E.E. Graves, *Effects of radiation on metastasis and tumor cell migration.* Cell Mol Life Sci, 2016. **73**(16): p. 2999-3007.
381. Ramirez-Castillejo, C., et al., *Pigment epithelium-derived factor is a niche signal for neural stem cell renewal.* Nature Neuroscience, 2006. **9**(3): p. 331-339.
382. Hallbergson, A.F., C. Gnatenco, and D.A. Peterson, *Neurogenesis and brain injury: managing a renewable resource for repair.* Journal of Clinical Investigation, 2003. **112**(8): p. 1128-1133.
383. Catchpole, T. and M. Henkemeyer, *EphB2 Tyrosine Kinase-Dependent Forward Signaling in Migration of Neuronal Progenitors That Populate and Form a Distinct Region of the Dentate Niche.* Journal of Neuroscience, 2011. **31**(32): p. 11472-11483.
384. Connor, B., et al., *Deviating From the Well Travelled Path: Precursor Cell Migration in the Pathological Adult Mammalian Brain.* Journal of Cellular Biochemistry, 2011. **112**(6): p. 1467-1474.
385. Kaneko, N., et al., *New Neurons Clear the Path of Astrocytic Processes for Their Rapid Migration in the Adult Brain.* Neuron, 2010. **67**(2): p. 213-223.
386. Wang, Y., et al., *Girdin Is an Intrinsic Regulator of Neuroblast Chain Migration in the Rostral Migratory Stream of the Postnatal Brain.* Journal of Neuroscience, 2011. **31**(22): p. 8109-8122.
387. Akane, H., et al., *Glycidol induces axonopathy by adult-stage exposure and aberration of hippocampal neurogenesis affecting late-stage differentiation by developmental exposure in rats.* Toxicol Sci, 2013. **134**(1): p. 140-54.
388. Morrison, R.S., et al., *p53-dependent cell death signaling in neurons.* Neurochemical Research, 2003. **28**(1): p. 15-27.
389. Limoli, C.L., et al., *Radiation response of neural precursor cells: Linking cellular sensitivity to cell cycle checkpoints, apoptosis and oxidative stress.* Radiation Research, 2004. **161**(1): p. 17-27.
390. Wood, K.A. and R.J. Youle, *The Role of Free-Radicals and P53 in Neuron Apoptosis in-Vivo.* Journal of Neuroscience, 1995. **15**(8): p. 5851-5857.
391. Akiyama, K., et al., *Cognitive dysfunction and histological findings in adult rats one year after whole brain irradiation.* Neurol Med Chir (Tokyo), 2001. **41**(12): p. 590-8.
392. Bao, S., et al., *Glioma stem cells promote radioresistance by preferential activation of the DNA damage response.* Nature, 2006. **444**(7120): p. 756-60.

393. Schneider, L., M. Fumagalli, and F. d'Adda di Fagagna, *Terminally differentiated astrocytes lack DNA damage response signaling and are radioresistant but retain DNA repair proficiency.* Cell Death Differ, 2012. **19**(4): p. 582-91.
394. Gong, L., et al., *Differential radiation response between normal astrocytes and glioma cells revealed by comparative transcriptome analysis.* Onco Targets Ther, 2017. **10**: p. 5755-5764.
395. Lu, L., et al., *Arachidonic acid has protective effects on oxygen-glucose deprived astrocytes mediated through enhancement of potassium channel TREK-1 activity.* Neurosci Lett, 2017. **636**: p. 241-247.
396. Diehn, M., et al., *Association of reactive oxygen species levels and radioresistance in cancer stem cells.* Nature, 2009. **458**(7239): p. 780-3.
397. Robb, S.J. and J.R. Connor, *Nitric oxide protects astrocytes from oxidative stress.* Ann N Y Acad Sci, 2002. **962**: p. 93-102.
398. Baxter, P.S. and G.E. Hardingham, *Adaptive regulation of the brain's antioxidant defences by neurons and astrocytes.* Free Radic Biol Med, 2016. **100**: p. 147-152.
399. Yoshida, T., et al., *Mitochondrial dysfunction, a probable cause of persistent oxidative stress after exposure to ionizing radiation.* Free Radic Res, 2012. **46**(2): p. 147-53.
400. Zhang, R., et al., *Morin (2',3,4',5,7-pentahydroxyflavone) protected cells against gamma-radiation-induced oxidative stress.* Basic Clin Pharmacol Toxicol, 2011. **108**(1): p. 63-72.
401. Oh, S.B., et al., *Baicalein attenuates impaired hippocampal neurogenesis and the neurocognitive deficits induced by gamma-ray radiation.* Br J Pharmacol, 2013. **168**(2): p. 421-31.
402. Cho, H.J., et al., *Role of NADPH oxidase in radiation-induced pro-oxidative and pro-inflammatory pathways in mouse brain.* International Journal of Radiation Biology, 2017. **93**(11): p. 1257-1266.
403. Lu, Z., et al., *Colistin-induced autophagy and apoptosis involves the JNK-Bcl2-Bax signaling pathway and JNK-p53-ROS positive feedback loop in PC-12 cells.* Chem Biol Interact, 2017. **277**: p. 62-73.
404. Wang, D.B., et al., *p53 and mitochondrial function in neurons.* Biochimica Et Biophysica Acta-Molecular Basis of Disease, 2014. **1842**(8): p. 1186-1197.
405. Quadrato, G. and S. Di Giovanni, *Gatekeeper Between Quiescence and Differentiation: p53 in Axonal Outgrowth and Neurogenesis.* Axon Growth and Regeneration, Pt 1, 2012. **105**: p. 71-89.
406. Makar, T.K., et al., *Vitamin E, ascorbate, glutathione, glutathione disulfide, and enzymes of glutathione metabolism in cultures of chick astrocytes and neurons: evidence that astrocytes play an important role in antioxidative processes in the brain.* J Neurochem, 1994. **62**(1): p. 45-53.
407. Cafe, C., et al., *Oxidative Events in Neuronal and Glial Cell-Enriched Fractions of Rat Cerebral-Cortex.* Free Radical Biology and Medicine, 1995. **19**(6): p. 853-857.
408. Hall, Z.J., et al., *Site-specific regulation of adult neurogenesis by dietary fatty acid content, vitamin E and flight exercise in European starlings.* Eur J Neurosci, 2014. **39**(6): p. 875-82.
409. Scanlon, J.M. and I.J. Reynolds, *Effects of oxidants and glutamate receptor activation on mitochondrial membrane potential in rat forebrain neurons.* J Neurochem, 1998. **71**(6): p. 2392-400.
410. Reynolds, I.J. and T.G. Hastings, *Glutamate induces the production of reactive oxygen species in cultured forebrain neurons following NMDA receptor activation.* J Neurosci, 1995. **15**(5 Pt 1): p. 3318-27.
411. Nicholls, D.G. and S.L. Budd, *Mitochondria and neuronal glutamate excitotoxicity.* Biochim Biophys Acta, 1998. **1366**(1-2): p. 97-112.

412. Day, R.M., A.L. Snow, and R.A. Panganiban, *Radiation-induced accelerated senescence: a fate worse than death?* Cell Cycle, 2014. **13**(13): p. 2011-2.
413. Waters, K.M., et al., *Annexin A2 modulates radiation-sensitive transcriptional programming and cell fate.* Radiat Res, 2013. **179**(1): p. 53-61.
414. !!! INVALID CITATION !!! {}.
415. Aelvoet, S.A., et al., *Long-Term Fate Mapping Using Conditional Lentiviral Vectors Reveals a Continuous Contribution of Radial Glia-Like Cells to Adult Hippocampal Neurogenesis in Mice.* PLoS One, 2015. **10**(11): p. e0143772.
416. Spadafora, R., et al., *Altered fate of subventricular zone progenitor cells and reduced neurogenesis following neonatal stroke.* Dev Neurosci, 2010. **32**(2): p. 101-13.
417. Torner, L., et al., *Prolactin prevents chronic stress-induced decrease of adult hippocampal neurogenesis and promotes neuronal fate.* J Neurosci, 2009. **29**(6): p. 1826-33.
418. Yanagisawa, M., et al., *Fate alteration of neuroepithelial cells from neurogenesis to astrocytogenesis by bone morphogenetic proteins.* Neurosci Res, 2001. **41**(4): p. 391-6.
419. Monje, M.L., H. Toda, and T.D. Palmer, *Inflammatory blockade restores adult hippocampal neurogenesis.* Science, 2003. **302**(5651): p. 1760-5.
420. Monje, M.L., et al., *Impaired human hippocampal neurogenesis after treatment for central nervous system malignancies.* Ann Neurol, 2007. **62**(5): p. 515-20.
421. Monje, M., *Cranial radiation therapy and damage to hippocampal neurogenesis.* Dev Disabil Res Rev, 2008. **14**(3): p. 238-42.
422. Monje, M. and J. Dietrich, *Cognitive side effects of cancer therapy demonstrate a functional role for adult neurogenesis.* Behav Brain Res, 2012. **227**(2): p. 376-9.
423. Fike, J.R., S. Rosi, and C.L. Limoli, *Neural precursor cells and central nervous system radiation sensitivity.* Semin Radiat Oncol, 2009. **19**(2): p. 122-32.
424. Mizumatsu, S., et al., *Extreme sensitivity of adult neurogenesis to low doses of X-irradiation.* Cancer Research, 2003. **63**(14): p. 4021-4027.
425. Lumniczky, K., T. Szatmari, and G. Safrany, *Ionizing Radiation-Induced Immune and Inflammatory Reactions in the Brain.* Front Immunol, 2017. **8**: p. 517.
426. Tang, F.R., W.K. Loke, and B.C. Khoo, *Postnatal irradiation-induced hippocampal neuropathology, cognitive impairment and aging.* Brain Dev, 2017. **39**(4): p. 277-293.
427. Prozorovski, T., et al., *Sirt1 contributes critically to the redox-dependent fate of neural progenitors.* Nat Cell Biol, 2008. **10**(4): p. 385-94.
428. Isozaki, T., et al., *Effects of carbon ion irradiation and X-ray irradiation on the ubiquitylated protein accumulation.* Int J Oncol, 2016. **49**(1): p. 144-52.
429. Yasuda, T., et al., *Irradiation-injured brain tissues can self-renew in the absence of the pivotal tumor suppressor p53 in the medaka (Oryzias latipes) embryo.* J Radiat Res, 2016. **57**(1): p. 9-15.
430. Huang, T.T., D. Leu, and Y. Zou, *Oxidative stress and redox regulation on hippocampal-dependent cognitive functions.* Arch Biochem Biophys, 2015. **576**: p. 2-7.
431. Ben Abdallah, N.M., L. Slomianka, and H.P. Lipp, *Reversible effect of X-irradiation on proliferation, neurogenesis, and cell death in the dentate gyrus of adult mice.* Hippocampus, 2007. **17**(12): p. 1230-40.
432. Corniola, R., et al., *Paradoxical relationship between Mn superoxide dismutase deficiency and radiation-induced cognitive defects.* PLoS One, 2012. **7**(11): p. e49367.
433. Zou, Y., et al., *Extracellular superoxide dismutase is important for hippocampal neurogenesis and preservation of cognitive functions after irradiation.* Proc Natl Acad Sci U S A, 2012. **109**(52): p. 21522-7.

434. Wilson, C. and C. Gonzalez-Billault, *Regulation of cytoskeletal dynamics by redox signaling and oxidative stress: implications for neuronal development and trafficking.* Front Cell Neurosci, 2015. **9**: p. 381.
435. Nunez, M.T., et al., *Iron toxicity in neurodegeneration.* Biometals, 2012. **25**(4): p. 761-76.
436. Chen, K., et al., *Loss of Frataxin induces iron toxicity, sphingolipid synthesis, and Pdk1/Mef2 activation, leading to neurodegeneration.* Elife, 2016. **5**.
437. Gerich, F.J., et al., *H(2)O(2)-mediated modulation of cytosolic signaling and organelle function in rat hippocampus.* Pflugers Arch, 2009. **458**(5): p. 937-52.
438. Janssen-Heininger, Y.M., et al., *Redox-based regulation of signal transduction: principles, pitfalls, and promises.* Free Radic Biol Med, 2008. **45**(1): p. 1-17.
439. Quinta, H.R., et al., *Ligand-mediated Galectin-1 endocytosis prevents intraneural H2O2 production promoting F-actin dynamics reactivation and axonal re-growth.* Exp Neurol, 2016. **283**(Pt A): p. 165-78.
440. Morinaka, A., et al., *Thioredoxin mediates oxidation-dependent phosphorylation of CRMP2 and growth cone collapse.* Sci Signal, 2011. **4**(170): p. ra26.
441. Wilson, C., M.T. Nunez, and C. Gonzalez-Billault, *Contribution of NADPH oxidase to the establishment of hippocampal neuronal polarity in culture.* J Cell Sci, 2015. **128**(16): p. 2989-95.
442. Wilson, C., et al., *A Feed-Forward Mechanism Involving the NOX Complex and RyR-Mediated Ca2+ Release During Axonal Specification.* J Neurosci, 2016. **36**(43): p. 11107-11119.
443. Rieger, S. and A. Sagasti, *Hydrogen peroxide promotes injury-induced peripheral sensory axon regeneration in the zebrafish skin.* PLoS Biol, 2011. **9**(5): p. e1000621.
444. Olguin-Albuerne, M. and J. Moran, *ROS produced by NOX2 control in vitro development of cerebellar granule neurons development.* ASN Neuro, 2015. **7**(2).
445. Munnamalai, V., et al., *Bidirectional interactions between NOX2-type NADPH oxidase and the F-actin cytoskeleton in neuronal growth cones.* J Neurochem, 2014. **130**(4): p. 526-40.
446. Tapon, N. and A. Hall, *Rho, Rac and Cdc42 GTPases regulate the organization of the actin cytoskeleton.* Curr Opin Cell Biol, 1997. **9**(1): p. 86-92.
447. Wilson, C., et al., *Actin filaments-A target for redox regulation.* Cytoskeleton (Hoboken), 2016. **73**(10): p. 577-595.
448. Munnamalai, V. and D.M. Suter, *Reactive oxygen species regulate F-actin dynamics in neuronal growth cones and neurite outgrowth.* J Neurochem, 2009. **108**(3): p. 644-61.
449. Hung, R.J., C.W. Pak, and J.R. Terman, *Direct redox regulation of F-actin assembly and disassembly by Mical.* Science, 2011. **334**(6063): p. 1710-3.
450. Terman, J.R. and A. Kashina, *Post-translational modification and regulation of actin.* Curr Opin Cell Biol, 2013. **25**(1): p. 30-8.
451. Um, K., et al., *Dynamic control of excitatory synapse development by a Rac1 GEF/GAP regulatory complex.* Dev Cell, 2014. **29**(6): p. 701-15.
452. Gao, S., R. Yu, and X. Zhou, *The Role of Geranylgeranyltransferase I-Mediated Protein Prenylation in the Brain.* Mol Neurobiol, 2016. **53**(10): p. 6925-6937.
453. Massaad, C.A. and E. Klann, *Reactive oxygen species in the regulation of synaptic plasticity and memory.* Antioxid Redox Signal, 2011. **14**(10): p. 2013-54.
454. Niggli, E., et al., *Posttranslational modifications of cardiac ryanodine receptors: Ca(2+) signaling and EC-coupling.* Biochim Biophys Acta, 2013. **1833**(4): p. 866-75.
455. Sun, Q.A., et al., *Oxygen-coupled redox regulation of the skeletal muscle ryanodine receptor/Ca2+ release channel (RyR1): sites and nature of oxidative modification.* J Biol Chem, 2013. **288**(32): p. 22961-71.

456. Sesti, F., *Oxidation of K(+) Channels in Aging and Neurodegeneration.* Aging Dis, 2016. **7**(2): p. 130-5.
457. Sesti, F., S. Liu, and S.Q. Cai, *Oxidation of potassium channels by ROS: a general mechanism of aging and neurodegeneration?* Trends Cell Biol, 2010. **20**(1): p. 45-51.
458. Liu, Y. and D.D. Gutterman, *Oxidative stress and potassium channel function.* Clin Exp Pharmacol Physiol, 2002. **29**(4): p. 305-11.
459. Caouette, D., et al., *Hydrogen peroxide modulates the Kv1.5 channel expressed in a mammalian cell line.* Naunyn Schmiedebergs Arch Pharmacol, 2003. **368**(6): p. 479-86.
460. Berube, J., D. Caouette, and P. Daleau, *Hydrogen peroxide modifies the kinetics of HERG channel expressed in a mammalian cell line.* J Pharmacol Exp Ther, 2001. **297**(1): p. 96-102.
461. Busch, A.E., et al., *Molecular basis of IsK protein regulation by oxidation or chelation.* J Biol Chem, 1995. **270**(8): p. 3638-41.
462. Ruppersberg, J.P., et al., *Regulation of fast inactivation of cloned mammalian IK(A) channels by cysteine oxidation.* Nature, 1991. **352**(6337): p. 711-4.
463. Stephens, G.J., D.G. Owen, and B. Robertson, *Cysteine-modifying reagents alter the gating of the rat cloned potassium channel Kv1.4.* Pflugers Arch, 1996. **431**(3): p. 435-42.
464. Gamper, N., et al., *Oxidative modification of M-type K(+) channels as a mechanism of cytoprotective neuronal silencing.* EMBO J, 2006. **25**(20): p. 4996-5004.
465. Hsieh, C.P., *Redox modulation of A-type K+ currents in pain-sensing dorsal root ganglion neurons.* Biochem Biophys Res Commun, 2008. **370**(3): p. 445-9.
466. Pal, S., et al., *Mediation of neuronal apoptosis by Kv2.1-encoded potassium channels.* J Neurosci, 2003. **23**(12): p. 4798-802.
467. Duprat, F., et al., *Pancreatic two P domain K+ channels TALK-1 and TALK-2 are activated by nitric oxide and reactive oxygen species.* J Physiol, 2005. **562**(Pt 1): p. 235-44.
468. Tang, X.D., et al., *Reactive oxygen species impair Slo1 BK channel function by altering cysteine-mediated calcium sensing.* Nat Struct Mol Biol, 2004. **11**(2): p. 171-8.
469. Zeidner, G., R. Sadja, and E. Reuveny, *Redox-dependent gating of G protein-coupled inwardly rectifying K+ channels.* J Biol Chem, 2001. **276**(38): p. 35564-70.
470. Avshalumov, M.V. and M.E. Rice, *Activation of ATP-sensitive K+ (K(ATP)) channels by H2O2 underlies glutamate-dependent inhibition of striatal dopamine release.* Proc Natl Acad Sci U S A, 2003. **100**(20): p. 11729-34.
471. Cotella, D., et al., *Toxic role of K+ channel oxidation in mammalian brain.* J Neurosci, 2012. **32**(12): p. 4133-44.
472. Wu, X., et al., *Molecular mechanisms underlying the apoptotic effect of KCNB1 K+ channel oxidation.* J Biol Chem, 2013. **288**(6): p. 4128-34.
473. Oddo, S., et al., *Triple-transgenic model of Alzheimer's disease with plaques and tangles: intracellular Abeta and synaptic dysfunction.* Neuron, 2003. **39**(3): p. 409-21.
474. Vergara, C., et al., *Calcium-activated potassium channels.* Curr Opin Neurobiol, 1998. **8**(3): p. 321-9.
475. Santarelli, L.C., et al., *Three methionine residues located within the regulator of conductance for K+ (RCK) domains confer oxidative sensitivity to large-conductance Ca2+-activated K+ channels.* J Physiol, 2006. **571**(Pt 2): p. 329-48.
476. Zhang, G., et al., *Cysteine oxidation and rundown of large-conductance Ca2+-dependent K+ channels.* Biochem Biophys Res Commun, 2006. **342**(4): p. 1389-95.

477. Gong, L., et al., *Redox modulation of large conductance calcium-activated potassium channels in CA1 pyramidal neurons from adult rat hippocampus.* Neurosci Lett, 2000. **286**(3): p. 191-4.
478. Streit, A.K., et al., *RNA editing in the central cavity as a mechanism to regulate surface expression of the voltage-gated potassium channel Kv1.1.* J Biol Chem, 2014. **289**(39): p. 26762-71.
479. Swain, S.M., et al., *Ca(2+)/calmodulin regulates Kvbeta1.1-mediated inactivation of voltage-gated K(+) channels.* Sci Rep, 2015. **5**: p. 15509.
480. Kline, D.D., et al., *Kv1.1 deletion augments the afferent hypoxic chemosensory pathway and respiration.* J Neurosci, 2005. **25**(13): p. 3389-99.
481. Simeone, K.A., et al., *Targeting deficiencies in mitochondrial respiratory complex I and functional uncoupling exerts anti-seizure effects in a genetic model of temporal lobe epilepsy and in a model of acute temporal lobe seizures.* Exp Neurol, 2014. **251**: p. 84-90.
482. Hu, C.L., et al., *Kv 1.1 is associated with neuronal apoptosis and modulated by protein kinase C in the rat cerebellar granule cell.* J Neurochem, 2008. **106**(3): p. 1125-37.
483. Binzen, U., et al., *Co-expression of the voltage-gated potassium channel Kv1.4 with transient receptor potential channels (TRPV1 and TRPV2) and the cannabinoid receptor CB1 in rat dorsal root ganglion neurons.* Neuroscience, 2006. **142**(2): p. 527-39.
484. Hellstrom, N.A., et al., *Differential recovery of neural stem cells in the subventricular zone and dentate gyrus after ionizing radiation.* Stem Cells, 2009. **27**(3): p. 634-41.
485. Schneider, L., et al., *DNA damage in mammalian neural stem cells leads to astrocytic differentiation mediated by BMP2 signaling through JAK-STAT.* Stem Cell Reports, 2013. **1**(2): p. 123-38.
486. Havelek, R., et al., *Ionizing radiation induces senescence and differentiation of human dental pulp stem cells.* Folia Biol (Praha), 2013. **59**(5): p. 188-97.
487. Shao, L., Y. Luo, and D. Zhou, *Hematopoietic stem cell injury induced by ionizing radiation.* Antioxid Redox Signal, 2014. **20**(9): p. 1447-62.
488. Manda, K., et al., *Low dose effects of ionizing radiation on normal tissue stem cells.* Mutat Res Rev Mutat Res, 2014.
489. Yao, X., et al., *Molecular cloning of a glibenclamide-sensitive, voltage-gated potassium channel expressed in rabbit kidney.* J Clin Invest, 1996. **97**(11): p. 2525-33.
490. Choi, J.S., et al., *Mechanism of fluoxetine block of cloned voltage-activated potassium channel Kv1.3.* J Pharmacol Exp Ther, 1999. **291**(1): p. 1-6.
491. Pompermayer, K., et al., *The ATP-sensitive potassium channel blocker glibenclamide prevents renal ischemia/reperfusion injury in rats.* Kidney Int, 2005. **67**(5): p. 1785-96.
492. Sung, M.J., et al., *Open channel block of Kv3.1 currents by fluoxetine.* J Pharmacol Sci, 2008. **106**(1): p. 38-45.
493. Reeve, H.L., P.F. Vaughan, and C. Peers, *Glibenclamide inhibits a voltage-gated K+ current in the human neuroblastoma cell line SH-SY5Y.* Neurosci Lett, 1992. **135**(1): p. 37-40.
494. Urrego, D., et al., *Potassium channels in cell cycle and cell proliferation.* Philos Trans R Soc Lond B Biol Sci, 2014. **369**(1638): p. 20130094.
495. Filippov, V., et al., *Subpopulation of nestin-expressing progenitor cells in the adult murine hippocampus shows electrophysiological and morphological characteristics of astrocytes.* Mol Cell Neurosci, 2003. **23**(3): p. 373-82.
496. Gibhardt, C.S., et al., *X-ray irradiation activates K+ channels via H2O2 signaling.* Sci Rep, 2015. **5**: p. 13861.

497. Sahoo, N., T. Hoshi, and S.H. Heinemann, *Oxidative modulation of voltage-gated potassium channels.* Antioxid Redox Signal, 2014. **21**(6): p. 933-52.
498. Zhou, Q.G., et al., *Regional-specific effect of fluoxetine on rapidly dividing progenitors along the dorsoventral axis of the hippocampus.* Sci Rep, 2016. **6**: p. 35572.
499. Encinas, J.M., A. Vaahtokari, and G. Enikolopov, *Fluoxetine targets early progenitor cells in the adult brain.* Proc Natl Acad Sci U S A, 2006. **103**(21): p. 8233-8.
500. Ortega, F.J., et al., *Glibenclamide enhances neurogenesis and improves long-term functional recovery after transient focal cerebral ischemia.* J Cereb Blood Flow Metab, 2013. **33**(3): p. 356-64.
501. Kurland, D.B., et al., *Glibenclamide for the treatment of acute CNS injury.* Pharmaceuticals (Basel), 2013. **6**(10): p. 1287-303.
502. Parga, J.A., et al., *Effect of inhibitors of NADPH oxidase complex and mitochondrial ATP-sensitive potassium channels on generation of dopaminergic neurons from neurospheres of mesencephalic precursors.* Dev Dyn, 2010. **239**(12): p. 3247-59.
503. Yang, J.Z., et al., *Iptakalim enhances adult mouse hippocampal neurogenesis via opening Kir6.1-composed K-ATP channels expressed in neural stem cells.* CNS Neurosci Ther, 2012. **18**(9): p. 737-44.
504. Fan, Y., et al., *ATP-sensitive potassium channels: uncovering novel targets for treating depression.* Brain Struct Funct, 2016. **221**(6): p. 3111-22.
505. Aimone, J.B., W. Deng, and F.H. Gage, *Resolving new memories: a critical look at the dentate gyrus, adult neurogenesis, and pattern separation.* Neuron, 2011. **70**(4): p. 589-96.

10. Abbreviations

IR	Ionising radiation
IQ	Intelegenz quoificent
CT	Computer tomography
CNS	Central nervous system
SGZ	Subgranular zone
DG	Dentate gyrus
SVZ	Subventricular zone
LV	Lateral ventricle
NSC	Neural stem cell
BrdU	bromodeoxyuridine
OB	Olfactory Bulb
GC	Granule Cell
RGG	Radial Gila Cell
EP	Early Progenitor
ßTub3	ß Tubulin 3
MAP2	Microtubule-associated protein 2
GFAP	Glial fibrillary acidic protein
EGF	Epidermal growth factor
FGF2	Fibroblast growth factor 2
BDNF	Brain derived neurotrophic factor
DCX	Doublecortin
PSD95	Post synaptic density protein 95
V_R	Resting membrane potential
K_{DR}	Delayed rectifier K^+ channel
K_{ir}	Inward rectifying K^+ channel
K_{ca}	Ca^{2+} sensitive K^+ channel
K_A	A-type K^+ channel
Na_V	Voltage gated Na^+ channel

PFA	Paraformaldehyde
RT	Room temperature
Ccas3	Cleaved caspase 3
syn	Synaptophysin
geph	Gephyrin
DAPI	4′,6-Diamidin-2-phenylindol
MEA	Multi electrode array
FS	Fate specification
CM	Cell maturation
EdU	5-Ethynyl-2´-deoxyuridine
SD	Standard Deviation
ESC	Embryonal stem cell
Gy	Gray
DNA	deoxyribonucleic acid
ROS	Reactive oxygen species
MTT	3-(4,5-dimethylthiazol-2-yl)-2,5-diphenyltetrazolium bromide
LET	Linear energy transfer
LD50	Median lethal dose
NOX	NADPH oxidase
LTP	Long term potential
PBS	phosphate buffered saline
JNK kinase	c-Jun NH2-terminal
ER	Endoplasmic reticulum
SOD	Superoxidedismutase
RyR	Ryanoide receptor
IP3	Inositol 1,4,5-trisphosphate
PKC	Protein kinase C
FL	Fluoxentine
Gl	Glibenclamide

ELISA	Enzyme-linked Immunosorbent Assay
CREB	cAMP response element-binding protein
ID	Inter spike distanze
MAP kinase	mitogen-activated protein kinase
DSB	DNA double strand break

11. Curriculum vitae

Name: Kerstin Rau

Address: Landgraf-Georg Str. 66

64283 Darmstadt

Contact: Kiki.Rau@gmail.com

Date of birth: November 19th, 1986

Education:

2013-2018:

Doctoral candidate at TU Darmstadt in the group of Prof. Dr. Bodo Laube, department of Neurophysiology and Neurosensory Systems. Participation in GRK 1657; DFG founded interdisciplinary Graduate college focusing “Molecular and cellular responses to ionizing radiation”.

2006-2013:

Sudies of Biology at TU Darmstadt. Specialisation in Animal Physiology, Cell-, Radiation- and Development- Biology and Plant Physiology; including 6-month intercourse at Boehringer Ingelheim, Bieberach, Department of Parkinson and Alzheimer Research.

Until 2006:

High school at Liebfrauen Schule Bensheim.

During my PhD thesis I had the opportunity to present my actual work in a poster presentation at DGDR in Mainz, 2014; EACR in Essen, 2015; GBS in Dresden, 2016 and Neuroscience in San Diego, 2016.

12. Acknowledgment:

First of all, I would like to thank Prof. Dr. Bodo Laube for giving me the opportunity to work on this very interesting project, for the scientific guidance, for the discussions and the suggestions about this project and for always having an open ear for your group members.

Furthermore, I want to thank Prof. Dr. Gerhard Thiel for being the co-referee of this thesis. Also, I want to thank Prof. Dr. Alexander Löwer and Prof. Dr. Franz Rödel.

Special thanks go to Dr. Bastian Roth who helped me on countless occasions and had an open ear for all my questions and for calming me down when needed. Additionally, to Bastian I want to thank my master student Selina Kahl for contributing to this thesis.

I want to thank GRK 1657 for supporting and enlarging my knowledge about radiobiology and allowing me to visit national and international conferences.

Katja, Henrik, Max, Basti, Raj, Michi, Axel, Kai, Gabi, Vito, Kirsten, Alex, Juliane and Selina thank you so much for creating such a nice working atmosphere!!! You are the best when it comes to eating cake...or even eating anything, fixing problems, creating new problems and getting around “Küchen- und Labordienst”. I could not imagine better colleagues than you, thank you.

Andyli, Bo and Hannahmaus, thank you for all the coffees, teas, beers and the wonderful time I had with you. Thank you for being really good friends I can count on.

Kili, I hope I told you every day how grateful I am for having you by my side, if not, I will make up for it with this. Your support was life-saving while I was PhD-thesis zombie, thank you!

Abschließend möchte ich meiner Familie meine besondere Dankbarkeit ausdrücken. Mama, Papa, Thomas ihr seid die Allerbesten. Danke, dass ihr mich bei all meinen wirren Tätigkeiten unterstützt und immer für mich da seid. Ohne euch hätte ich das alles nicht geschafft, ich hoffe das ist euch bewusst! Tausend Dank dafür…..und jetzt habe ich hoffentlich auch mal wieder Zeit nach Hause zukommen <3